Stanford Geothermal Program
Interdisciplinary Research in
Engineering and Earth Sciences
STANFORD UNIVERSITY
Stanford, California

SGP-TR-65

PRESSURE TRANSIENT ANALYSIS OF RESERVOIRS WITH LINEAR OR INTERNAL CIRCULAR BOUNDARIES

By

Abraham Sageev

June 1983

Financial support was provided through the Stanford Geothermal Program under Department of Energy Contract No. DE-AT03-80SF11459 and by the Department of Petroleum Engineering, Stanford University.

I certify that I have read this thesis and that in my opinion it is fully adequate, in scope and quality, as a dissertation for the degree of Doctor of Philosophy.

(Principal Adviser)

I certify that I have read this thesis and that in my opinion it is fully adequate, in scope and quality, as a dissertation for the degree of Doctor of Philosophy.

I certify that I have read this thesis and that in my opinion it is fully adequate, in scope and quality, as a dissertation for the degree of Doctor of Philosophy.

Approved for the University Committee
on Graduate Studies:

Dean of Graduate Studies & Research

to Michal

ACKNOWLEDGMENT

The author wishes to thank professor Roland N. Horne, principal adviser of this research.

Thanks are extended to professors H.J. Ramey Jr., W.E. Brigham, M.B. Standing and K. Aziz for their insight, participation and support.

Financial support was provided by Stanford University and by the Geothermal & Hydrology Technologies Division of the U.S. Dept. of Energy, project No.: DE-AT03-80SF11459.

ABSTRACT

In this work, a practical pressure transient analysis method is presented for a drawdown test in a well near an internal circular boundary. Both no-flow and constant pressure boundaries are considered. The problem is mathematically posed and solved using Green's Function theory and the Laplace Transformation. Both the Laplace solutions and the analytical solutions are presented.

Linear boundaries are viewed as circles with infinite radii and act as a known limiting case for finite radii internal boundaries. The size of an internal circular boundary and the distance ito it can be estimated using generalized type curves. Using a new method developed here, the distance to a linear boundary can be determined by semilog type curve matching without using the usual double straight line technique.

In developed systems containing compressible subregions, interference testing can provide estimates of the sizes of these subregions. However, detecting no-flow subregions with interference testing is not practical. Also presented are type curves for interference between a well flowing at a constant rate and one at constant pressure. These type curves may be applied to interpretation of pressure interference between oil and gas fields sharing a common aquifer.

The superposition method which can be used for assembling circular subregions intersected by linear faults is discussed as well.

Finally, a new generalized semilog type curve is presented that can be used for analyzing pressure transient data for both the linear and circular boundary cases.

TABLE OF CONTENTS

LIST OF FIGURES

LIST OF TABLES

CHAPTER 1 : INTRODUCTION

In this chapter, we discuss the need for a pressure transient analysis method for reservoirs with internal circular boundaries and the conditions under which this method is applicable. Then, we present a general discussion of the problem followed by a background review. Finally, we conclude this chapter with a statement of the problem.

1.1 APPLICATIONS

Constant pressure internal subregions occur naturally in oil fields as gas caps and in geothermal fields as steam or noncondensable gas caps. These subregions can also be induced artificially during steam flooding, in-situ combustion, immiscible gas drive, aquifer gas storage and growth of steam or gas bubbles below the bubble point pressure. In any of these cases, testing a well completed in the liquid zone, exterior to the circular discontinuity, can provide estimates of the size of this internal gaseous subregion and the distance to it if a technique can be derived to analyze such tests.

In this research, we are concerned with drawdown testing in a well exterior to a circular boundary such as a gas cap. Ramey (1983) and Standing (1983) were concerned about the effect such a gas cap can have on pressure responses during well tests. Ramey (1983) has observed a high total system compressibility when analyzing interference tests in such systems.

The new method presented here for pressure transient analysis is applicable whenever a two composite system resembles an infinite system containing an internal circular boundary.

This method offers a way to detect naturally occuring compressible regions when exploratory wells are completed in the liquid zone. Even a locally small gas cap would have a large impact on pressure transients in nearby wells. Using this method, we can distinguish between the total system compressibility and an effect of a compressible subregion.

We can apply this analysis method to study pressure interference between oil and gas fields sharing the same aquifer. If the oil field is far enough from the gas field and is relatively small, it can be approximated as a line source. The gas field can be relatively large, resembling a constant pressure circle, or small and resembling a constant pressure line source.

In developed systems, the method derived here permits monitoring of the location of fronts without having to shut in the injectors, which in many cases is undesirable.

The analysis assumes a horizontal slab reservoir with the compressible subregion completely penetrating the vertical thickness. However, the analysis is applicable to systems with liquid zones underlying gas bubbles in thin formations. Examples of such cases are naturally occurring gas caps or gas storage in aquifers.

Internal subregions with no-flow boundaries occur when a low mobility and compressibility fluid is injected into a reservoir containing a mobile compressible fluid. This condition may occur during reinjection of geothermal water into steam or two phase zones. Some enhanced oil recovery processes, such as polymer flooding or water injection during gas fillup, may develop similar conditions. The analysis of pressure transient tests in the mobile region may yield estimates of the size of the affected zone.

It is demonstrated here that useful results from interference testing are limited to the cases of constant pressure boundaries and only in systems where the location of the bubble is known. Interference testing may lead to an estimate of the shape of the affected zone, whether it is circular or not.

The application of pressure transient analysis methods for linear boundary cases is discussed extensively in the water and petroleum literature. A new method which improves the semilog portion of the analysis is developed as a corollary to this work. The use of a single semilog type curve replaces the straight line analysis method for determining the distance to the linear boundary.

1.2 PKOBLEM DESCRIPTION

Composite reservoirs are flow systems composed of two or more different regions. In this work, we consider models of oil, gas or geothermal reservoirs as two region infinite slab systems. One region is continuous and homogeneous and is bounded internally by a circular subregion. A production well and interference wells are exterior to the internal circular region, which may be conveniently described as a "hole" in the exterior region.

In a fully composite system, each region has its own flow characteristics. We have taken a simplifying approach, where the interface conditions of the internal circular region are specified as boundary conditions to the exterior regions instead of allowing the pressure transients to travel through the internal region. If the mobility and compressibility of the hole are high in comparison to the other region, the hole acts like a constant pressure source. On the other hand, if the mobility and compressibility of the hole are low in comparison to the extended region, the hole acts like a no-flow internal boundary. Hence, we consider both the no-flow and the constant pressure boundary conditions.

A linear boundary is a limiting case of a circular boundary with an infinite radius. If a linear boundary were to be wrapped around the well, it would form the known case of a well located within a circular boundary. If a linear boundary were to be wrapped away from the well, it forms an internal circular region that does not include the well.

The thrust of this research is to develop a pressure transient analysis method for a drawdown constant rate test for a well near an internal circular boundary. This reservoir limit test may be analyzed to determine the distance to and the size of the circular discontinuity.

1.3 BACKGROUND

Pressure transient tests are performed in order to gain knowledge about reservoir flow properties. The early and intermediate time pressure data can provide estimates of the flow characteristics of the local area around the well. The late time pressure data can provide information about the extent or the limits of the reservoir. This research is mainly concerned with the effects of internal reservoir limits on the pressure response of a well, but is nevertheless heavily dependent on the ability to determine the flow characteristics of the area near the well. Hence, both the intermediate and late time pressure responses are needed.

Carslaw and Jaeger (1946) and Van Everdingen and Hurst (1949) presented the solutions for a constant flow rate line source well and for a finite radius well in an infinite slab system. At intermediate times, many wells follow this behavior, known as "infinite - acting". Ramey (1970) presented an interpretation method for early time pressure data in the presence of wellbore storage and skin effect. The present study does not consider the effects of storage and skin on reservoir limit testing.

Carslaw and Jaeger (1946) and Bixel, et al. (1963) presented the most general analysis for an infinite reservoir with a linear discontinuity. They considered two regions with different flow properties and continuity of pressure and flow rate at the linear boundary.

Other authors simplified the approach to the composite system by specifying the condition at the linear boundary using the method of images. Stallman (1952) published log–log type curves for both the no–flow and the constant pressure linear boundaries. His curves are applicable for the analysis of single well tests and also for interference tests. These curves may be used to find the distance to the linear boundary and its orientation. Superposition of line source images was used by Jones (1961), Ferris, et al. (1962), Miller (1963), Miller, et al. (1966), Ramey, et al. (1970), Vela (1977), Tiab and Crichlow (1979) and Tiab and Kumar (1980) to generate the pressure response of a well in the presence of linear boundaries.

Davis and Larkin (1963), Standing (1964), Witherspoon, et al. (1967) and Kruseman and De Ridder (1970) extended the log-log method for a single linear boundary. They introduced the semilog method for determining the distance to a linear boundary. This method is based on identifying the intersection of two semilog straight lines representing the superposition of two line source solutions.

Cinco, et al. (1976) presented a solution to the transient pressure behavior of a well near a conductive linear fracture. This is a unique paper since they considered the fracture as an internal finite linear boundary.

Composite systems with circular discontinuities have been studied extensively in the literature. However, very few authors have considered internal circular discontinuities. Carslaw and Jaeger (1946) presented the Green's function for a point source external to an infinite cylinder with specified boundary conditions. Miller (1963) and Witherspoon, et al. (1967) considered testing near gas storage bubbles to be the same as testing near a constant pressure linear boundary. Most of the work using composite systems considered concentric systems with wells in the central region. Mathematically oriented works, describing heat conduction in composite materials were presented by Jaeger (1938 and 1943). Jaeger presented the Green's source function for an instantaneous line source centered and noncentered in a two system.

Larkin (1963) and Temeng and Horne (1983) applied Jaeger's work (1938 and 1934) on an eccentric line source to the flow of fluids in reservoirs. Hantush and Jacob (1960) considered an eccentric well within a bounded aquifer with a leaky caprock.

Loucks and Guerrero (1961) and Bixel and Van Poolen (1967) presented type curves for a well centered in a two region radial flow system. Ramey (1970) presented approximate solutions for unsteady liquid flow for a well centered in a radially concentric composite system.

Katz, et al. (1959) and Coats, et al. (1959) studied gas storage in aquifers. Although the gas bubble may ride on top of the aquifer, they treated the aquifer as a radially concentric two region system. This approach is valid when the underlying aquifer is relatively thin. Coats (1962) included vertical flow under the gas bubble in his solution to this aquifer problem.

Hurst (1960) and Mortada (1960) considered interference between oil fields sharing a common aquifer. Their common approach was to treat the oil fields as line sources, hence, avoiding the dependence of the pressure on the angle of rotation.

The present work concentrates on internal circular boundaries, yet, the same mathematical methods apply also to linear boundary configurations.

1.4 PROBLEM STATEMENT

The objective of this study is to provide a practical method for estimating the size of and the distance to an internal circular discontinuity.

In order to achieve this objective, we pose a mathematical description of the pressure change in a reservoir due to a constant rate line source exterior to a circular boundary with a specified boundary condition. We consider both no-flow and constant pressure boundaries.

We use the mathematical solutions to generate type curves that can be used in practical type curve matching procedures for analyzing transient pressure drawdown data from well tests.

First, we describe the limiting linear boundary cases, and then we consider constant pressure and no-flow internal circular boundary cases.

CHAPTER 2 : LINEAR BOUNDARIES

In this chapter, we consider a drawdown pressure transient analysis method for determining the distance between a well and a nearby constant pressure or no-flow linear boundary.

First, we pose and solve the problem using the method of images. Then, we describe the current log-log and semilog methods of analysis. Finally, we present a new semilog method followed by a type curve matching example. Some of the techniques developed In this chapter are useful in later chapters considering internal circular boundaries.

2.1 PROBLEM STATEMENT

The problem is two dimensional with one axis of symmetry along the line perpendicular to the linear boundary that includes the line source well (see Fig. 2.1).

It is assumed that the system has : an infinite radial extent, constant thickness, viscosity, porosity and compressibility, and constant and isotropic permeability. It is also assumed that the pressure gradients are small. so that the gradient squared terms can be neglected and that the flow is isothermal. Gravity effects are neglected.

The pressure $p(r,\theta,t)$ must satisfy the following equation and boundary conditions :

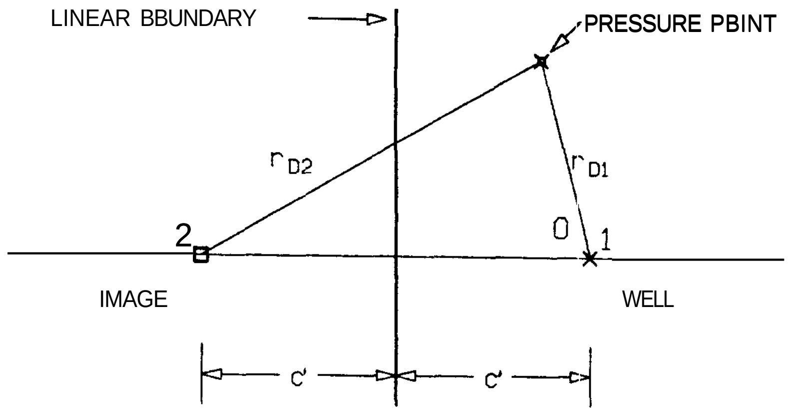

FIGURE 2.1 : A SCHEMATIC DIAGRAM OF THE **CONSTANT** PRESSURE **LINEAR BOUNDARY** SYSTEM

$$\frac{\partial^2 p}{\partial r^2} + \frac{1}{r}\frac{\partial p}{\partial r} + \frac{1}{r^2}\frac{\partial^2 p}{\partial \theta^2} = \frac{1}{\eta}\frac{\partial p}{\partial t} \tag{2.1}$$

$$p(\infty,\theta,t) = 0 \tag{2.2}$$

$$p \text{ at the boundary} = 0 \tag{2.3}$$

$$\lim_{r\to 0} r\frac{\partial p}{\partial r} = -\frac{q\mu}{2\pi kh} \tag{2.4}$$

$$p(r,\theta,0) = 0 \tag{2.5}$$

2.2 SOLUTION

The solution uses the method of images for generating linear boundaries, superposing the line source due to the infinite acting well and an opposing line source or sink due to an image well. A constant pressure linear boundary is generated by a line source well and a line sink image. A no-flow linear boundary is generated by a line source well and a line source image. The use of imaging for generating linear boundaries was discussed by Carslaw and Jaeger (1946), Ferris, et al. (1962) and Ramey, et al. (1973).

The dimensionless pressure drop for a line source near a constant pressure linear boundary takes the form :

$$p_D = -\frac{1}{2} \left[E_i(-X_1) - E_i(-X_2) \right] \qquad (2.6)$$

For a no-flow linear boundary the solution is :

$$p_D = -\frac{1}{2} \left[E_i(-X_1) + E_i(-X_2) \right] \qquad (2.7)$$

where :

$$X_i = \frac{r_{Di}^2}{4t_D} \qquad (2.8)$$

E_i denotes the Exponential Integral. The dimensionless terms are defined in the conventional manner :

$$p_D = \frac{2\pi kh(p_i - p)}{qB\mu} \tag{2.9}$$

$$t_D = \frac{kt}{\phi\mu c_t r_w^2} \tag{2.10}$$

$$r_{Di} = \frac{r_i}{r_w} \tag{2.11}$$

2.3 LOG-LOG AND SEMILOG ANALYSIS METHODS

Stallman (1952) presented log-log type curves for a line source well near a linear boundary (see Fig. 2.2). The curves below the line source curve approach steady state values and represent constant pressure linear boundaries. The curves that deviate above the line source curve are for no-flow linear boundaries. The parameter of the various curves is the ratio of the distance between the pressure point and the image well to the distance between the pressure point and the production well:

$$\frac{r_{D2}}{r_{D1}} = \frac{r_2}{r_1} = \sqrt{H} = \text{constant} \tag{2.12}$$

Stallman's type curve (Fig. 2.2) can be used for analyzing pressure responses from production wells and interference wells.

Brigham (1979) has shown that Eq. 2.12 represents circles that are centered at :

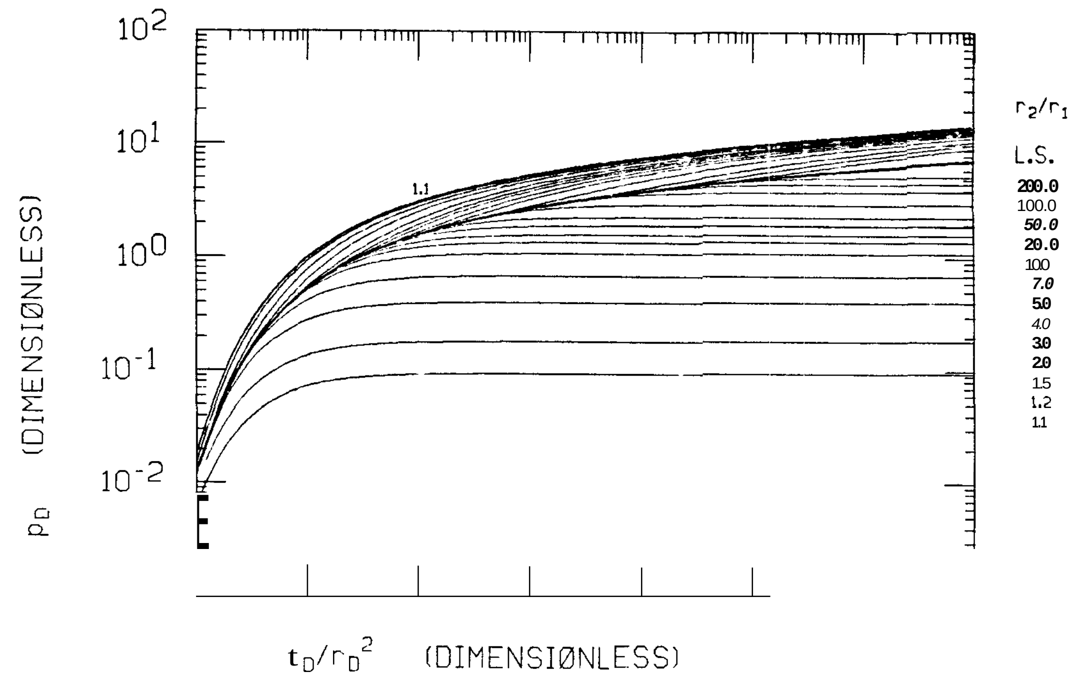

FIGURE **2.2 : LOG-LOG** TYPE CURVES FOR THE LINEAR **BOUNDARY** CASE.
AFTER STALLMAN (1952)

$$\left[c' \frac{1 + H}{1 - H} , \ 0 \right] \tag{2.13}$$

and have radii of :

$$2c' \frac{\sqrt{H}}{1 - H} \tag{2.14}$$

The distance between the well and the linear boundary is denoted by c' (see Fig. 2.1). The derivation of Eqs. 2.13 and 2.14 is presented in Appendix A.

Also, interference points which lie on the circles having the same r_2/r_1 ratio have the same dimensionless pressure response as a function of reduced dimensionless time (p_D vs. t_D/r_D^2), hence, the use of the parameter r_2/r_1 in Stallman's type curve. This behavior is discussed in Appendix B.

Using Stallman's type curves, we can match the pressure response to one of the curves and determine the ratio r_2/r_1. However, it is difficult to interpolate between the curves. Addressing this difficulty, Davis and Hawkins (1963) and Witherspoon, et al. (1970) extended Stallman's log-log type curve matching analysis using a double straight line semilog method. They observed that when the pressure - time data are graphed in a semilog fashion, two straight lines develop. Figure 2.3 presents an example of these two straight lines taken from Witherspoon, et al. (1970). The first straight line is the infinite acting period of the production well and develops after a dimensionless time of 10. The second straight line has a slope which is double that of the first line and represents the sum of two line sources. This second straight line develops when both the exponential integrals can be represented by the logarithmic approximation :

$$- E_1(-X) = - \gamma - \ln(X) \qquad (2.15)$$

where γ is the Euler constant.

Davis and Hawkins (1963) showed that for a production well, the distance to the linear boundary can be determined from the intersection point of the two straight lines :

$$d = [\, 0.561 \eta t_1 \,]^{\frac{1}{2}} \qquad (2.16)$$

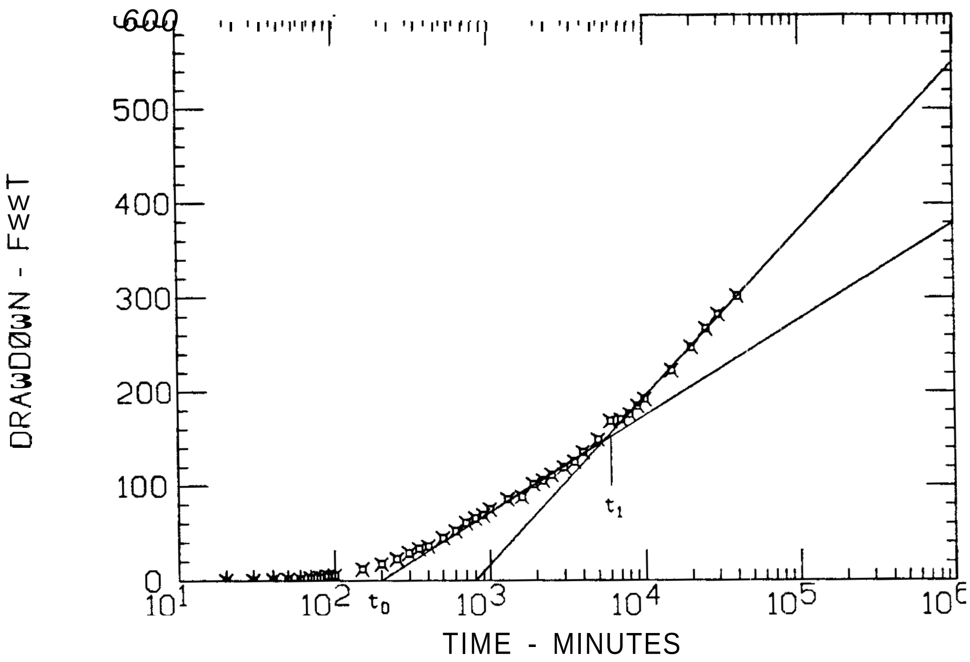

FIGURE **2.3** : EXAMPLE OF THE DOUBLE STRAIGHT LINE ANALYSIS METHOD. AFTER WITHERSPOON (**1970)**

where :

d = distance between the well and the boundary

and :

$$\eta = \frac{k}{\phi \mu c_t} \tag{2.17}$$

and t_1 is the time of the intersection point (see Fig. 2.3).

Witherspoon, et al. (1970) presented a method based on two intersection points. The first point is the intersection of the first straight line and the time axis. The second point is the intersection point of the two straight lines. The ratio r_2/r_1 becomes :

$$\frac{r_2}{r_1} = \sqrt{t_1/t_o} \tag{2.18}$$

Davis and Hawkins (1963) and Witherspoon, et al. (1970) pointed out several limitations of the double straight line method. If either of the straight lines did not fully develop, the method cannot be used. Furthermore, if the first straight line has a small slope, a small error in the location of the straight line will have a large effect on the calculated distance between the well and the image well.

So far, we have discussed the existing log–log and semilog methods for determining the distance between a well and an image well. In the next section, we present a new semilog type curve matching method for determining this distance.

2.4 A NEW SEMILOG TYPE CURVE MATCHING METHOD

In this section, we present a new semilog method for determining the ratio r_2/r_1 based on type curve matching. First, we describe how the type curve was generated. Then, a procedure for using the type curve is presented. Finally, we discuss the advantages of the new semilog method.

Figure 2.4 presents the same pressure - time data of Stallman's type curve (Fig. 2.2) in a semilog scale. The curves branching off horizontally from the line source curve represent constant pressure linear boundaries. The curves branching off above the line source curve represent no–flow linear boundaries.

Except for the early time transition part, prior to a dimensionless time of 10, all these curves can be collapsed to a single curve. We

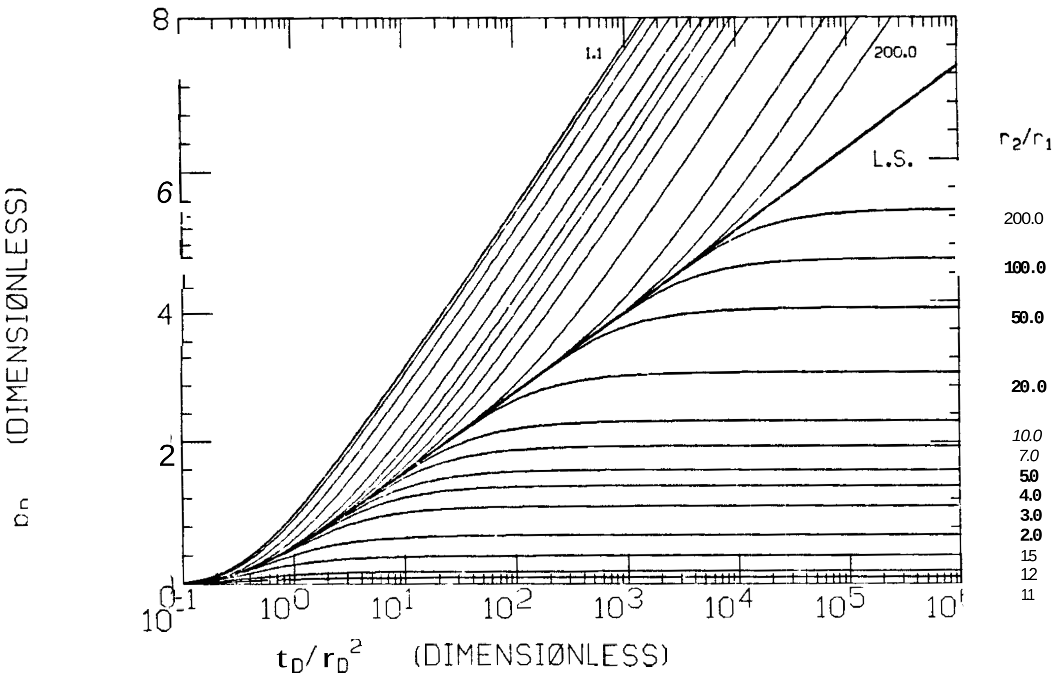

FIGURE 2.4 : A SEMILOG TYPE CURVE FOR THE LINEAR BOUNDARY CASE

have chosen arbitrarily to shift all the curves and match them to the curve where $r_2/r_1 = 100$. The shifting method is discussed in Appendix C. As a result of this shifting of all the curves in Fig. 2.4, we generated a generalized semilog type curve presented in Fig. 2.5. The dimensionless pressure and time are modified based on the derivations presented in Appendix C.

The new semilog type curve can be used for both production and interference wells. An early time infinite acting period is needed in order to use this semilog type curve. The early time log-log match to the line source curve enables us to convert pressures to dimensionless pressures. The following procedure describes the use of the generalized semilog type curve (Fig. 2.5) :

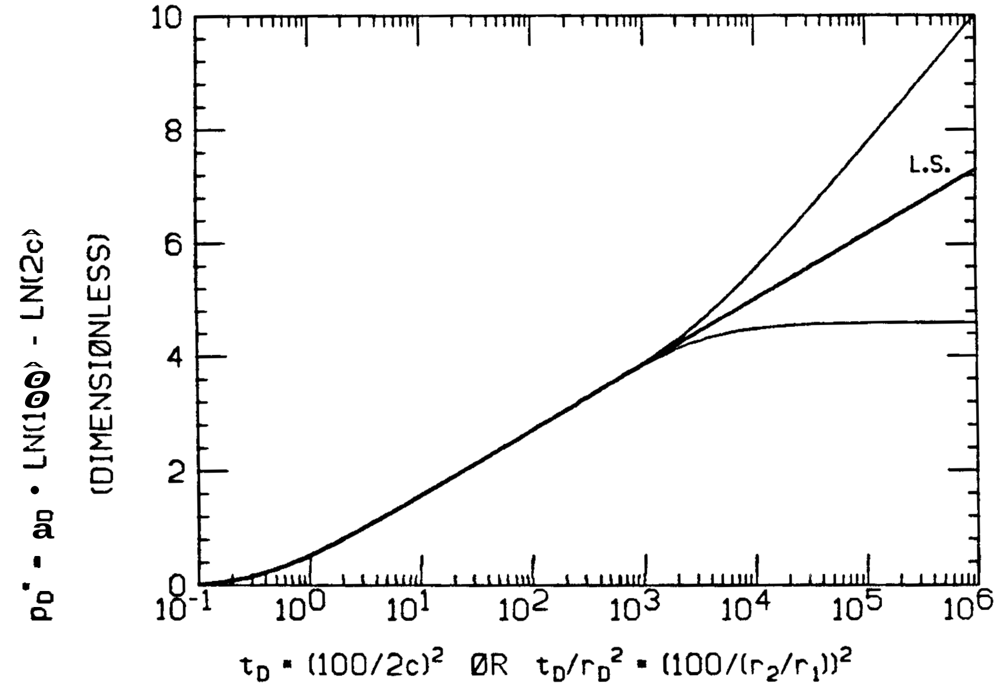

FIGURE 2.5 : A GENERALIZED SEMILOG TYPE CURVE FOR THE LINEAR BOUNDARY CASE

1) Make a log–log graph of the pressure - time response using the same scales as the log–log line source type curve.

2) Match the early time part of the data to the line source curve and pick a match point.

3) Convert all the pressures to a dimensionless form.

4) Make a semilog graph of the dimensionless pressure - time response using the same scale as in the generalized semilog type curve.

5) Match to one of the curves (constant pressure or no-flow boundary) and pick a match point. The transition and the late time data are the most important portion of the match.

6) Using the match point and the modified pressure equation, solve for the ratio r_2/r_1 , which in the case of a production well is approximately twice the distance to the linear boundary.

A type curve matching example is presented in the next section.

There are several advantages in using this semilog type curve matching method in comparison to the double straight line method. The new method can be used under all the conditions when the double straight line method is applicable. The first semilog straight line corresponds to an early time match to the line source curve, hence, pressures can be converted to a dimensionless form. However, there are conditions when the new method can be used and the previous method fails. Such a condition may occur when a test is terminated early, and only the first straight line and the transition between the two lines have developed. Another condition may occur when the first straight line is not defined, but we can still have a log-log match to the line source curve prior to a dimensionless time of 10.

In both these conditions, the new method can be used to determine the distance between a production well and the linear boundary or the distance between an interference well and the image well.

Note that the time axis can remain in real time units since the time scale remains logarithmic.

2.5 TYPE CURVE MATCHING EXAMPLE

In this section, a synthetic drawdown test is analyzed using the new generalized semilog type curve. Table 2.1 presents hypothetical drawdown data given by Witherspoon, et al. (1970). The pressures are for an observation well, 325 feet away from the pumping well.

Figure 2.6 is a log–log graph of the data. Figure 2.7 is a log–log match of the data to the line source log–log type curve. The log–log match yields an approximate value for r_2/r_1 and a conversion factor between p and p_D.

The match point is :

$$p_D = p / 90 \tag{2.19}$$

Next, we convert the pressures to dimensionless pressures using Eq. 2.19 and make a semilog graph of the dimensionless pressure vs. real time (Fig. 2.8). Note that the time axis need not be converted to a dimensionless form. This can simplify the procedure by graphing the semilog data on the same sheet of paper with the log–log graph (see Fig. 2.9).

TABLE 2.1

DRAWDOWN DATA FOR A LINEAR BOUNDARY CASE TEST

Time (min)	Drawdown (feet)	Time (min)	Drawdown (feet)
20	0.15	1000	74.61
30	0.31	1300	a5.33
40	0.56	1600	87.70
50	1.31	1900	101.41
60	1.50	2200	105.36
70	2.51	2500	111.17
80	3.50	3000	119.60
90	4.56	3500	125.01
100	3.33	4000	135.12
150	11.87	5000	148.81
200	17.42	6000	168.34
250	22.40	7000	170.01
300	28.61	8000	176.12
350	33.04	9000	184.40
400	36.31	10000	191.93
500	44.70	15000	222.41
600	52.13	20000	247.33
700	60.46	25000	267.00
800	65.03	30000	282.13
900	68.50	40000	301.24

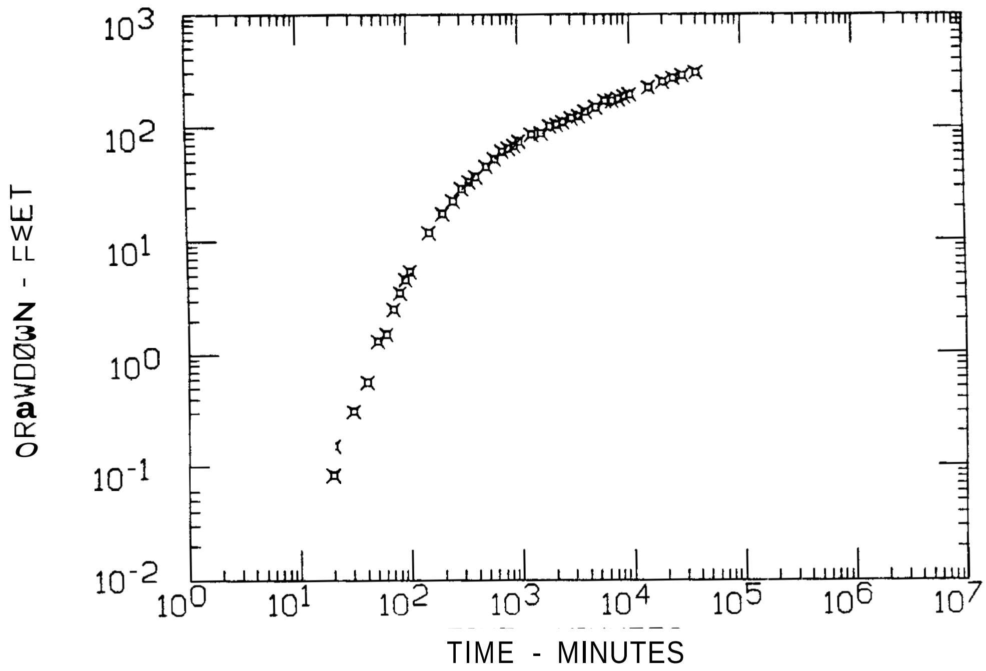

FIGURE **2.6** : **LOG-LOG** GRAPH OF THE DRAWDOWN DATA **FOR** *AN* INTERFERENCE **WELL.** AFTER WITHERSPOON (1970)

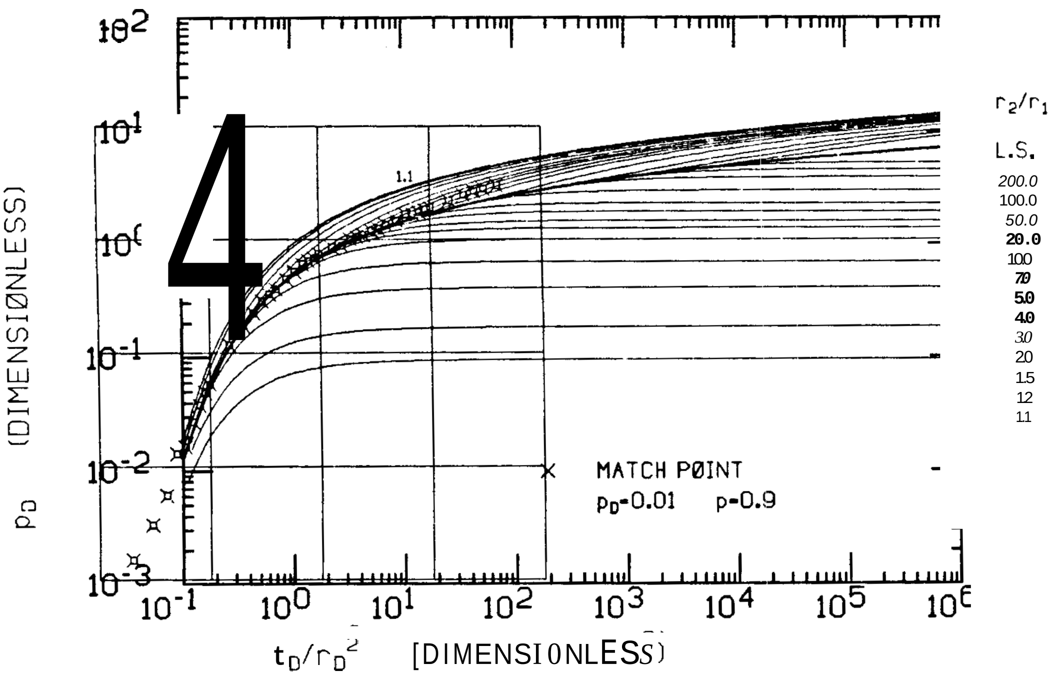

FIGURE **2.7** : LOG-LOG MATCH **FOR** THE DRAWDOWN DATA **FOR** *AN* INTERFERENCE **WELL.** AFTER WITHERSPOON (1970)

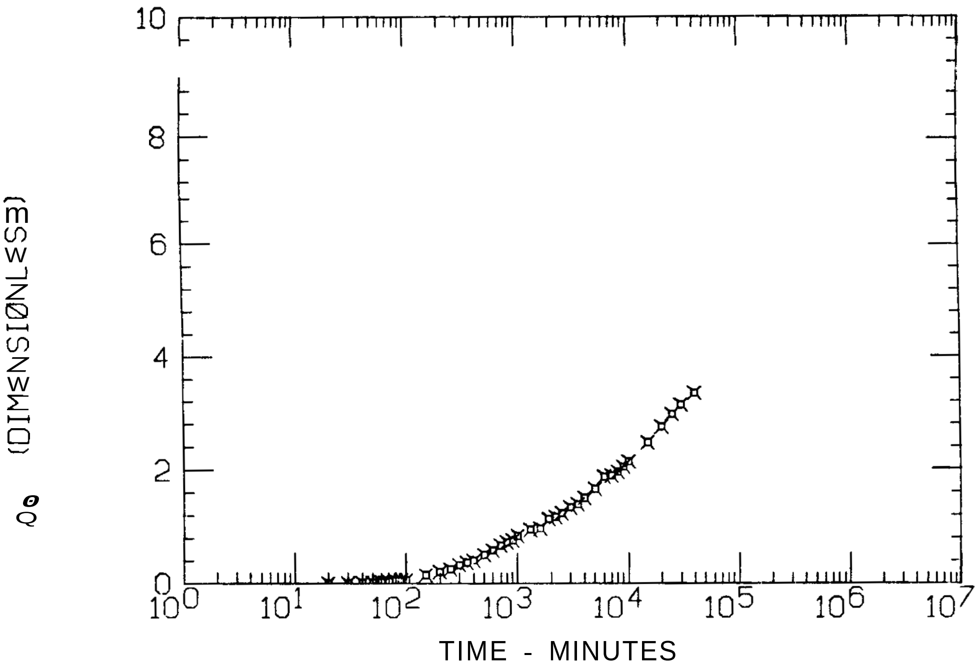

FIGURE 2.8 : SEMILOG GRAPH OF THE DRAWDOWN DATA IN DIMENSIONLESS PRESSURE FORM

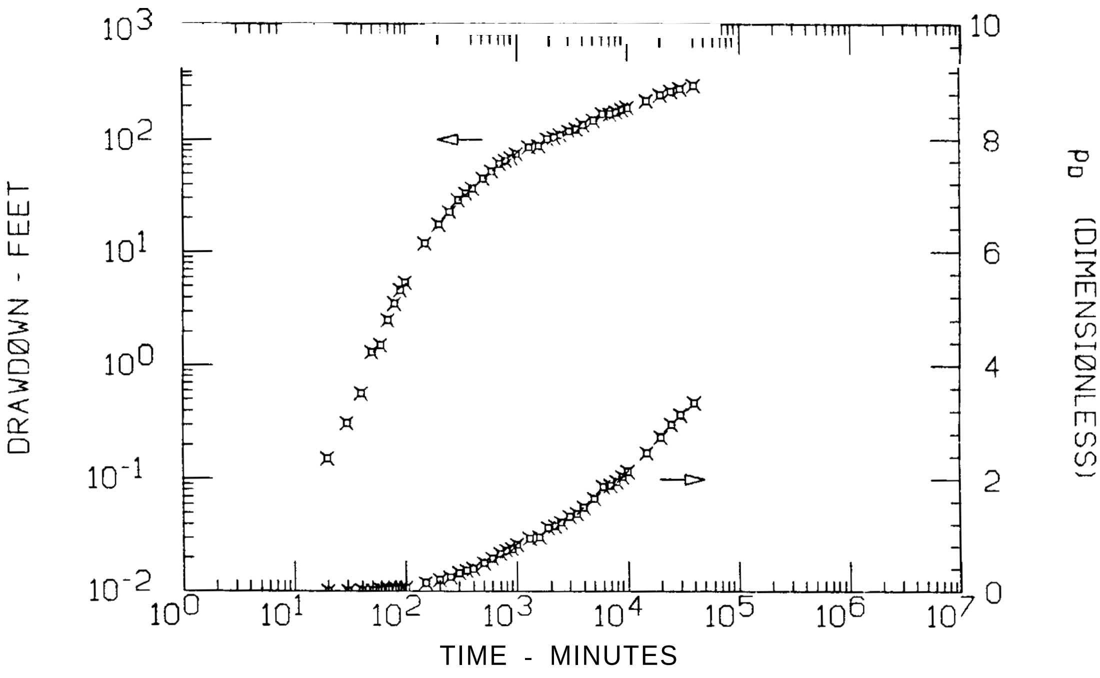

FIGURE 2.9 : LOG-LOG AND SEMILOG GRAPHS FOR THE DRAWDOWN DATA IN DIMENSIONLESS PRESSURE FORM

Finally, the semilog graph of the data is matched to the generalized semilog type curve in Fig. 2.10. This match concentrates on the late time data and on the transition. The early time data, that do not match to the first straight line, correspond to early time line source behavior prior to a dimensionless time of 10. This early time portion of the data can be matched to the lowermost portion of the type curve. This is an example where the first straight line has not fully developed, yet, we have a good log-log match to the line source curve. At the match point :

$$p_D = -1 \qquad p_D^* = 1.6$$

Next, we solve for 2c' in the equivalent system using the modified pressure equation :

$$p_D^* = p_D + \ln(100) - \ln(2c') \tag{2.20}$$

$$2c' = 7.427$$

Since, in this case, the pressure is measured at the production well, $r_{D2} + r_{D1} = r_{D2} + 1 = 2c'$, therefore :

$$\frac{r_2}{r_1} = 6.427$$

hence :

$$r_2 = 6.427 \; r_1 = 2089 \text{ ft}$$

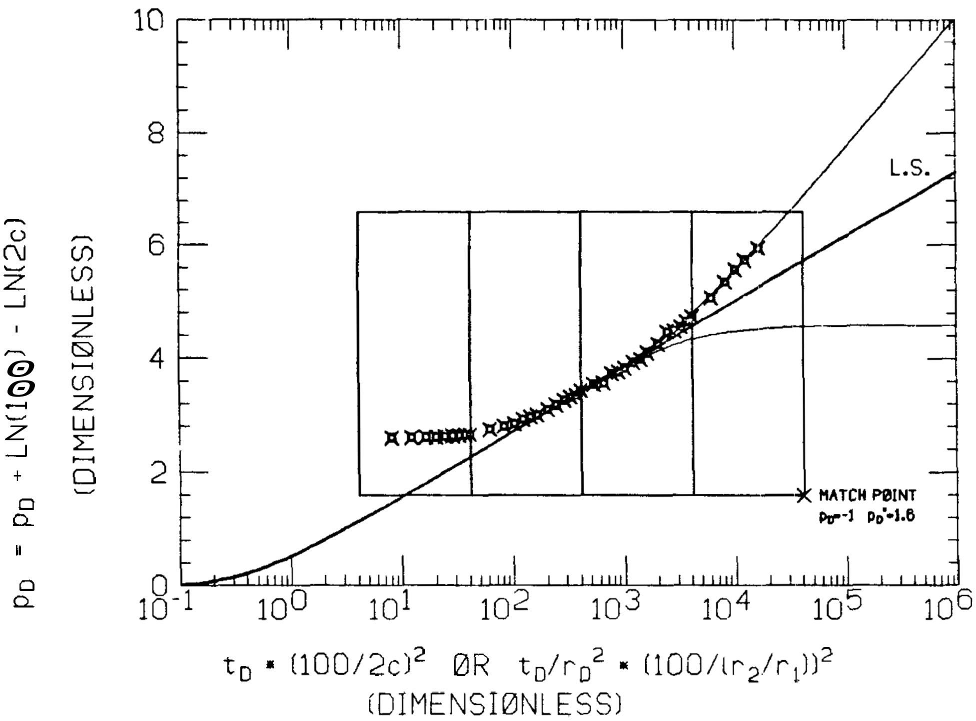

FIGURE 2.10 : SEMILOG MATCH OF THE DRAWDOWN DATA TO THE GENERALIZED TYPE CURVE

Using the double straight line method, Witherspoon, et al. (1970) found r_2 to be 2025 ft.

In summary, two type curves are used in this new method. The log-log type curve of the line source is used to convert the pressure data to a dimensionless form. The new generalized semilog type curve (Fig. 2.5) is used to determine the distance between the pressure point and the image well. If the pressure point is at the production well, this distance is twice the distance between the well and the linear boundary.

The method of shifting the semilog curves and the semilog type curve matching technique are used in establishing the analysis method for internal circular boundaries presented in the next two chapters.

CHAPTER 3 : CONSTANT PRESSURE INTERNAL CIRCULAR BOUNDARY

This chapter presents the transient pressure analysis for a constant flow rate well near a constant pressure circular boundary. The problem is mathematically stated and solved using the Laplace transformation method. Then, the practical applications of the solution are discussed.

3.1 PROBLEM STATEMENT

The problem is two dimensional with one axis of symmetry along the line between the well and the center of the hole (see Fig. 3.1). The constant pressure hole cannot be treated as a line source if it is of finite radius, hence, the pressure at a given point is a function of three parameters: distance r, angle θ and time t.

It is assumed that the system has: an infinite radial extent, constant thickness, constant and isotropic permeability, constant viscosity, porosity and compressibility. It is also assumed that the pressure gradients are small so that the gradient squared terms can be neglected and that the flow is isothermal. The well produces at a constant flow rate.

The pressure $p(r,\theta,t)$ must satisfy the following equation and boundary conditions :

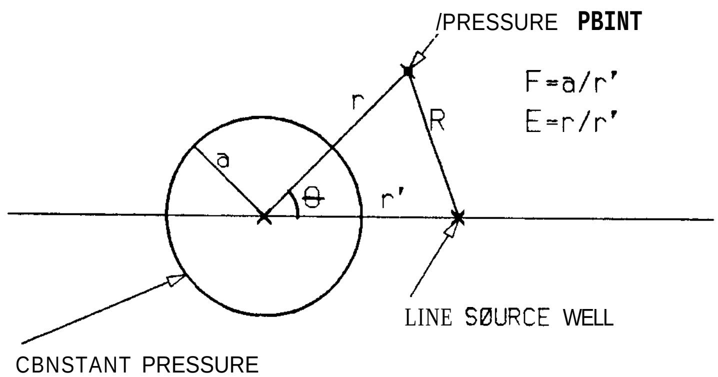

FIGURE 3.1 : A SCHEMATIC DIAGRAM OF THE **CONSTANT PRESSURE** HOLE SYSTEM

$$\frac{\partial^2 p}{\partial r^2} + \frac{1}{r}\frac{\partial p}{\partial r} + \frac{1}{r^2}\frac{\partial^2 p}{\partial \theta^2} = \frac{1}{\eta}\frac{\partial p}{\partial t} \tag{3.1}$$

$$p(\infty,\theta,t) = 0 \qquad \text{or } p_i \tag{3.2}$$

$$p(a,\theta,t) = 0 \qquad \text{or } p_i \tag{3.3}$$

$$\lim_{R\to 0} R\frac{\partial p}{\partial R} = -\frac{q\mu}{2\pi kh} \tag{3.4}$$

$$p(r,\theta,0) = 0 \qquad \text{or } p_i \tag{3.5}$$

where :

$$R^2 = r^2 + r'^2 - 2rr'\cos\theta \tag{3.6}$$

and :

$$\eta = \frac{k}{\phi\mu c_t} \tag{3.7}$$

Equation *3.4* is the condition at the line source well exterior to the constant pressure boundary. The derivation of Eq. *3.4* follows.

The flow around the well is assumed radial :

$$q(R) = -\frac{2\pi Rkh}{\mu}\frac{\partial p}{\partial R}$$

Now, as R tends to 0, q(R) tends to q, so that the rate of production out of the system is maintained constant, hence Eq. *3.4* :

$$\lim_{R\to 0} R\frac{\partial p}{\partial R} = -\frac{q\mu}{2\pi kh}$$

3.2 LAPLACE TRANSFORMATION

We transform Eqs. 3.1 through 3.4 into Laplace space using the initial condition of Eq. 3.5. In general :

$$p(r,\theta,t) \rightarrow \bar{p}(r,\theta,s)$$

$$\frac{\partial^2 \bar{p}}{\partial r^2} + \frac{1}{r}\frac{\partial \bar{p}}{\partial r} + \frac{1}{r^2}\frac{\partial^2 \bar{p}}{\partial \theta^2} - \sqrt{s/\eta}\;\bar{p} = 0 \tag{3.8}$$

$$\bar{p}(\infty,\theta,s) = 0 \tag{3.9}$$

$$\bar{p}(a,\theta,s) = 0 \tag{3.10}$$

$$\lim_{R\rightarrow 0} R\frac{\partial \bar{p}}{\partial R} = \frac{q\mu}{2\pi skh} \tag{3.11}$$

3.3 THE LAPLACE TRANSFORMATION SOLUTION

The solution for the homogeneous boundary conditions, Eqs. 3.8, 3.9 and 3.11, in a coordinate system centered at the well is :

$$\bar{p} = \frac{q\mu}{2\pi skh} K_0(R\sqrt{s/\eta}\,) \tag{3.12}$$

By the addition theorem for Bessel Functions, Carslaw and Jaeger

(1946, p. 377), we translate Eq. 3.12 to a coordinate system centered at the center of the hole :

$$\bar{p} = \frac{q\mu}{2\pi skh} \sum_{n=-0}^{\infty} \cos(n\theta)\ I_n(r\sqrt{s/\eta})K_n(r'\sqrt{s/\eta})$$

$$\text{for } r < r' \tag{3.13}$$

$$\bar{p} = \frac{q\mu}{2\pi skh} \sum_{n=-\infty}^{\infty} \cos(n\theta)\ I_n(r'\sqrt{s/\eta})K_n(r\sqrt{s/\eta})$$

$$\text{for } r > r' \tag{3.14}$$

In order to satisfy the condition of constant: pressure at the internal boundary, we assume that $\bar{p}$ takes the following form :

$$\bar{p} = \frac{q\mu}{2\pi skh} \sum_{n=-\infty}^{\infty} \cos(n\theta)\left[I_n(r\sqrt{s/\eta})K_n(r'\sqrt{s/\eta}) + A_n K_n(r\sqrt{s/\eta}) \right]$$

$$\text{for } r < r' \tag{3.15}$$

$$\bar{p} = \frac{q\mu}{2\pi skh} \sum_{n=-\infty}^{\infty} \cos(n\theta)\left[I_n(r'\sqrt{s/\eta})K_n(r\sqrt{s/\eta}) + A_n K_n(r\sqrt{s/\eta}) \right]$$

$$\text{for } r > r' \tag{3.16}$$

where the constants A_n are to be set by the boundary condition. The particular solution, K_n, is picked in order to satisfy the condition at infinite radii. A similar method for constructing the solution to the problem of an eccentric well within a circular subregion was presented by Carslaw and Jaeger (1946).

Equations 3.15 and 3.16 can be written as :

$$\bar{p} = \frac{q\mu}{2\pi skh} \sum_{n=0}^{\infty} \varepsilon_n \cos(n\theta) \left[I_n(r\sqrt{s/\eta}\,) K_n(r'\sqrt{s/\eta}\,) + A_n K_n(r\sqrt{s/\eta}\,) \right]$$

$$\text{for } r < r' \tag{3.17}$$

$$\bar{p} = \frac{q\mu}{2\pi skh} \sum_{n=0}^{\infty} \varepsilon_n \cos(n\theta) \left[I_n(r'\sqrt{s/\eta}\,) K_n(r\sqrt{s/\eta}\,) + A_n K_n(r\sqrt{s/\eta}\,) \right]$$

$$\text{for } r > r' \tag{3.18}$$

where :

for $n = 0$, $\varepsilon_n = 1$

for $n > 0$, $\varepsilon_n - 2$

The internal boundary condition determines the coeficients A_n :

$$A_n = - \frac{I_n(a\sqrt{s/\eta}\,) K_n(r'\sqrt{s/\eta}\,)}{K_n(a\sqrt{s/\eta}\,)} \tag{3.19}$$

Substituting Eq. 3.19 into Eqs. 3.17 and 3.18 yields :

$$\bar{p} = \frac{q\mu}{2\pi skh} \sum_{n=0}^{\infty} \varepsilon_n \cos(n\theta) \Big[I_n(r\sqrt{s/\eta})K_n(r'\sqrt{s/\eta})$$

$$- \frac{I_n(a\sqrt{s/\eta})K_n(r'\sqrt{s/\eta})}{K_n(a\sqrt{s/\eta})} K_n(r\sqrt{s/\eta}) \Big]$$

$$\text{for } r < r' \tag{3.20}$$

$$\bar{p} = \frac{q\mu}{2\pi skh} \sum_{n=0}^{\infty} \varepsilon_n \cos(n\theta) \Big[I_n(r'\sqrt{s/\eta})K_n(r\sqrt{s/\eta})$$

$$- \frac{I_n(a\sqrt{s/\eta})K_n(r'\sqrt{s/\eta})}{K_n(a\sqrt{s/\eta})} K_n(r\sqrt{s/\eta}) \Big]$$

$$\text{for } r > r' \tag{3.21}$$

Next, we make the problem dimensionless using the standard definitions :

$$p_D = \frac{2\pi kh(p_i - p)}{qB\mu} \tag{3.22}$$

$$t_D = \frac{kt}{\phi\mu c_t r_w^2} \tag{3.23}$$

$$r_D = \frac{r}{r_w} \tag{3.24}$$

$$r'_D = \frac{r'}{r_w} \tag{3.25}$$

$$a_D = \frac{a}{r_w} \tag{3.26}$$

$$R_D = \frac{R}{r_w} \tag{3.27}$$

Substituting Eqs. 3.22 through 3.27 into Eqs. 3.20 and 3.21 yields :

$$\bar{p}_D = \frac{1}{s} \sum_{n=0}^{\infty} \varepsilon_n \cos(n\theta) \Big[I_n(r_D\sqrt{s})K_n(r'_D\sqrt{s}) - \frac{I_n(a_D\sqrt{s})K_n(r'_D\sqrt{s})}{K_n(a_D\sqrt{s})} K_n(r_D\sqrt{s}) \Big]$$

$$\text{for} \quad r_D < r'_D \tag{3.28}$$

$$\bar{p}_D = \frac{1}{s} \sum_{n=0}^{\infty} \varepsilon_n \cos(n\theta) \Big[I_n(r'_D\sqrt{s})K_n(r_D\sqrt{s}) - \frac{I_n(a_D\sqrt{s})K_n(r'_D\sqrt{s})}{K_n(a_D\sqrt{s})} K_n(r_D\sqrt{s}) \Big]$$

$$\text{for} \quad r_D > r'_D \tag{3.29}$$

Note that Eq. 3.29 is Eq. 3.28 with r_D and r'_D interchanged. The Laplace solution was inverted numerically using an algorithm developed by Stehfest (1970). A description of the algorithm is presented in Section 3.5.

3.4 THE ANALYTICAL SOLUTION

The following presents the analytical inversion of the Laplace solution into the real time solution using the method of residues.

The Laplace solution of Eq. 3.28 can be written as :

$$\bar{p}_D = \frac{1}{s} \sum_{n=0}^{\infty} \varepsilon_n \cos(n\theta) \frac{1}{K_n(a_D\sqrt{s})} \left[I_n(r_D\sqrt{s})K_n(r'_D\sqrt{s})K_n(a_D\sqrt{s}) \right.$$

$$\left. - K_n(r_D\sqrt{s})I_n(a_D\sqrt{s})K_n(r'_D\sqrt{s}) \right]$$

$$\text{for} \quad r_D < r'_D \tag{3.30}$$

At $s=0$ we have a single pole, hence, we can use the small argument approximations for the Modified Bessel Functions :

$$K_0(z) = -(\ln \frac{z}{2} + \gamma) \tag{3.31}$$

$$K_n(z) = 2^{n-1}(n-1)!\ z^{-n} \tag{3.32}$$

$$I_0(z) = 1 \qquad (3.33)$$

$$I_n(z) = 2^{-n}z^n/n! \qquad (3.34)$$

As s tends to 0, t tends to ∞ and the residue at $s=0$ is the steady state pressure drop, p_{Dss}. Substituting Eqs. *3.31* through *3.34* into Eq. *3.30* yields :

$$\bar{p}_{D1} = \frac{1}{s} \ln \frac{r_D}{a_D} + \sum_{n=1}^{\infty} \frac{\cos(n\theta)}{n} \left[\left(\frac{r_D}{r'_D}\right)^n - \left(\frac{a_D^2}{r_D r'_D}\right)^n \right\} \qquad (3.35)$$

Using the following relation :

$$\sum_{k=1}^{\infty} \frac{1}{k} p^k \cos(k\theta) = \frac{1}{2} \ln(1-2p\cos\theta + p^2) \qquad (3.36)$$

and the Laplace inversion formula :

$$\frac{1}{s}(b) \rightarrow b \qquad (3.37)$$

Equation *3.35* inverts into the following :

$$p_{Dss} = \ln\left(\frac{r_D}{a_D}\right) + \frac{1}{2}\ln \frac{1 - 2\dfrac{a_D^2}{r_D r'_D}\cos\theta + \left(\dfrac{a_D^2}{r_D r'_D}\right)^2}{1 - 2\dfrac{r_D}{r'_D}\cos\theta + \left(\dfrac{r_D}{r'_D}\right)^2}$$

$$\text{for } r_D < r'_D \tag{3.38}$$

This steady state solution can also be derived using superposition of line sources, with an identical result. This derivation is presented in Appendix D.

For $r_D > r'_D$ we interchange r_D and r'_D in Eq. **3.38** :

$$p_{Dss} = \ln\left(\frac{r'_D}{a_D}\right) + \frac{1}{2}\ln \frac{1 - 2\dfrac{a_D^2}{r_D r'_D}\cos\theta + \left(\dfrac{a_D^2}{r_D r'_D}\right)^2}{1 - 2\dfrac{r'_D}{r_D}\cos\theta + \left(\dfrac{r'_D}{r_D}\right)^2}$$

$$\text{for } r_D > r'_D \tag{3.39}$$

Factoring the term $(r'_D/r_D)^2$ out of the denominator of the last term in Eq. **3.39**, and joining it to the first term, Eq. **3.39** becomes identical to Eq. **3.38.** This is expected from the reciprocity principle.

When $s \neq 0$ we use the residues at the roots of $K_n(a_D\sqrt{s})$. Let $\xi_{n/m}$ denote the m^{th} zero of $K_n(a_D\sqrt{s}) = K_n(\xi a_D)$. $K_n(z)$ has n zeroes in the second and third quadrants, Macdonald **(1898)**, Watson **(1948)** and Abramowitz **(1964).** Using the method of residues we evaluate the inversion of p_{D2} :

$$RES(\xi_{n/m}) = \lim_{s \to \xi^2_{n/m}} \sum_{n=0}^{\infty} \varepsilon_n \cos(n\theta) \frac{(s - \xi^2_{n/m}) e^{st_D} K_n(r'_D \sqrt{s})}{sK_n(a_D \sqrt{s})}$$

$$\cdot \left[I_n(r_D \sqrt{s}) K_n(a_D \sqrt{s}) - K_n(r_D \sqrt{s}) I_n(a_D \sqrt{s}) \right\} \qquad (3.40)$$

Rearranging Eq. *3.40* :

$$RES(\xi^2_{n/m}) = \sum_{n=0}^{\infty} \varepsilon_n \cos(n\theta) B_n \frac{e^{\xi^2_{n/m} t_D} K_n(r'_D \sqrt{s})}{\xi^2_{n/m}} \qquad (3.41)$$

where :

$$B_n = \lim_{s \to \xi^2_{n/m}} \frac{(s - \xi^2_{n/m})}{K_n(a_D \sqrt{s})}$$

$$\cdot \left[I_n(r_D \sqrt{s}) K_n(a_D \sqrt{s}) - K_n(r_D \sqrt{s}) I_n(a_D \sqrt{s}) \right] \qquad (3.42)$$

Using L'Hôpital's rule, we evaluate B_n :

$$B_n = - \frac{2\xi_{n/m} K_n(\xi_{n/m} r_D) I_n(\xi_{n/m} a_D)}{a_D K'_n(\xi_{n/m} a_D)} \qquad (3.43)$$

From Abramowitz *(1964, p.361)* :

$$K_n'(z) = \frac{n}{z} K_n(z) - K_{n+1}(z) \tag{3.44}$$

Using Eq. *3.44* and the fact that $K_n(\xi_{n/m} a_D) = 0$, we find that :

$$B_n = \frac{2\xi_{n/m} K_n(\xi_{n/m} r_D) I_n(\xi_{n/m} a_D)}{a_D K_{n+1}(\xi_{n/m} a_D)} \tag{3.45}$$

Substituting Eq. *3.45* into Eq. *3.41* yields :

$$\mathrm{RES}(\xi^2_{n/m}) = \sum_{n=0}^{\infty} \varepsilon_n \cos(n\theta) \frac{e^{\xi^2_{n/m} t_D} K_n(\xi_{n/m} r_D')}{a_D \xi^2_{n/m}}$$

$$\cdot \frac{2\xi_{n/m} K_n(\xi_{n/m} r_D) I_n(\xi_{n/m} a_D)}{K_{n+1}(\xi_{n/m} a_D)} \tag{3.46}$$

Now, in order to complete the inversion of $\bar{p}_{D2}$, we use the residues from Eq. *3.46* :

$$p_{D2} = 2 \sum_{n=0}^{\infty} \sum_{m=0}^{n} \varepsilon_n \cos(n\theta)\, e^{\xi^2_{n/m} t_D}$$

$$\cdot \frac{K_n(\xi_{n/m} r_D') K_n(\xi_{n/m} r_D) I_n(\xi_{n/m} a_D)}{a_D \xi_{n/m} K_{n+1}(\xi_{n/m} a_D)} \tag{3.47}$$

We can express p_{D2} in terms of Bessel Functions instead of Modified Bessel Functions. We use the following relations :

$$I_n(z) = i^{-n} J_n(iz) \tag{3.48}$$

$$K_n(z) = \frac{\pi}{2}\, i^{n+1}\left[\, J_n(iz) + iY_n(iz)\,\right] = \frac{\pi}{2}\, i^{n+1} H_n^{(1)}(iz) \tag{3.49}$$

The second and third quadrants for $K_n(z)$ correspond to the third and fourth quadrants for $H_n^{(1)}(z)$ since the argument of the Hankel Function is rotated by $\pi/2$.

Substituting Eqs. *3.48* and *3.49* into Eq. *3.30* yields :

$$\bar{p}_{D2} = \frac{\pi i}{2s} \sum_{n=0}^{\infty} \varepsilon_n \cos(n\theta) \frac{H_n^{(1)}(ir_D'\sqrt{s}\,)}{H_n^{(1)}(ia_D\sqrt{s}\,)} \left[\, J_n(ir_D\sqrt{s}\,) H_n^{(1)}(ia_D\sqrt{s}\,) - J_n(ia_D\sqrt{s}\,) H_n^{(1)}(ir_D\sqrt{s}\,)\,\right] \tag{3.50}$$

$H_n^{(1)}(ia_D\sqrt{s}\,)$ has zeroes at $ia_D\sqrt{s} = \mu_1\ ,\ \mu_2\ ,\ \ldots\mu_m$ and $\bar{p}_{D2}$ has simple poles at :

$$s = -\left(\frac{\mu_m}{a_D}\right)^2 = -\alpha_m^{\ 2} \tag{3.51}$$

or :

$$\alpha_m = \left(\frac{\mu_m}{a_D}\right) = i\sqrt{s} \tag{3.52}$$

$\alpha_{n/m}$ denotes the m^{th} zero of $H_n^{(1)}(ia_D\sqrt{s}\,) = H_n^{(1)}(\alpha a_D)$.
Using the method of residues we evaluate the inversion of $\bar{p}_{D2}$:

$$\text{RES}(-\alpha^2_{n/m}) = \frac{\pi}{2} \lim_{s\to-\alpha^2_{n/m}} \sum_{n=0}^{\infty} \varepsilon_n \cos(n\theta)$$

$$\cdot \frac{i(s+\alpha_{n/m}^2)\; e^{st_D}\; H_n^{(1)}(ir_D'\sqrt{s}\,)}{sH_n^{(1)}(ia_D\sqrt{s}\,)}$$

$$\cdot \left[J_n(ir_D\sqrt{s}\,)H_n^{(1)}(ia_D\sqrt{s}\,) - J_n(ia_D\sqrt{s}\,)H_n^{(1)}(ir_D\sqrt{s}\,) \right] \tag{3.53}$$

Rearranging Eq. 3.53 :

$$\text{RES}(-\alpha^2_{n/m}) = \frac{\pi}{2} \sum_{n=0}^{\infty} \varepsilon_n \cos(n\theta)\; A_n \frac{e^{-\alpha^2_{n/m} t_D}}{-a^2_{n/m}} H_n^{(1)}(\alpha_{n/m} r_D') \tag{3.54}$$

where :

$$A_n = \lim_{s\to-\alpha^2_{n/m}} \frac{i(s + a^2_{n/m})}{H_n^{(1)}(ia_D\sqrt{s}\,)}$$

$$\cdot \left[J_n(ir_D\sqrt{s}\,)H_n^{(1)}(ia_D\sqrt{s}\,) - J_n(ia_D\sqrt{s}\,)H_n^{(1)}(ir_D\sqrt{s}\,) \right] \tag{3.55}$$

Using L'Hôpital's rule, we evaluate A_n :

$$A_n = \lim_{s\to-\alpha^2_{n/m}} \frac{i}{H_n'^{(1)}(ia_D\sqrt{s})\left(\frac{ia_D}{2\sqrt{s}}\right)}$$

$$\cdot \left\{ \left[J_n(ir_D\sqrt{s})H_n^{(1)}(ia_D\sqrt{s}) - J_n(ia_D\sqrt{s})H_n^{(1)}(ir_D\sqrt{s}) \right] \right.$$

$$+ (s + \alpha^2_{n/m}) \frac{d}{ds} \left[J_n(ir_D\sqrt{s})H_n^{(1)}(ia_D\sqrt{s}) \right.$$

$$\left. \left. - J_n(ia_D\sqrt{s})H_n^{(1)}(ir_D\sqrt{s}) \right] \right\} =$$

$$= \lim_{s\to-\alpha^2_{n/m}} - \frac{J_n(ia_D\sqrt{s})H_n^{(1)}(ir_D\sqrt{s})}{\frac{a_D}{2\sqrt{s}} H_n^{(1)}(ia_D\sqrt{s})}$$

Substituting $s = -\alpha^2_{n/m}$ yields :

$$A_n = - \frac{2\sqrt{s}\, J_n(\alpha_{n/m}a_D)H_n^{(1)}(\alpha_{n/m}r_D)}{a_D\, H_n'^{(1)}(\alpha_{n/m}a_D)} \tag{3.56}$$

From Abramowitz (1964, p. 361) :

$$H_n^{'(1)}(z) = - H_{n+1}^{(1)}(z) + \frac{n}{z} H_n^{(1)}(z) \tag{3.57}$$

Using Eq. 3.57 and the fact that $H_n^{(1)}(\alpha_{n/m} a_D) = 0$, we find that :

$$A_n = \frac{2\alpha n/m \, J_n(\alpha_{n/m} a_D) \, H_n^{(1)}(\alpha_{n/m} r_D)}{a_D \, H_{n+1}^{(1)}(\alpha_{n/m} a_D)} \tag{3.58}$$

Substituting Eq. 3.58 into Eq. 3.54 yields :

$$\text{RES}\ (-a_{n/m}^2) = \frac{\pi}{2} \sum_{n=0}^{\infty} \varepsilon_n \cos(n\theta) \frac{e^{-a_{n/m}^2 t_D} H_n^{(1)}(\alpha_{n/m} r_D')}{-a_{n/m}^2}$$

$$\cdot \frac{2\alpha n/m \, J_n(\alpha_{n/m} a_D) \, H_n^{(1)}(\alpha_{n/m} r_D)}{a_D \, H_{n+1}^{(1)}(\alpha_{n/m} a_D)} \tag{3.59}$$

Now, in order to complete the inversion of $\bar{p}_{D2}$, we use the residues from Eq. 3.59 :

$$p_{D2} = - \pi \sum_{n=0}^{\infty} \sum_{m=0}^{n} \varepsilon_n \cos(n\theta) \, e^{-a_{n/m}^2 tD}$$

$$\cdot \frac{H_n^{(1)}(\alpha_{n/m} r_D') H_n^{(1)}(\alpha_{n/m} r_D) J_n(\alpha_{n/m} a_D)}{a_D \alpha_{n/m} \, H_{n+1}^{(1)}(\alpha_{n/m} a_D)} \tag{3.60}$$

Finally, the complete real time solution is $p_D = p_{D1} + p_{D2}$. In terms of Modified Bessel Functions, the solution is :

$$p_D = \ln\left(\frac{r_D}{a_D}\right) + \frac{1}{2}\ln \frac{1 - 2\dfrac{a_D^2}{r_D r_D'}\cos\theta + \left(\dfrac{a_D^2}{r_D r_D'}\right)^2}{1 - 2\dfrac{r_D}{r_D'}\cos\theta + \left(\dfrac{r_D}{r_D'}\right)^2}$$

$$+ \sum_{n=0}^{\infty} \sum_{m=0}^{n} \varepsilon_n \cos(n\theta)\, e^{-\xi_{n/m}^2 t_D}$$

$$\cdot \frac{K_n(\xi_{n/m} r_D')\,K_n(\xi_{n/m} r_D)\,I_n(\xi_{n/m} a_D)}{a_D\, \xi_{n/m}\, K_{n+1}(\xi_{n/m} a_D)}$$

$$\text{for} \quad r_D < r_D' \tag{3.61}$$

In terms of Bessel Functions the solution is :

$$p_D = \ln\left(\frac{r_D}{a_D}\right) + \frac{1}{2}\ln \frac{1 - 2\frac{a_D^2}{r_D r'_D}\cos\theta + \left(\frac{a_D^2}{r_D r'_D}\right)^2}{1 - 2\frac{r_D}{r'_D}\cos\theta + \left(\frac{r_D}{r'_D}\right)^2}$$

$$- \pi \sum_{n=0}^{\infty} \sum_{m=0}^{n} \varepsilon_n \cos(n\theta) \; e^{-\alpha_{n/m}^2 t_D}$$

$$\cdot \frac{H_n^{(1)}(\alpha_{n/m} r'_D) H_n^{(1)}(\alpha_{n/m} r_D) J_n(\alpha_{n/m} a_D)}{a_D \, a_{n/m} \, H_{n+1}^{(1)}(\alpha_{n/m} a_D)}$$

$$\text{for} \quad r_D < r'_D \qquad (3.62)$$

For $r_D > r'_D$, we interchange r_D and r'_D in Eqs. ,61 and ,62.

The transient part of the real time solution was not used in the numerical evaluations due to complexities of computaion. However, the general behavior of the pressure response can be deduced from the real time solution. The steady state part of the solution is a limiting value for the numerically evaluated pressures at late time.

3.5 NUMERICAL INVERSION OF THE LAPLACE TRANSFORM

Due to the complexity of the numerical evaluation of Eq. 3.62, we use the Laplace form of the solution, Eqs. 3.28 and 3.29 and invert the transform numerically. The numerical Laplace transform inverter was presented by Stehfest in 1970.

If $\bar{p}(s)$ is the Laplace transform of $p(t)$, then, the equations used in the algorithm are :

$$p(t) = \frac{\ln 2}{t} \sum_{i=1}^{N} V_i \, \bar{p}\left(\frac{\ln 2}{t} i\right) \tag{3.63}$$

where :

$$V_i = (-1)^{\left(\frac{N}{2}+1\right)} \sum_{k=1}^{\min\left(i, \frac{N}{2}\right)} \frac{k^{\frac{N}{2}} (2k)!}{\left(\frac{N}{2} - k\right)! \, k! \, (k-1)! \, (i-k)! \, (2k-i)!} \tag{3.64}$$

N is the number of sampling points where $\bar{p}(s)$ is evaluated for each inversion. Some of the limitations of the Stehfest algorithm are described by Stehfest (1970) and Shinohara (1980). The pressure function should be continuous, moderately varying and not rapidly oscillating. The number of sampling points, N, vas taken as 8. For the 64 bit arithmetic that was used, a value of N=16 is the best in terms of accuracy for the type of function presented here. With N=16 it is possible to produce an accuracy of 6 to 7 digits in most ranges. The program was tested at various N's. With N=8 the accuracy is within 4 to

5 digits which is sufficient for practical purposes and requires significantly less computer time than with N=16.

The Laplace solutions are given by Eqs. 3.28 and 3.29. In the numerical inversion, only Eq. 3.28 was used. Although Eq. 3.28 is written for $r_D < r'_D$, it can be used for $r_D > r'_D$ making use of the reciprocity principle. The pressure drop at r_D due to the well at r'_D is the same as the pressure drop at r'_D due to a well at r_D.

The computer program for the Stehfest algorithm is presented in Appendix G.

3.6 TYPE CURVE MATCHING FOR THE PRODUCTION WELL

In this section we show how to type curve match for the size of the hole and the distance to it, using the production well pressure data.

3.6.1 GENERAL DISCUSSION

The pressure point representing the production well is one dimensionless radius away from the line source, at angle zero and in the direction of the hole. The pressure - time behavior depends on two factors:

a. The ratio F, which is the ratio of the diameter of the hole to the distance between the center of the hole and the line

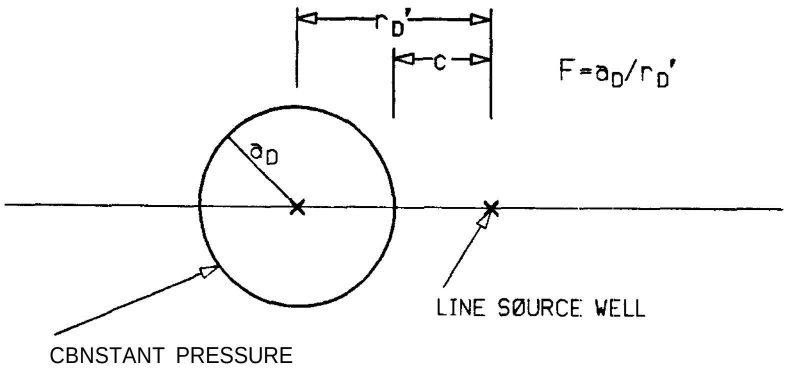

FIGURE 3.2 : THE GEOMETRY FOR TYPE CURVE MATCHING.
CONSTANT PRESSURE HOLE

source (see Fig. 3.2).

b. The actual size of the system, c (see .Fig. 3.2).

Figures 3.3 and 3.4 present the pressure - time behavior for a constant c=50 and various ratios of F, from 0.1 to 0.9. Figure 3.3 is in log-log scale and Fig. 3.4 is in semilog scale. Every curve starts off on the line source solution then undergoes a transition to approach a steady state value. The steady state values of p_D can be calculated directly using Eq. 3.38 with an angle of zero.

At long time, the system will approach a steady state condition which can be represented simply by a doublet model. This is because at steady state all the equipotential lines are circles (see Appendix A). We can find the location of the image well at steady state (see Fig. 3.5). Using the radius of the constant pressure circle of Eq. 2.13, and denoting the distance between the well and the image as 2c', we find :

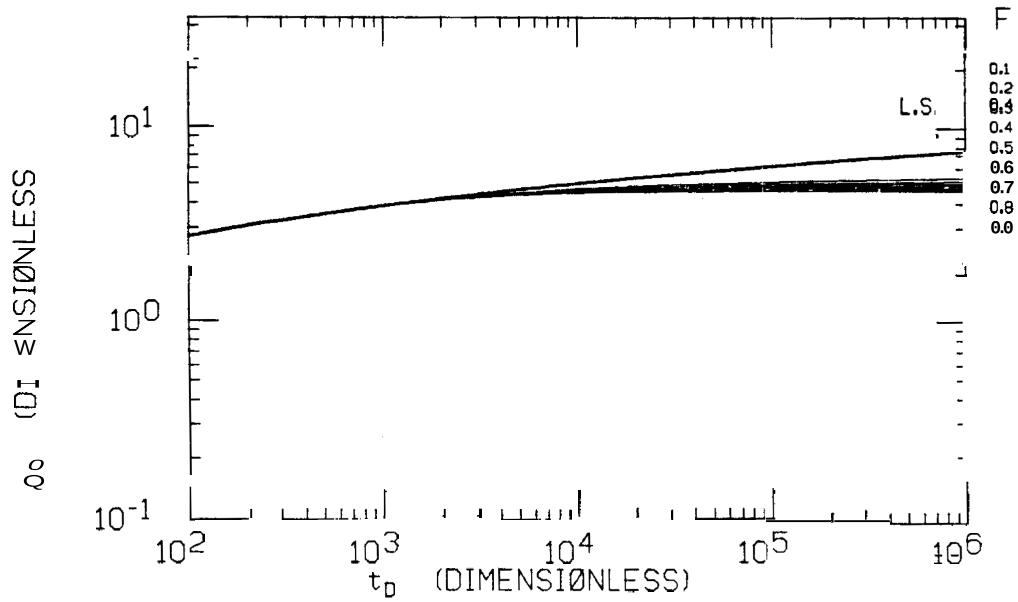

FIGURE 3.3 : LOG-LOG CURVES FOR 2c=100 AND F FROM 0.1 TO 0.9.

CONSTANT PRESSURE HOLE

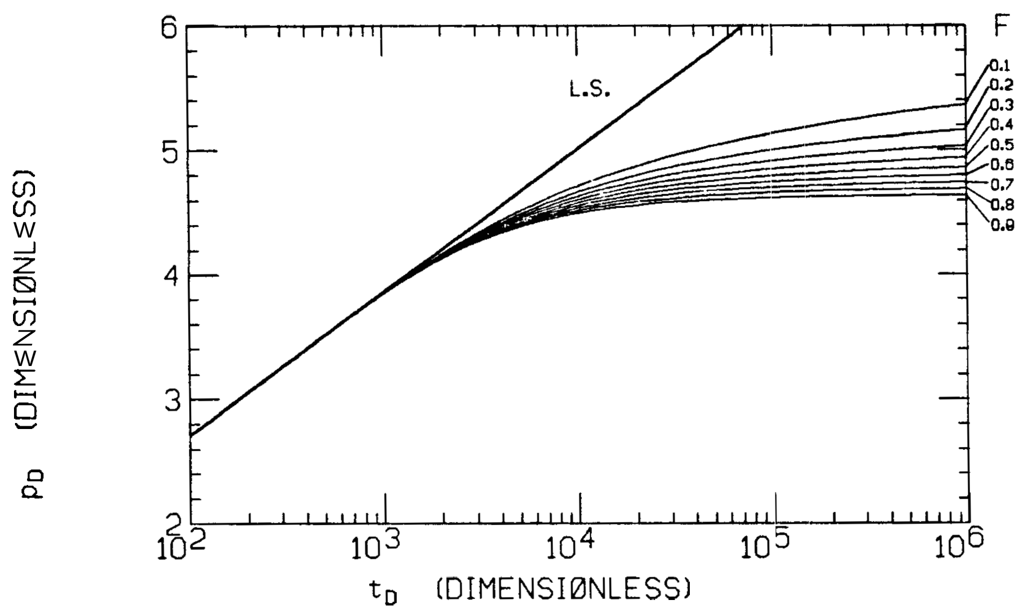

FIGURE 3.4 : SEMILOG CURVES FOR 2c=100 AND F FROM 0.1 TO 0.9.

CONSTANT PRESSURE HOLE

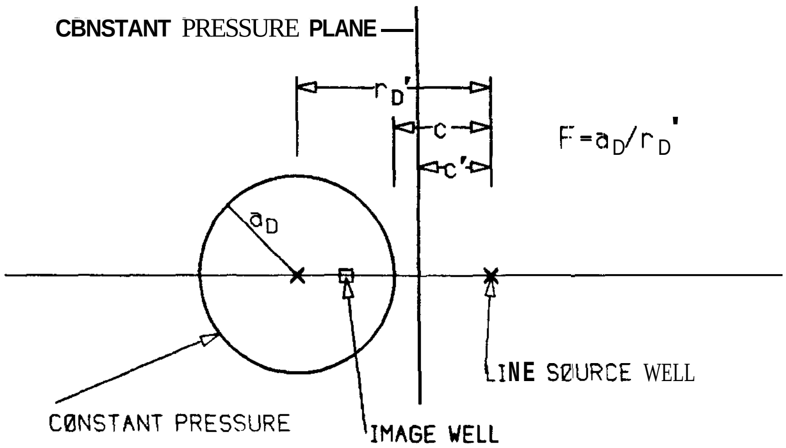

FIGURE 3.5 : THE DOUBLET MODEL FOR THE CONSTANT PRESSURE HOLE AT STEADY STATE

$$a_D = 2c' \frac{\sqrt{H}}{1-H} \tag{3.65}$$

where :

$$\sqrt{H} = \frac{r_{D2}}{r_{D1}} = \frac{2c' - r_D' + a_D}{r_D' - a_D} \tag{3.66}$$

Substituting Eq. 3.66 into 3.65 and simplifying :

$$c' = \frac{r_D'^2 - a_D^2}{2r_D'} \tag{3.67}$$

As the normalized radius of the hole, F, approaches 1, the system response approaches that of a well near a constant pressure linear boundary. This can be seen in Fig. 3.6. This figure is a combination of Fig. 3.4 for the constant pressure hole and Fig. 2.4 tor the constant pressure linear boundary. The fine curves above the curve for 2c=100 are for the constant pressure hole. The curve for F=0.9 is closer to the linear boundary curve, and the curve for F=0.1 is the uppermost one. As F approaches 1, the transient responses become similar to that of the constant pressure linear boundary response as do the long time steady state values. This is discussed in Appendix C.

As F approaches zero, the system becomes a set of two line sources. One source produces at a constant rate, and the other source maintains a constant pressure. Although the long time pressure drop is twice that of the source - sink model, the transient pressure drop is not. This is discussed in Section 3.8.

Another set of curves for the constant pressure hole is presented in Fig. 3.6. These curves are for 2c=250 and F varying from 0.1 to 0.9. The set of curves for 2c=100 (see Fig. 3.6) can be shifted and matched to the set of curves for 2c=250. This shifting and the numerical fit are discussed in Appendix C.

Figure 3.7 presents the pressure points and the curves for two cases:

a) 2c=500 , F=0.5

b) 2c=100 , F=0.5 shifted to fit case a.

The fit is closer than ±1% for $t_D<100$. Mathematically, the two curves are not identical since E, the relative distance to the pressure point, is not the same for both cases. For the curve where 2c=500 E=499/500 and for the curve where 2c=100 E=99/100. Yet, the curves are similar due to the fact that E is close to 1.

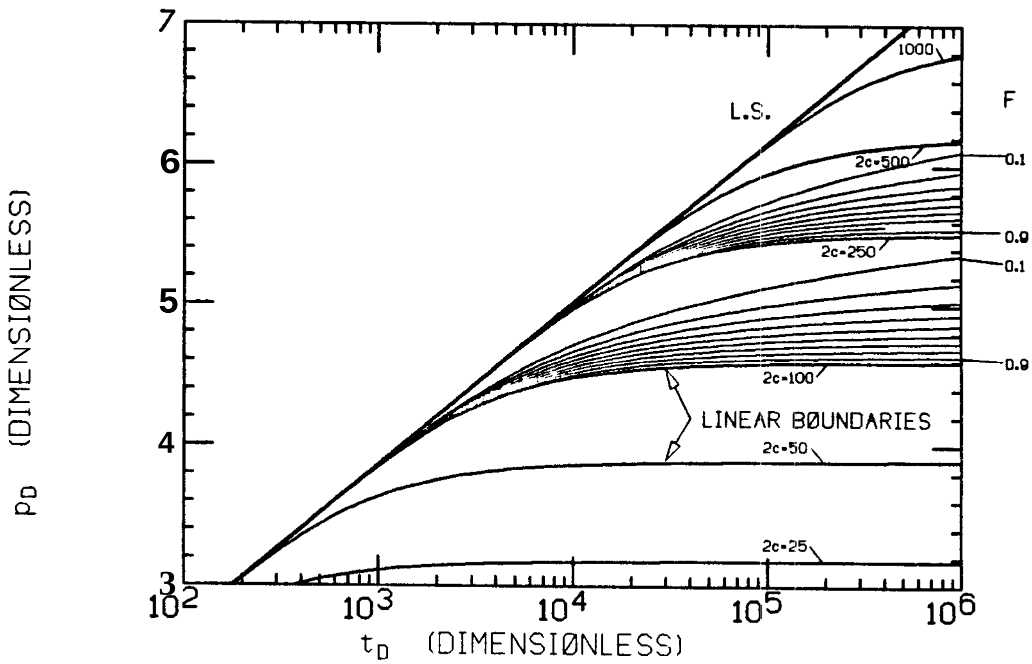

FIGURE 3.6 : SEMILOG CURVES **FOR 2c=100,250** AND **F=0.1 TO 0.9.**

CONSTANT PRESSURE LINEAR BOUNDARY AND HOLE

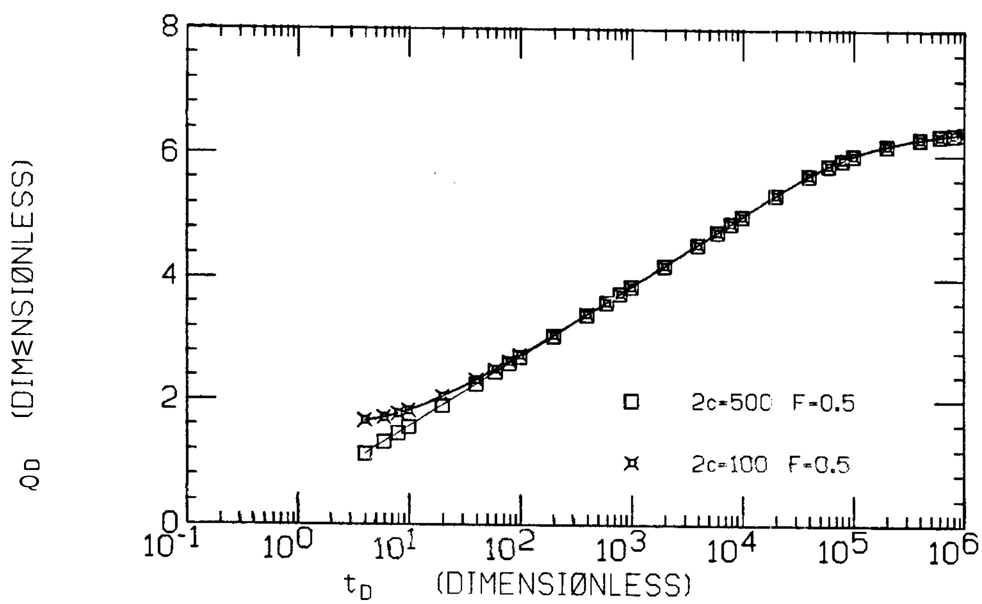

FIGURE **3.7** : SEMILOG **CURVE FOR 2c=500 W0.5 MATCHED** WITH **A SHIFTED**

CURVE **FOR** 2c=100 F=0.5. **CONSTANT** PRESSURE **HOLE**

We can collapse all sets of curves for various $2c$ values to one set of curves. This collapsing implies that after reducing the pressure data to dimensionless values, we can type curve match for the value of F and hence for the radius of the hole.

Finally, we can determine the value of c, the shortest distance between the well and the boundary. This is based upon finding the limiting linear boundary model corresponding to the data we have. The linear boundary model analysis is presented in Chapter 2.

Figure 3.8 presents generalized semilog type curves for the constant pressure hole case. The pressure and time scales are modified based on the shifting of the semilog curves described in Appendix C. The uppermost straight curve represents the line source. The lowermost curve for $F=1.0$ represents the limiting constant pressure linear boundary. This curve for the linear boundary is identical to the curves presented in the generalized semilog type curve for constant pressure linear boundaries (see Fig. 2.5). Thus, finding the curve appropriate to a set of measured data also allows estimation of the closest distance to the circular boundary. A synthetic type curve match example is presented in the following section.

In summary, we can type curve match first for the radius of the hole and then for the distance to its center. We should note that theoretically, two more wells are needed to fix the location of the constant pressure hole. Interference testing is discussed in Section 3.7.

From a practical viewpoint, each family of curves for the constant pressure hole, along with the limiting curve for the constant pressure linear boundary, depart from the line source at the same time. Taking a

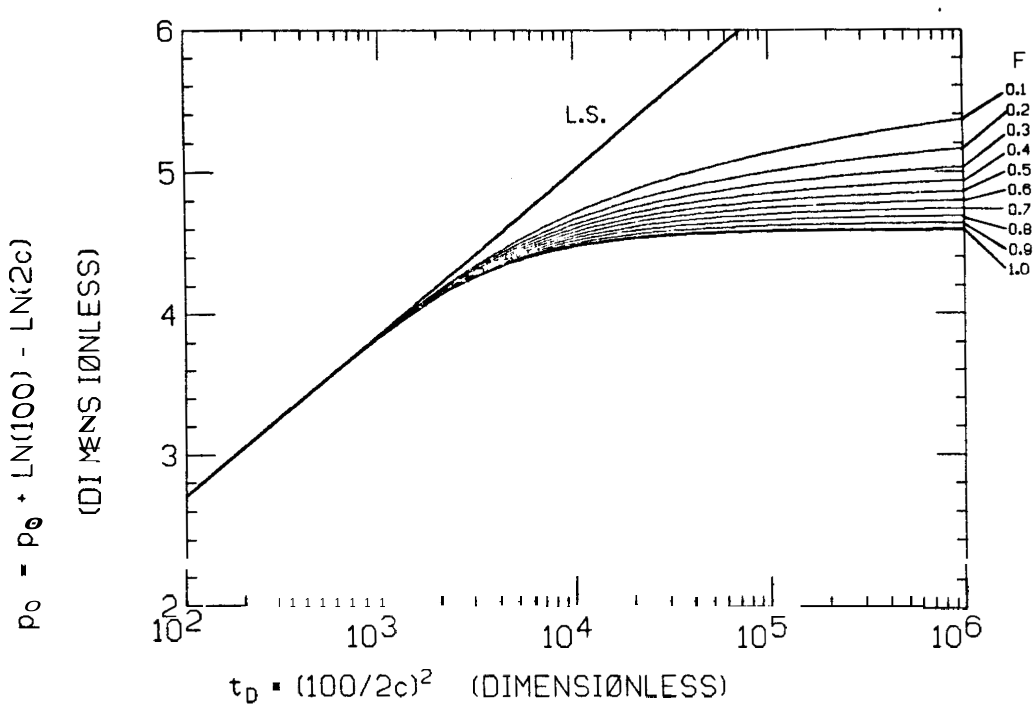

FIGURE 3.8 : A GENERALIZED SEMILOG TYPE CURVE FOR THE CONSTANT PRESSURE INTERNAL CIRCULAR BOUNDARY

1% variation from the line source as the point of departure, suggested by Ramey et. al. (1973), we can evaluate the departure times for various values of 2c (see Fig. 3.9). This is discussed in Appendix D.

3.6.2 TYPE CURVE MATCHING EXAMPLE

The following presents the application of the type curves using synthetic data. Figure 3.10 presents the pressure - time points for a system where 2c=20 and F=0.5 on log-log scale. The data are matched on the log-log type curve for the constant pressure linear boundary (see Fig. 3.11). The type curve used for the match of the data is the Stallman type curve for constant pressure linear boundaries. From this

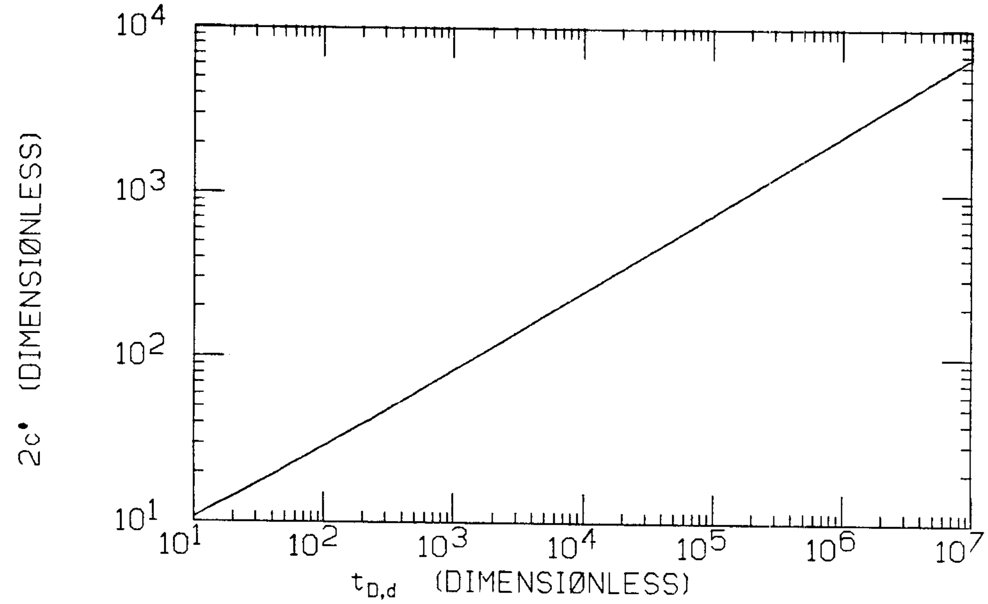

FIGURE 3.9 : ONE PERCENT DIMENSIONLESS DEPARTURE TIME FROM THE LINE SOURCE AS A FUNCTION OF 2c'

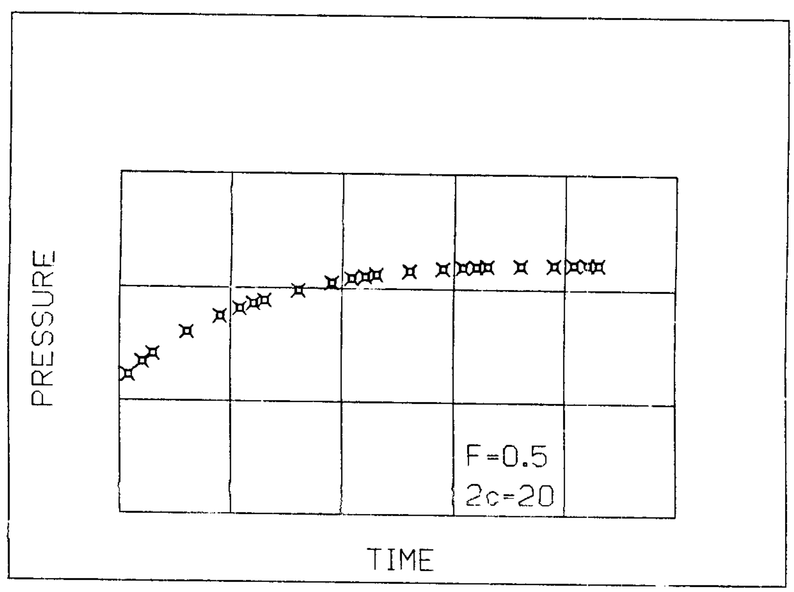

FIGURE 3.10 : TYPE CURVE MATCH EXAMPLE : DATA FOR 2c=20 F=0.5. CONSTANT PRESSURE HOLE

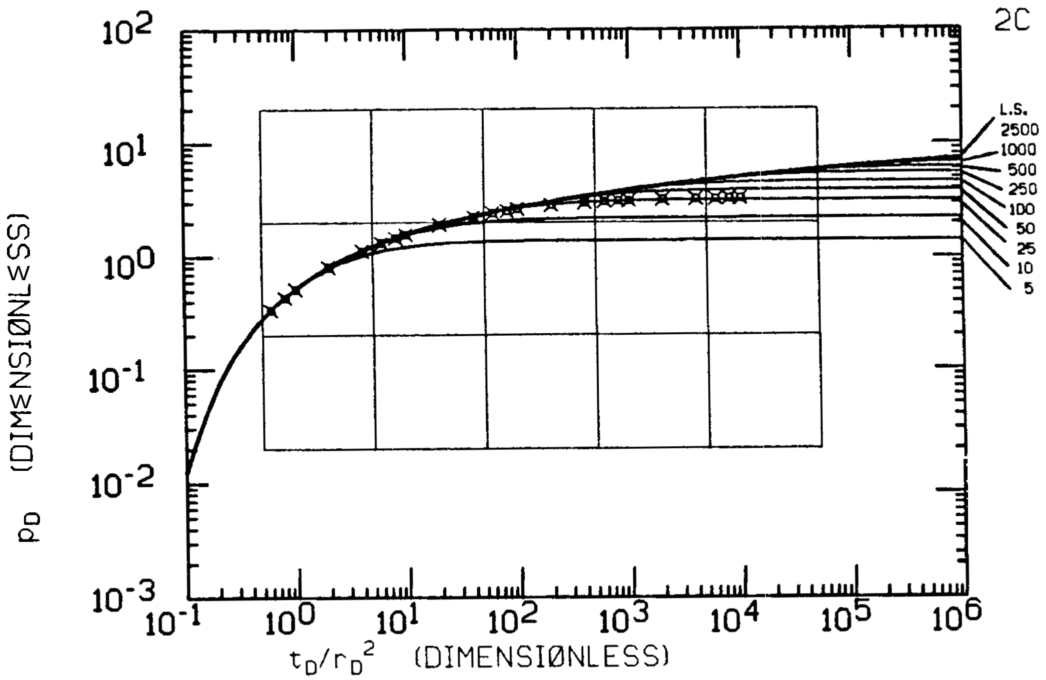

FIGURE 3.11 : TYPE CURVE MATCH EXAMPLE : LOG–LOG MATCH TO THE LINE SOURCE AND A PRELIMINARY VALUE OF 2c

match, we find an approximate value of $2c \approx 25$ and the conversion factor between pressure and dimensionless pressure.

The dimensionless pressure data as a function of time are graphed on the same semilog scale as the generalized semilog type curve presented in Fig. 3.8. Now, we match for the most similar curve and find that F=0.5 (see Fig, 3.12).

The next step is to determine the distance between the well and the hole, c. Using a pressure match point on Fig. 3.12 together with the modified pressure equation for p_D^* (derived in Appendix C) we solve for the value of 2c :

$$2c = \exp\left[\, p_D + \ln(100) - p_D^* \,\right] = \exp\left[\, 10 + \ln(100) - 2.6 \,\right] = 20.1$$

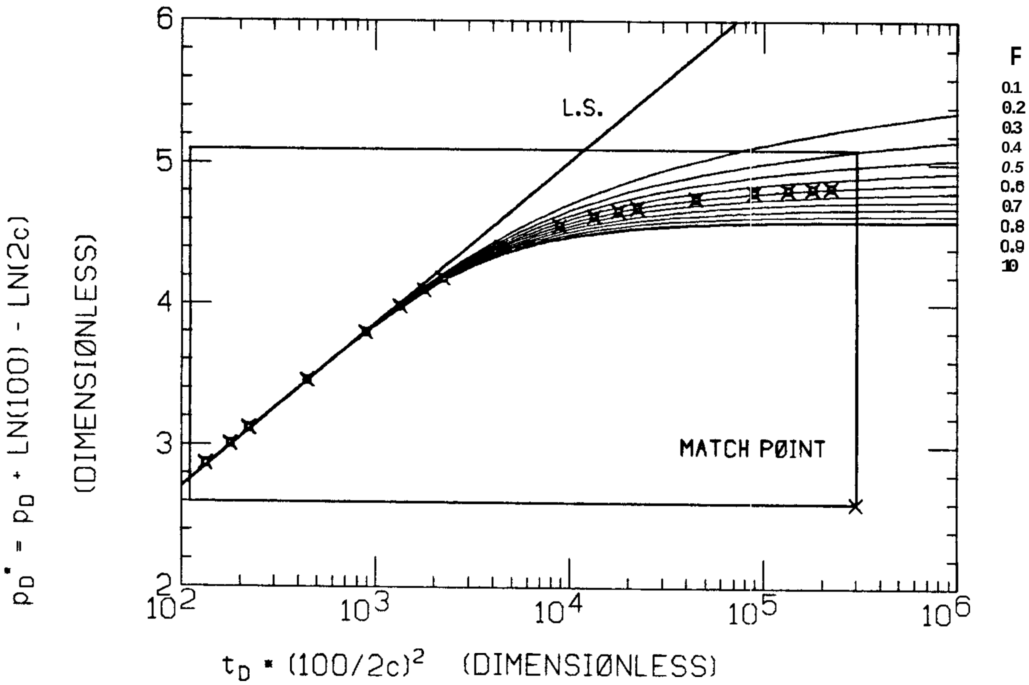

FIGURE 3.12 : TYPE CURVE MATCH EXAMPLE : SEMILOG MATCH FOR THE RELATIVE SIZE OF THE HOLE AND THE DISTANCE TO IT

It should be noted that the time axis of the semilog graph of the data need not be converted to a dimensionless form. The time axis can remain in real time units since only the pressure match is used to determine the value of 2c.

3.7 INTERFERENCE TYPE CURVE MATCHING

This section presents some theoretical and practical aspects of interference testing in the presence of a constant pressure internal boundary.

3.7.1 GENERAL DISCUSSION

The following discussion of interference testing is closely related to interference applications described in the introduction. We consider two basic cases:

a) Interference testing without a known geometry.

b) Interference testing with a known geometry.

Three parameters control the interference behavior: the relative size of the hole, F, the relative distance to the observation point, E and the angle of rotation of the pressure point, θ.

Figure **3.13** presents an example of some log-log interference curves. Five observation points are used, shown in Fig. **3.14.** Figure **3.13** presents one of the problems with interference log-log type curve matching. The curves break off from the line source solution at early times. As the observation point moves away from the production well, the curves break off earlier. Hence, we do not have an early line source behavior to match to the line source type curve.

In order to test systems with unknown geometries (E, F and θ are unknown), we must span the interference domain with a small number of type curves. Our efforts to collapse this domain were unsuccessful.

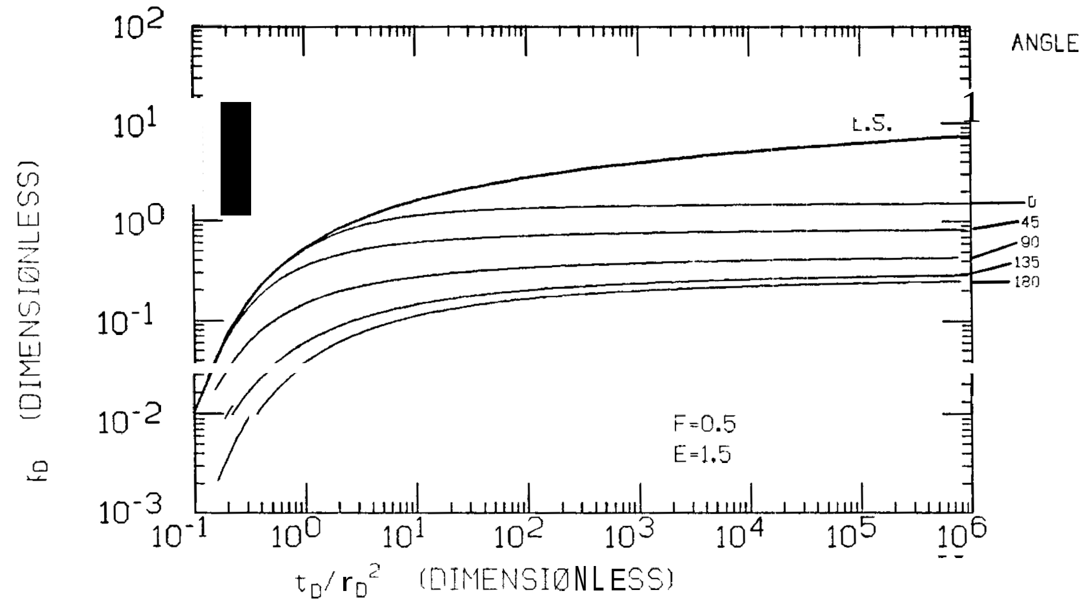

FIGURE 3.13 : INTERFERENCE LOG–LOG **CURVES** FOR **F=0.5 , E=1.5 AND** θ**=0,**

45,90,135,180 **DEG. CONSTANT PRESSURE** HOLE

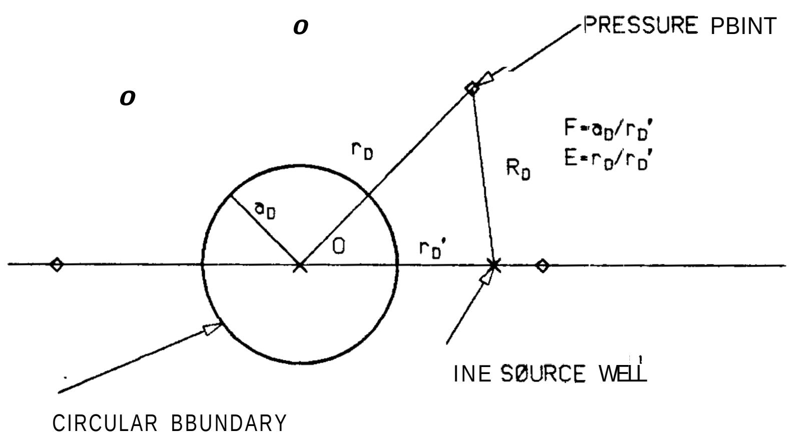

FIGURE 3.14 : THE GEOMETRY OF THE OBSERVATION POINTS IN THE CONSTANT

PRESSURE HOLE **SYSTEM**

Stallman (1952) presented a method for spanning the interference domain with one set of curves for the constant pressure linear boundary case. This method is based on the long time steady state circles. The method does not apply to a system with a constant pressure hole. Figure 3.15 presents three log-log curves for three interference points on a long time constant pressure circle. All three curves have the same long time pressure, but the transients are different. For the limiting case of a constant pressure linear boundary, these curves would be identical. This is discussed in Appendix E.

Figure 3.16 presents an attempt to collapse interference curves for fixed E and θ with a varying F. Figure 3.17 presents the same data of Fig. 3.16 normalized to the steady state dimensionless pressure. In Fig. 3.17, the dimensionless pressure values are devided by the corresponding steady state dimensionless pressure evaluated by Eq. 3.38.

Figure 3.18 presents an attempt to collapse interference curves for fixed F and θ and varying E. Figure 3.19 presents the same data of Fig. 3.18 normalized to the steady state dimensionless pressures.

Figure 3.20 presents an attempt to collapse interference curves for fixed E and F with varying angles. Fig. 3.21 presents the normalized version of Fig 3.20.

The next three efforts correspond to straight .Lines parallel to the axes in an E, F and θ space. In the first case, E and F were kept constant and the angle of rotation was varied. This corresponds to a straight line parallel to the angle axis. In the second case, θ and E were kept constant and the relative size of the hole was varied. In the third case, θ and F were kept constant and the relative distance to the pressure point was varied.

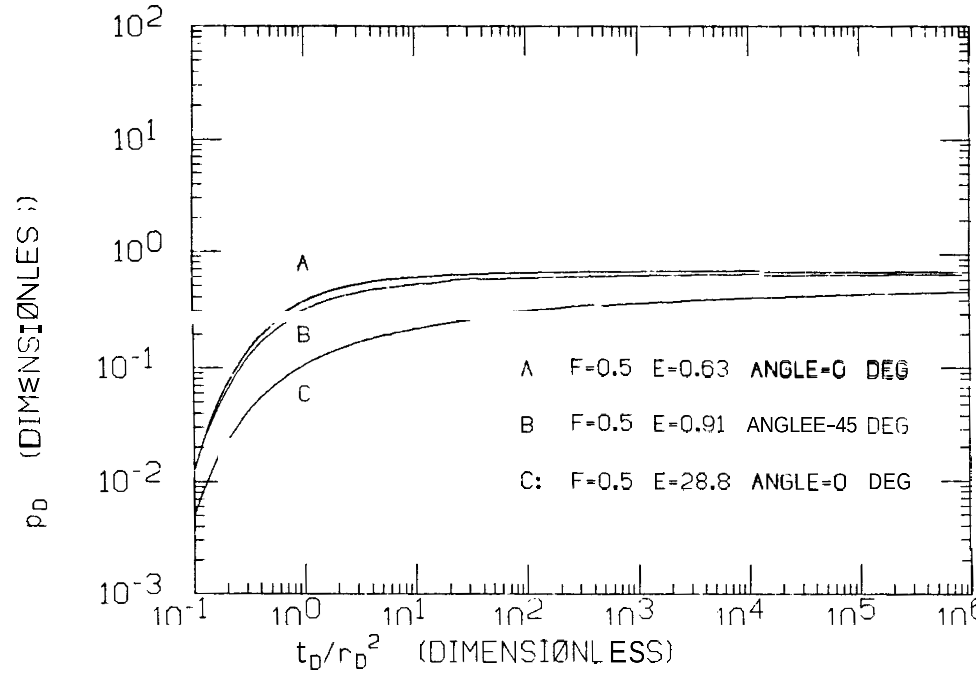

FIGURE 3.15 : INTERFERENCE LOG-LOG CURVES FOR THREE POINTS ON THE LONG TIME CONSTANT PRESSURE CIRCLE

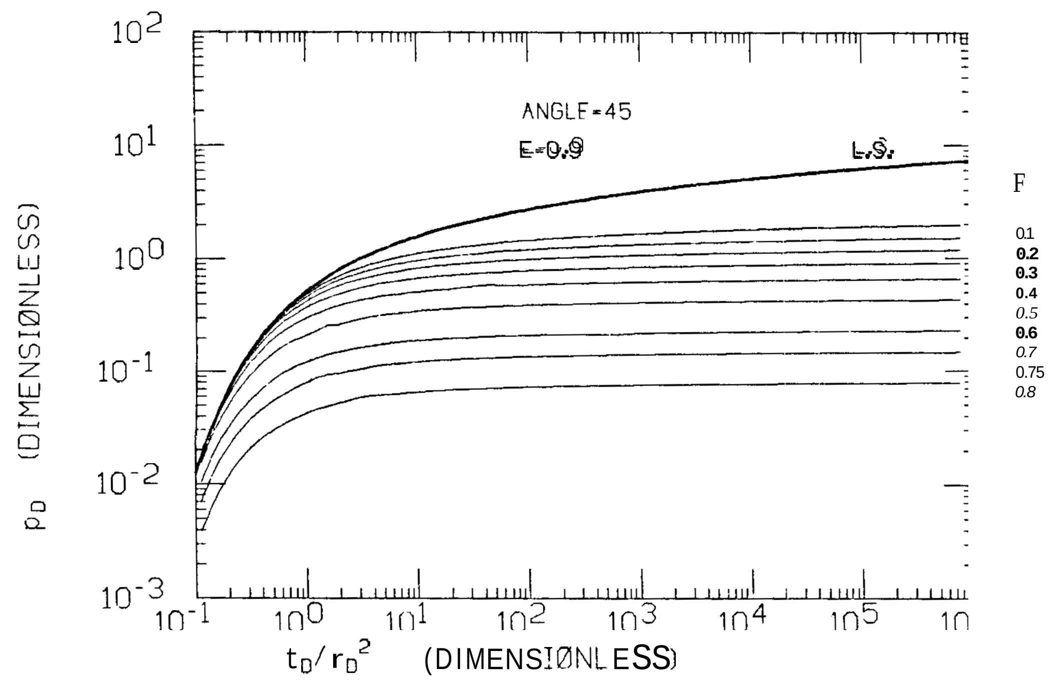

FIGURE 3.16 : INTERFERENCE LOG–LOG CURVES FOR E=0.9 F=0.1 TO 0.8 AND θ=45 DEG. CONSTANT PRESSURE HOLE

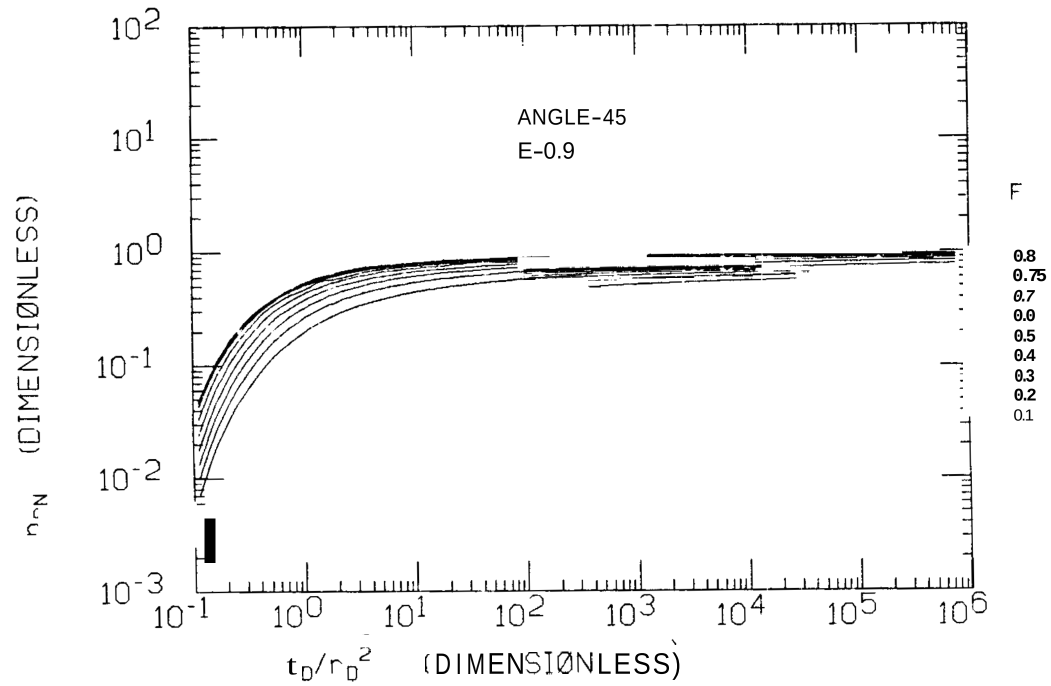

FIGURE 3.17 : INTERFERENCE NORMALIZED LOG–LOG CURVES FOR **E=0.9**

F=0.1 TO 0.8 AND θ=45 DEG. CONSTANT PRESSURE HOLE

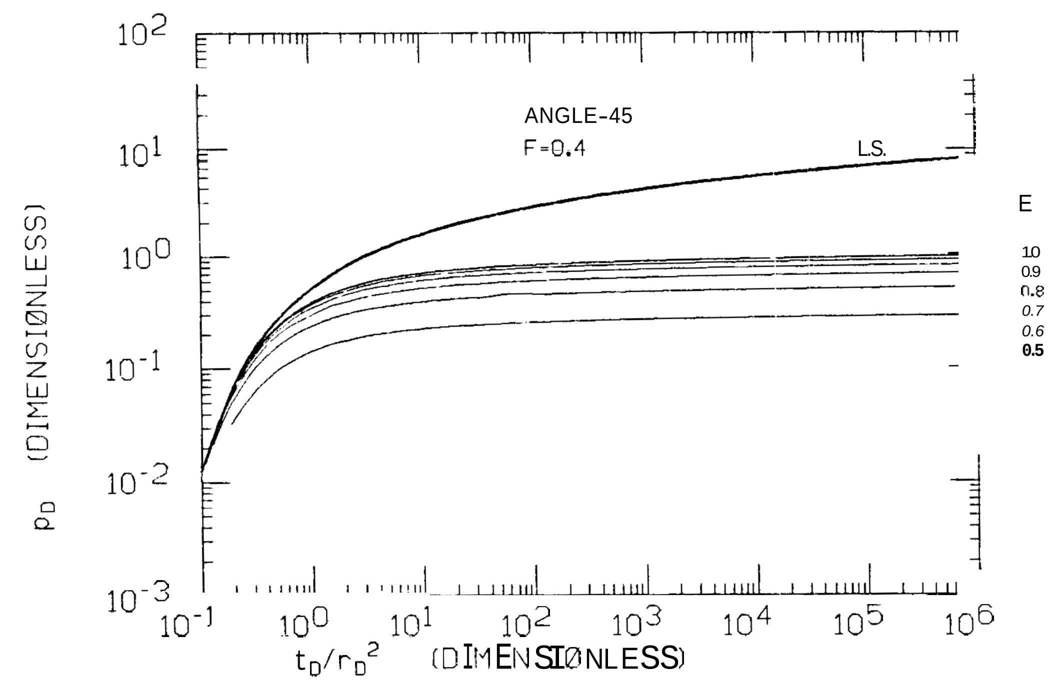

FIGURE 3.18 : INTERFERENCE **LOG-LOG** CURVES FOR F=0.4 E=0.5 TO 1.0 AND

θ=45 DEG. CONSTANT PRESSURE HOLE

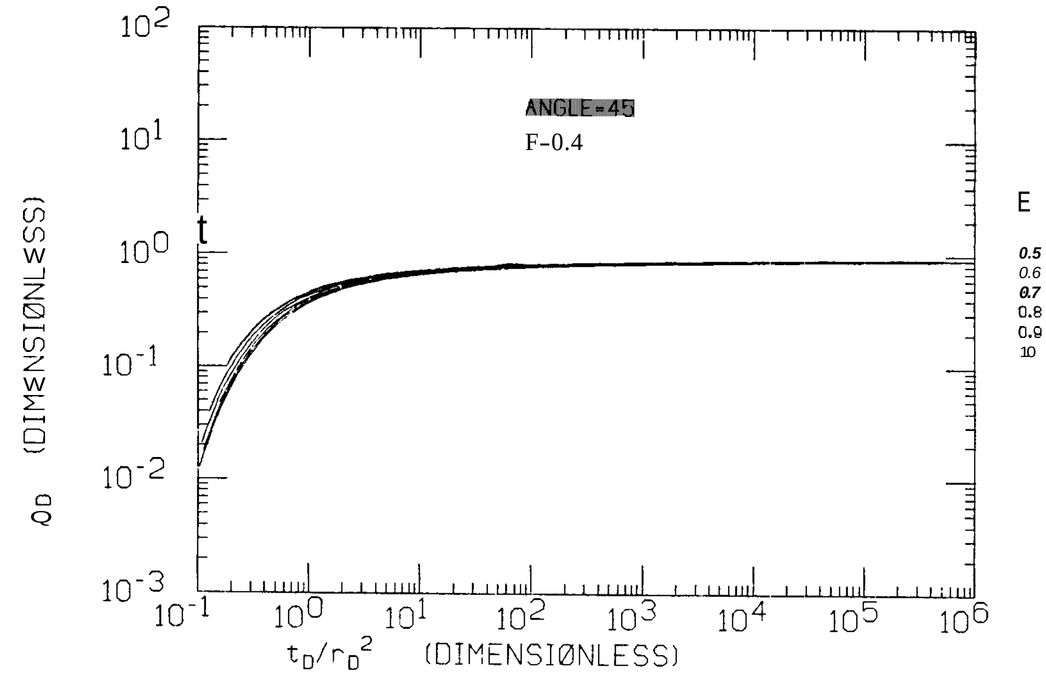

FIGURE 3.19 : INTERFERENCE NORMALIZED LOG-LOG CURVES FOR F=0.4

E=0.5 TO 1.0 AND θ=45 DEG. CONSTANT PRESSURE HOLE

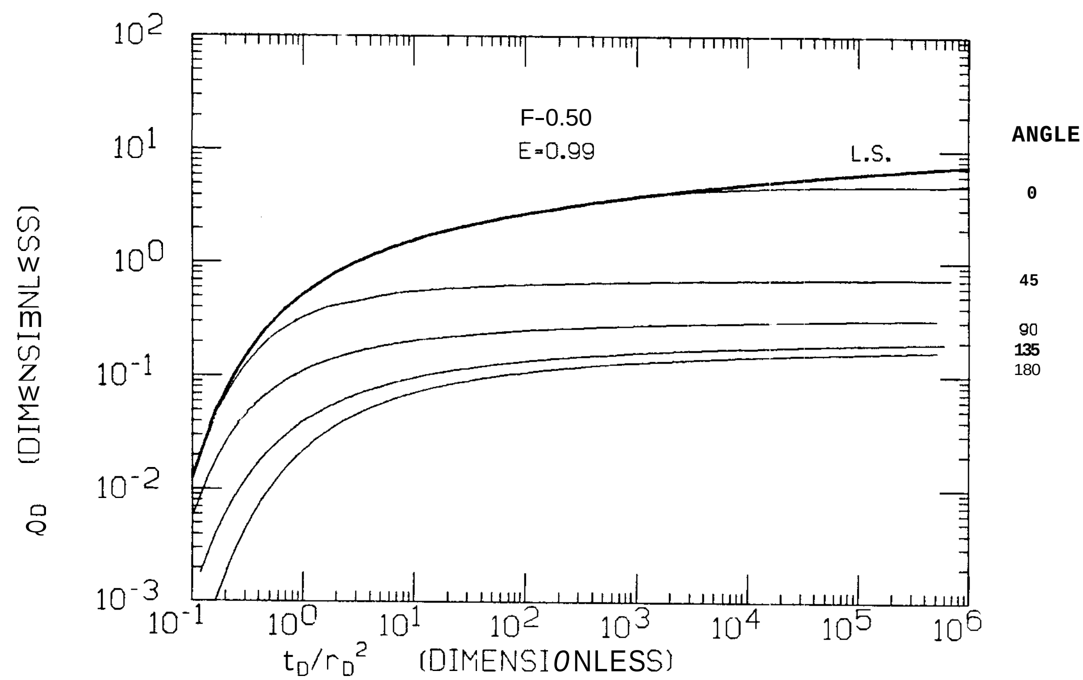

FIGURE 3.20 : INTERFERENCE LOG-LOG CURVES FOR F=0.5 E=0.99 AND

θ=0,45,90,135,180 DEG. CONSTANT PRESSURE HOLE

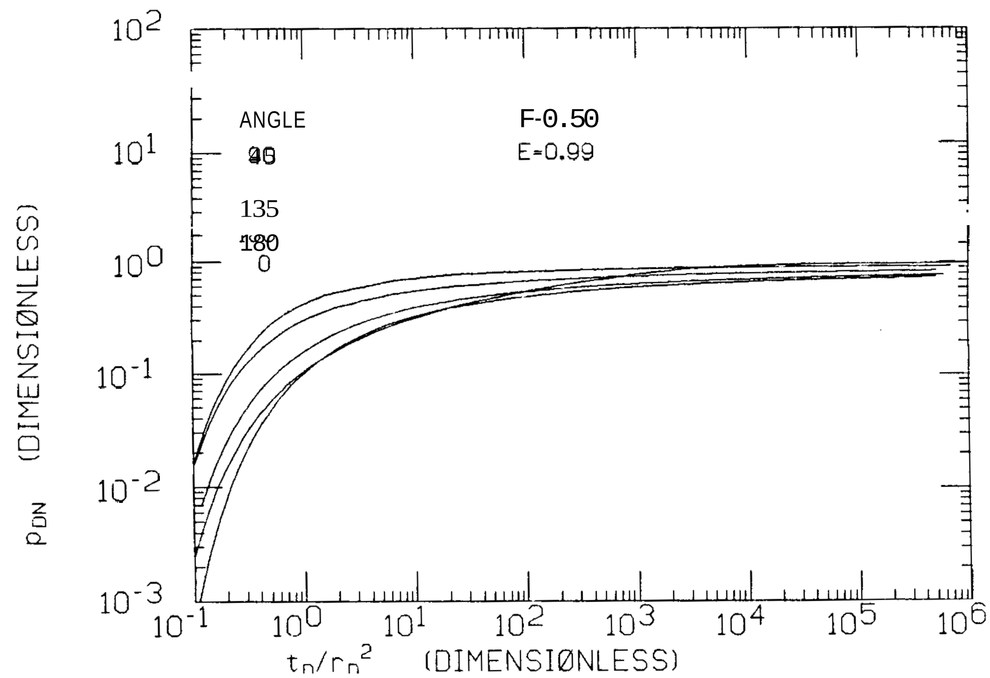

FIGURE 3.21 : INTERFERENCE NORMALIZED LOG-LOG CURVES FOR F=0.5 E=0.99 AND θ=0,45,90,135,180 DEG. CONSTANT PRESSURE HOLE

All three efforts did not span the interference domain in a practical manner.

Two additional efforts for interference analysis are presented. The first attempt considers a constant angle and a constant distance between the pressure point and the hole. This corresponds to E-F=constant. Figure 3.22 presents the normalized log-log curves for this unsuccessful effort.

The second attempt considers the ratio E-F/1-F a constant. This is a ratio of the distance between the observation point and the hole to the distance between the well and the hole. Figure 3.23 presents the normalized log-log curves for this unsuccessful effort.

It should be noted that all these attempts to span the interference

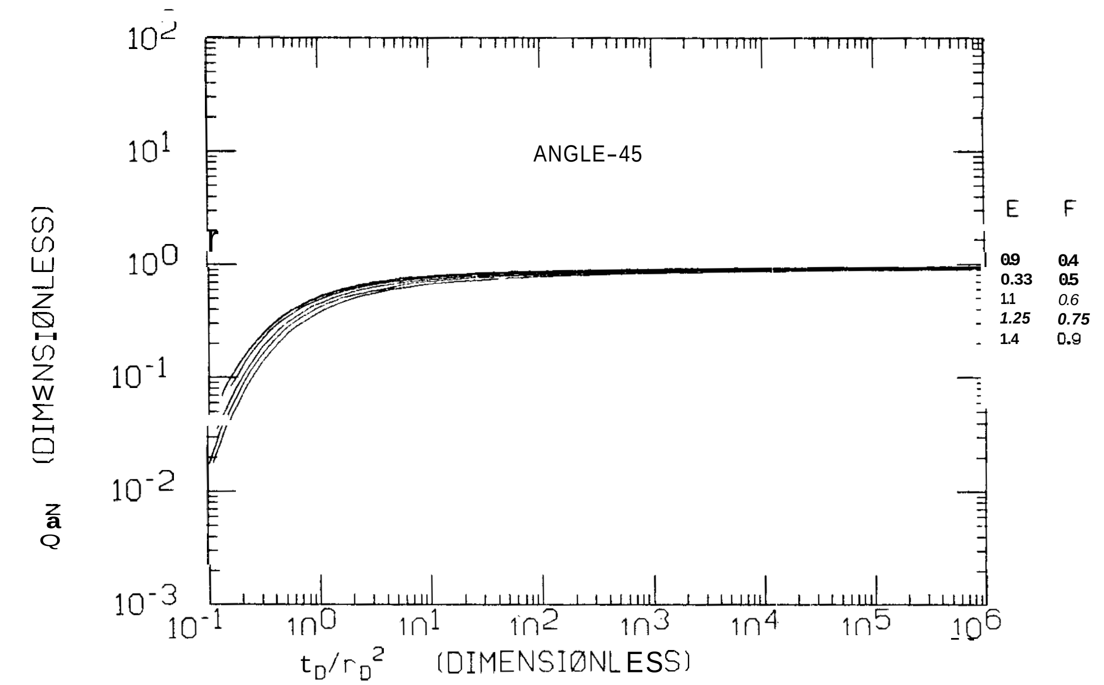

FIGURE 3.22 : INTERFERENCE NORMALIZED LOG-LOG CURVES FOR $\theta=45$ DEG. AND E-F=0.5. CONSTANT PRESSURE HOLE

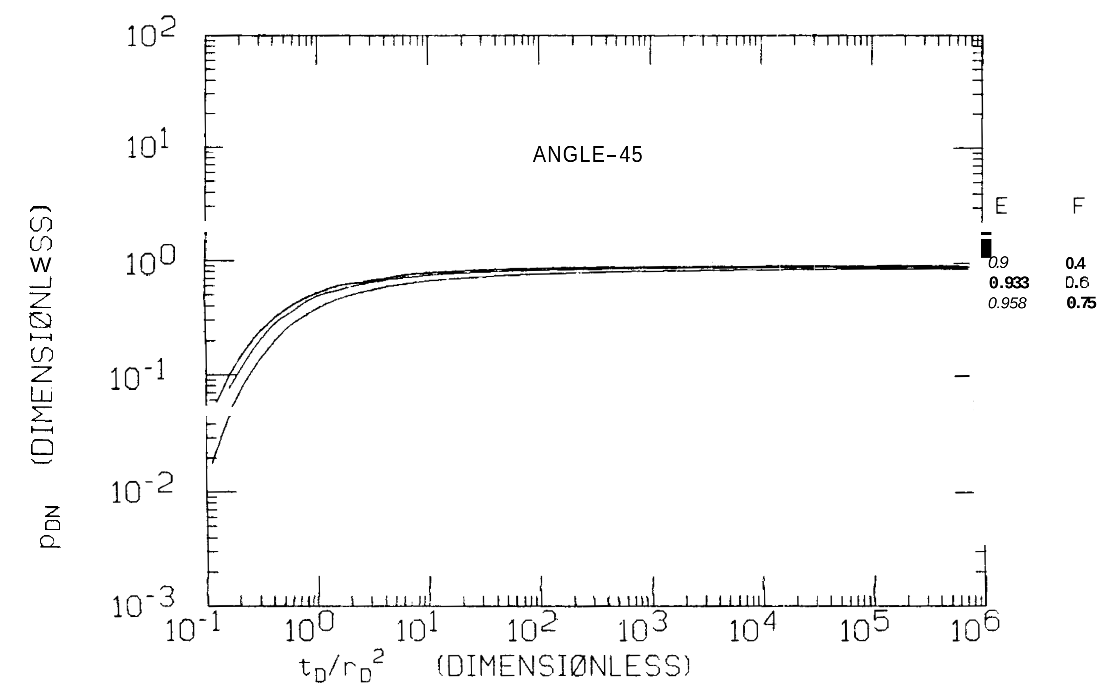

FIGURE 3.23 : INTERFERENCE NORMALIZED LOG-LOG CURVES FOR $\theta=45$ DEG. AND (E-F)/(1-F)=5/6. CONSTANT PRESSURE HOLE

domain have no theoretical support.

Based on this lack of success, it is suggested. that interference testing without any knowledge of the geometry is not practical. Various different configurations of E, F and θ will match the same set of pressure - time data.

Systems where we know one or more of the controlling parameters are defined as systems with a known geometry. In developed systems, such as in a geothermal field or a certain developed pattern (5 spot etc.), E and 8 are known and F will vary with time. In these cases we may have the value of F if the production well data are analyzed. When testing undeveloped systems, such as a gas cap, only the value of F is known. In summary, we can have three different cases under the unknown geometry category:

a) F known, E and θ unknown.

b) E and θ **known** , F unknown.

c) E, F and 8 known.

The following is a discussion of these three cases.

a) <u>F known, E and θ unknown</u>

This case is very similar to a case where F is not known. Figure 3.24 presents interference log–log curves for a constant F and various values of E and 8 . This figure demonstrates the difficulty in trying to log–log type curve match interference data.

However, when the same data are normalized as semilog curves, they segregate according to the angle for values of E < **2. This** segregation can be seen in Fig. **3.25.** Even so, this type curve has no practical use. In order to use Fig. 3.25, we need the conversion constant for

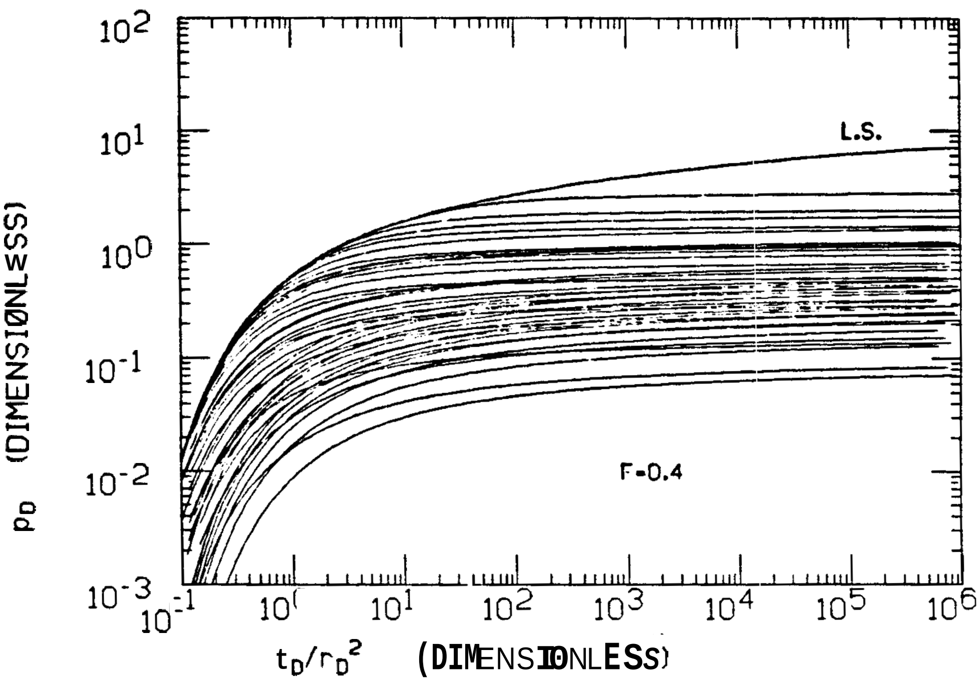

FIGURE 3.24 : INTERFERENCE LOG-LOG CURVES FOR F=0.4 θ=0,45,90,135,180 DEG. AND E-0.5 TO 2.0. CONSTANT PRESSURE HOLE

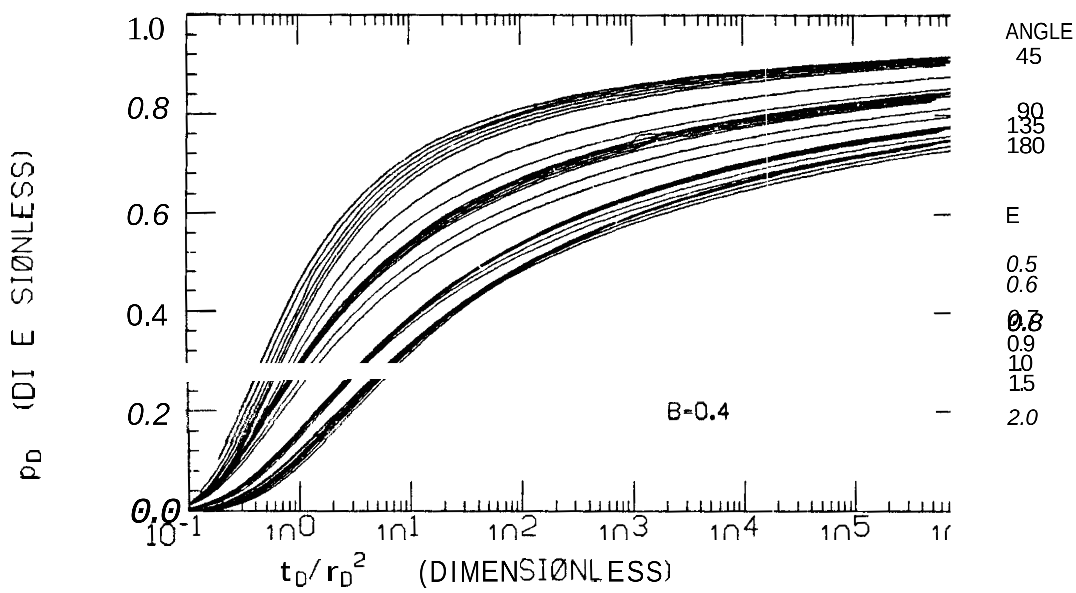

FIGURE 3.25 : INTERFERENCE NORMALIZED SEMILOG CURVES FOR F=0.4, θ-45, 90,135,180 DEG. AND E=0.5 TO 2.0. CONSTANT PRESSURE HOLE

the dimensionless pressure as well as the steady state pressure which are not available.

b) E and 8 known, F unknown

This case is typical of interference testing where the production well data is not used. Here, the pressure - time data must first be converted into a dimensionless form. This can be done only if we have a portion of the curve matching the line source solution. Figure 3.26 presents interference log-log curves for fixed values of E and 8.

For values of F < 0.5 we can get reasonably close to the line source solution. Then, we take the converted dimensionless pressure - time data and match for F on a semilog interference type curve presented in Fig. 3.27.

c) E, F and 8 known

This case is typical of interference testing in a developed system where the data from the producing well are analyzed. This analysis gives us the conversion coefficient for the dimensionless pressure for both the producing and the interference wells. Then, the interference data are matched for F on a semilog type curve such as Fig. 3.27. In this figure, the interference well is located at an angle of 45 Deg. Three values of the relative distance to the interference well are considered. The relative size of the hole, F, varies between a value of 0.1 and the largest value it can assume. For example, in the case where E- 0.7, F=0.1 to 0.6. Figure 3.27 is used to match for the value of F. This is actually a check for the value of F generated by analyzing the production well data.

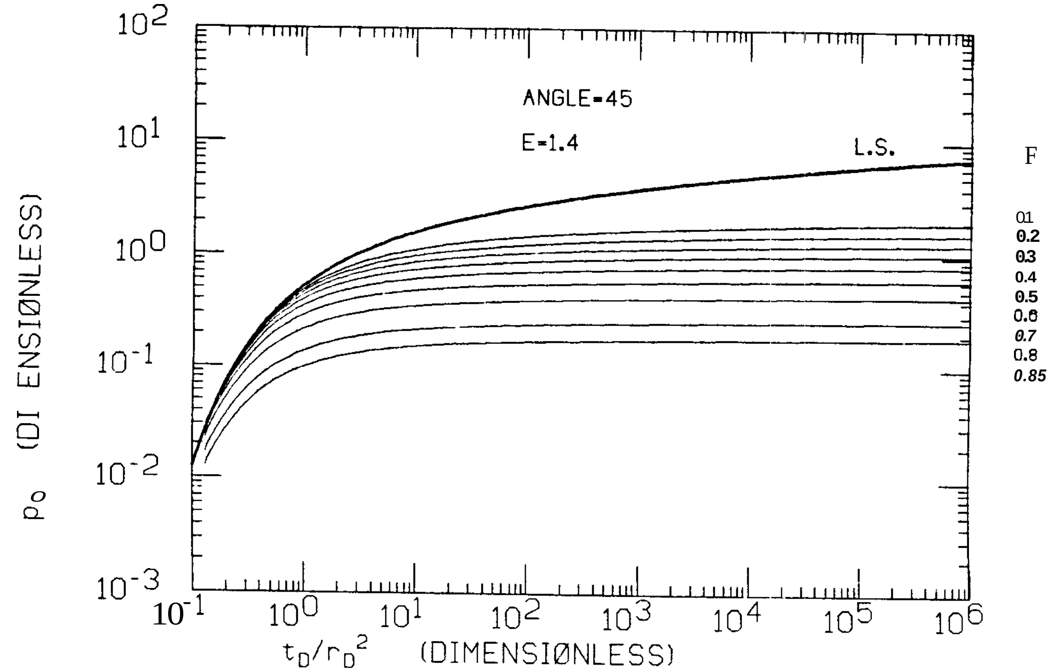

FIGURE 3.26 : INTERFERENCE LOG–LOG TYPE CURVE FOR E=1.4 AND θ=45 DEG.
CONSTANT PRESSURE HOLE

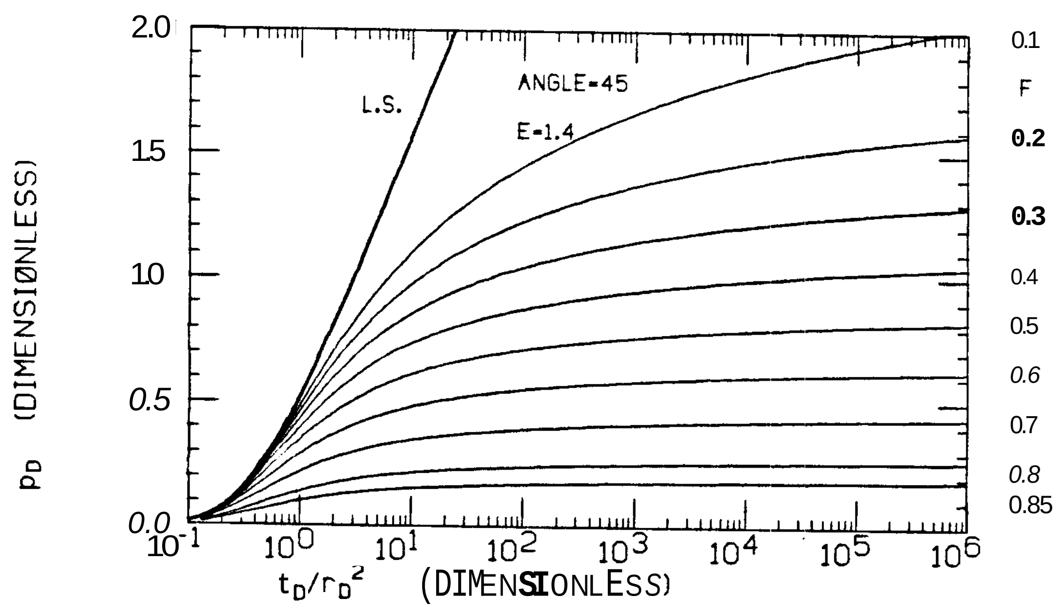

FIGURE 3.27 : INTERFERENCE SEMILOG TYPE CURVES FOR E=1.4 AND θ=45 DEG.
CONSTANT PRESSURE HOLE

3.7.2 INTERFERENCE TESTING IN AN UNKNOWN GEOMETRY

Interference testing when E and θ are not known is not practical. It is possible to fit several systems to a set of interference data. The difficulties in type curve matching were discussed in Section 3.7.1.

3.7.3 INTERFERENCE TESTING IN A KNOWN GEOMETRY

a) E, F and θ known

The data from the production well are used to determine F and the conversion factor to dimensionless pressure. The interference data are converted to dimensionless values using this factor. F is matched on the corresponding semilog type curve (odd-numbered Figs. 3.29 through 3.55). This analysis is a check for the value of F. This check can give an indication of how circular the constant pressure boundary is. The closer the boundary is to the interference point, the smaller the values of the dimensionless pressure. Hence, if the match is below the F line, the distance between the boundary and the observation well is shorter than the distance predicted by the production well. This indicates that the internal boundary may be elliptical in shape and not circular.

b) E and θ known, F unknown

This condition may arise when aquifers are tested near a gas storage bubble, and the production well is not monitored. It is recommended to have two interference wells, where one is close to the production well and the other is closer to the constant pressure boundary. In this case, the first well is used to find the conversion factor to dimensionless pressure, and the second well is used to determine the value of F using the semilog type curves.

If, however, only one interference well is available, the data must first be matched to the corresponding log-log type curve (even-numbered Figs. 3.28 through 3.54). This match yields the conversion factor and an approximate value for F. Then, the semilog type curves are used to get a better value for F.

The log-log match is subject to errors due to the fact that some curves depart from the line source at early time.

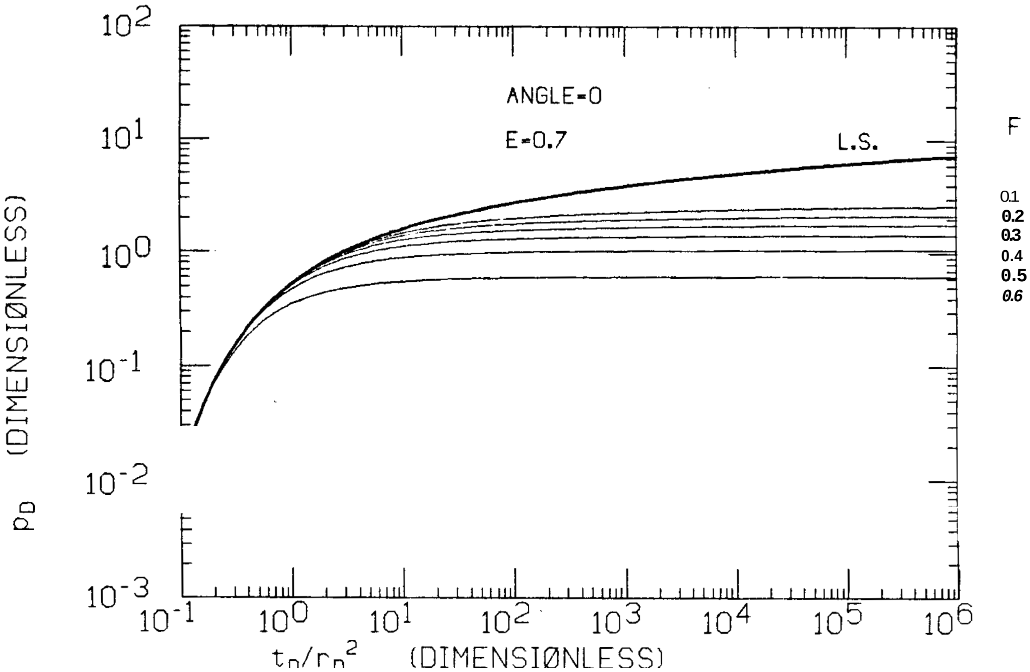

FIGURE 3.28 : INTERFERENCE LOG-LOG TYPE CURVES FOR E=0.7 AND θ=0 DEG. CONSTANT PRESSURE HOLE

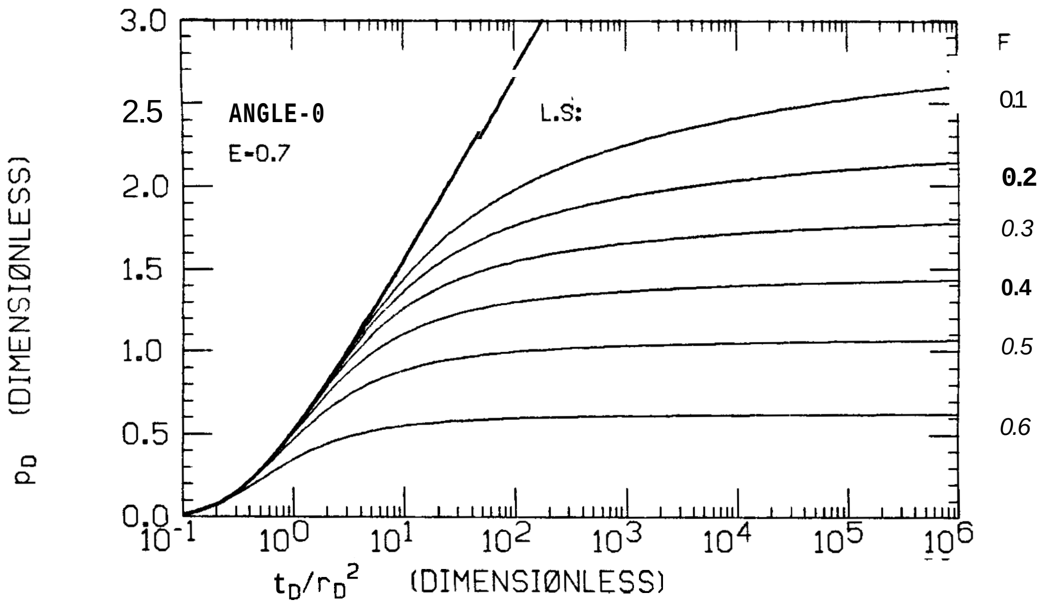

FIGURE 3.29 : INTERFERENCE SEMILOG TYPE CURVES FOR E=0.7 AND θ=0 DEG. CONSTANT PRESSURE HOLE

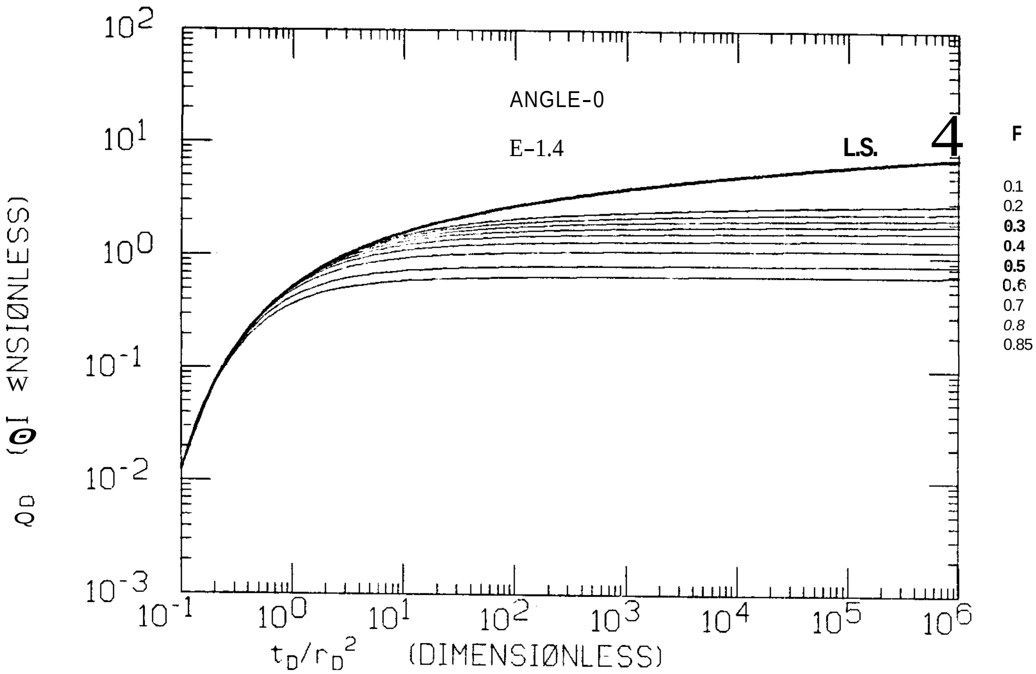

FIGURE **3.30** : INTERFERENCE LOG–LOG TYPE CURVES FOR **E=1.4** AND **θ=0** DEG.

CONSTANT PRESSURE HOLE

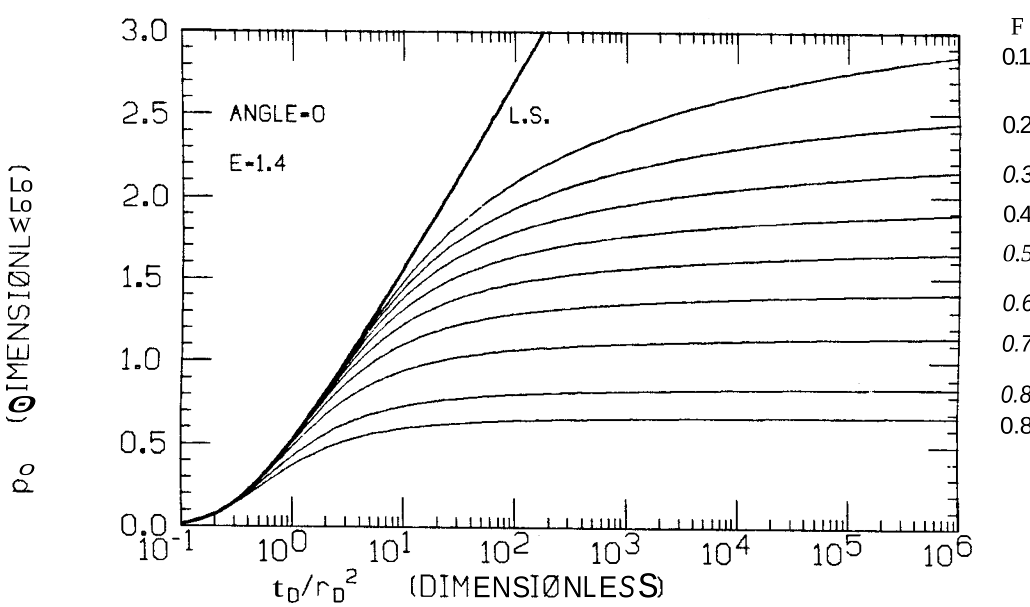

FIGURE **3.31** : INTERFERENCE SEMILOG TYPE CURVES FOR **E=1.4** AND **θ=0** DEG.

CONSTANT PRESSURE HOLE

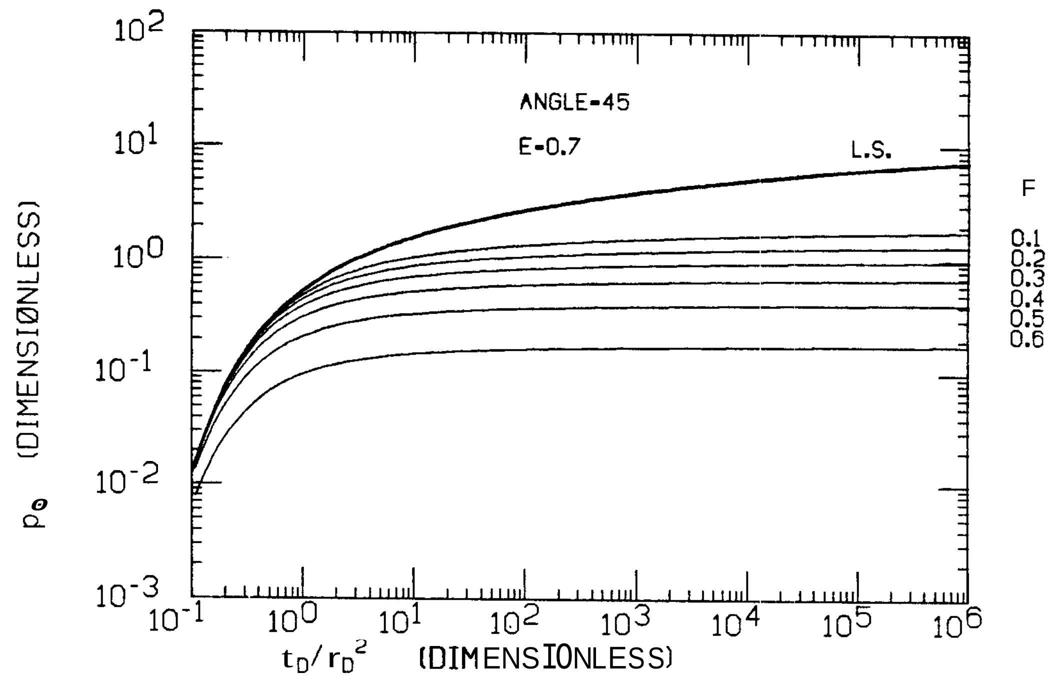

FIGURE 3.32 : INTERFERENCE LOG–LOG TYPE CURVES FOR E=0.7 AND *8-45* DEG.

CONSTANT PRESSURE HOLE

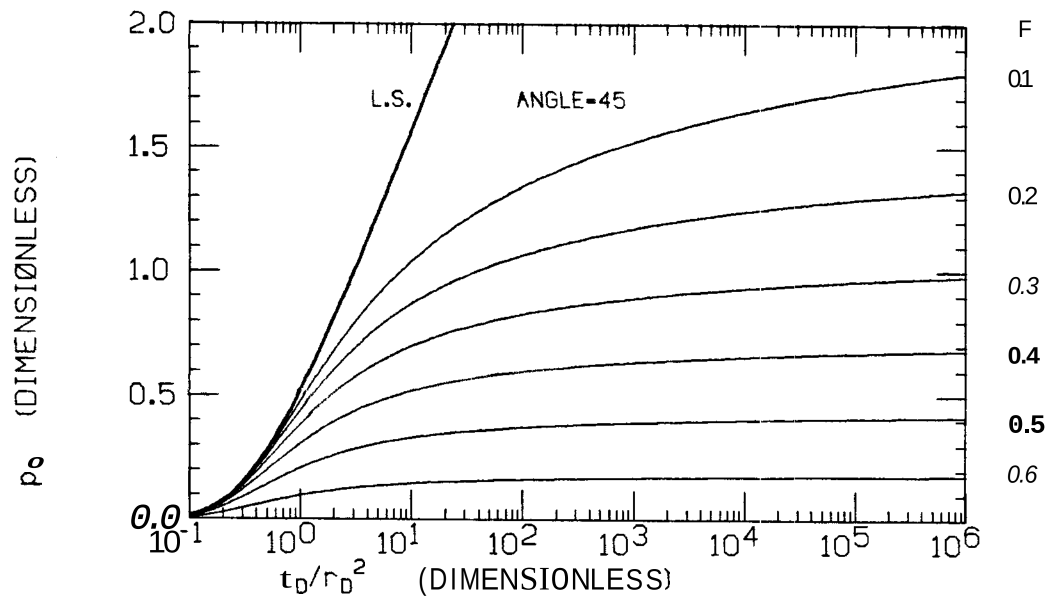

FIGURE 3.33 : INTERFERENCE SEMILOG TYPE CURVES FOR **E=0.7 AND θ=45** DEG.

CONSTANT PRESSURE HOLE

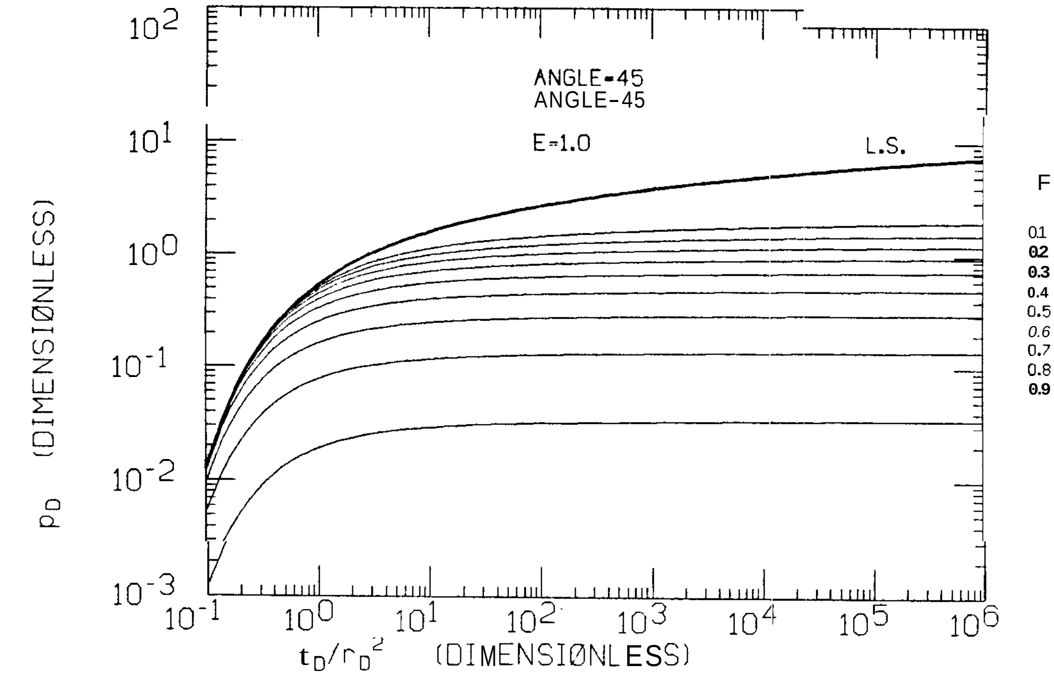

FIGURE 3.34 : INTERFERENCE LOG-LOG TYPE CURVES FOR E=1.0 AND θ=45 DEG.

CONSTANT PRESSURE HOLE

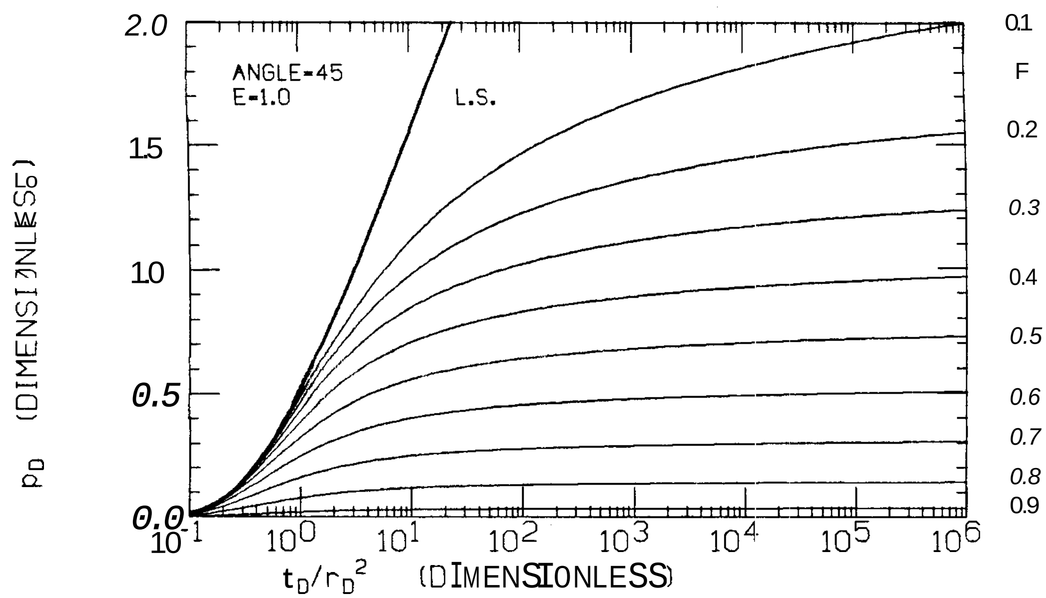

FIGURE 3.35 : INTERFERENCE SEMILOG TYPE CURVES FOR E=1.0 AND θ=45 DEG.

CONSTANT PRESSURE HOLE

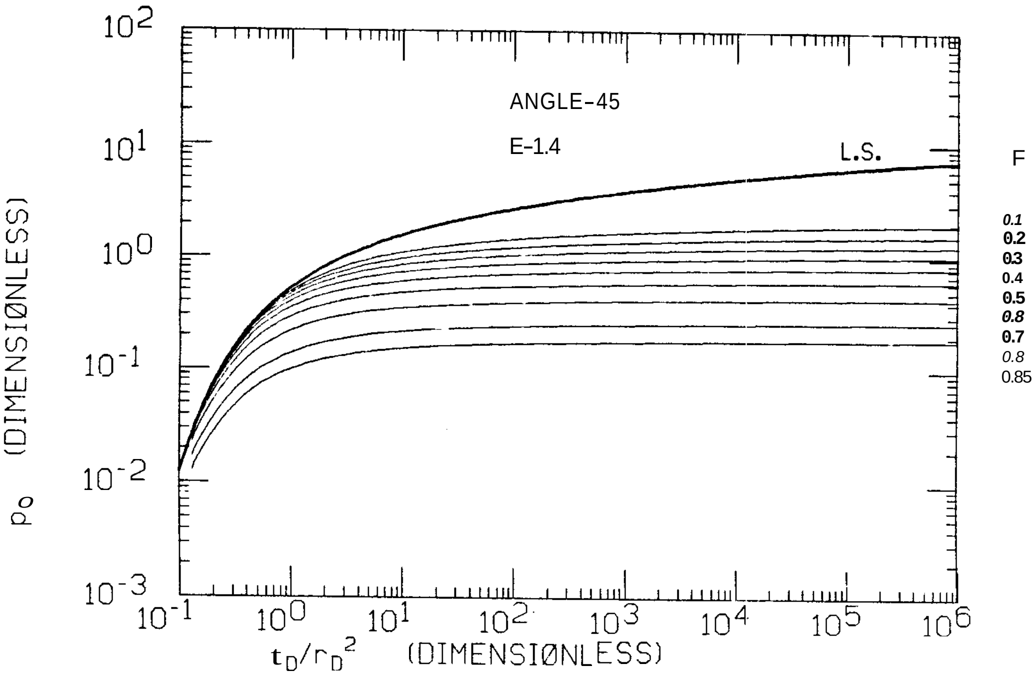

FIGURE 3.36 : INTERFERENCE LOG-LOG TYPE CURVES FOR E=1.4 AND θ=45 DEG. CONSTANT PRESSURE HOLE

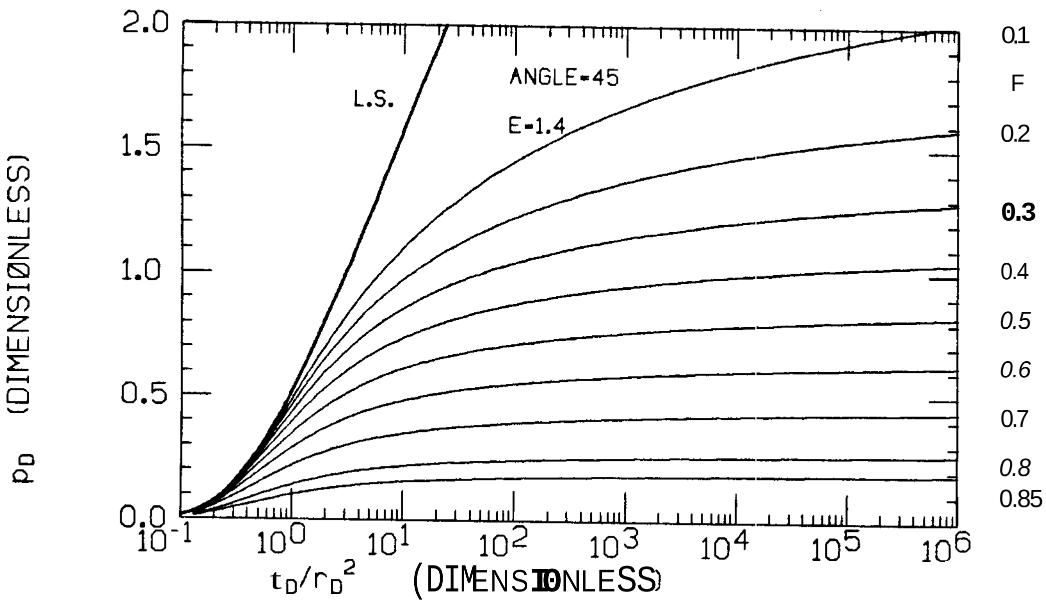

FIGURE 3.37 : INTERFERENCE SEMILOG TYPE CURVES FOR E=1.4 AND 8-45 DEG. CONSTANT PRESSURE HOLE

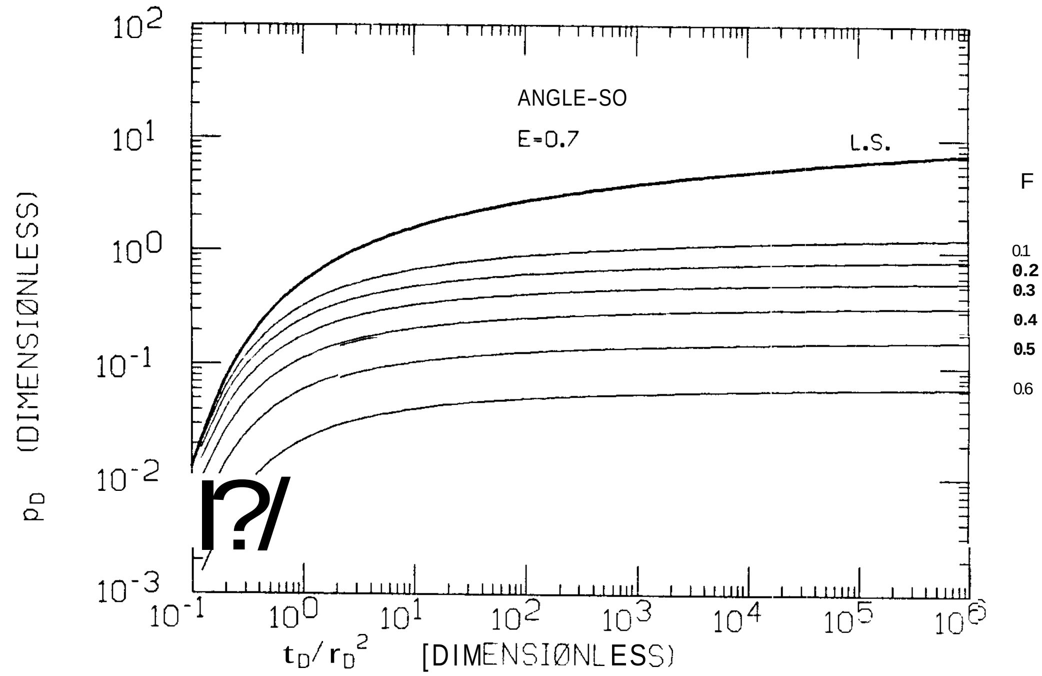

FIGURE 3.38 : INTERFERENCE LOG–LOG TYPE CURVES FOR E=0.7 AND θ=90 DEG. CONSTANT PRESSURE HOLE

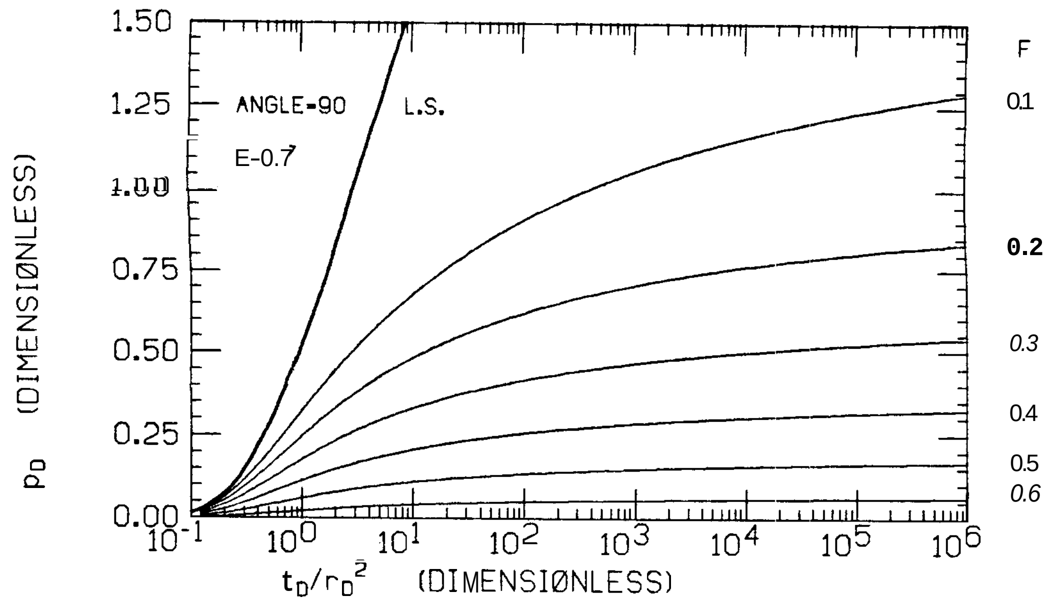

FIGURE 3.39 : INTERFERENCE SEMILOG TYPE CURVES FOR E=0.7 AND θ=90 DEG. CONSTANT PRESSURE HOLE

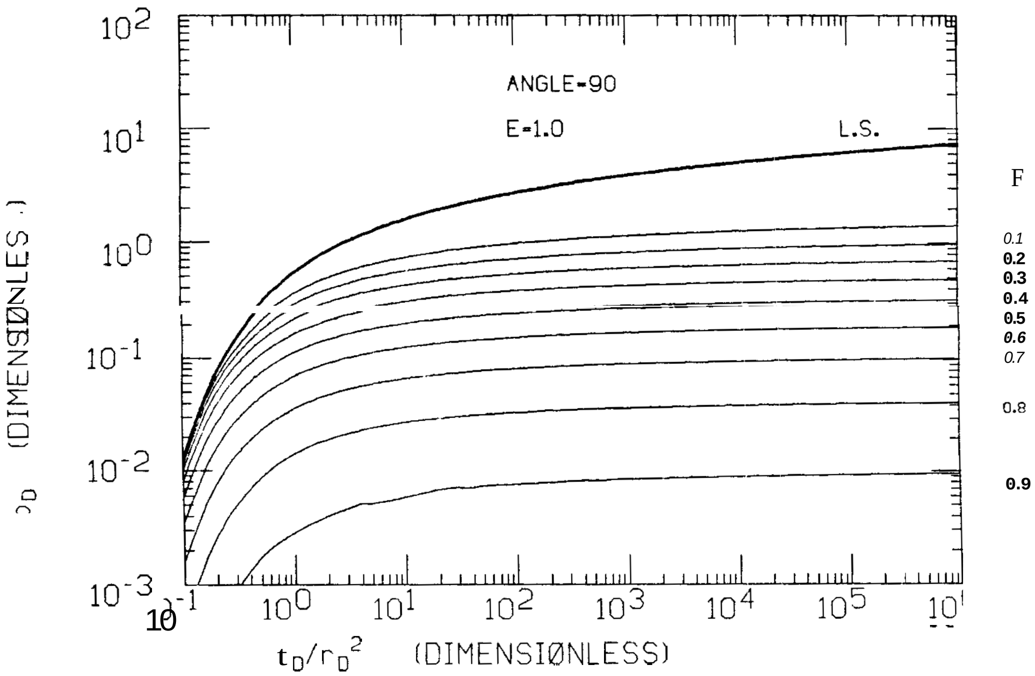

FIGURE 3.40 : INTERFERENCE LOG–LOG TYPE CURVES FOR E=1.0 AND θ=90 DEG.

CONSTANT PRESSURE HOLE

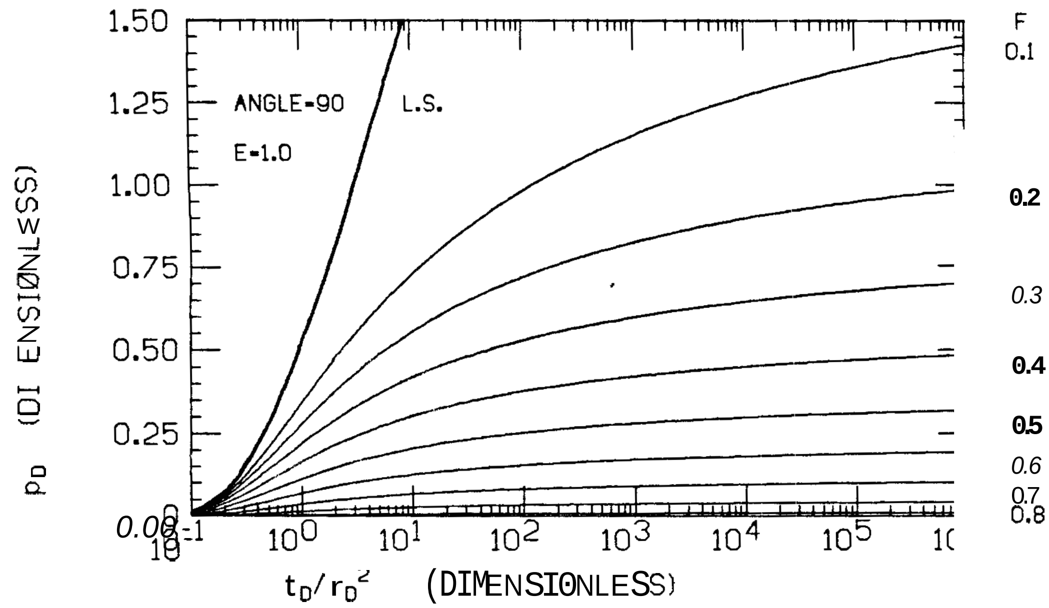

FIGURE 3.41 : INTERFERENCE SEMILOG TYPE CURVES FOR E=1.0 AND θ=90 DEG.

CONSTANT PRESSURE HOLE

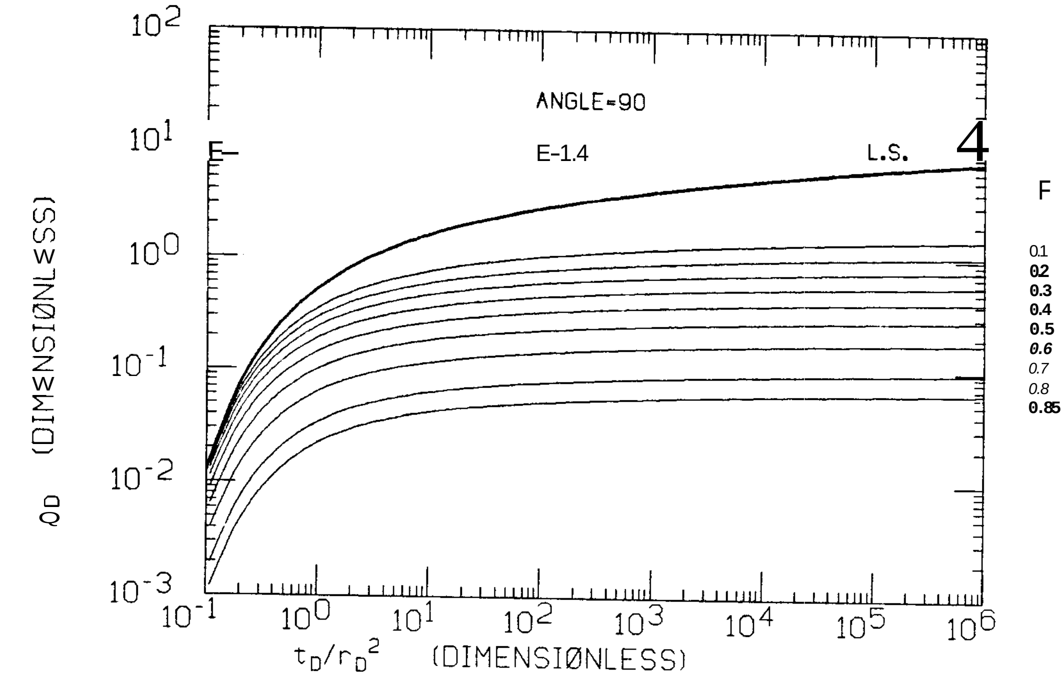

FIGURE 3.42 : INTERFERENCE LOG–LOG TYPE CURVES FOR E=1.4 AND θ=90 DEG.

CONSTANT. PRESSURE HOLE

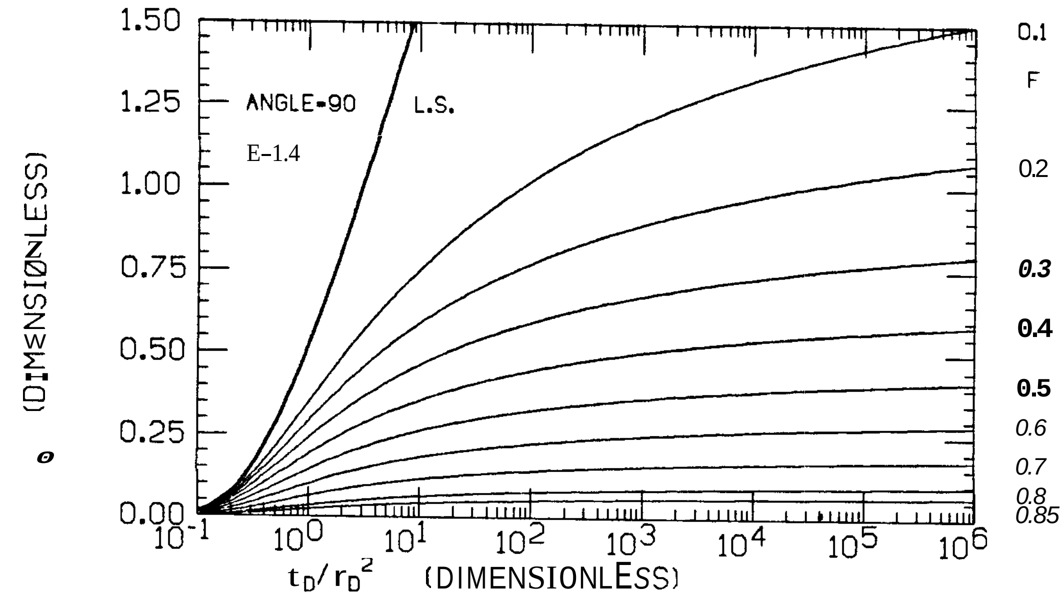

FIGURE 3.43 : INTERFERENCE SEMILOG TYPE CURVES FOR E=1.4 AND θ=90 DEG.

CONSTANT PRESSURE HOLE

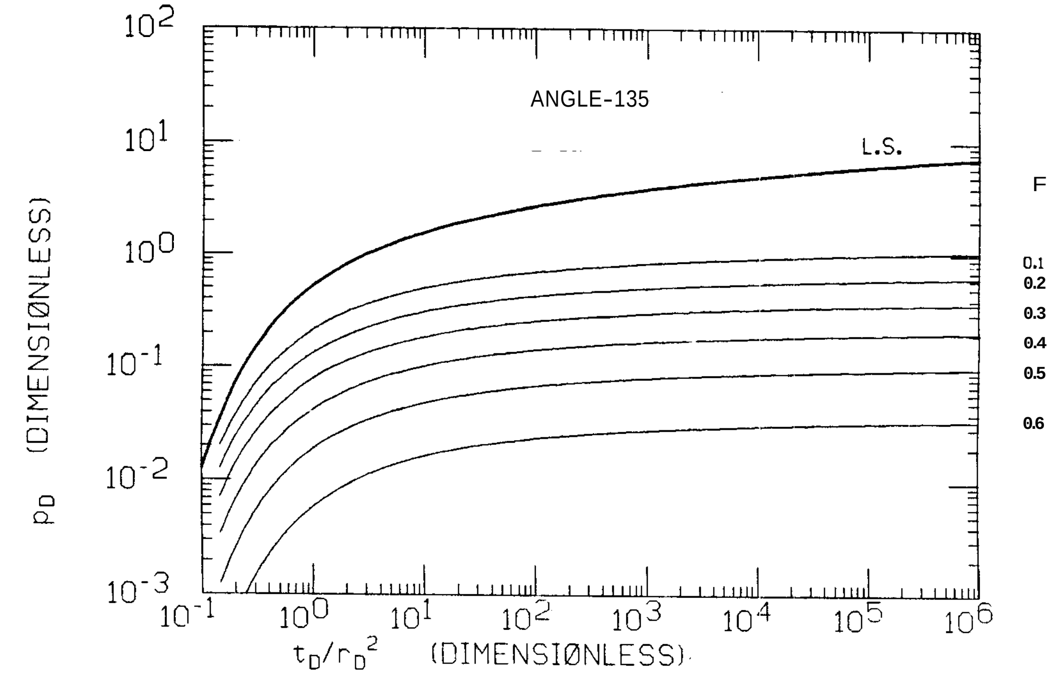

FIGURE *3.44* : INTERFERENCE LOG–LOG TYPE CURVES FOR E=0.7 **AND** θ=135 DEG. CONSTANT PRESSURE **HOLE**

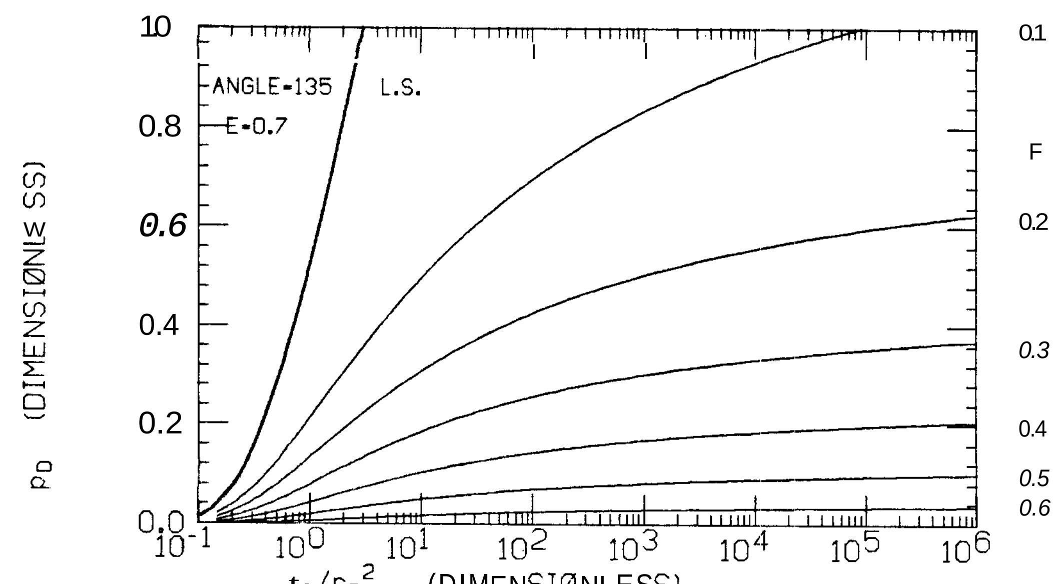

FIGURE *3.45* : INTERFERENCE SEMILOG TYPE CURVES FOR E=0.7 AND θ=135 DEG. CONSTANT PRESSURE **HOLE**

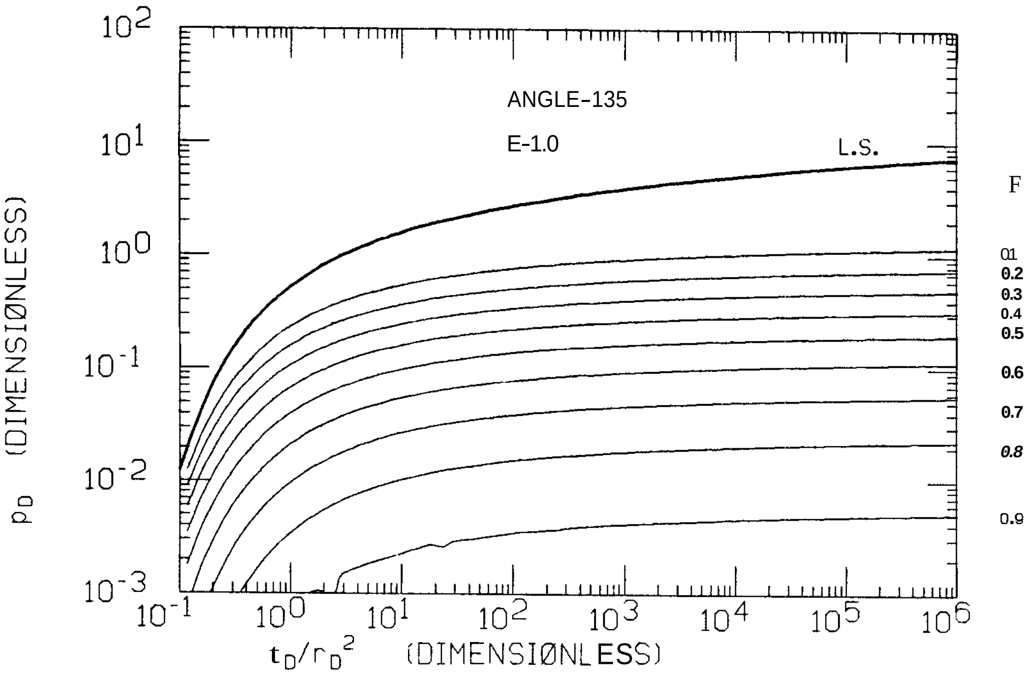

FIGURE 3.46 : INTERFERENCE LOG–LOG TYPE CURVES **FOR** E=1.0 AND θ=135 DEG.

CONSTANT PRESSURE HOLE

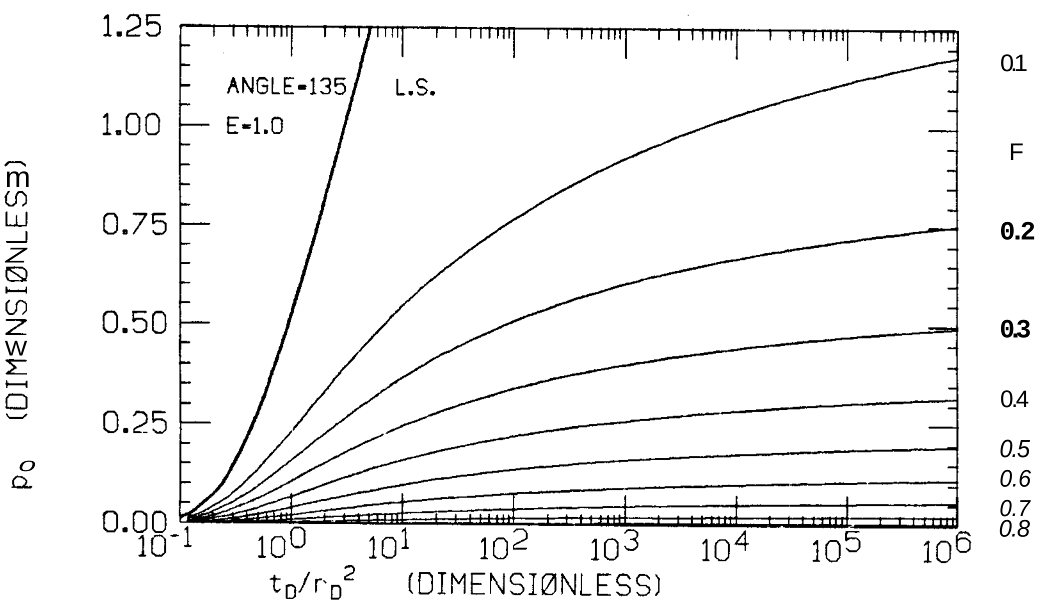

FIGURE 3.47 : INTERFEKENCE SEMILOG TYPE CURVES FOR **E=1.0** AND θ=135 DEG.

CONSTANT PRESSURE HOLE

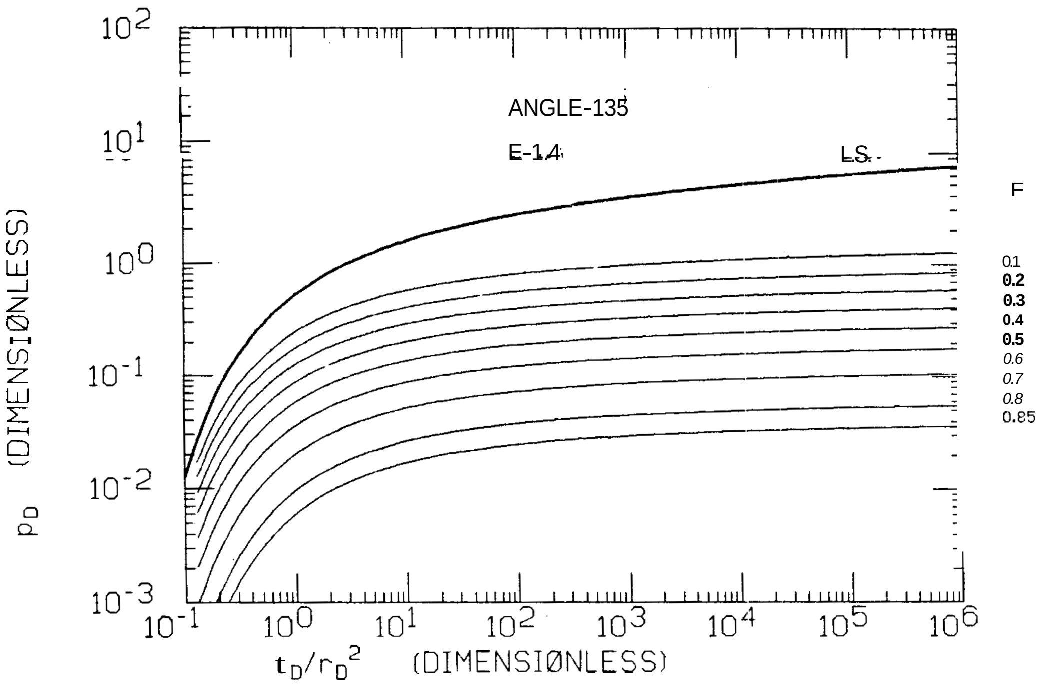

FIGURE 3.48 : INTERFERENCE LOG–LOG TYPE CURVES FOR E=1.4 AND θ=135 DEG. CONSTANT PRESSURE HOLE

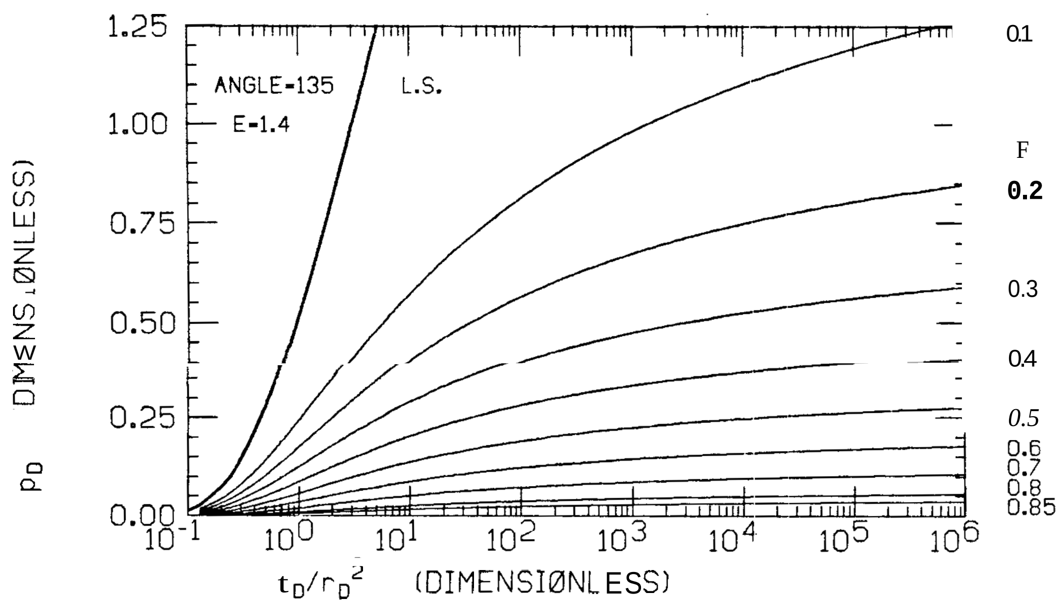

FIGURE 3.49 : INTERFERENCE SEMILOG TYPE CURVES FOR E=1.4 AND θ=135 DEG. CONSTANT PRESSURE HOLE

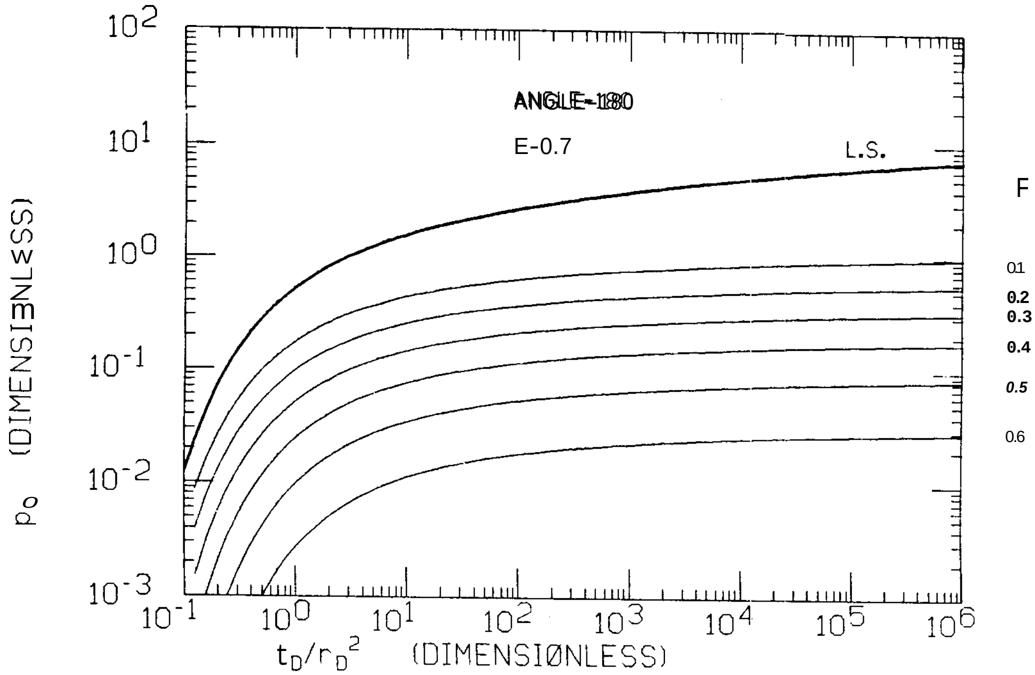

FIGURE 3.50 : INTERFERENCE LOG-LOG TYPE CURVES FOR E=0.7 AND θ=180 DEG.
CONSTANT PRESSURE HOLE

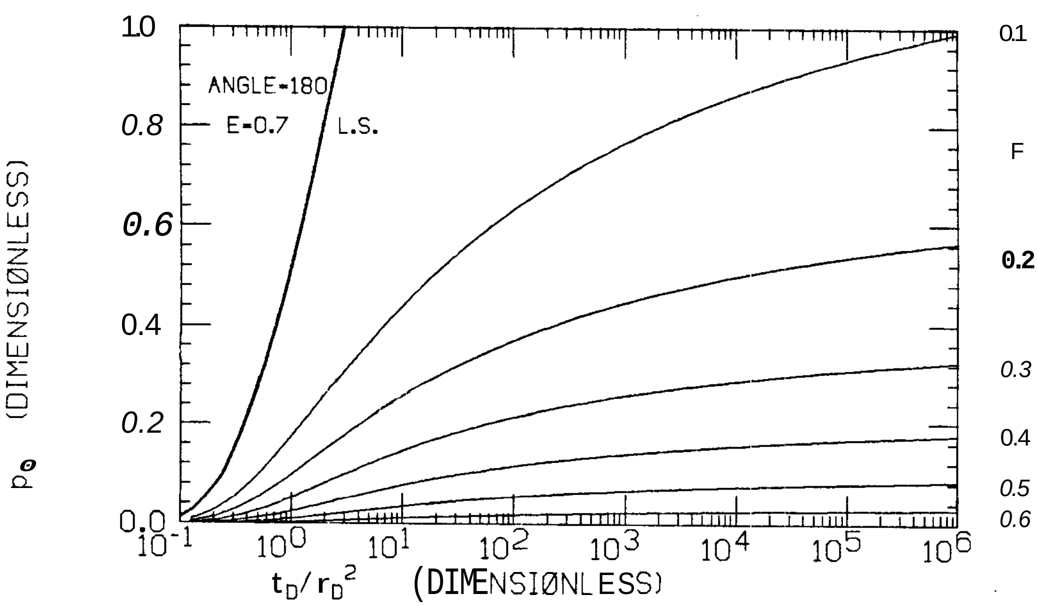

FIGURE 3.51 : INTERFERENCE SEMILOG TYPE CURVES FOR E-0.7 AND θ=180 DEG.
CONSTANT PRESSURE HOLE

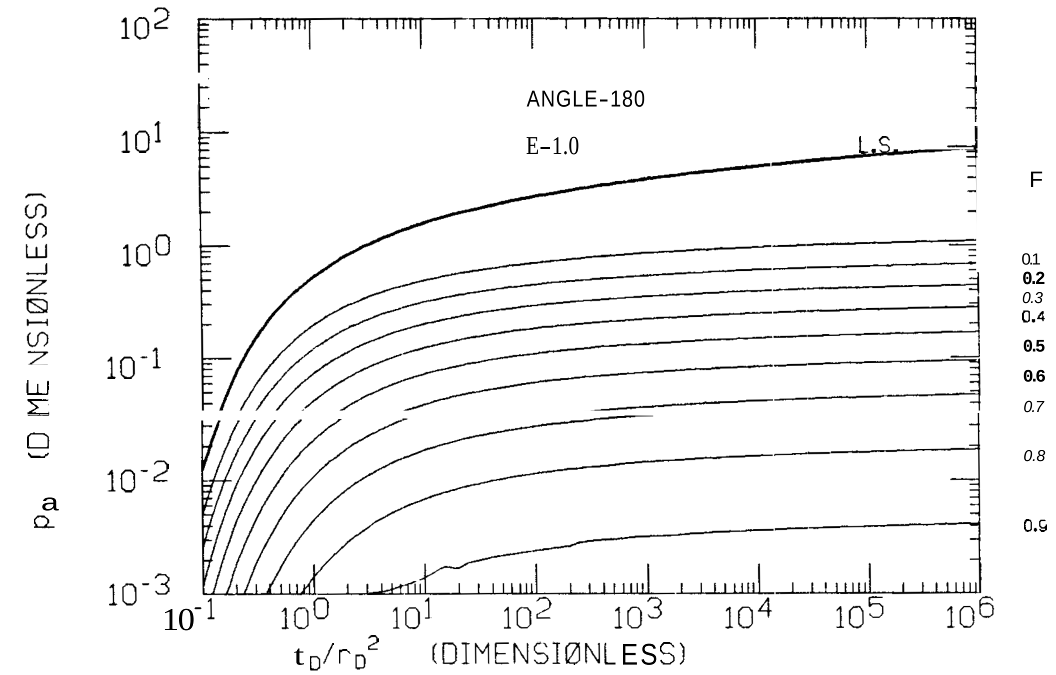

FIGURE 3.52 : INTERFERENCE LOG-LOG **TYPE** CURVES **FOR** E=1.0 AND θ=180 DEG.

CONSTANT PRESSURE HOLE

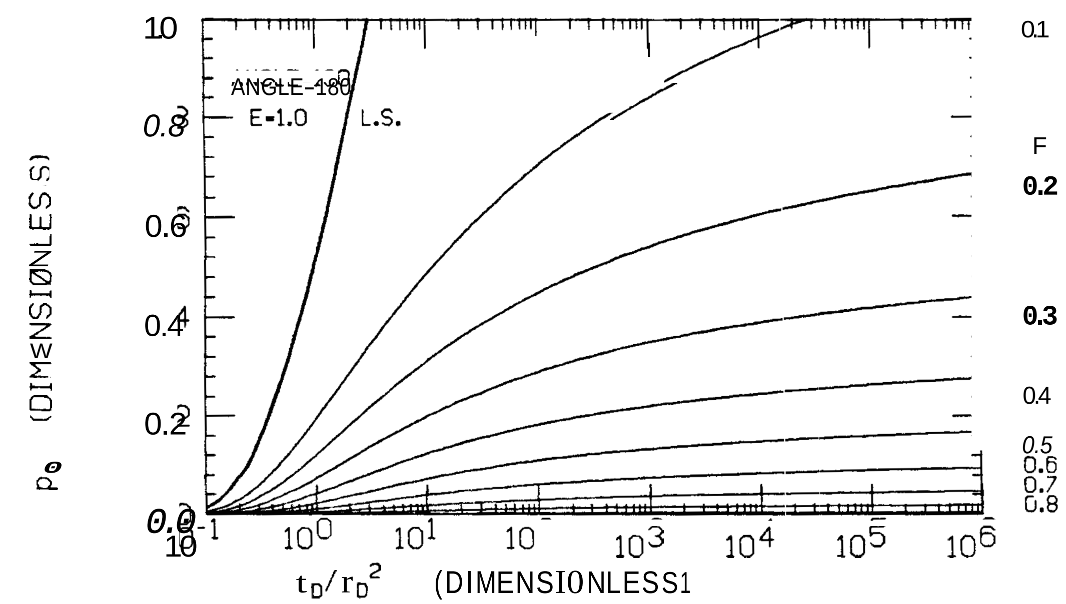

FIGURE 3.53 : INTERFERENCE SEMILOG **TYPE CURVES** FOR E=1.0 AND θ=180 DEG.

CONSTANT **PRESSURE** HOLE

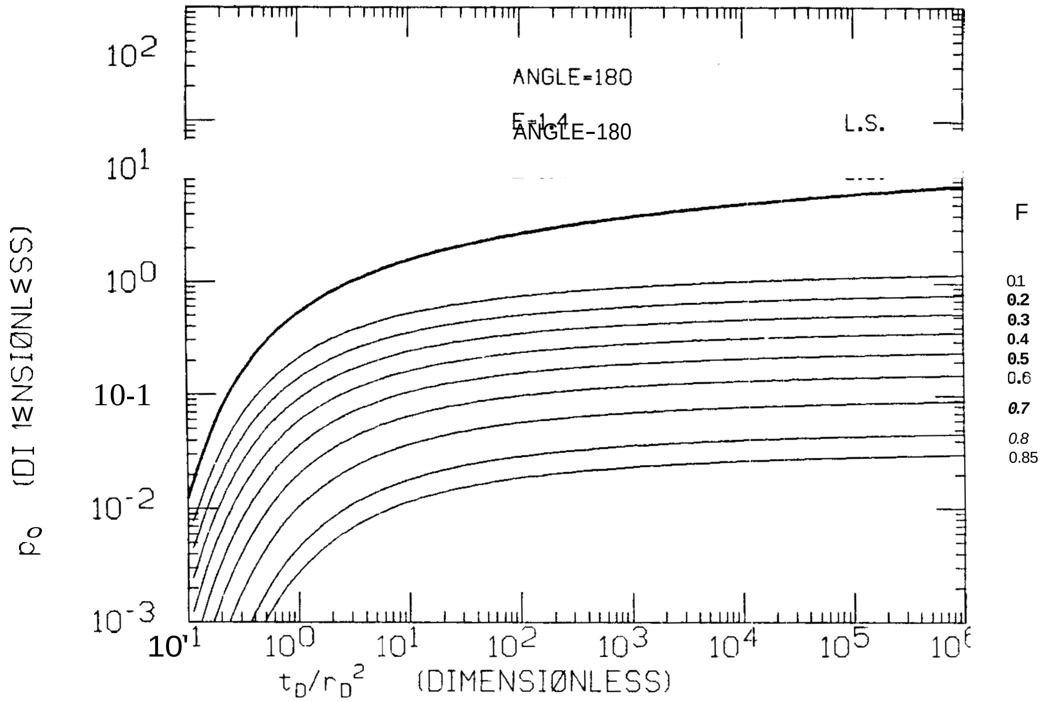

FIGURE 3.54 : INTERFERENCE LOG–LOG TYPE CURVES FOR E=1.4 AND θ=180 DEG. CONSTANT PRESSURE HOLE

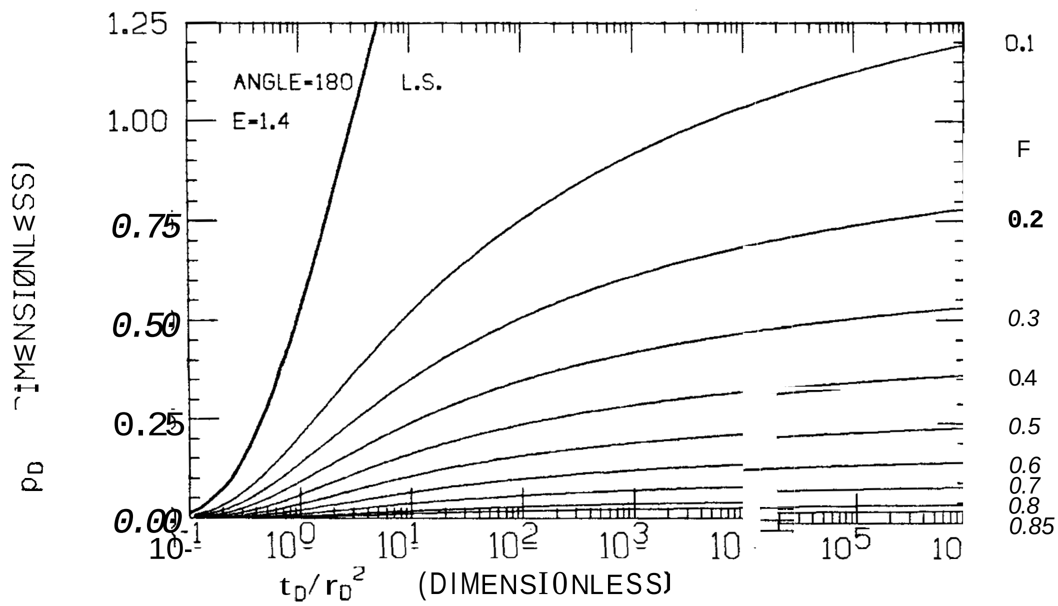

FIGURE 3.55 : INTERFERENCE SEMILOG TYPE CURVES FOR E=1.4 AND θ=180 DEG, CONSTANT PRESSURE HOLE

3.8 INTERFERENCE BETWEEN OIL AND GAS FIELDS

Two or more reservoirs can share a common aquifer. If one of the reservoirs is a gas field and the other is an oil field, the gas field may be considered as a constant pressure source. Then, the analysis presented in the previous sections can be used, the oil field being treated as a production line source.

A special case occurs when the distance between the fields is large. We can approximate both fields as line sources. This is the same as a model where one well produces at a constant rate and another well maintains a constant pressure and may be represented in the present analysis by taking a hole of a small radius.

For a source - sink model with two constant flow rate wells :

$$p_{Dss} = 2\ln(2c'-1) \approx 2\ln(2c') \tag{3.68}$$

for large c'

For the rate - pressure mdel based on the constant pressure hole model, the steady state pressure drop is given by Eq. 3.38 :

$$p_{Dss} = \ln\left(\frac{r_D}{a_D}\right) + \frac{1}{2}\ln\frac{1 - 2\dfrac{a_D^2}{r_D r_D'}\cos\theta + \left(\dfrac{a_D^2}{r_D r_D'}\right)^2}{1 - 2\dfrac{r_D}{r_D'}\cos\theta + \left(\dfrac{r_D}{r_D'}\right)^2}$$

$$\text{for } r_D < r_D' \tag{3.69}$$

Letting :

$$a_D = 1$$

$$\theta = 0$$

$$r_D = r'_D - 1$$

Equation **3.69** becomes :

$$p_{Dss} = \ln\left[\, r'_D\,(r'_D - 1)\,\right] \approx 2\,\ln(r'_D) \qquad \textbf{(3.70)}$$

for large r'_D

Equation **3.70** is equivalent to Eq. **3.68** for large r'_D since $r'_D \approx 2c'$ for the rate - pressure model. Figure 3.56 presents the transient pressure behavior for a case where $2c' = r'_D = 50$. Curve 1 is for the rate - pressure model and curve 2 is for the constant flow rate source - sink doublet model. Both these Curves have the same limiting steady state pressures. The transient part of curve 1 extends over a long time period due to the fact that the constant pressure source is not injecting any fluid at the start of the test and gradually increases the injection rate. At late time, the injection rate becomes equal to the production rate. Figure 3.57 presents semilog type curves for the rate - pressure model, for various distances between the sources.

Table 3.1 presents a comparison between the steady state pressures of the two models. As the distance between the wells becomes larger, the agreement of the long time pressures is better.

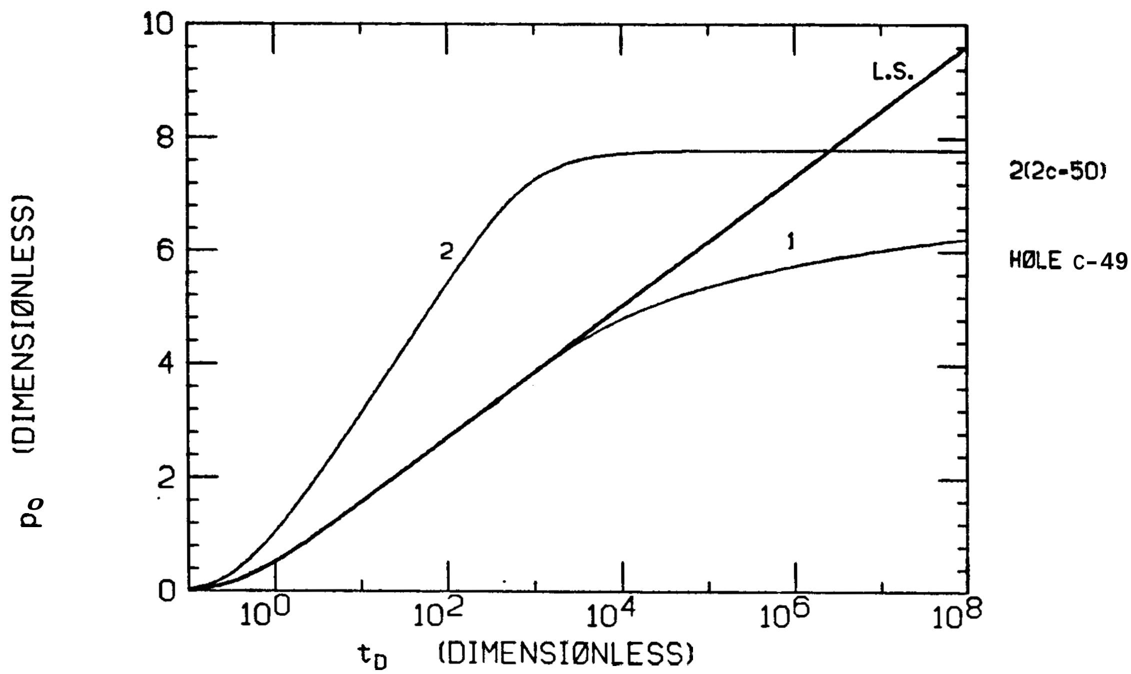

FIGURE 3.56 : A COMPARISON BETWEEN TWO CASES :

1 : A CONSTANT RATE WELL AND A CONSTANT PRESSURE WELL

2 : **TWO** CONSTANT RATE **WELLS**

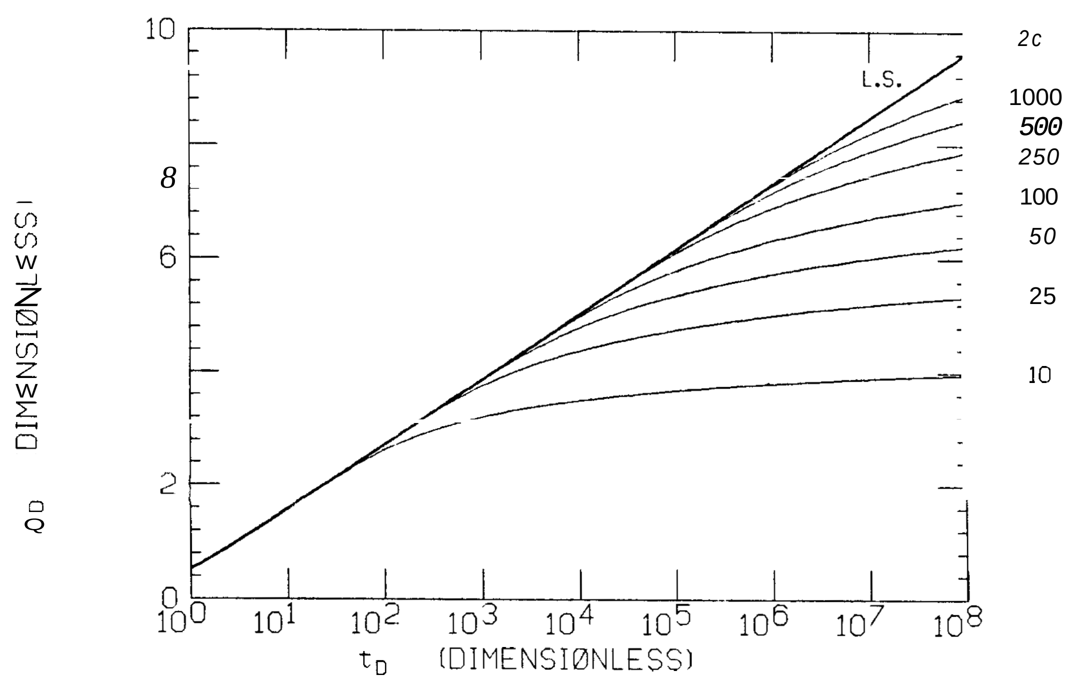

FIGURE 3.57 : SEMILOG TYPE CURVES FOR THE RATE - PRESSURE MODEL

TABLE 3.1

A COMPARISON BETWEEN THE STEADY STATE DIMENSIONLESS PRESSURE FOR TWO MODELS : 1. RATE - RATE 2. RATE - PRESSURE

(1) $r'_D = 2c'$	(2) P_{Dss} CASE 1	(3) P_{Dss} CASE 2	(4) (2)/(3) %
10	4.3944	4.4886	97.90
25	6.3561	6.3953	99.39
50	7.7836	7.8034	99.75
100	9.1902	9.2002	99.89
250	11.035	11.039	99.96
500	12.425	12.427	99.98
1000	13.814	13.815	99.99

3.9 SEMICIRCULAR AND QUARTERCIRCULAR SUBREGIONS

It is possible to have a compressible gas region near one or more sealing faults. Using the method of images, we can assemble these configurations with the circular hole solutions obtained in section 3.3.

Figures 3.58 and 3.59 present two examples of linear boundaries intersecting the constant pressure hole. Two conditions must be satisfied: the boundaries must pass through the center of the hole, and the angle between the boundaries must be an even integral part of the

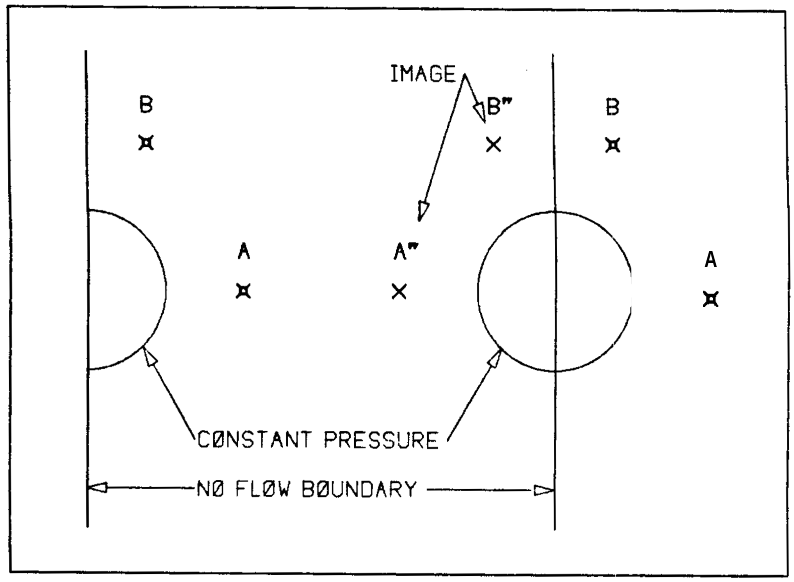

FIGURE 3.58 : SUPERPOSITION **FOR** A CONSTANT PRESSURE SEMI–CIRCLE **AND** A NO-FLOW LINEAR BOUNDARY

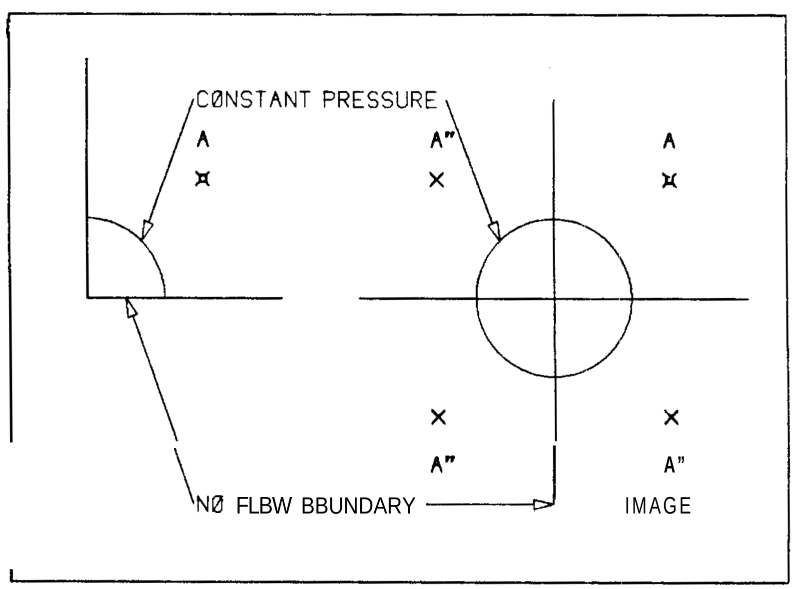

FIGURE **3.59** : SUPERPOSITION FOR A CONSTANT PRESSURE QUARTER CIRCLE BOUNDED BY NO-FLOW LINEAR BOUNDARIES full circle. In any other case, the superposition gives rise to images on Riemann surfaces. The image wells in Figs. 3.58 and 3.59 are all producers like the production well, generating the no-flow boundaries. Various combinations of injection and production images can be used to generate no-flow or constant pressure boundaries.

Figure 3.58 presents a case where a half circular gas field is bounded by an infinite no-flow linear boundary. Figure 3.60 presents the pressure behavior of well "B" for two hole sizes. For a relatively small hole, the no-flow boundary interferes with the production well and causes the pressure drop to rise above the line source, as if the constant pressure hole did not exist (curve 1). However, as time progresses, the influence of the constant pressure hole dominates the pressure behavior and the pressure approaches steady state (curve 1). The same geometry without the linear boundary is presented for comparison (curve 2).

For a relatively large hole, the effect of the hole starts dominating the pressure at an earlier time (curve 3), making it difficult to detect the no-flow boundary. The same geometry without a linear boundary is presented for comparison (curve 4).

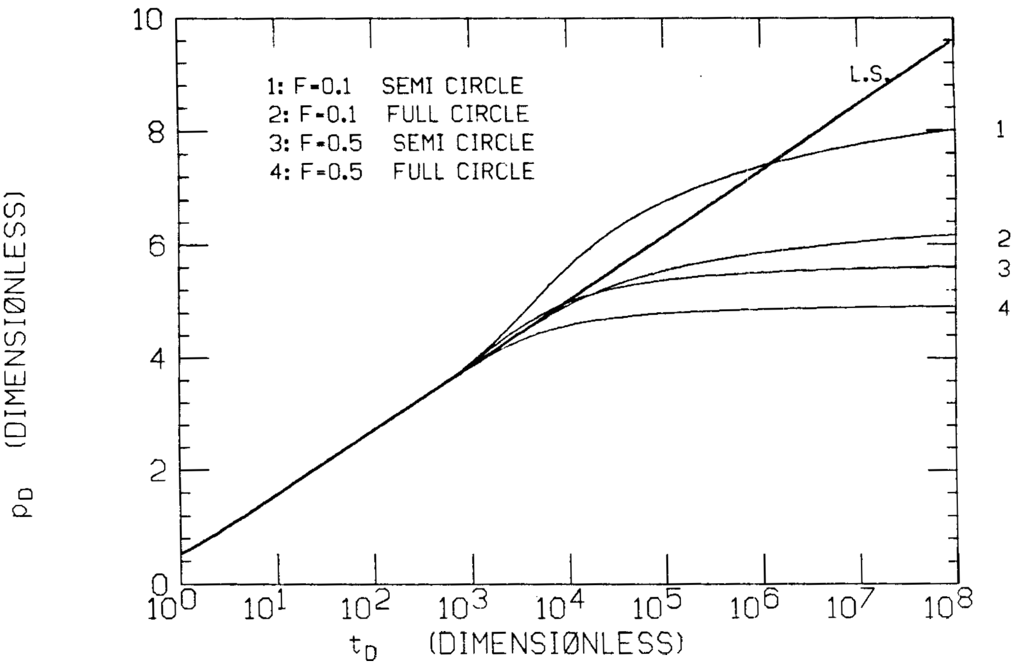

FIGURE *3.60* : SUPERPOSITION SEMILOG CURVES FOR A SEMI-CIRCLE. F=0.5 AND 0.1. ANGLE BETWEEN THE WELL AND THE BOUNDARY 22.5 DEG. CONSTANT PRESSURE HOLE

CHAPTER 4 : NO-FLOW INTERNAL CIRCULAR BOUNDARY

This chapter presents the transient pressure analysis for a well near an impermeable circular boundary. The problem is mathematically stated and solved using the Laplace transformation method. Then, the practical applications of the solution are discussed.

4.1 PROBLEM STATEMENT

The problem is two dimensional with one axis of symmetry along the line between the well and the center of the hole (see Fig. 4.1). We assume that the system has: an infinite radial extent, a constant thickness, viscosity, porosity and permeability, small pressure gradients and single phase laminar isothermal flow.

The pressure at any given point is a function of three parameters: distance r, angle θ and time t, Hence, $p(r,\theta,t)$ must satisfy the following equations :

$$\frac{\partial^2 p}{\partial r^2} + \frac{1}{r}\frac{\partial p}{\partial r} + \frac{1}{r^2}\frac{\partial^2 p}{\partial \theta^2} = \frac{1}{\eta}\frac{\partial p}{\partial t} \tag{4.1}$$

$$p(\infty,\theta,t) = 0 \qquad \text{or } p_i \tag{4.2}$$

$$\frac{\partial p(a,\theta,t)}{\partial r} = 0 \tag{4.3}$$

$$\lim_{R\to 0} R\,\frac{\partial p}{\partial R} = -\frac{q\mu}{2\pi kh} \tag{4.4}$$

$$p(r,\theta,t) = 0 \qquad \text{or } p_i \tag{4.5}$$

where :

$$R^2 = r^2 + r'^2 - 2rr'\cos(\theta) \tag{4.6}$$

$$\eta = \frac{k}{\phi\mu c_t} \tag{4.7}$$

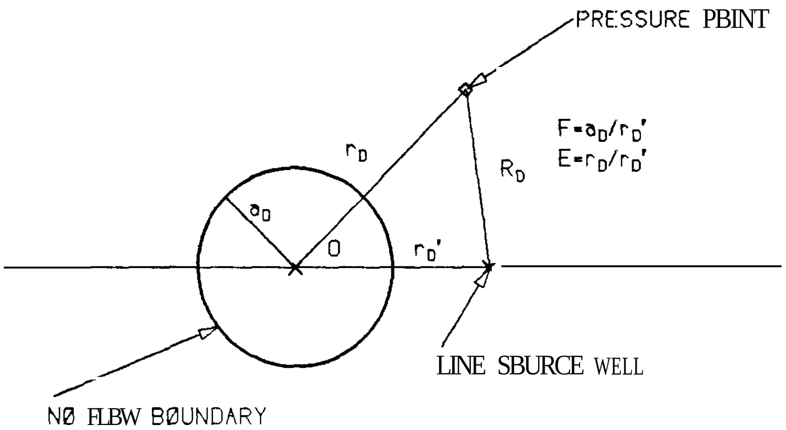

FIGURE 4.1 : A SCHEMATIC DIAGRAM OF THE NO-FLOW BOUNDARY HOLE SYSTEM

4.2 LAPLACE TRANSFORMATION

We transform Eqs. 4.1 to 4.4 into Laplace space using the initial boundary condition of Eq. 4.5. In general :

$$p(r,\theta,t) \rightarrow \bar{p}(r,\theta,s)$$

$$\frac{\partial^2 \bar{p}}{\partial r^2} + \frac{1}{r}\frac{\partial \bar{p}}{\partial r} + \frac{1}{r^2}\frac{\partial^2 \bar{p}}{\partial \theta^2} - \frac{s}{\eta}\bar{p} = 0 \qquad (4.8)$$

$$\bar{p}(\infty,\theta,s) = 0 \qquad (4.9)$$

$$\frac{\partial \bar{p}(a,\theta,s)}{\partial r} = 0 \qquad (4.10)$$

$$\lim_{R\to 0} R\,\frac{\partial \bar{p}}{\partial R} = -\frac{\quad}{\quad} \qquad (4.11)$$

4.3 THE LAPLACE TRANSFORMATION SOLUTION

The solution for the homogeneous boundary conditions, Eqs. 4.8, 4.9 and 4.11, in a coordinate system centered at the well is :

$$\bar{p} = \frac{q\mu}{2\pi s k h} K_0(R\sqrt{s/\eta}\,) \qquad (4.12)$$

By the addition theorem for Bessel Functions, Carslaw and Jaeger (1946, p. 377), we translate Eq. 4.12 to a coordinate system centered at the center of the hole :

$$\bar{p} = \frac{q\mu}{2\pi skh} \sum_{n=-\infty}^{\infty} \cos(n\theta)\ I_n(r\sqrt{s/\eta})K_n(r'\sqrt{s/\eta})$$

$$\text{for } r < r' \tag{4.13}$$

$$\bar{p} = \frac{q\mu}{2\pi skh} \sum_{n=-\infty}^{\infty} \cos(n\theta)\ I_n(r'\sqrt{s/\eta})K_n(r\sqrt{s/\eta})$$

$$\text{for } r > r' \tag{4.14}$$

In order to satisfy the condition of no-flow at the internal boundary, we assume that $\bar{p}$ takes the following form :

$$\bar{p} = \frac{q\mu}{2\pi skh} \sum_{n=-\infty}^{\infty} \cos(n\theta)\ [\ I_n(r\sqrt{s/\eta})K_n(r'\sqrt{s/\eta}) + A_nK_n(r\sqrt{s/\eta})\ ]$$

$$\text{for } r < r' \tag{4.15}$$

$$\bar{p} = \frac{q\mu}{2\pi skh} \sum_{n=-\infty}^{\infty} \cos(n\theta)\ [\ I_n(r'\sqrt{s/\eta})K_n(r\sqrt{s/\eta}) + A_nK_n(r\sqrt{s/\eta})\ ]$$

$$\text{for } r > r' \tag{4.16}$$

The constants A_n are set by the boundary condition. The particular solution, K_n , is picked in order to satisfy the condition at infinite radii. Equations 4.15 and 4.16 can be written as :

$$\bar{p} = \frac{q\mu}{2\pi skh} \sum_{n=0}^{\infty} \varepsilon_n\cos(n\theta)\ [\ I_n(r\sqrt{s/\eta})K_n(r'\sqrt{s/\eta}) + A_nK_n(r\sqrt{s/\eta})\ ]$$

$$\text{for } r < r' \tag{4.17}$$

$$\bar{p} = \frac{q\mu}{2\pi skh} \sum_{n=0}^{\infty} \varepsilon_n \cos(n\theta) \left[I_n(r'\sqrt{s/\eta})K_n(r\sqrt{s/\eta}) + A_n K_n(r\sqrt{s/\eta}) \right]$$

$$\text{for } r > r' \tag{4.18}$$

where :

for $n = 0$, $\varepsilon_n = 1$

for $n > 1$, $\varepsilon_n = 2$

The internal boundary condition determines the coeficients A_n :

$$A_n = - \frac{K_n(r'\sqrt{s/\eta})I_n'(a\sqrt{s/\eta})}{K_n'(a\sqrt{s/\eta})} \tag{4.19}$$

where $K_n'(z)$ and $I_n'(z)$ denote the derivatives of the Modified Bessel Functions.

Substituting **Eq.** 4.19 into **Eqs.** 4.17 and 4.18 yields :

$$\bar{p} = \frac{q\mu}{2\pi skh} \sum_{n=0}^{\infty} \varepsilon_n \cos(n\theta) \Big[I_n(r\sqrt{s/\eta})K_n(r'\sqrt{s/\eta})$$

$$- \frac{K_n(r'\sqrt{s/\eta})I_n'(a\sqrt{s/\eta})}{K_n'(a\sqrt{s/\eta})} K_n(r\sqrt{s/\eta}) \Big]$$

$$\text{for } r < r' \tag{4.20}$$

$$\bar{p} = \frac{q\mu}{2\pi skh} \sum_{n=0}^{\infty} \varepsilon_n \cos(n\theta) \Big[I_n(r'\sqrt{s/\eta})K_n(r\sqrt{s/\eta})$$

$$- \frac{K_n(r'\sqrt{s/\eta})I_n'(a\sqrt{s/\eta})}{K_n'(a\sqrt{s/\eta})} K_n(r\sqrt{s/\eta}) \Big]$$

$$\text{for } r > r' \tag{4.21}$$

Using Eqs. *3.22* to *3.27* yields :

$$\bar{p}_D = \frac{1}{s} \sum_{n=0}^{\infty} \varepsilon_n \cos(n\theta) \Big[I_n(r_D\sqrt{s})K_n(r_D'\sqrt{s})$$

$$- \frac{K_n(r_D'\sqrt{s})I_n'(a_D\sqrt{s})}{K_n'(a_D\sqrt{s})} K_n(r_D\sqrt{s})$$

$$\text{for } r_D < r_D' \tag{4.22}$$

$$\bar{p}_D = \frac{1}{s} \sum_{n=0}^{\infty} \varepsilon_n \cos(n\theta) \Big[I_n(r_D'\sqrt{s})K_n(r_D\sqrt{s}$$

$$- \frac{K_n(r_D'\sqrt{s})I_n'(a_D\sqrt{s})}{K_n(a_D\sqrt{s})} K_n(r_D\sqrt{s})$$

$$\text{for } rD > rD \tag{4.23}$$

Equation *4.22* is identical to Eq. *4.23* with r_D and r_D' interchanged.

The Laplace solution was inverted numerically using the algorithm developed by Stehfest *(1970)*. A description of the algorithm is presented in Sections 3.5 and 4.5, and the computer application is discussed in Appendix G.

4.4 THE ANALYTICAL SOLUTION

The following presents the analytical inversion of the Laplace solution into the real time solution using the method of residues.

The Laplace solution of Eq. 4.22 can be written as :

$$\bar{p}_D = \frac{1}{s} \sum_{n=0}^{\infty} \varepsilon_n \cos(n\theta) \frac{1}{K_n'(a_D\sqrt{s})} \Big[I_n(r_D\sqrt{s})K_n(r_D'\sqrt{s})K_n'(a_D\sqrt{s})$$

$$- K_n(r_D\sqrt{s})I_n'(a_D\sqrt{s})K_n(r_D'\sqrt{s}) \Big]$$

$$\text{for} \quad r_D < r_D' \tag{4.24}$$

At $s=0$ we have a single pole, hence, we can use the following small argument approximations for the Modified Bessel Functions :

$$K_0(z) = -\left[\ln\left(\frac{z}{2}\right) + \gamma \right] \tag{4.25}$$

$$K_n(z) = 2^{n-1}(n-1)!z^{-n} \tag{4.26}$$

$$K_0'(z) = - K_1(z) \tag{4.27}$$

$$K_n'(z) = -\frac{1}{2} \left[K_{n-1}(z) + K_{n+1}(z) \right] \tag{4.28}$$

$$I_0(z) = 1 \tag{4.29}$$

$$I_n(z) = 2^{-n} z^n / n! \tag{4.30}$$

$$I_0'(z) = I_1(z) \tag{4.31}$$

$$I_n'(z) = \frac{1}{2} \left[I_{n-1}(z) + I_{n+1}(z) \right] \tag{4.32}$$

Substituting Eqs. 4.25 to 4.32 into Eq. 4.24 yields :

$$p_{D1} = \frac{1}{s} - \ln\left(\frac{r'_D}{2}\right) - \gamma - \frac{1}{2} \ln(s) + \sum_{n=1}^{\infty} \frac{\cos(n\theta)}{n} \left[\left(\frac{r_D}{r'_D}\right)^n + \left(\frac{a_D^2}{r_D r'_D}\right)^n \right] \tag{4.33}$$

Using the following relations :

$$\sum_{k=1}^{\infty} \frac{1}{k} p^k \cos(k\theta) = \frac{1}{2} \ln(1 - 2p\cos\theta + p^2) \tag{4.34}$$

$$\frac{1}{s} \; \text{-b} \rightarrow b \tag{4.35}$$

$$\frac{\ln(s)}{s} \rightarrow -\gamma - \ln(t_D) \tag{4.36}$$

we find that :

$$p_{D1} = -\ln\left(\frac{r'_D}{2}\right) - \frac{\gamma}{2} + \frac{1}{2}\ln(t_D) - \frac{1}{2}\ln\left\{\left[1 - 2\frac{r_D}{r'_D}\cos\theta + \left(\frac{r_D}{r'_D}\right)^2\right]\right.$$

$$\left. * \left[1 - 2\frac{a_D^2}{r_D r'_D}\cos\theta + \left(\frac{a_D^2}{r_D r'_D}\right)^2\right]\right\}$$

$$\text{for } r_D < r'_D \tag{4.37}$$

$$p_{D1} = -\ln\left(\frac{r_D}{2}\right) - \frac{\gamma}{2} + \frac{1}{2}\ln(t_D) - \frac{1}{2}\ln\left\{\left[1 - 2\frac{r'_D}{r_D}\cos\theta + \left(\frac{r'_D}{r_D}\right)^2\right]\right.$$

$$\left. \cdot \left[1 - 2\frac{a_D^2}{r_D r'_D}\cos\theta + \left(\frac{a_D^2}{r_D r'_D}\right)^2\right]\right\}$$

$$\text{for } r_D > r'_D \tag{4.38}$$

We can see that by factoring the term $(r'_D/r_D)^2$ out of the last term in Eq. *4.38*, the equation becomes identical to Eq. *4.37*. This is expected due to the reciprocity principle.

Equation *4.38* can be written as follows :

$$p_{D1} = -\ln\left(\frac{r_D}{2}\right) - \frac{\gamma}{2} + \ln(t_D) - \frac{1}{2}\ln\left[1 - 2\frac{r'_D}{r_D}\cos\theta + \left(\frac{r'_D}{r_D}\right)^2\right]$$

$$- \frac{1}{2}\ln\left[1 - 2\frac{a_D^2}{r_D r'_D}\cos\theta + \left(\frac{a^2}{r_D r'_D}\right)^2\right] \tag{4.39}$$

Using the definition of R_D in Eq. *4.6* yields :

$$p_{D1} = \frac{1}{2}\left[\ln\left(\frac{t_D}{R_D^2}\right) + 0.80907 \right] - \frac{1}{2} \ln\left[1 - 2 \frac{a_D^2}{r_D R_D} \cos\theta + \left(\frac{a_D^2}{r_D R_D}\right)^2 \right] \tag{4.40}$$

The first term in Eq. 4.40 is the long time approximation for the line source exponential integral solution. Hence, the long time behavior of p_D has a line source term and a deviation term.

When $s \neq 0$, we use the residues at the roots of $K_n'(a_D\sqrt{s})$. Letting $\xi_{n/m}$ denote the m^{th} zero of $K_n'(a_D\sqrt{s}) = K_n'(\xi a_D)$ and using the method of residues, we evaluate the inversion of p_{D2}:

$$\mathrm{RES}(\xi_{n/m}^2) = \lim_{s \to \xi_{n/m}^2} \sum_{n=0}^{\infty} \varepsilon_n \cos(n\theta)$$

$$\cdot \frac{(s - \xi_{n/m}^2)\, e^{st_D}\, K_n(r_D'\sqrt{s})}{s\, K_n'(a_D\sqrt{s})}$$

$$\cdot \left[I_n(r_D\sqrt{s})K_n'(a_D\sqrt{s}) - K_n(r_D\sqrt{s})I_n'(a_D\sqrt{s}) \right] \tag{4.41}$$

Rearranging Eq. 4.41 yields :

$$\mathrm{RES}(\xi^2_{n/m}) = \sum_{n=0}^{\infty} \varepsilon_n \cos(n\theta)\, B_n \frac{e^{\xi^2_{n/m} t_D} K_n(\xi_{n/m} r'_D)}{\xi^2_{n/m}} \tag{4.42}$$

where :

$$B_n = \lim_{s \to \xi^2_{n/m}} \frac{(s + \xi^2_{n/m})}{K_n'(a_D\sqrt{s}\,)}$$

$$\cdot \left[\, I_n(r_D\sqrt{s}\,)K_n'(a_D\sqrt{s}\,) - K_n(r_D\sqrt{s}\,)I_n'(a_D\sqrt{s}\,)\,\right] \tag{4.43}$$

Using L'Hôpital's rule, we evaluate B_n :

$$B_n = -\frac{2\xi_{n/m} K_n(\xi_{n/m} r_D) I_n'(\xi_{n/m} a_D)}{a_D\, K_n''(\xi_{n/m} a_D)} \tag{4.44}$$

where $K_n''(z)$ denotes the second derivative of K. From Bickley (1957) we find that :

$$K_n''(z) = \frac{1}{4}\left[\, K_{n-2}(z) + 2K_n(z) + K_{n+2}(z)\,\right] \tag{4.45}$$

$$K_{n-1}(z) = -\frac{2n}{z} K_n(z) + K_{n+1}(z) \tag{4.46}$$

$$K_n'(z) = -K_{n+1}(z) + \frac{2n}{z} K_n(z) \tag{4.47}$$

Using Eqs. 4.46 and 4.47 and the fact that $K_n'(z) = 0$, Eq. 4.45 reduces to the following :

$$K_n''(z) = (1 + \frac{n^2}{z^2})\, K_n(z) \qquad (4.48)$$

In Bickley (1957), we find that :

$$I_n'(z) = I_{n-1}(z) - \frac{n}{z}\, I_n(z) \qquad (4.49)$$

Substituting Eqs. 4.48 and 4.49 into Eq. 4.44 yields :

$$B_n = - \frac{2\xi_{n/m} K_n(\xi_{n/m} r_D) [\, I_{n-1}(\xi_{n/m} a_D) - \frac{n}{\xi_{n/m} a_D} I_n(\xi_{n/m} a_D)}{a_D\, (1 + \frac{n^2}{\xi^2_{n/m} a_D})\, K_n(\xi_{n/m} a_D)} \qquad (4.50)$$

substituting Eq. 4.50 into Eq. 4.42 yields :

$$\mathrm{RES}(\xi^2_{n/m}) = \sum_{n=0}^{\infty} \varepsilon_n \cos(n\theta)\, \frac{e^{\xi^2_{n/m} t_D}\, K_n(\xi_{n/m} r_D')}{a_D\, \xi^2_{n/m}}$$

$$\cdot \frac{2\xi_{n/m} K_n(\xi_{n/m} r_D) [\, \frac{n}{\xi_{n/m} a_D} I_n(\xi_{n/m} a_D) - I_{n-1}(\xi_{n/m} a_D)\,]}{(1 + \frac{n^2}{\xi^2_{n/m} a_D^2})\, K_n(\xi_{n/m} a_D)} \qquad (4.51)$$

Now, in order to complete the inversion of $\bar{p}_{D2}$, we use the residues from Eq. 4.51 :

$$p_{D2} = 2 \sum_{n=0}^{w} \sum_{m \text{ roots}} \varepsilon_n \cos(n\theta)\ e^{\xi^2_{n/m} t_D}$$

$$\cdot \frac{K_n(\xi_{n/m} r'_D) K_n(\xi_{n/m} r_D) \left[\frac{n}{\xi_{n/m} a_D} I_n(\xi_{n/m} a_D) - I_{n-1}(\xi_{n/m} a_D) \right]}{\left(1 + \frac{n^2}{\xi^2_{n/m} a^2_D}\right) K_n(\xi_{n/m} a_D)} \tag{4.52}$$

We can express p_{D2} in terms of Bessel Functions instead of Modified Bessel Functions using the following relations :

$$I_n(z) = i^{-n} J_n(iz) \tag{4.53}$$

$$K_n(z) = \frac{\pi}{2} i^{n+1} \left[J_n(iz) + Y_n(iz) \right] = \frac{\pi}{2} i^{n+1} H_n^{(1)}(z) \tag{4.54}$$

$$I_n'(z) = i^{-n+1} J_n'(iz) \tag{4.55}$$

$$K_n'(z) = \frac{\pi}{2} i^{n+2} \left[J_n'(iz) + iY_n'(iz) \right] = \frac{\pi}{2} i^{n+2} H_n'^{(1)}(z) \tag{4.56}$$

Substituting Eqs. 4.53 to 4.56 into 4.24 yields :

$$\bar{p}_{D2} = \frac{\pi}{2is} \sum_{n=0}^{\infty} \varepsilon_n \cos(n\theta) \frac{H_n^{(1)}(ir_D'\sqrt{s})}{H_n'^{(1)}(ia_D\sqrt{s})} \left[H_n'^{(1)}(ia_D\sqrt{s}) J_n(ir_D\sqrt{s}) \right.$$

$$\left. - H_n^{(1)}(ir_D\sqrt{s}) J_n'(ia_D\sqrt{s}) \right] \tag{4.57}$$

$H_n'^{(1)}(ia_D\sqrt{s})$ has zeroes at $ia_D\sqrt{s} = \mu_1, \mu_2, \ldots \mu_m$ and $\bar{p}_{D2}$ has simple poles at :

$$s = -\left(\frac{\mu_m}{a_D}\right)^2 = -\alpha_m^2 \tag{4.58}$$

$$\alpha_m = \left(\frac{\mu_m}{a_D}\right) = i\sqrt{s} \tag{4.59}$$

where $\alpha_{n/m}$ denotes the m^{th} zero of $H_n'^{(1)}(ia_D\sqrt{s})$. Using the method of residues, we evaluate the inversion of $\bar{p}_{D2}$:

$$RES(-\alpha^2_{n/m}) = \frac{\pi}{2} \lim_{s \to \alpha^2_{n/m}} \sum_{n=0}^{\infty} \varepsilon_n \cos(n\theta)$$

$$\cdot \frac{(s + \alpha^2_{n/m})\ e^{st_D}\ H_n^{(1)}(ir_D'\sqrt{s})}{is\ H_n'^{(1)}(ia_D\sqrt{s})}$$

$$\cdot \left[H_n'^{(1)}(ia_D\sqrt{s}) J_n(ir_D\sqrt{s}) - H_n^{(1)}(ir_D\sqrt{s}) J_n'(ia_D\sqrt{s}) \right]$$

$$(4.60)$$

Rearranging Eq. 4.60 :

$$\mathrm{RES}(-\alpha^2_{n/m}) = \frac{\pi}{2} \sum_{n=0}^{\infty} \varepsilon_n \cos(n\theta)\, A_n \frac{e^{-\alpha_{n/m}^2 t_D} H_n^{(1)}(\alpha_{n/m} r_D)}{-\alpha^2_{n/m}} \tag{4.61}$$

where :

$$A_n = \lim_{s \to \alpha^2_{n/m}} \frac{(s + \alpha^2_{n/m})}{i H_n'^{(1)}(i a_D \sqrt{s})}$$

$$\cdot \left[H_n'^{(1)}(i a_D \sqrt{s}) J_n(i r_D \sqrt{s}) - H_n^{(1)}(i r_D \sqrt{s}) J_n'(i a_D \sqrt{s}) \right] \tag{4.62}$$

Using L'Hôpital's rule, we evaluate A_n :

$$A_n = \lim_{s \to \alpha^2_{n/m}} \frac{1}{H_n''^{(1)}(i a_D \sqrt{s}) \left(\frac{a_D i^2}{2\sqrt{s}} \right)}$$

$$\cdot \left\{ \left[H_n'^{(1)}(i a_D \sqrt{s}) J_n(i r_D \sqrt{s}) - H_n^{(1)}(i r_D \sqrt{s}) J_n'(i a_D \sqrt{s}) \right] \right.$$

$$+ (s + \alpha^2_{n/m}) \frac{d}{ds} \left[H_n'^{(1)}(i a_D \sqrt{s}) J_n(i r_D \sqrt{s}) \right.$$

$$\left. \left. - H_n^{(1)}(i r_D \sqrt{s}) J_n'(i a_D \sqrt{s}) \right] \right\}$$

$$= \lim_{s \to \alpha^2_{n/m}} - \frac{2\sqrt{s}\, J_n'(ia_D\sqrt{s})H_n^{(1)}(ir_D\sqrt{s})}{a_D\, H_n''^{(1)}(ia_D\sqrt{s})}$$

Substituting $s = - a^2_{n/m}$ yields :

$$A_n = - \frac{2i\alpha_{n/m} J_n'(ia_D\sqrt{s})H_n^{(1)}(ir_D\sqrt{s})}{a_D\, H_n''^{(1)}(ia_D\sqrt{s})} \tag{4.63}$$

From Bickley (1957, p. xxxiii), we find that :

$$H_n''(z) = \frac{1}{4}\left[H_{n-2}(z) - 2\, H_n(z) + H_{n+2}(z) \right] \tag{4.64}$$

$$H_{n-1}(z) = - H_{n+1}(z) + \frac{2n}{z} H_n(z) \tag{4.65}$$

$$H_n'(z) = - H_{n-1}(z) + \frac{n}{z} H_n(z) \tag{4.66}$$

Using Eqs. *4.65* and *4.66* and the fact that $H_n'(z) = 0$, Eq. *4.64* becomes :

$$H_n''^{(1)}(\alpha_{n/m}a_D) = H_n^{(1)}(\alpha_{n/m}a_D)\left(\frac{n^2}{\alpha^2_{n/m}\, a^2_D} - 1\right) \tag{4.67}$$

Equation *4.49* holds for $J_n(z)$, hence :

$$J_n'(\alpha_{n/m}a_D) = J_{n-1}(\alpha_{n/m}a_D) - \left(\frac{n}{\alpha_{n/m}a_D}\right) J_n(\alpha_{n/m}a_D) \tag{4.68}$$

Substituting Eqs. *4.67* and *4.68* into *4.63* yields :

$$A_n = \frac{2i\left(J_{n-1}(\alpha_{n/m}a_D) - \frac{n}{\alpha_{n/m}a_D} J_n(\alpha_{n/m}a_D)\right)H_n^{(1)}(\alpha_{n/m}r_D)}{a_D\left(1 - \frac{n^2}{\alpha^2_{n/m}\, a^2_D}\right) H_n^{(1)}{}_D(\alpha_{n/m}a_D)} \qquad (4.69)$$

Substituting Eq. 4.69 into Eq. 4.61 yields :

$$\text{RES}\ (-a^2_{n/m}) = \frac{\pi}{2} \sum_{n=0}^{\infty} \varepsilon_n \cos(n\theta)\ \frac{2i\ e^{-\alpha^2_{n/m} t_D}\ H_n^{(1)}(\alpha_{n/m}r'_D)}{-\ \alpha^2_{n/m}\ a_D}$$

$$\cdot \frac{\left[\ J_{n-1}(\alpha_{n/m}a_D) - \frac{n}{a_{n/m}a_D} J_n(\alpha_{n/m}a_D)\ \right] H_n^{(1)}(\alpha_{n/m}r_D)}{\left(1 - \frac{n^2}{a2_{n/m}\ a2_D}\right) H_n^{(1)}(\alpha_{n/m}a_D)}$$

(4.70)

Now, in order to complete the inversion of $\bar{p}_{D2}$, we use the residues of Eq. 4.70 :

$$p_{D2} = -\ \pi \sum_{n=0}^{\infty} \sum_{m\ \text{roots}} \varepsilon_n \cos(n\theta)\ e^{-\alpha^2_{n/m} t_D}\ \frac{H_n^{(1)}(\alpha_{n/m}r'_D)}{\alpha^2_{n/m}\ a_D}$$

$$\cdot \frac{\left[\ J_{n-1}(\alpha_{n/m}a_D) - \frac{n}{a_{n/m}a_D} J_n(\alpha_{n/m}a_D)\ \right] H_n^{(1)}(\alpha_{n/m}r_D)}{\left(1 - \frac{n^2}{a^2_{n/m}\ a^2_D}\right) H_n^{(1)}(\alpha_{n/m}a_D)} \qquad (4.71)$$

Finally, the complete real time solution is $p_D = p_{D1} + p_{D2}$. In terms of Modified Bessel Functions, the solution is :

$$p_D = \frac{1}{2}\left[\ln\left(\frac{t_D}{R_D^2}\right) + 0.80907 \right] - \frac{1}{2}\ln\left[1 - 2\frac{a_D^2}{r_D r_D'}\cos\theta + \left(\frac{a_d^2}{r_D r_D'}\right)^2 \right]$$

$$+ 2\sum_{n=0}^{\infty}\sum_{m\ \mathrm{roots}} \varepsilon_n \cos(n\theta)\, e^{\xi_{n/m}^2 t_D}$$

$$\cdot \frac{K_n(\xi_{n/m} r_D')K_n(\xi_{n/m} r_D)\left[\frac{n}{\xi_{n/m} a_D} I_n(\xi_{n/m} a_D) - I_{n-1}(\xi_{n/m} a_D) \right]}{\left(1 + \frac{n^2}{\xi_{n/m}^2 a_D^2}\right) K_n(\xi_{n/m} a_D)}$$

$$\text{for} \quad r_D < r_D' \qquad (4.72)$$

In terms of Bessel Functions, the solution is :

$$p_D = \frac{1}{2}\left[\ln\left(\frac{t_D}{R_D^2}\right) + 0.80907 \right] - \frac{1}{2}\ln\left[1 - 2\frac{a_D^2}{r_D r_D'}\cos\theta + \left(\frac{a_D^2}{r_D r_D'}\right)^2 \right]$$

$$- \pi \sum_{n=0}^{\infty}\sum_{m\ \mathrm{roots}} \varepsilon_n \cos(n\theta)\, e^{-\alpha_{n/m}^2 t_D} \frac{i\, H_n^{(1)}(\alpha_{n/m} r_D')}{\alpha_{n/m}^2 a_D}$$

$$\cdot \frac{\left[J_{n-1}(\alpha_{n/m} a_D) - \frac{n}{\alpha_{n/m} a_D} J_n(\alpha_{n/m} a_D) \right] H_n^{(1)}(\alpha_{n/m} r_D)}{\left(1 - \frac{n^2}{\alpha_{n/m}^2 a_D^2}\right) H_n^{(1)}(\alpha_{n/m} a_D)}$$

$$\text{for} \quad r_D < r_D' \qquad (4.73)$$

For $r_D > r'_D$, we interchange r_D and r'_D in Eqs. 4.72 and 4.73.

The terms in Eq. 4.72 corresponding to s=0 (the first and second terms in square brackets) contain the long time pressure response of the system. The first term is the long time approximation of the line source, and the second term is a constant fixed by the geometry of the system. The transient part of the real time solution, the last double summation term, was not used in the numerical evaluations due to computation complexities. However, the general behavior of the pressure response can be deduced from the real time solution and will be discussed in Section 4.6.

4.5 NUMERICAL INVERSION OF THE LAPLACE TRANSFORMATION

The Stehfest algorithm presented in section 3.5 is used to invert Eqs. 4.22 and 4.23. The numerical evaluation of $\bar{p}(s)$ for the no-flow boundary case is more complex than for the constant pressure case, for two reasons : 1) In the no-flow boundary case the derivatives of the Modified Bessel Functions are needed. 2) Larger values of the relative size of the hole, F, are used, approaching slow convergence conditions.

The second complication arises from the fact that a system with a constant pressure source approaches a steady state condition while a system with a no-flow boundary will keep dropping in pressure. Hence, small no-flow boundary holes have little effect on the pressure transients at the production well. Therefore, large values of F are needed to see any effect. The Laplace solutions are given by Eqs. 4.22

and 4.23. In the numerical inversion, only Eq. 4.22 was used. Although Eq. 4.22 is written for $r_D < r'_D$, it can be used for cases where $r_D > r'_D$, due to the reciprocity principle. The computer program for the Stehfest algorithm is presented in Appendix G.

4.6 TYPE CURVE MATCHING FOR THE PRODUCTION WELL

The use of the type curves for the no-flow boundary case is similar to that of the constant pressure boundary case, presented in Chapter 3.

Figure 4.2 presents a family of curves for a geometrical configuration with 2c=100. As the relative diameter of the hole, F, becomes small, the curves approach the line source response. For values of F < 0.3, the effect of the hole is insignificant. As F increases, the curves approach the limiting no-flow linear boundary response. For a finite radius case, all the curves eventually form a straight line parallel to the line source curve. This is expected, since at long time, the area around the well and the hole produces very little by expansion. The straight line stresses the fact that the expansion is taking place beyond the area of the well and the hole. The response shows no pseudo - steady state behavior.

Figure 4.3 presents a family of curves for a geometrical configuration with 2c=250. Figure 4.3 can be shifted to match the curves of Fig. 4.2. The shifting is done in the same way as for the linear boundary case, presented in Appendix C.

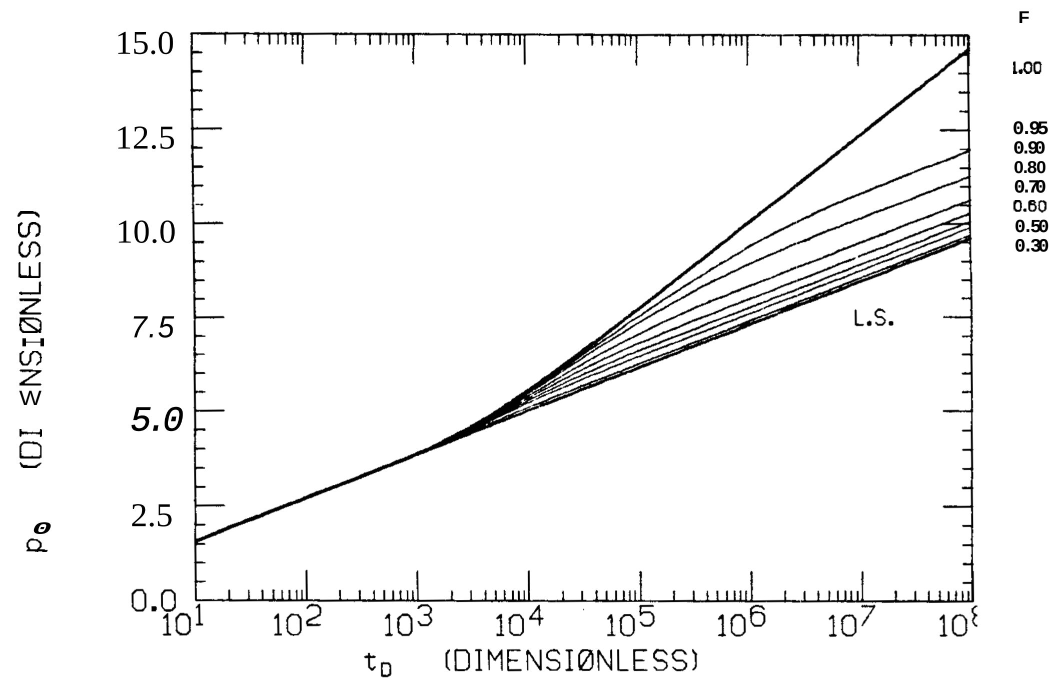

FIGURE 4.2 : SEMILOG CURVES FOR P0.3 TO 0.95 AND 2c=100.

NO-FLOW BOUNDARY HOLE

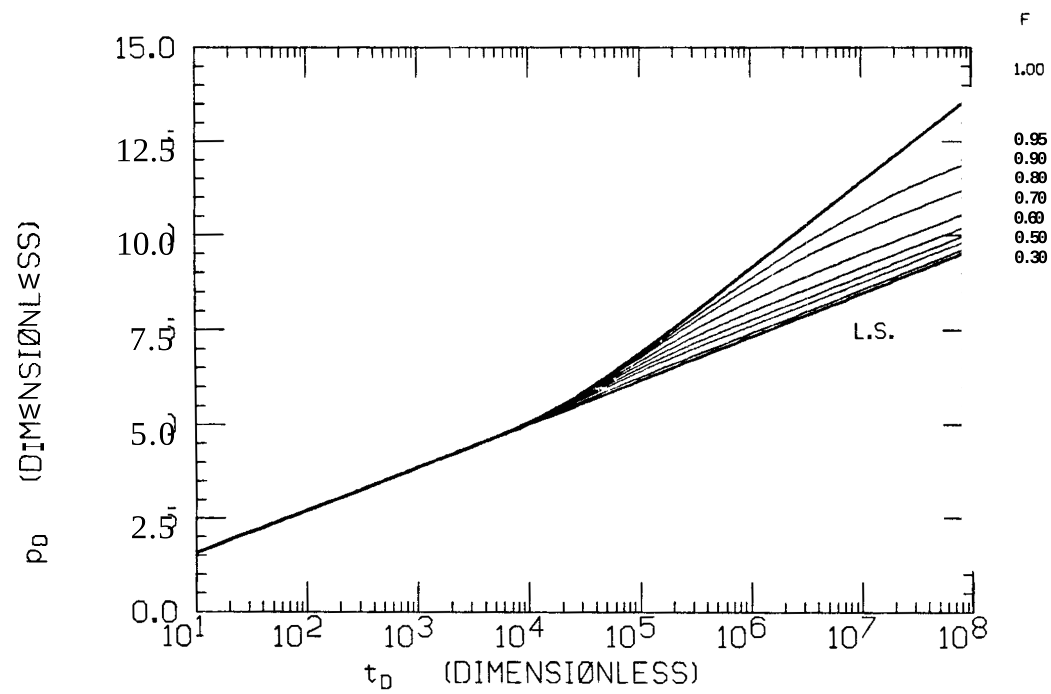

FIGURE *4.3* **: SEMILOG CURVES FOR F=0.3 TO 0.95** AND **2c=250.**

NO-FLOW BOUNDARY HOLE

Figure 4.4 presents the curve for F=0.5 and 2c=100 shifted over the curve for F=0.5 and 2c=500. The numerical data are presented in Appendix C.

Figure 4.5 is a generalized semilog type curve with modified scales for the no-flow boundary case. A match on this curve yields the values of F and 2c. The use of this type curve is similar to the use of the type curve for constant pressure holes presented in Chapter 3 and is discussed further in Chapter 5.

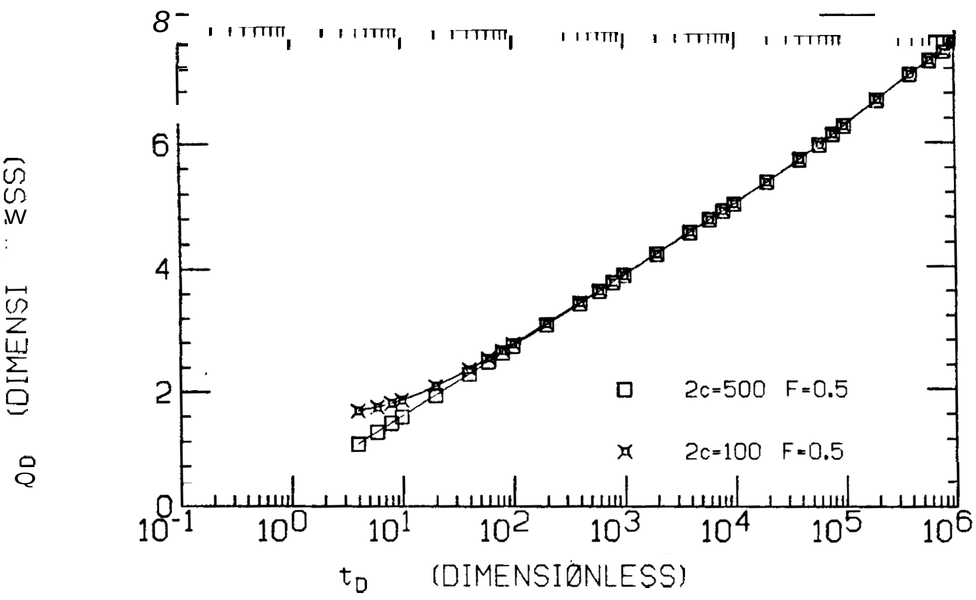

FIGURE 4.4 : SEMILOG CURVE FOR 2c=100 AND F=0.5 MATCHED WITH A SHIFTED CURVE FOR 2c=500 AND F=0.5. NO-FLOW BOUNDARY HOLE

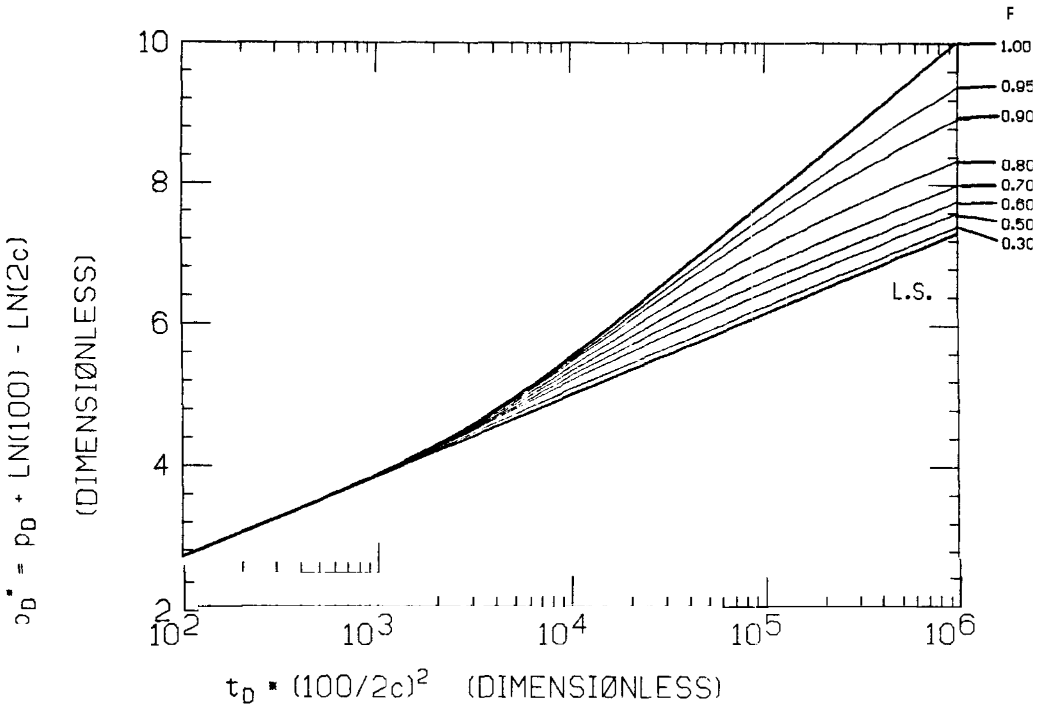

FIGURE 4.5 : A GENERALIZED SEMILOG TYPE CURVE **FOR THE** NO-FLOW INTERNAL CIRCULAR BOUNDARY

4.7 INTERFERENCE

Interference testing is not practical in the case of a no–flow boundary hole even when the geometry is known.

Figures 4.6 and 4.7 present log–log and semilog curves, respectively, for a case where $E=0.9999$, $F=0.9$ and $\theta = 0,45,90,135$ and 180 Deg. These two figures point out several problems in interference testing. Even for **a** relatively large hole **($F=0.9$),** the log–log curves are not markedly different than the line source curve and get closer to each other as time progresses. For the constant pressure hole the curves behave in the opposite manner. At long time, all the curves

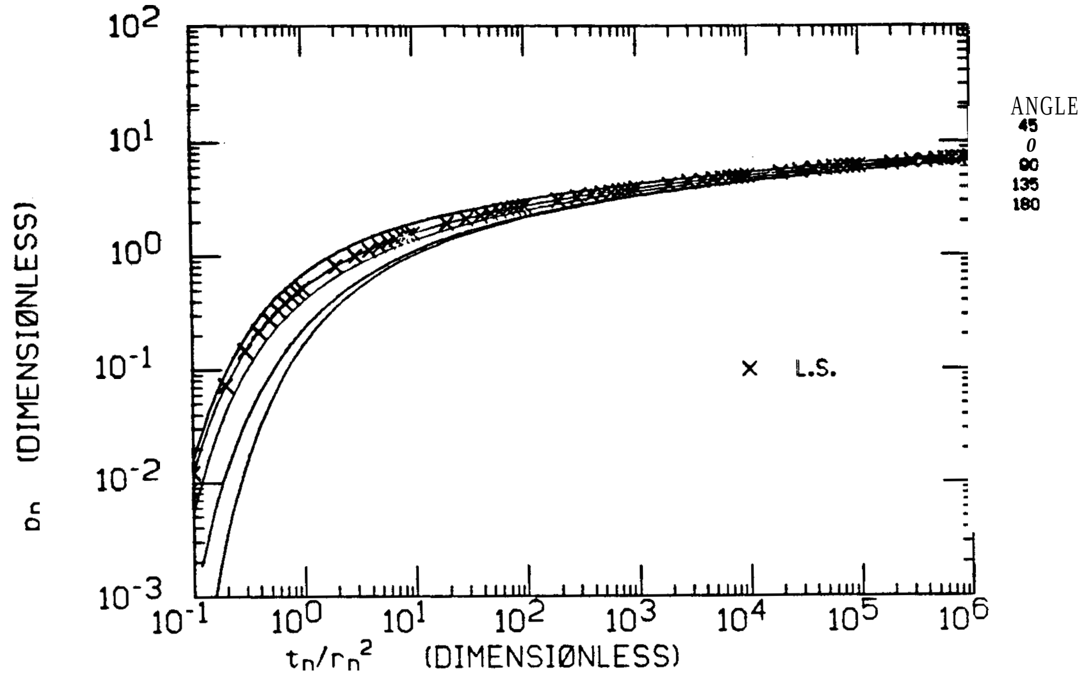

FIGURE 4.6 : INTERFERENCE LOG-LOG CURVES FOR E=0.9999, F=0.9 AND

θ=0,45,90,135,180 DEG. NO-FLOW BOUNDARY HOLE

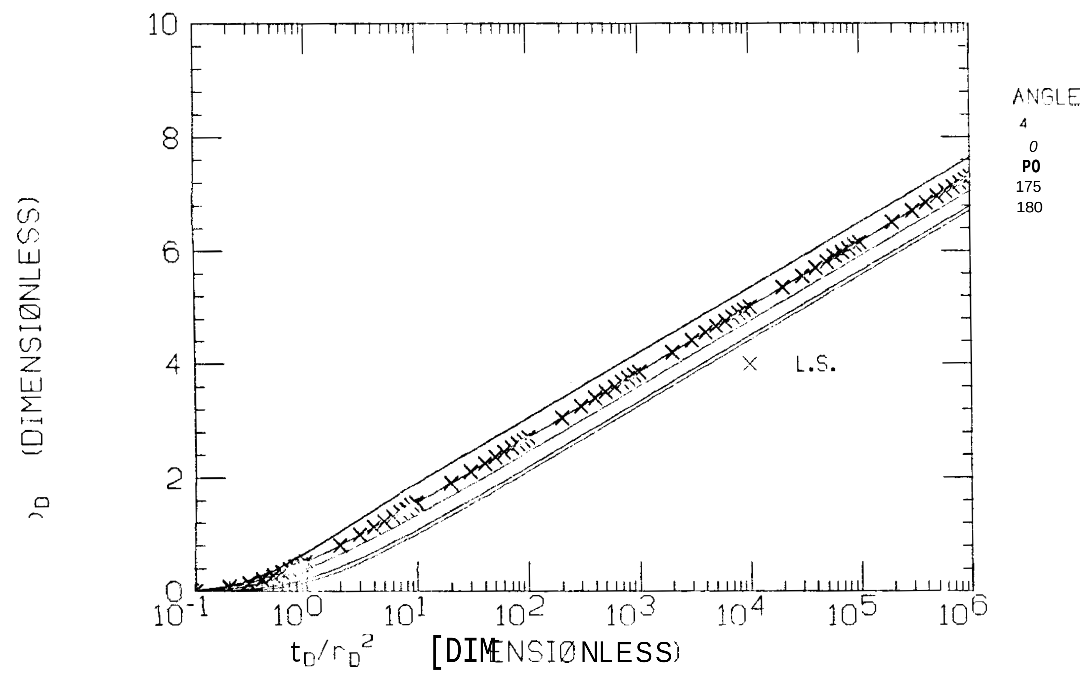

FIGURE 4.7 : INTERFERENCE SEMILOG CURVES FOR E=0.9999, F=0.9 AND

θ=0,45,90,135,180 DEG. NO-FLOW BOUNDARY HOLE follow semilog straight line curves (see Fig. 4.7). The curves are parallel to each other and are displaced vertically by a constant. This "skin-like" behavior is expressed in Eq. 4.72. The constant pressure displacement is a function of the geometry of the system. The parallel semilog curves make semilog type curve matching ambiguous and difficult.

The presence of a no-flow circular boundary divides the reservoir into two parts, having pressure drops greater or smaller than the line source. At times when the semilog curves are parallel (the exponential term in Eq. 4.72 vanishes), the partition line is a straight line perpendicular to the axis of symmetry. The x coordinate is: $x_D = F^2/2$ and is derived by setting the second term of Eq. 4.72 equal to zero. Figure 4.8 presents the location of partition lines for various hole sizes. Observation wells located at angles of 45 to 90 Deg. produce pressure - time behaviors similar to that of the line source, hence, reducing the practical use of interference testing.

Figures 4.9 to 4.13 present log-log interference curves for a fixed value of E=0.7. The curves for θ=90 Deg. are almost identical to the line source curve (see Fig. 4.11). We can also observe that the curves for θ=0 and 45 Deg. are below the line source curve, and the curves for θ=135 and 180 Deg. are above the line source curve. At angles of about 90 Deg. (see Fig 4.11), interference testing in the normal way can be validly used to estimate the parameters of the system, but there is no indication of the existence of a no-flow boundary close to the interference well.

The ineffectiveness of interference testing in a system with a no-flow internal boundary stems from the nature of the source of the flow in the system. Production comes from fluid expansion and the discontinuity can be treated as a skin, once most of this expansion takes place beyond the discontinuity.

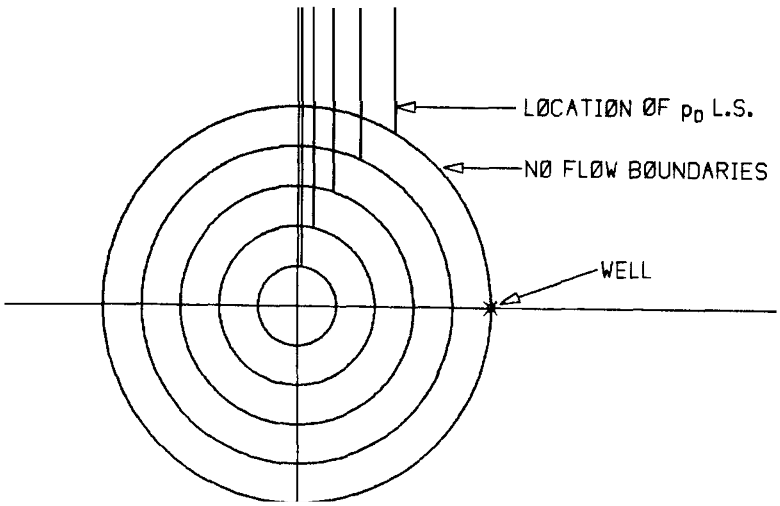

FIGURE 4.8 : LONG TIME LOCATION OF p_D L.S.

NO-FLOW BOUNDARY HOLE

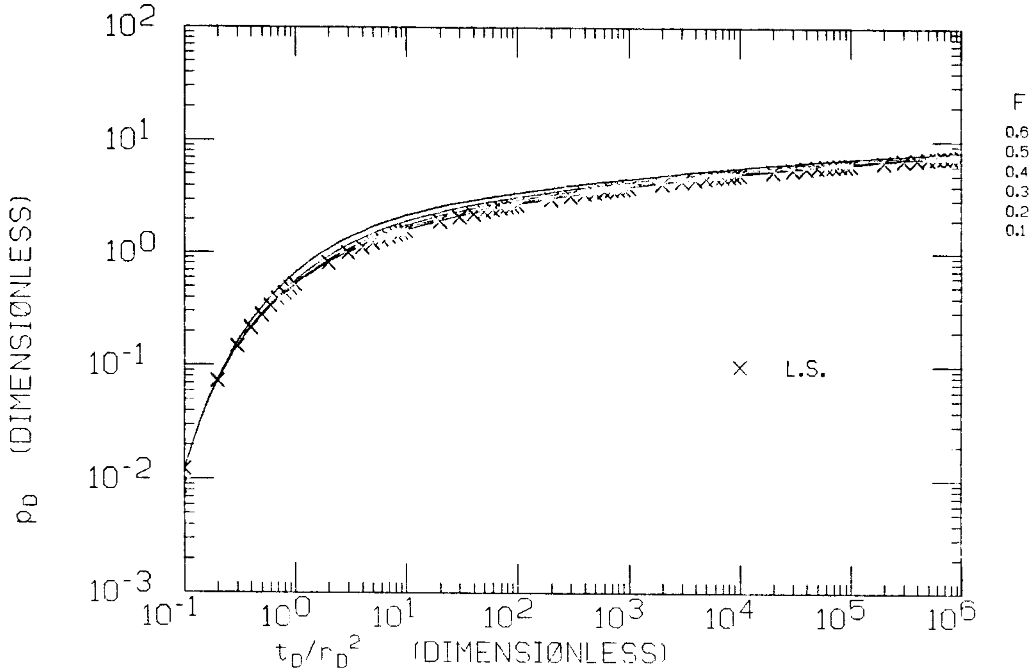

FIGURE 4.9 : INTERFERENCE LOG-LOG CURVES FOR E=0.7, F=0.1 TO 0.6 AND

θ=0 **Deg.** NO—FLOW BOUNDARY HOLE

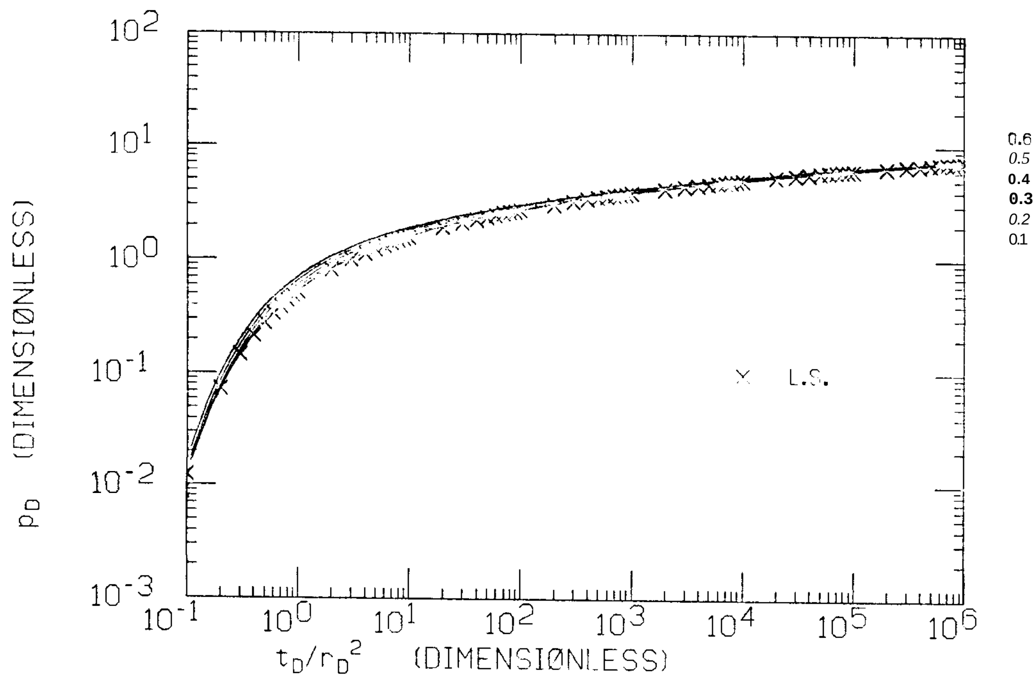

FIGURE 4.10 : INTERFERENCE LOG-LOG CURVES FOR E=0.7 , F=0.1 TO 0.6

AND θ=45 DEG. NO—FLOW BOUNDARY HOLE

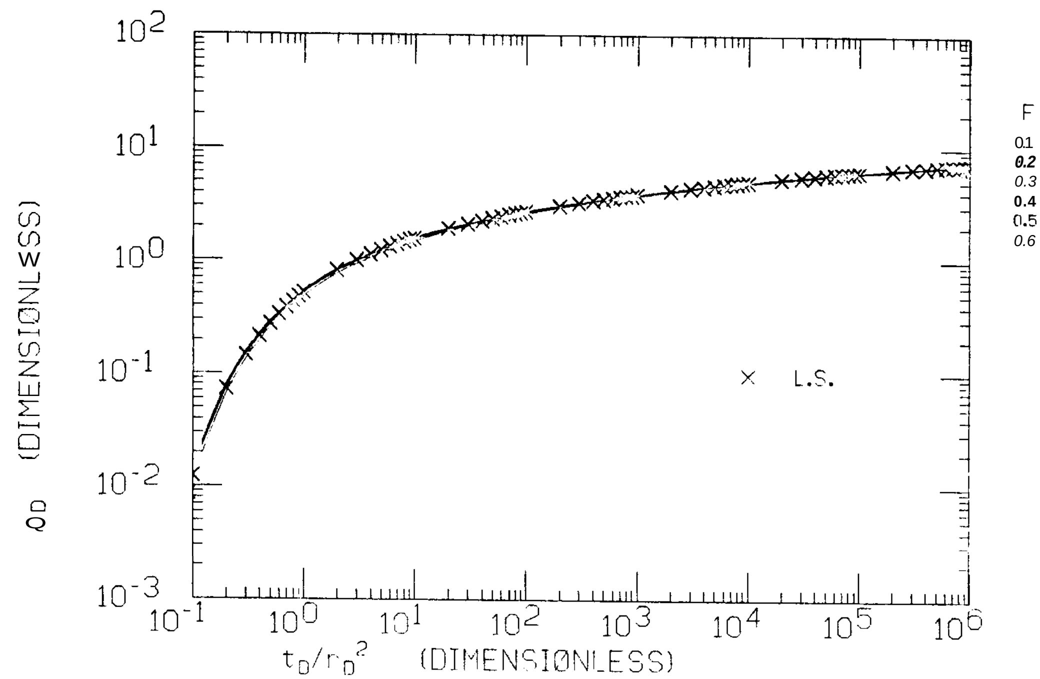

FIGURE 4.11 : INTERFERENCE LOG–LOG CURVES FOR E=0.7, F=0.1 TO 0.6 AND θ=90 Deg. NO-FLOW BOUNDARY HOLE

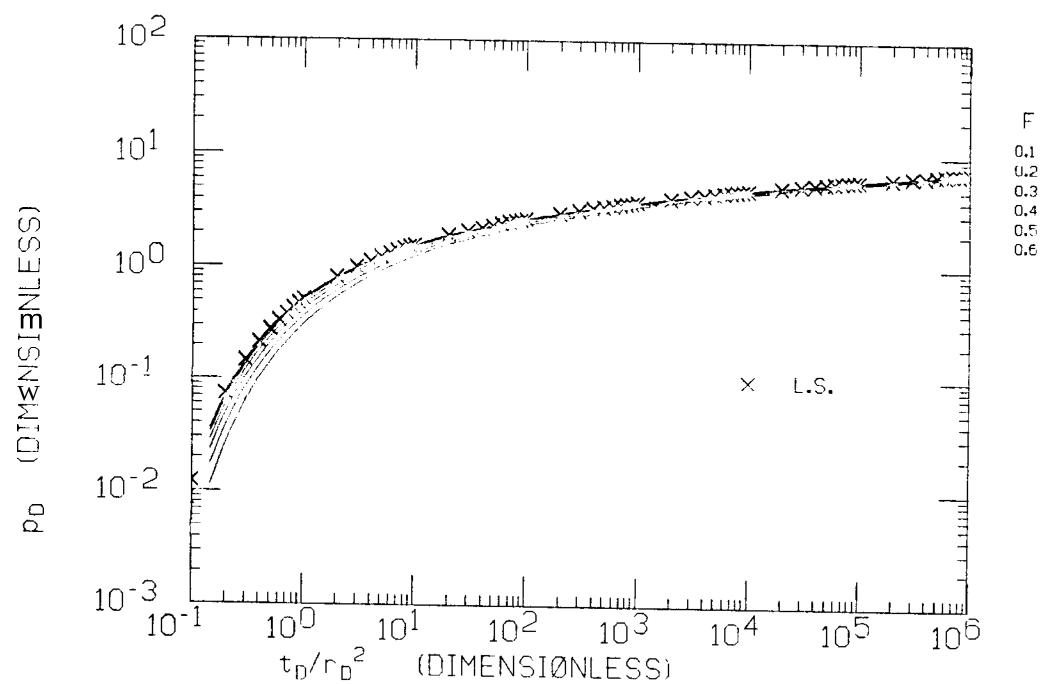

FIGURE 4.12 : INTERFERENCE LOG–LOG CURVES FOR E=0.7, F=0.1 TO 0.6 AND θ=135 DEG. NO-FLOW BOUNDARY HOLE

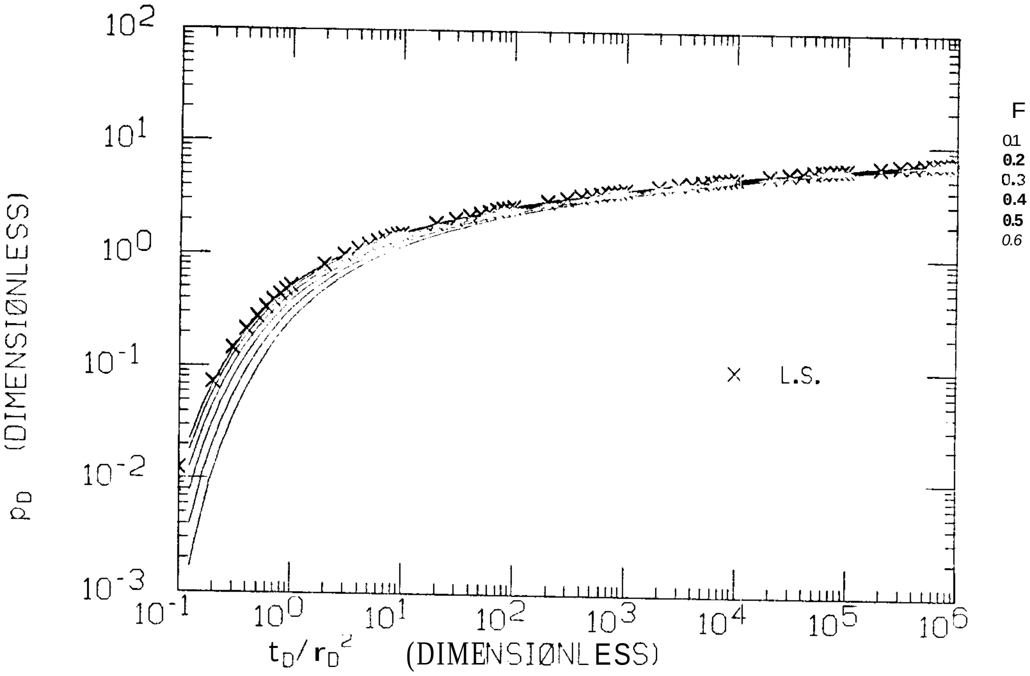

FIGURE 4.13 : INTERFERENCE LOG-LOG CURVES FOR E=0.7, F=0.1 TO 0.6 AND θ=180 DEG. NO-FLOW BOUNDARY HOLE

CHAPTER 5 : A GENERALIZED SEMILOG TYPE CURVE

The solutions for the internal circular boundairy include the linear boundary solutions as particular cases where the radii of the holes are infinite. So far, we presented three separate generalized semilog type curves. The first type curve was for linear boundaries, Chapter 2 Fig. 2.5. The second type curve was for constant pressure holes, Chapter 3 Fig. 3.8, and the third type curve was for no-flow boundary holes, Chapter 4 Fig. 4.5. Now, we combine the three generalized semilog curves into one generalized type curve (Fig. 5.1). This type curve can be used for analyzing limit tests in reservoirs with linear or internal circular boundaries. In the linear boundary cases, we can analyze interference tests as well as production well tests. In the internal circular boundary cases, only production well tests can be analyzed using the generalized type curve.

There are two families of curves in Fig. 5.1. The lower family of curves represents constant pressure boundaries. The lowermost curve is for a constant pressure linear boundary, denoted with F=1.0. The uppermost curve in this group of curves is for a relatively small hole denoted with F=0.1. All the constant pressure curves have limiting steady state values that can be calculated using Eq. 3.38. Constant pressure holes with F>0.9 cannot be distinguished from a constant pressure linear boundary.

The second family of curves in Fig. 5.1 is for no-flow boundaries. The uppermost curve is for a no-flow linear boundary, denoted with F=1.0. As the relative size of the hole becomes smaller, its effect on the pressure response becomes smaller, and the curves

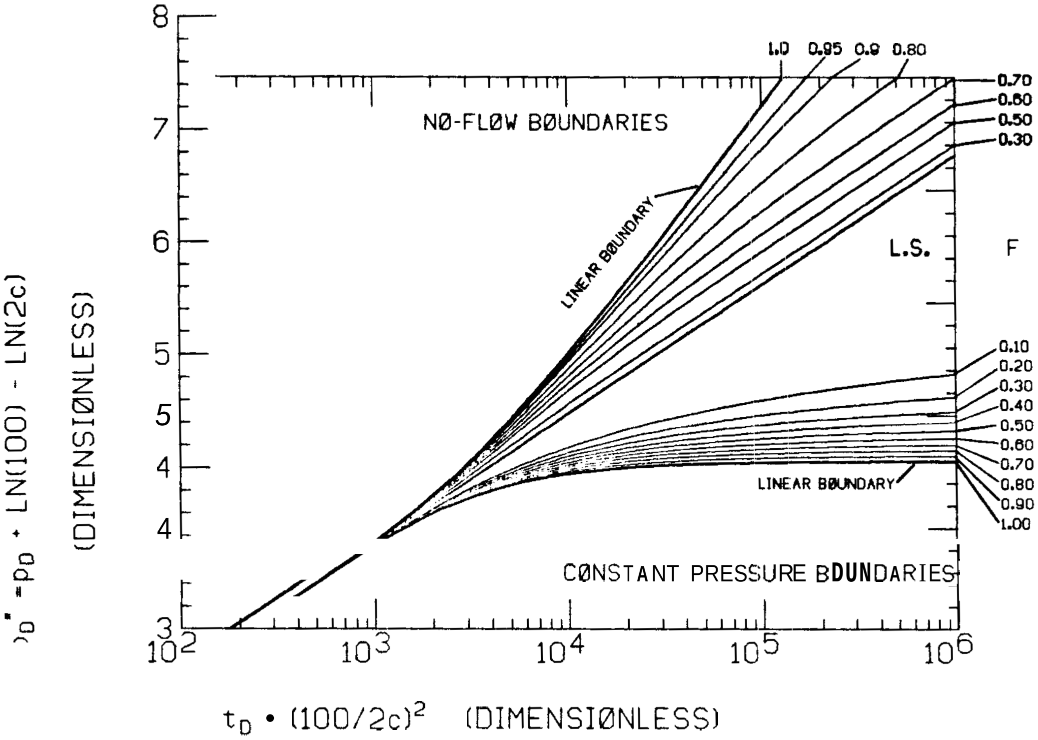

FIGURE 5.1 : A GENERALIZED SEMILOG TYPE CURVE FOR THE INTERNAL CIRCULAR BOUNDARY CASE INCLUDING LINEAR BOUNDARIES

approach the line source curve. No–flow boundary holes with $F<0.3$ have no effect on the pressure response of the production well.

All the curves in Fig. 5.1 depart from the line source curve at the same time. This is discussed in Chapter 2 and in Appendix D.

In Chapter 2, we presented an example of the use of the new semilog type curve matching method for a no–flow linear boundary, and in Chapter 3, we presented an example for a constant pressure hole. The following procedure describes the use of this new generalized semilog type curve (Fig. 5.1) :

1) Make a log–log graph of the pressure - time response on the same log–log scale as that of the line source type curve.

2) Match the early time data to the line source curve and pick a match point.

3) Convert the pressures to a dimensionless form.

4) Graph the dimensionless pressure - time response on the same semilog scale as that of the generalized semilog type curve.

5) Match to one of the curves on the generalized semilog type curve and pick a match point.

6) Determine the value of F by noting which curve matches best and evaluate the value of 2c using the pressure match point.

CHAPTER 6 : CONCLUSIONS

In this study, we consider a drawdown pressure transient analysis for a well produced at constant rate near an internal circular boundary. Linear boundaries are also treated since they are a special case of circular boundaries with infinite radii. The objective of this reservoir limit pressure transient analysis method is to estimate the distance to the discontinuity and its size.

The following conclusions are drawn :

Linear Boundaries

1. The distance between a production well and a linear boundary can be estimated by a new semilog type curve matching method derived here. The same generalized semilog type curve can be used to estimate the distance between an interference well and an image well.

2. An infinite acting period is required in order to use the generalized semilog type curve. An early time line source match must be achieved in order to determine the mapping between actual and dimensionless pressure drops.

3. The use of the semilog generalized type curve supercedes the double straight line analysis. The type curve can be used with data that extend through an early time line source period and a transition period. In this case, neither of the two semilog straight lines would exist. A match to the line source curve can be achieved prior to a dimensionless time of 10, which is the

approximate start of the semilog straight line.

Internal Circular Boundaries

4. The size of and the distance to an internal circular boundary can be estimated using semilog type curve matching of production well data.

5. A no-flow boundary hole with a relative size of 0.3 or less ($F<0.3$) cannot be detected.

6. The drawdown pressure response of a well near a no-flow boundary hole exhibits an infinite acting period, a transition period and a second infinite acting period. The two semilog straight lines have the same slope but are displaced by a constant pressure drop. The system shows a "skin-like" behavior at late time, when fluid expansion takes place away from the well and the hole.

7. A constant pressure hole with a relative size of 0.9 or more ($F>0.9$) cannot be distinguished from a constant pressure linear boundary.

8. Interference testing in the presence of a no-flow boundary hole is not useful in diagnosing the presence of this impermeable boundary. However, if &he interference well is located at an angle of 90 Deg., a log-log match can be validly analyzed in the conventional manner, since the pressure response is similar to the line source response.

9. In the case of a well producing near a no-flow boundary hole, two different pressure regions are developed, which are separated by a line perpendicular to the axis of symmetry. One region that contains the production well has a pressure drop higher than the line source, and the other region has a pressure drop lower than the line source.

10. Interference testing in the presence of a constant pressure hole in a developed system, where the geometry is known, can yield the relative size of the hole.

11. Interference testing in the presence of a constant pressure hole in a system with an unknown geometry, can yield qualitative information about the existence of a pressure source in the system.

12. Interference between oil and gas fields can be analyzed using the rate-pressure model type curves. The same type curves can also be applied to interference between constant rate and constant pressure wells.

13. The superposition method can be used to generate type curves for a semicircular boundary bounded by an infinite linear boundary and also for a quadrant bounded by two perpendicular semi-infinite linear boundaries.

General

14. A single generalized semilog type curve is presented. This type curve can be used to analyze pressure responses of production wells

near an internal circular boundary and of both production and interference wells near a linear boundary. Both the distance to the boundary and the size of it can be determined. In order to use this type curve, only the pressure data need be converted to a dimensionless form.

NOMENCLATURE

B	FORMATION VOLUME FACTOR
C_t	TOTAL SYSTEM COMPRESSIBILITY
E	NORMALIZED DISTANCE TO THE PRESSURE POINT
$E_i(X)$	EXPONENTIAL INTEGRAL OF ARGUMENT X
F	NORMALIZED RADIUS OF THE HOLE
H	RADII RATIO (CONSTANT)
$H_n^{(1)}(z)$	BESSEL FUNCTION OF THE THIRD KIND OF ORDER n OF THE FIRST TYPE
$H_n^{(2)}(z)$	BESSEL FUNCTION OF THE THIRD KIND OF ORDER n OF THE SECOND TYPE
$I_n(z)$	MODIFIED BESSEL FUNCTION OF THE FIRST KIND OF ORDER n
$J_n(z)$	BESSEL FUNCTION OF THE FIRST KIND OF ORDER n
$K_n(z)$	MODIFIED BESSEL FUNCTION OF THE SECOND KIND OF ORDER n
$Y_n(z)$	BESSEL FUNCTION OF THE SECOND KIND OF ORDER n
R	DISTANCE BETWEEN THE WELL AND THE PRESSURE POINT
R_D	DIMENSIONLESS DISTANCE BETWEEN THE WELL AND THE PRESSURE POINT
a	RADIUS OF THE INTERNAL CIRCULAR BOUNDARY
a_D	DIMENSIONLESS RADIUS OF THE HOLE
c	SHORTEST DIMENSIONLESS DISTANCE BETWEEN THE WELL AND THE CIRCULAR BOUNDARY
c'	SHORTEST DIMENSIONLESS DISTANCE BETWEEN THE WELL AND THE LINEAR BOUNDARY
d	DISTANCE BETWEEN 'ME WELL AND THE LINEAR BOUNDARY
h	THICKNESS OF THE FORMATION
k	PERMEABILITY
p	PRESSURE
p_D	DIMENSIONLESS PRESSURE DROP
p_i	INITIAL PRESSURE
p_{Dss}	DIMENSIONLESS STEADY STATE PRESSURE
$p_{D\ L.S.}$	DIMENSIONLESS LINE SOURCE PRESSURE
q	WELL FLOW RATE
t	TIME

t_D .... DIMENSIONLESS TIME

$t_{D,d}$ .... DIMENSIONLESS DEPARTURE TIME

r .... DISTANCE TO THE PRESSURE POINT

r' .... DISTANCE BETWEEN THE WELL AND THE CENTER OF THE HOLE

r_w .... RADIUS OF THE WELL

r_D .... DIMENSIONLESS DISTANCE TO THE PRESSURE POINT

r_D .... DIMENSIONLESS DISTANCE BETWEEN THE WELL AND THE CENTER OF THE HOLE

z............. ARGUMENT OF BESSEL FUNCTIONS

θ .... ANGLE OF ROTATION TO THE PRESSURE POINT

η .... DIFFUSIVITY CONSTANT

ϕ .... POROSITY

μ .... VISCOSITY

γ .... EULER CONSTANT

REFERENCES

Abramowitz, M., and Stegun, I.A.: "Handbook of Mathematical Functions, National Bureau of Standards, Washington D.C. (1964).

Bickley, W.G.: Bessel Functions and Formulae, University Press, Cambridge (1957).

Bixel, H.C., Larkin, B.K., and Van Poollen, H.K.: "Effect of Linear Discontinuities on Pressure Build-Up and Drawdown Behavior," J. Pet. Tech. (Aug. 1963), 885-895.

Bixel, H.C., and Van Pollen, H.K.: "Pressure Drawdown and Buildup in the Presence of Radial Discontinuities," SPE J. (Sep. 1967), 301.

Brigham, W.E.: Advanced Reservoir Engineering Class, 270A, Stanford University, Stanford, California (1979).

Carslaw, H.S., and Jaeger, J.C.: "Conduction of Heat in Solids, Oxford at the Clarendon press (1959).

Cinco, H., Samaniego, F.V., and Dominguez, N.A.: "Unsteady-state Flow Behavior for a Well Near a Natural Fracture," Paper SPE 6019 Presented at the 51 st Annual Fall Technical Conference and Exhibition of the Society of Petroleum Engineers of AIME, New Orleans (Oct. 1976).

Coats, K.H.: "A Mathematical Model Water Movement about a Bottom-Water-Drive Reservoirs," SPE J. (March 1962), 44-52.

Coats, K.H., Tek, M.R., and Katz, D.L.: "Method for Predicting the Behavior of Mutually Interfering Gas Reservoirs Adjacent to a Common Aquifer," Trans., AIME (1959), 216, 247-251.

Davis, G.E., and Hawkins, M.F.: "Linear Fluid-Barrier Detection by Well Pressure Measurements," J. Pet. Tech. (Oct. 1963), 1077-1079.

Ferris, J.G., Knowles, D.B., Brown, R.H., and Stallman, R.W.: "Theory of Aquifer Tests," U.S. Geol. Surv., Water Supply Paper 1536 E (1962).

Hantush, M.S., and Jacob, C.E.: "Flow to an Eccentric Well in a Leaky Circular Aquifer," J. Geoph. Res. (Oct. 1966), Vol. 65, No. 10, 3425-3431.

Hurst, W.: "Interference Between Oil Fields," Trans., AIME (1960), 219, 175-192.

Jaeger, J.C.: "Heat Conduction in Composite Circular Cylinders," Phil. Mag. (1941) Vol. 7, 324-335.

Jaeger, J.C. : "Some Problems Involving Line Sources in Conduction of Heat," Phil. Mag. (1944) Vol. 35, 169-179.

Jones, P.: "Reservoir Limit Test on Gas Wells," J. Pet. Tech. (June 1962), 613-619.

Katz, D.L., Tek, M.R., and Coats, K.H.: "Effect of Unsteady-State Aquifer Motion on the Size of an Adjacent Gas Storage Reservoir," Trans., AIME (1959), 216, 18-22.

Kruseman, G.P., and De Ridder, N.A.: "Analysis and Evaluation of Pumping Test Data," International Institute for Land Reclamation and Improvement, Wageningen, The Netherlands (1970).

Larkin, B.K.: "Solutions to the Diffusion Equation for a Region Bounded By a Circular Discontinuity," SPE J. (June 1963), 113-115.

Loucks, T.L., and Guerrero, E.T.: "Pressure Drop in a Composite Reservoir," SPE J. (Sep. 1961), 170-176.

Macdonald, H.M. : "Zeroes of the Bessel Functions," Proceedings of the London Mathematical Society, Vol. XXX (Nov. 1898 - March 1899), 165-179.

Miller, M.C.: "Relationship Between Unsteady State Well Performance and Insitu Reservoir Characteristics," Ph.D. Thesis, The University of Michigan, Ann Arbor, Michigan (1963).

Miller, M.C, Tek, R.M., and Katz, D.L.: "Effect of Adjacent Expansible Fluids and Caprock Leakage on Build-Up and Drawdown Behavior of Wells in an Aquifer," SPE J. (Sep. 1966), 239-246.

Mortada, M.: "Oilfield Interference in Aquifers of Non-Uniform Properties," Trans., AIME (1960), 219, 412-414.

Ramey, H.J., Jr.: "Short-Time Well Test Data Interpretation in the Presence of Skin Effect and Wellbore Storage," J. Pet. Tech. (Jan. 1970), 97-104.

Ramey, H.J., Jr.: "Approximate Solutions for Unsteady Liquid Flow in Composite Reservoirs," J. Can. Pet. Tech. (Jan.-March 1970), 32-37.

Ramey, H.J., Jr., Kumar, A., and Gulati, M.S.: "Gas Well Test Analysis Under Water Drive Conditions, American Gas Association, Arlington, Virginia (1973).

Ramey, H.J., Jr.: Personal Communication (Feb. 1983).

Shinohara, K.: "A Study of Inertial Effect in the Wellbore in Pressure Transient Well Testing," Ph.D. Thesis, Stanford University, Stanford, California (1980).

Stallman, R.W. : "Nonequilibrium Type Curves Modified for Two-Well Systems," U.S. Geol. Surv., Groundwater Note 3 (1952).

Standing, M.B.: "Linear Fluid-Barrier Detection by Well Pressure Measurements," - Discussion, J. Pet. Tech. (March 1964), 259-260.

Standing, M.B.: Personal Communication (Feb. 1983).

Stehfest, H.: "Algorithm 368, Numerical Inversion of Laplace Transforms," D-5 Communications of the ACM (Jan. 1970), 13, No. 1, 47-49.

Temeng, K.O., and Horne, R.N. : "Pressure Distributions in Eccentric Circular Systems," Paper SPE 11223, Presented at the 1982 SPE Annual Technical Conference, New Orleans, Sept. 26-29, 1982, to appear in J. Pet. Tech. (1983).

Tiab, D., and Crichlow, H.B. : "Pressure Analysis of Multiple-Sealing-Fault Systems and Bounded Reservoirs by Type-Curve Matching," SPE J. (Dec. 1979), 379-392.

Tiab, D., and Kumar, A.: "Detection and Location of Two Parallel Sealing Faults Around a Well," J. Pet. Tech. (Oct. 1980), 1701-1708.

Van Everdingen, A.F., and Hurst, W.: "The Application of the Laplace Transformation to Flow Problems in Reservoirs," Trans., AIME (Dec. 1949), 186, 305-324.

Vela, S.: "Effect of a Linear Boundary on Interference and Pulse Tests-The Elliptical Inference Area," J. Pet. Tech. (Aug. 1977), 947-950.

Watson, G.N.: A Treatise on the Theory of Bessel Functions, (2nd Ed.), Cambridge University Press (1944).

Witherspoon, P.A., Javandel, I., Neuman, S.P., and Freeze, R.A.: Interpretation of Aquifer Gas Storage Conditions From Water Pumping Tests, Monograph on Project NS-38, American Gas Association, Inc., New York (1967).

APPENDIX A : CIRCLES WITH A CONSTANT r_2/r_1 RATIO

Brigham (1979) observed that points with a constant r_2/r_1 ratio formed circles.

Let :

$$\left(\frac{r_{D2}}{r_{D1}}\right)^2 = H \qquad (A.1)$$

where :

$$r_{D1}^2 = (c' - x)^2 + y^2 \qquad (A.2)$$

$$r_{D2}^2 = (c' + x)^2 + y^2 \qquad (A.3)$$

and c' is the distance between the well and the linear boundary (see Fig. 2.1).

Substituting Eqs. A.2 and A.3 into Eq. A.1 yields :

$$\left[x - c'\left(\frac{1 + H}{1 - H}\right) \right]^2 + y^2 = \left[\frac{2c'\sqrt{H}}{1 - H} \right]^2 \qquad (A.4)$$

Equation A.4 represents a circle, centered at :

$$\left[c'\left(\frac{1 + H}{1 - H}\right) , 0 \right] \qquad (A.5)$$

with a radius of :

$$2c' \frac{\sqrt{H}}{1 - H} \qquad (A.6)$$

Brigham (1979) showed that in the case of a constant pressure linear boundary, these circles are late time isopressure lines. At late time, when $t_D/r_D^2 > 10$, the exponential integral is approximated by the following equation :

$$E_i(-X) = \gamma + \ln(X) \tag{A.7}$$

The dimensionless pressure drop for this case is given by Eq. 2.6 :

$$p_D = -\frac{1}{2}\left[\,E_i(-X_1) - E_i(-X_2)\,\right] \tag{A.8}$$

where :

$$X_i = \frac{r_{Di}^2}{4t_D} \tag{A.9}$$

Substituting Eq. A.7 into Eq. A.8 yields :

$$p_{Dss} = \ln\left(\frac{r_{D2}}{r_{D1}}\right) \tag{A. 10}$$

Hence, points with the same r_2/r_1 ratio form constant pressue circles at late time.

APPENDIX B : DIMENSIONLESS PRESSURE VS. REDUCED DIMENSIONLESS TIME FOR POINTS WITH A CONSTANT r_2/r_1 RATIO

In this Appendix we show that pressure points with the same r_2/r_1 have the same dimensionless pressure response as a function of reduced dimensionless time (p_D vs. t_D/r_D^2) .

In Appendix A, we showed that the constant pressure linear boundary case at late time, the isopressure lines are circles. Using superposition, the pressure drops at two points A and B on one of these late time constant pressure circles (see Fig. B.1) are given by :

$$p_{D,A} = \frac{1}{2} \left[E_i\left(-\frac{r^2_{D2,A}}{4t_{D,A}}\right) - E_i\left(-\frac{r^2_{D1,A}}{4t_{D,A}}\right) \right] \tag{B.1}$$

$$p_{D,B} = \frac{1}{2} \left[E_i\left(-\frac{r^2_{D2,B}}{4t_{D,B}}\right) - E_i\left(-\frac{r^2_{D1,B}}{4t_{D,B}}\right) \right] \tag{B.2}$$

From Abramowitz (1964, p. 229), the series expansion for the exponential integral is :

$$- E_i(-X) = - \gamma - \ln (X) - \sum_{n=1}^{\infty} \frac{(-1)^n (X)^n}{n\ n!} \tag{B.3}$$

Substituting Eq. B.3 into Eqs. B.1 and B.2 yields :

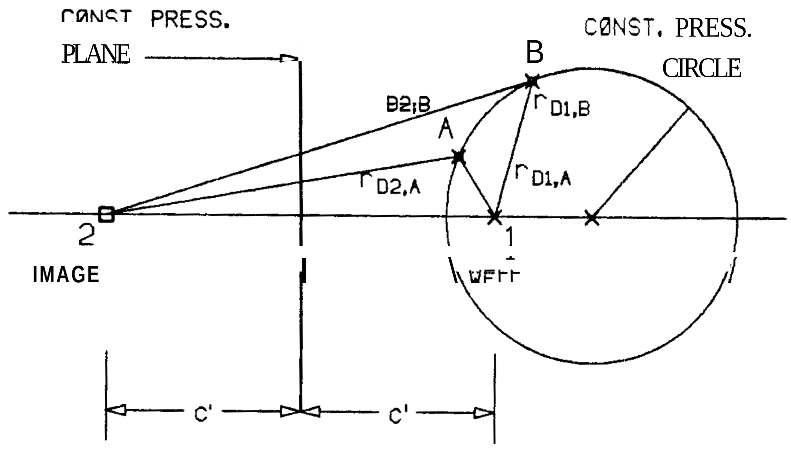

FIGURE B.1 : THE GEOMETRY FOR THE POINTS ON THE LATE TIME CONSTANT PRESSURE CIRCLE.

$$p_{D,A} = \frac{1}{2}\left[\gamma + \ln\left(\frac{r_{D2,A}^2}{4t_{D,A}}\right) + \sum_{n=1}^{\infty} \frac{(-1)^n \left(\frac{r_{D2,A}^2}{4t_{D,A}}\right)^n}{n\, n!} - \gamma - \ln\left(\frac{r_{D1,A}^2}{4t_{D,A}}\right) - \sum_{n=1}^{\infty} \frac{(-1)^n \left(\frac{r_{D1,A}^2}{4t_{D,A}}\right)^n}{n\, n!} \right] \qquad \text{(B.4)}$$

$$p_{D,B} = \frac{1}{2}\left[\gamma + \ln\left(\frac{r_{D2,B}^2}{4t_{D,B}}\right) + \sum_{n=1}^{\infty}\frac{(-1)^n\left(\frac{r_{D2,B}^2}{4t_{D,B}}\right)^n}{n\,n!}\right.$$

$$\left. - \gamma - \ln\left(\frac{r_{D1,B}^2}{4t_{D,B}}\right) - \sum_{n=0}^{\infty}\frac{(-1)^n\left(\frac{r_{D1,B}^2}{4t_{D,B}}\right)^n}{n\,n!}\right] \tag{B.5}$$

or :

$$p_{D,A} = \frac{1}{2}\left\{ 2\ln\left(\frac{r_{D2,A}}{r_{D1,A}}\right) + \sum_{n=1}^{\infty}\frac{(-1)^n}{n\,n!\,4^n}\left[\left(\frac{r_{D2,A}^2}{t_{D,A}}\right)^n - \left(\frac{r_{D1,A}^2}{t_{D,A}}\right)^n\right]\right\} \tag{B.6}$$

$$p_{D,B} = \frac{1}{2}\left\{ 2\ln\left(\frac{r_{D2,B}}{r_{D1,B}}\right) + \sum_{n=1}^{\infty}\left(\frac{(-1)^n}{n\,n!\,4^n}\right)\left[\left(\frac{r_{D2,B}^2}{t_{D,B}}\right)^n - \left(\frac{r_{D1,B}^2}{t_{D,B}}\right)^n\right]\right\} \tag{B.7}$$

Points A and B are on the long time isopressure circles, hence :

$$\frac{r_{D2,A}}{r_{D1,A}} = \frac{r_{D2,B}}{r_{D1,B}} = \sqrt{H} \tag{B.8}$$

Now, suppose that we pick two different times, $t_{D,A}$ and $t_{D,B}$ such that :

$$\frac{t_{D,A}}{r_{D1,A}^2} = \frac{t_{D,B}}{r_{D1,B}^2} \tag{B.9}$$

Using Eq. B.8, we can show that :

$$\frac{t_{D,A}}{r^2_{D2,A}} = \frac{t_{D,B}}{r^2_{D2,B}} \qquad (B.10)$$

Subtracting Eq. B.7 from Eq. B.6 yields :

$$p_{D,A} - p_{D,B} = \frac{1}{2} \{ 2\ln(\frac{r_{D2,A}}{r_{D1,A}}) - 2\ln(\frac{r_{D2,B}}{r_{D1,B}}] + \sum_{n=1}^{\infty} \frac{(-1)^n}{n\, n!\, 4^n}$$

$$\cdot [(\frac{r^2_{D2,A}}{t_{D,A}})^n - (\frac{r^2_{D1,A}}{t_{D,A}})^n - (\frac{r^2_{D2,B}}{t_{D,B}})^n + (\frac{r^2_{D1,B}}{t_{D,B}})^n] \} \qquad (B.11)$$

Applying Eqs. B.8, B.9 and B.10 to Eq. B.11 yields :

$$p_{D,A} = p_{D,B} \qquad (B.12)$$

This implies that the pressure drop at points A and B which lie on the late time constant pressure circles are identical functions of t_D/r^2_D. Figure B.2 presents identical curves for two points on the late time isopressure circles.

For no-flow linear boundary cases, points with the same r_2/r_1 ratio have identical p_D vs. t_D/r^2_D responses. This is proved in the same manner as for the constant pressure linear boundary case. Hence :

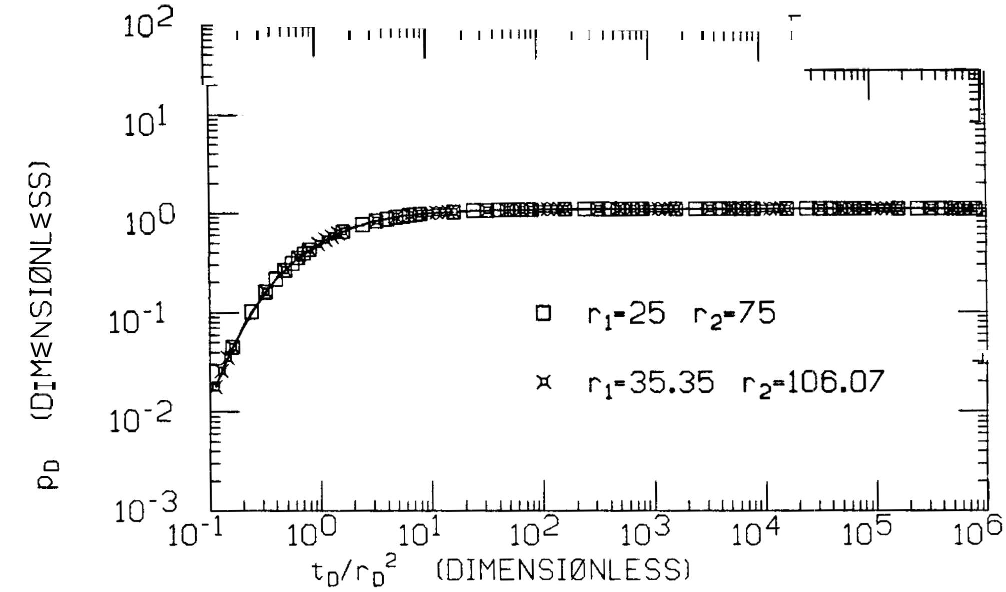

FIGURE B.2 : CURVES FOR TWO POINTS ON THE LATE TIME CONSTANT PRESSURE CIRCLES. CONSTANT PRESSURE LINEAR BOUNDARY.

$$p_{D,A} - p_{D,B} = \frac{1}{2} [\gamma + \ln\left(\frac{r_{D2,A}^2}{4t_{D,A}}\right) + \sum_{n=1}^{\infty} \frac{(-1)^n \left(\frac{r_{D2,A}^2}{4t_{D,A}}\right)^n}{n\ n!}$$

$$+ \gamma + \ln\left(\frac{r_{D1,A}^2}{4t_{D,A}}\right) + \sum_{n=1}^{\infty} \frac{(-1) \left(\frac{r_{D1,A}^2}{4t_{D,A}}\right)^n}{n\ n!}]$$

$$- \frac{1}{2} [\gamma + \ln\left(\frac{r_{D2,B}^2}{4t_{D,B}}\right) + \sum_{n=1}^{\infty} \frac{(-1)^n \left(\frac{r_{D2,B}^2}{4t_{D,B}}\right)^n}{n\ n!}$$

$$+ \gamma + \ln\left(\frac{r^2_{D1,B}}{4t_{D,B}}\right) + \sum_{n=1}^{\infty} \frac{(-1)^n \left(\frac{r^2_{D1,B}}{4t_{D,B}}\right)^n}{n\,n!} \qquad \text{(B.12)}$$

or :

$$p_{D,A} + p_{D,B} = \ln\left(\frac{t_{D,B}\, r_{D2,A}\, r_{D1,A}}{t_{D,A}\, r_{D2,B}\, r_{D2,A}}\right) + \frac{1}{2} \sum_{n=1}^{\infty} \frac{(-1)^n}{n\,n!\,4^n}$$

$$\cdot \left[\left(\frac{r^2_{D2,A}}{t_{D,A}}\right)^n + \left(\frac{r^2_{D1,A}}{t_{D,A}}\right)^n + \left(\frac{r^2_{D2,B}}{t_{D,B}}\right)^n + \left(\frac{r^2_{D1,B}}{t_{D,B}}\right)^n \right] \qquad \text{(B.13)}$$

Using Eqs. B.8 and B.9, the summation term in Eq. B.13 becomes zero. Using Eqs. B.7 and B.8, the first term in Eq. B.13 becomes :

$$\ln\left(\frac{t_{D,A}\, r_{D2,A}\, r_{D1,A}}{t_{D,B}\, r_{D2,B}\, r_{D1,B}}\right) = \ln(1) = 0 \qquad \text{(B.14)}$$

hence :

$$p_{D,A} = p_{D,B} \qquad \text{(B.15)}$$

Equations B.11 and B.15 imply that we can type curve match pressure responses and determine the ratio r_2 / r_1. Stallman (1952) presented log-log type curves (see Fig. 2.2) for linear boundary cases as a function of this ratio.

APPENDIX C : SHIFTING OF THE SEMILOG CURVES

In this appendix we show how one semilog curve denoted as curve B, can be shifted to match another curve denoted as curve A. We consider linear and internal circular boundaries.

Constant Pressure Linear Boundary

Equation A-10 can be written for $r_{D1} = 1$ in the direction of the image well. Hence, $r_{D2} = 2c' - 1$ and :

$$p_{Dss} = \ln(2c' - 1) \tag{C.1}$$

For the two cases, A and B :

$$p_{Dss,A} = \ln(2c'_A - 1) \tag{C.2}$$

$$p_{Dss,B} = \ln(2c'_B - 1) \tag{C.3}$$

The shift in p_D , denoted as Dp_D is :

$$Dp_D = \ln\left(\frac{2c'_A - 1}{2c'_B - 1}\right) \tag{C.4}$$

The shift in time is determined by the early time line source behavior of the curves :

$$p_{D,A} = \frac{1}{2}\left[\ln(t_{D,A}) + 0.80907\right] \tag{C.5}$$

$$p_{D,B} = \frac{1}{2} \left[\ln(t_{D,B}) + 0.80907 \right] \tag{C.6}$$

Subtracting Eq. C.6 from Eq. C.5 and equating to Eq. C.4 yields :

$$\frac{1}{2} \ln\left(\frac{t_{D,A}}{t_{D,A}}\right) = \ln\left(\frac{2c'_A - 1}{2c'_B - 1}\right) \tag{C.7}$$

In summary, curve B is shifted according to the following :

$$p_{D,B,\text{shifted}} = p_{D,B} + \ln\left(\frac{2c'_A - 1}{c'_B - 1}\right) \tag{C.8}$$

$$t_{D,B,\text{shifted}} = t_{D,B} \left(\frac{2c'_A - 1}{2c'_B - 1}\right)^2 \tag{C.9}$$

Equations C.8 and C.9 were used to shift curves with 2c' values of 25, 50, 100, 250, 500, 1000 and 2500 on to a base case of 2c' = 5000. Table C.1 presents the numerical values of the shift. For $t_D > 100$ the fits are within one percent accuracy. Note that for large values of c', the shifting equations simplify to the following :

$$p_{D,B,\text{ shifted}} = p_{D,B} + \ln\left(\frac{c'_A}{c'_B}\right) \tag{C.10}$$

$$t_{D,B,\text{shifted}} = t_{D,B} \left(\frac{c'_A}{c'_B}\right)^2 \tag{C.11}$$

Constant Pressure Hole

Letting $\theta = 0$ and $r_D' = r_D = 1$ in Eq. 3.38 yields :

$$p_{Dss} = \ln\left(\frac{r_D r_D'}{a_D} - a_D \right) \tag{C.12}$$

Since $F = a_D / r_D'$ and $c = r_D' - a_D$, Eq. c.12 becomes :

$$p_{Dss} = \ln\left(\frac{c - 1}{F} + c \right) \tag{C.13}$$

As F approaches 1, the hole is infinitely large and acts like a constant pressure linear boundary. When F = 1 :

$$p_{Dss} = \ln(2c - 1) \tag{C.14}$$

Which is identical to Eq. C.1 for the doublet model.

The shifting of the semilog curves is done in the same manner as for the linear boundary case. Hence :

$$p_{D,B,\mathrm{shifted}} = p_{D,B} + \ln\left[\frac{c_A(1 + F) - 1}{c_B(1 + F) - 1} \right] \tag{C.15}$$

$$t_{D,B,\mathrm{shifted}} = t_{D,B} \left[\frac{c_A(1 + F) - 1}{c_B(1 + F) - 1} \right]^2 \tag{C.16}$$

Note, that for large values of c, the shifting equations simplify to :

$$p_{D,B,shifted} = p_{D,B} + \ln\left(\frac{c_A}{c_B}\right) \qquad (C.17)$$

$$t_{D,B,\ shifted} = t_{D,B} \left(\frac{c_A}{c_B}\right)^2 \qquad (C.18)$$

These equations are identical to those for the linear boundary case. Hence, at large values of c, both sets of curves can be shifted together.

Figure 3.7 presents an example of collapsing two curves for the constant pressure hole. The numerical values for this example are presented in Table C.2.

No-flow linear boundary

The curves for the no-flow linear boundary cases are shifted in the same manner as the constant pressure curves. Based on Eq. C.9, the time shift must satisfy :

$$\frac{t_{DA}}{t_{DB}} = \left(\frac{2c'_A - 1}{2c'_B - 1}\right)^2 \qquad (C.19)$$

Equation C.19 is derived based on the line source portion of the curves. For the no-flow linear boundary case, the dimensionless pressure drops at the well for cases A and B are :

$$p_{D,A} = \ln(t_{DA}) - \ln(2c'_A - 1) + 0.80907 \qquad (C.20)$$

$$p_{D,B} = \ln(t_{DB}) - \ln(2c'_B - 1) + 0.80907 \qquad (C.21)$$

Subtracting C.21 from C.20 yields :

$$p_{D,A} - p_{D,B} = \ln\left(\frac{2c'_B - 1}{2c'_A - 1} \right) + \ln\left(\frac{t_{DA}}{t_{DB}}\right) \qquad (C.22)$$

Substituting Eq. C.19 into C.22 yields :

$$p_{D,A} - p_{D,B} = \ln\left(\frac{2c'_A - 1}{2c'_B - 1} \right) \qquad (C.23)$$

which is identical to the dimensionless pressure shift for the constant pressure linear boundary case.

No-flow internal circular boundary

The shifting for the no-flow internal circular boundary is done in the same manner as for the constant pressure hole. Figure *4.4* presents an example of collapsing two curves for the no-flow boundary hole. The numerical values for this example are presented in Table C.3.

TABLE C.1 :

NUMERICAL DATA FOR SHIFTING A SEMILOG CURVE FOR THE CONSTANT PRESSURE LINEAR BOUNDARY CASE

BASE CASE A : 2C=5000
SHIFTED CASE B : 2C=1000

TDA	PDA	TDB	PDB	TDB,SHIF	PDB,SHIF	%ERROR
0.1000000160 02	0.1568254280 01	0.3993601940 00	0.2156976730 00	0.1000000160 02	0.1825936070 01	-0.1643112260 00
0.2000000330 02	0.1908636090 01	0.7987203870 00	0.4372255230 00	0.2000000330 02	0.2047463920 01	-0.7273666700-01
0.3000000490 02	0.2109296120 01	0.1198080580 01	0.5940333620 00	0.3000000490 02	0.2204271750 01	-0.4502716860-01
0.4000000660 02	0.2252099280 01	0.1597440770 01	0.7140328090 00	0.4000000660 02	0.2524271200 01	-0.3204650960-01
0.5000000820 02	0.2363047810 01	0.1996800970 01	0.8110065420 00	0.5000000820 02	0.2421244930 01	-0.2462799250-01
0.6000000980 02	0.2453792880 01	0.2396161160 01	0.8923103480 00	0.6000000980 02	0.2502548740 01	-0.1986959260-01
0.6999999280 02	0.2530571040 01	0.2795520610 01	0.9622827660 00	0.6999999280 02	0.2572521160 01	-0.1657733310-01
0.7999998330 02	0.2597113840 01	0.3194880360 01	0.1023686990 01	0.7999998330 02	0.2633925390 01	-0.1417402060-01
0.8999997380 02	0.2655831960 01	0.3594240110 01	0.1078387990 01	0.8999997380 02	0.2688626380 01	-0.1234807690-01
0.1000000160 03	0.2708373740 01	0.3993601940 01	0.1127703080 01	0.1000000160 03	0.2737941480 01	-0.1091715430-01
0.2000000330 03	0.3054322920 01	0.7987203870 01	0.1458988140 01	0.2000000330 03	0.3069226530 01	-0.4879514480-02
0.3000000490 03	0.3256847250 01	0.1198080580 02	0.1656571450 01	0.3000000490 03	0.3266809850 01	-0.3058970340-02
000(03	0.3400584150 01	0.1597440770 02	0.1797827820 01	0.4000000660 03	0.3408066210 01	-0.2200226640-02
000(03	0.3512093450 01	0.1996800970 02	0.1907845560 01	0.5000000820 03	0.3518083950 01	-0.1705679210-02
0 6000000980 03	0.3603212570 01	0.2396161160 02	0.1997968970 01	0.6000000980 03	0.3608207360 01	-0.1386204790-02
0 6999999280 03	0.3680258020 01	0.2795520610 02	0.2074302530 01	0.6999999280 03	0.3684540930 01	-0.1163751690-02
0.799999(03	0.3747001350 01	0.3194880360 02	0.2140511580 01	0.7999998330 03	0.3750749960 01	-0.1000434970-02
( )99999? 03	0.3805675460 01	0.3594240110 02	0.2198969940 01	0.8999997380 03	0.3809208330 01	-0.8757168130-03
(00000(04	0.3858542060 01	0.3993601940 02	0.2251303790 01	0.1000000160 04	0.3861542180 01	-0.7775275260-03
20 04	0.4205053160 01	0.7987203870 02	0.2596316050 01	0.2000000330 04	0.4206554440 01	-0.3570184230-03
30 04	0.4407764880 01	0.1198080580 03	0.2798527610 01	0.3000000490 04	0.4408766010 01	-0.2271277420-03
40 04	0.4551595500 01	0.1597440770 03	0.2942108050 01	0.4000000660 04	0.4552346450 01	-0.1649852390-03
0.5000000820 04	0.4663161030 01	0.1996800970 03	0.3053523440 01	0.5000000820 04	0.4663761830 01	-0.1288408720-03
0.6000000980 04	0.4754317640 01	0.2396161160 03	0.3144579940 01	0.6000000980 04	0.4754818340 01	-0.1053145030-03
0.6999999280 04	0.4831389870 01	0.2795520610 03	0.3221580660 01	0.6999999280 04	0.4831819050 01	-0.8883302350-04
0.7999998330 04	0.4898153280 01	0.3194880360 03	0.3288290440 01	0.7999998330 04	0.4898528830 01	-0.7667166170-04
0.8999997380 04	0.4957043020 01	0.3594240110 03	0.3347138460 01	0.8999997380 04	0.4957376850 01	-0.6734446210-04
0.1000000160 05	0.5009722120 01	0.3993601940 03	0.3599784170 01	0.1000000160 05	0.5010022570 01	-0.5997373610-04
0.2000000330 05	0.5356289460 01	0.7987203870 03	0.3746201300 01	0.2000000330 05	0.5356439690 01	-0.2804891360-04
0.3000000490 05	0.5559019930 01	0.1198080580 04	0.3948881700 01	0.3000000490 05	0.5559120090 01	-0.1801782530-04
0.4000000660 05	0.5702859920 01	0.1597440770 04	0.4092696650 01	0.4000000660 05	0.5702935040 01	-0.1317270760-04
0.5000000820 05	0.5814451070 01	0.1996800970 04	0.4204252780 01	0.5000000820 05	0.5814491170 01	-0.1033603690-04
)0000098D 05	0.5905591430 01	0.2396161160 04	0.4295403120 01	0.6000000980 05	0.5905641520 01	-0.8480451790-05
99999928D 05	0.5982666340 01	0.2795520610 04	0.4372470880 01	0.6999999280 05	0.5982709270 01	-0.7175342130-05
0.7999999330 05	0.6049431760 01	0.3194880360 04	0.4439231930 01	0.7999998330 05	0.6049469320 01	-0.6209150340-05
0.8999997380 05	0.6108323071) 01	0.3594240110 04	0.4498118060 01	0.8999997380 05	0.6108356450 01	-0.5466045650-05
0.1000000160 06	0.6161003410 01	0.3993601940 04	0.4550795070 01	0.1000000160 06	0.6161033460 01	-0.4877383450-05
) 3D 06	0.6507576380 01	0.7987203870 04	0.4897353010 01	0.2000000330 06	0.6507591400 01	-0.2308833500-05
) 9D 06	0.6710308720 01	0.1198080580 05	0.5100080350 01	0.3000000490 06	0.6710318740 01	-0.1492723280-05
4000000066D 06	0.6854149650 01	0.1597440770 05	0.5243918770 01	0.4000000660 06	0.6854157160 01	-0.1096049270-05
0.5000000820 06	0.6965721230 01	0.1996800970 05	0.5355488850 01	0.5000000820 06	0.6965727240 01	-0.8627955770-06
0.6000000980 06	0.7056880780 01	0.2396161160 05	0.5446647400 01	0.6000000980 06	0.7056885790 01	-0.7097088310-06
0.6999999280 06	0.7133950520 01	0.2795520610 05	0.5523716420 01	0.6999999280 06	0.7133954820 01	-0.6017504050-06
0.7999990330 06	0.7200699610 01	0.3194880360 05	0.5590464980 01	0.7999998330 06	0.7200703370 01	-0.5216509650-06
0.8999997380 06	0.7259552690 01	0.3594240110 05	0.5649317640 01	0.8999997380 06	0.7259556030 01	-0.4599307630-06
0.1000000160 07	0.7312159210 01	0.3993601940 05	0.5701923020 01	0.1000000160 07	0.7312162210 01	-0.4109595460-06
0.2000000330 07	0.7653291040 01	0.7987203870 05	0.6043054150 01	0.2000000330 07	0.7653292540 01	-0.1963210370-06
0.3000000490 07	0.7839776830 01	0.1198080580 06	0.6229539440 01	0.3000000490 07	0.7839777830 01	-0.1277674500-06
0.4000000660 07	0.7959806020 01	0.1597440770 06	0.6349568380 01	0.4000000660 07	0.7959806770 01	-0.9438060710-07
0.5000000820 07	0.8043749660 01	0.1996800970 06	0.6433511870 01	0.5000000320 07	0.8043750260 01	-0.7471693590-07
0.6000000980 07	0.8105767420 01	0.2396161160 06	0.6495529530 01	0.6000000980 07	0.8105767920 01	-0.6178739890-07
0.6999999280 07	0.8153450190 01	0.2795520610 06	0.6543212220 01	0.6999999280 07	0.8155450610 01	-0.5265092090-07
0.7999998330 07	0.8191246750 01	0.3194880360 06	0.6581008730 01	0.7999998330 07	0.8191247130 01	-0.4585698490-07

TABLE C.2 :

NUMERICAL DATA FOR SHIFTING A SEMILOG CURVE FOR THE CONSTANT PRESSURE HOLE

BASE CASE A :F=0.5 2C=500
SHIFTED CASE B :F=0.5 2C=100

TDA	PDA	PDB,SHIF	%ERROR
0.3999999900 01	0.112834613D 01	0.166107173D 01	-0.472129629D 00
0.5999999850 01	0.1320939180 01	0.171671837D 01	-0.2996195460 00
0.7999999800 01	0.145966981D 01	0.177410143D 01	-0.215412838D 00
0.9999999750 01	0.156816201D 01	0.182880611D 01	-0.166209936D 00
0.199999995D 02	0.190854578D 01	0.204863777D 01	-0.734024756D-01
0.3999999900 02	0.225200893D 01	0.2324507990 01	-0.321930619D-01
0.5999999850 02	0.245370237D 01	0.250247112D 01	-0.198755762D-01
0.799999980D 02	0.2597023420 01	0.263368843D 01	-0.141180875D-01
0.999999975D 02	0.270828308D 01	0.2737606830 01	-0.108274322D-01
0.199999995D 03	0.305423214D 01	0.306868905D 01	-0.473340022D-02
0.3999999900 03	0.340049334D 01	0.3407420900 01	-0.203722486D-02
0.5999999850 03	0.3603121740 01	0.3607524790 01	-0.122201103D-02
0.7999999800 03	0.3746910720 01	0.3750046730 01	-0.837490798D-03
0.9999999750 03	0.385845135D 01	0.3860829430 01	-0.616330280D-03
0.1999999950 04	0.4204964650 01	0.4205820910 01	-0.203629557D-03
0.3999999900 04	0.455148392D 01	0.4551570260 01	-0.207262481D-04
0.5999999850 04	0.475417234D 01	0.4754012540 01	0.336133073D-04
0.7999999800 04	0.489802441D 01	0.489773758D 01	0.5855934190-04
0.9999999750 04	0.500958674D 01	0.5009223650 01	0.7247854990-04
0.1999999950 05	0.5352158960 01	0.535163660D 01	0.975985582D-04
0.399999990D 05	0.5667590220 01	0.5666945120 01	0.113823374D-03
0.5999999850 05	0.5825835910 01	0.5025105630 01	0.125351224D-03
0.7999999800 05	0.592334057D 01	0.592254018D 01	0.135124772D-03
0.9999999750 05	0.5990327980 01	0.598946822D 01	0.1435253340-03
01 999999950 06	8.6154094670 01	0.6153013720 01	0.17239771 7D-03
0.3999999900 06	0.6264036500 01	0.6262772390 01	0.201804085D-03
0.599999985D 06	0.631043262D 01	0.6309057090 01	0.217977471D-03
0.799999980D 06	0.6337372530 01	0.6335922480 01	0.228809715D-03
0.9999999750 06	0.6355470830 01	0.6353965650 01	0.236831 900D-03
0.1999999950 07	0.639965020D 01	0.6397987940 01	0.259742347D-03
0.3999999900 07	0.6430918470 01	0.642911814D 01	0.279950322D-03
0.5999999850 07	0.6445170810 01	0.644329739D 01	0.2906708780-03
0.7999999800 07	0.6453938560 01	0.6452016420 01	0.297824357D-03
0.9999999750 07	0.646010112D 01	0.645814289D 01	0.303126713D-03
0.19999999513 08	0.6476406290 01	0.6474344780 01	0.318310622D-03

TABLE C.3 :

NUMERICAL DATA FOR SHIFTING A SEMILOG CURVE FOR THE NO–FLOW BOUNDARY HOLE

BASE CASE A :F=0.5 2C=500
SHIFTED CASE O :F=0.5 2C=100

TDA	PDA	PDB,SHIF	%ERROR
0.399999990D+01	0.1 128346130+01	0.165960201D+01	-0.470827049D+00
0.599999985D+01	0.132093918D+01	0.171562896D+01	-0.298794817D+00
0.799999980D+01	0.145966981D+01	0.177329356D+01	-0.214859379D+00
0.999999975D+01	0.156816201D+01	0.182820744D+01	-0.165828171D+00
0.199999995D+02	0.190854578D+01	0.204857370D+01	-0.733689054D-01
0.399999990D+02	0.225200892D+01	0.232478180D+01	-0.323146494D-01
0.599999985D+02	0.245370237D+01	0.250286963D+01	-0.200379916D-01
0.799999980D+02	0.259702342D+01	0.263415172D+01	-0.142964812D-01
0.999999975D+02	0.270828308D+01	0.273810979D+01	-0.110131443D-01
0.199999995D+03	0.305423214D+01	0.306927323D+01	-0.492467004D-02
0.3999999900'03	0.340049333D+01	0.340804669D+01	-0.222125244D-02
0.599999985D+03	0.360312173D+01	0.3608164590101	-0.139958125D-02
0.7999999300'03	0.374691067D+01	0.375069552D+01	-0.101012555D-02
0.999999975D+03	0.385845111D+01	0.386148027D+01	-0.785071217D-03
0.199999995D+04	0.420496053D+01	0.420647633D+01	-0.360480930D-03
0.399999990D+04	0.455152353D+01	0.4552282190+01	-0.166682157D-03
0.599999985D+04	0.475426649D+01	0.475477207D+01	-0.106342455D-03
0.7999999800'04	0.489807723D+01	0.489845589D+01	-0.773089757D-04
0.999999975D+04	0.500964936D+01	0.500995443D+01	-0.608972645D-04
0.199999995D+05	0.535956364D+01	0.535980007D+01	-0.441143853D-04
0.399999990D+05	0.572878257D+01	0.572925560D+01	-0.825714963D-04
0.599999985D+05	0.595979173D+01	0.596051972D+01	-0.122150063D-03
0.7999999300'05	0.612990536D+01	0.613084156D+01	-0.152644908D-03
0.999999975D+05	0.626434304D+01	0.626544671D+01	-0.176183301D-03
0.199999995D+06	0.668519680D+01	0.668682515D+01	-0.243574549D-05
0.3999999900106	0.709206427D+01	0.70941 7118D+01	-0.297079847D-03
0.599999985D+06	0.731839981D+01	0.732073246D+01	-0.318738781D-03
0.799999980D+06	0.747387170D+01	0.747633049D+01	-0.328985592D-03
0.999999975D+06	0.759197412D+01	0.759451045D+01	-0.334080478D-03
0.1999999950'07	0.794894577D+01	0.795162524D+01	-0.337084857D-03
0.399999990D+07	0.829778303D+01	0.830050926D+01	-0.328548784D-03
0.599999985D+07	0.850036850D+01	0.850310090D+01	-0.321445095D-03
0.799999980D+07	0.864385986D+01	0.864659231D+01	-0.316114810D-03
0.999999975D+07	0.875510274D+01	0.875783390D+01	-0.311950456D-03
0.199999995D+08	0.910063785D+01	0.910336218D+01	-0.299355654D-03

APPENDIX D : DERIVATION OF THE LATE TIME DIMENSIONLESS PRESSURE FOR THE CONSTANT PRESSURE HOLE USING THE DOUBLET MODEL

In this appendix , we derive Eq. 3.38 using the doublet model presented in Chapter 2. Using Eq. 2.9 and referring to Fig. D.1, we can write the dimensionless steady state pressure as follows :

$$p_{Dss}(r_D,\theta) = p_{Dss}(4\text{-}3) = p_{Dss}(4\text{-}5) - p_{Dss}(3\text{-}5) =$$

$$- \ln\left(\frac{r_{1-4}}{r_{2-4}}\right) + \ln\left(\frac{r_{1-3}}{r_{2-3}}\right) = - \ln\left(\frac{R_D}{r_{D2}}\right) + \ln\left(\frac{r'_D - a_D}{2c' - r'_D + a_D}\right) =$$

$$\ln\left[\frac{r_{D2}(r'_D - a_D)}{R_D(2c' - r'_D + a_D)}\right] \qquad (D.1)$$

Using the radius of the hole from Eq. 2.13, we solve **for** the value of c' :

$$c' = \frac{r'^{\,2}_D - a^2_D}{2r'_D} \qquad (D.2)$$

Now, we evaluate r_{D2} and R_D :

$$r^2_{D2} = r^2_D \left[1 - 2\frac{a^2_D}{r_D r'_D}\cos\theta + \left(\frac{a^2_D}{r_D r'_D}\right)^2 \right] \qquad (D.3)$$

$$R^2_D = r'^{\,2}_D \left[1 - 2\frac{r_D}{r'_D}\cos\theta + \left(\frac{r_D}{r'_D}\right)^2 \right] \qquad (D.4)$$

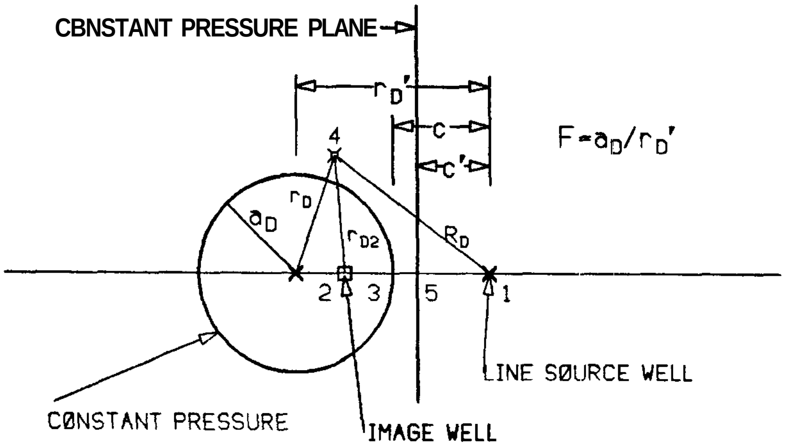

FIGURE D.1 : THE GEOMETRY OF THE DOUBLET MODEL FOR THE CONSTANT PRESSURE HOLE AT STEADY STATE

Substituting Eqs. D.2, D.3 and D.4 into Eq. D.1 yields :

$$p_{Dss} = \ln\left(\frac{r_D}{a_D}\right) + \frac{1}{2}\ln \frac{1 - 2\dfrac{a_D^2}{r_D r_D'}\cos\theta + \left(\dfrac{a_D^2}{r_D r_D'}\right)^2}{1 - 2\dfrac{r_D}{r_D'}\cos\theta + \left(\dfrac{r_D}{r_D'}\right)^2} \tag{D.5}$$

Equation D.5 is identical to Eq. 3.38.

APPENDIX E : DIMENSIONLESS DEPARTURE TIME FROM THE LINE SOURCE

The dimensionless departure time is defined as the dimensionless time at which the deviation from the line source is one percent. This definition was suggested by Ramey, et al. (1973). Stallman (1952) showed that the constant pressure and no–flow linear boundaries have the same departure time. This observation is based on the superposition of two exponential integrals.

For practical purposes, a system containing a circular boundary has the sam departure time as the limiting linear boundary system. This can be observed in Fig. 3.8.

Using the following two equations and the Newton - Raphson iterative method, we generated the departure times shown in Fig. 3.9 :

$$f(2c,t_D) = E_i(-X_1) - 0.01 \; E_i(-X_2) = 0 \tag{E.1}$$

The Newton - Raphson method uses the derivatives of the function to find the next *guess* of the zero of the function. Hence :

$$\frac{df(2c,t_D)}{dt_D} = -\frac{1}{t_D}\left(e^{-X_1} - e^{-X_2} \right) \tag{E.2}$$

where :

$$X_1 = \frac{(2c-1)^2}{4t_D} \tag{E.3}$$

$$X_2 = \frac{1}{4t_D} \tag{E.4}$$

APPENDIX F : ASYMPTOTIC EXPANSIONS FOR MODIFIED BESSEL FUNCTIONS

In this appendix, we point out to some computational problems in evaluating Modified Bessel Functions using asymptotic expansions.

The asymptotic expansions for $I_n(z)$ and $K_n(z)$ are :

$$I_n(z) = \frac{1}{\sqrt{2\pi z}}\, e^{z} \left[1 - \frac{v-1}{8z} + \frac{(v-1)(v-9)}{2!\,(8z)^2} - \frac{(v-1)(v-9)(v-25)}{3!\,(8z)^3} + \cdots \right] \tag{F.1}$$

$$K_n(z) = \sqrt{\pi/2z}\; e^{-z} \left[1 + \frac{v-1}{8z} + \frac{(v-1)(v-9)}{2!\,(8z)^2} - \frac{(v-1)(v-9)(v-25)}{3!\,(8z)^3} - \cdots \right] \tag{F.2}$$

where : $\qquad v = 4n^2$

or :

$$I_n(z) = \frac{1}{\sqrt{2\pi z}}\, e^{z}\, F_n(z) \tag{F.3}$$

$$K_n(z) = \sqrt{\pi/2z}\; e^{-z}\, G_n(z) \tag{F.4}$$

where :

$$F_n(z) = 1 + \sum_{m=1}^{\infty} (-1)^m \frac{\prod_{j=1}^{m} \left[v - (2j-1)^2 \right]}{m!\,(8z)^m} \tag{F.5}$$

$$G_n(z) = 1 + \sum_{m=1}^{\infty} \frac{\prod_{j=1}^{m} [\, v - (2j - 1)^2 \,]}{m!\ (8z)^m} \qquad \text{(F.6)}$$

The terms $F_n(z)$ and $G_n(z)$ differ by the alternating sign. Let us examine the convergence of $G_n(z)$.

Let R_n^m be the convergence ratio :

$$R_{n,m} = \left\| \frac{G_{n,m}(z)}{G_{n,m}(z)} \right\| \qquad \text{(F.7)}$$

where $G_{n,m}(z)$ denotes the m^{th} term in $G_n(z)$. Substituting Eq. D.6 into Eq. F.7 yields :

$$R_{n,m} = \left\| \frac{4n^2 - (2m - 1)^2}{8mz} \right\| \qquad \text{(F.8)}$$

For G to converge, $R_{n,m}$ must be less than 1 :

$$\| m - m^2 + n^2 - 1/4 \| < 2mz \qquad \text{(F.9)}$$

For a fixed z and n, we can find the range of m that satisfies the convergence criterion. Let :

$$L(m) = \| m - m^2 + n^2 + 1/4 \| \qquad \text{(F.10)}$$

$$R(m) = 2mz \qquad \text{(F.11)}$$

Figure F.1 presents L(m) and R(m) as a function of m for n = 50 and z = 5,10 and 20. The ranges of m where R(m) is "above" L(m) satisfy the convergence condition.

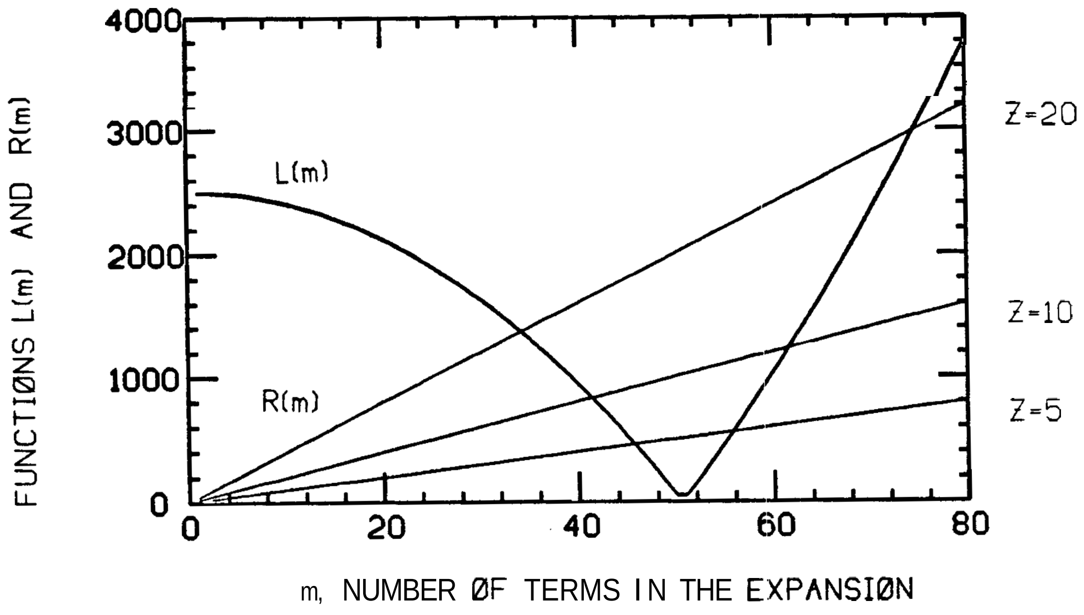

FIGURE F.1 : R(m) and L(m) AS A FUNCTION OF m IN THE ASYMPTOTIC EXPANSION OF $K_{50}(5)$, $K_{50}(10)$ and $K_{50}(20)$

Let m_{min} and m_{max} be the ends of these ranges. Then :

$$m_{min} = \frac{1}{2} \{ 1 - 2z + [(2z - 1)2 + 4n^2 - 1]^{\frac{1}{2}} \} \tag{F.12}$$

$$m_{max} = \frac{1}{2} \{ 1 + 2z + [(1 + 2z)^2 + 4n^2 - 1]^{\frac{1}{2}} \} \tag{F.13}$$

As m increases from 1, $R_{n,m} > 1$. Then, $R_{n,m}$ enters the convergence range, and finally, $R_{n,m} > 1$ for all $m > m_{max}$. This explains why we use asymptotic expansions for large arguments. As z increases, the range between m_{min} and m_{max} increases, and we have more terms in the series that satisfy the covergence criterion. Eqs. F.12 and F.13 offer a simple way to limit the number of terms used when evaluating Modified Bessel Functions using asymptotic expansions.

Figure F.2 presents the estimate of $K_{50}(5)$ as a function of the number of terms in the expansion, m. $K_{50}(5)$ levels off at a value close to its actual value. The accuracy in this case is 4 digits. The expansion starts to diverge in the 56^{th} term, and by the 70^{th} term the expansion is off the scale. In Fig. F.2 the absolute value of the estimate of $K_{50}(5)$ is graphed. At large values of m, the function alternates signs and diverges.

In the asymptotic expansion for $I_n(z)$, the terms in the series alternate signs up to a certain value of m, therefore all the terms take on either a positive or a negative sign. The sign depends upon the m at which $[\, v - (2m - 1)^2 \,]$ becomes negative.

The use of asymptotic expansions for evaluating $I_n(z)$ and $K_n(z)$ has a limited accuracy, not always satisfying our needs. In these cases, other methods should be used. Using m_{min} and m_{max}, we can set the limit on the number of terms used in the expansion, hence, simplifying the calculations.

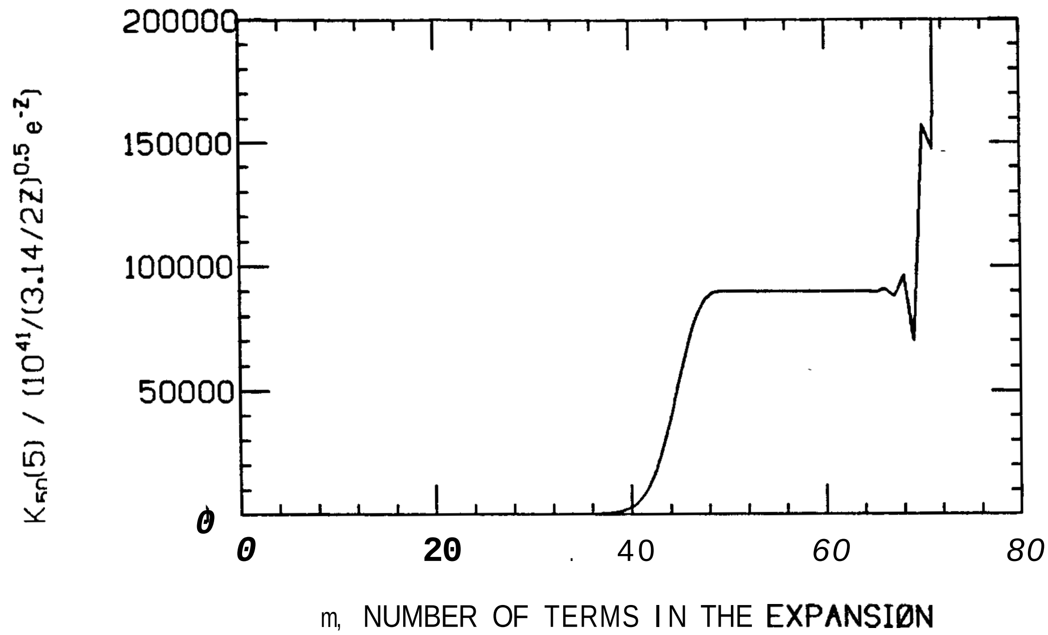

FIGURE F.2 : ASYMPTOTIC EXPANSION FOR $K_{50}(5)$ AS A FUNCTION OF THE NUMBER OF TERMS IN THE EXPANSION, m

APPENDIX G : THE COMPUTER PROGRAM

In this appendix, we presents the general approach taken in the numerical evaluation of the solutions. A detailed description of the various equations used in evaluating F(s) is presented. A listing of the program is presented at the end.

The numerical evaluation uses the Stehfest (1970) for the numerical inversion of the Laplace solutions. The Laplace solutions are :

For a constant pressure boundary :

$$p_D = \frac{1}{s} \left[K_0(SRRRD) - \frac{K_0(SRWD)\, I_0(SAAD)\, K_0(SRRD)}{K_0(SAAD)} \right.$$

$$\left. - 2 \sum_{n=1}^{\infty} \cos\theta \, \frac{K_n(SRWD)\, I_n(SAAD)\, K_n(SRRD)}{K_n(SAAD)} \right] \tag{G.1}$$

For a no-flow boundary :

$$p_D = \frac{1}{s} \left\{ K_0(SRRRD) + \frac{K_0(SRWD)\, I_1(SAAD)\, K_0(SRRD)}{K_1(SAAD)} \right.$$

$$\left. + 2 \sum_{n=1}^{\infty} \cos\theta \, \frac{K_n(SRWD) \left[I_{n-1}(SAAD) + I_{n+1}(SAAD) \right] K_n(SRRD)}{\left[K_{n-1}(SAAD) + K_{n+1}(SAAD) \right]} \right\}$$

(G.2)

where :

s = The Laplace variable

$$SRRRD = \sqrt{s}\, R_D$$

$$SAAD = \sqrt{s}\, a_D$$

$$SRWD = \sqrt{s}\, r_D'$$

$$SRRD = \sqrt{s}\, r_D$$

The solutions consist of the line source term (the first term) and an infinite series. This series is separated into two parts. The first part contains terms with Modified Bessel Functions of order zero. The second part contains terms with Modified Bessel Functions of order greater than zero.

Figure G.1 presents a flow diagram for the computer program. Since we are interested in interference testing, the program takes advantage of the nature of the solutions. The infinite series terms contain two types of geometrical variables, radii and angles, which are separated. Hence, for a fixed set of radii (AAD,RRD,RWD) we evaluate p_D for various angles. The radii dependent terms are evaluated once for various angles. Therefore, the angle loop is within the time loop. This approach requires more active storage but reduces the CPU time needed to evaluate p_D for a second angle by an order of magnitude or more.

The "navigation" section of the program chooses the method for evaluating the terms in the series of F(s). The complexity in evaluating F(s) stems from the infinite series on the order of the Modified Bessel Functions. Figure G.2 and Tab. G.1 describe the navigation decision tree program.

The following terms are used :

$$EKAAD = \| \log K_n(SAAD) \|$$

$$EKRWD = \| \log K_n(SRWD) \|$$

$$EKRRD = \| \log K_n(SRRD) \|$$

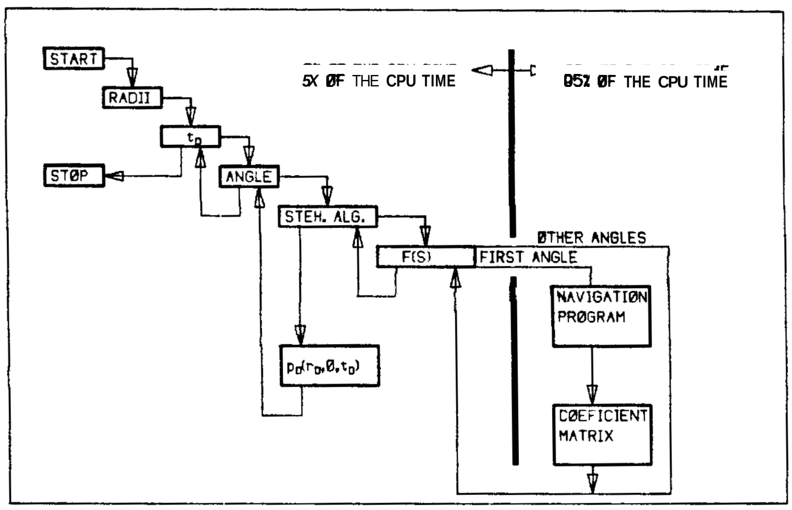

FIGURE G.1 : A FLOW DIAGRAM FOR THE COMPUTER PROGRAM

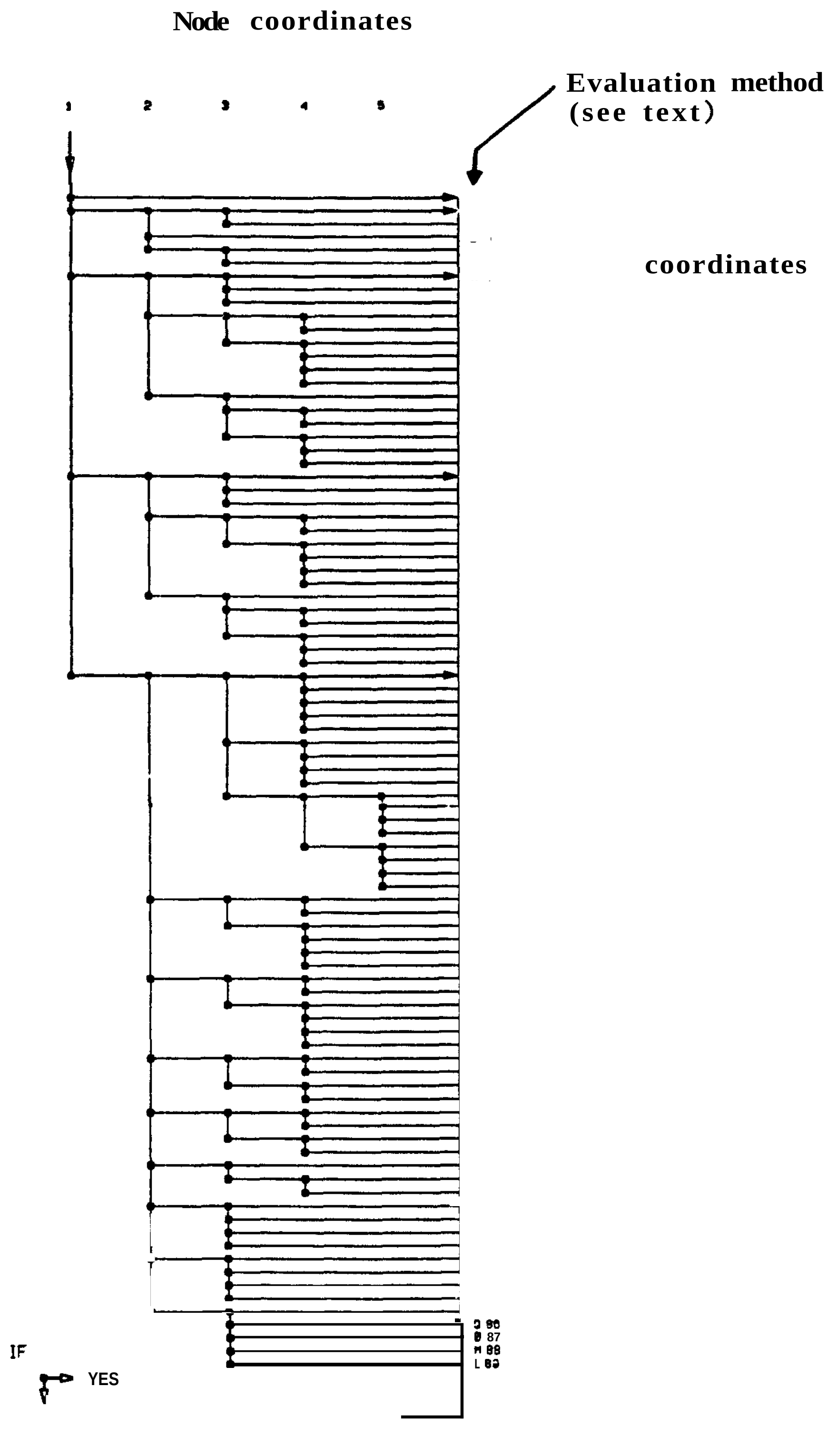

FIGURE G.2 : A SCHEMATIC FLOW DIAGRAM OF THE NAVIGATION PROGRAM

TABLE G-1 :

THE NAVIGATION PROGRAM DECISION TREE

COORDINATES		IF CONDITION	
1	1	SAAD>100	
1	2	SRWD>100	SRRD≥100
1	7	SRWD>100	SRRD<100
1	22	SRWD<100	SRRD>100
1	37	SRWIK 100	SRRD<100
2	2	SAAD>20	
2	4	SAAD≥2	
2	5	SAAD<1	
2	7	SAAD>20	SRRD 220
2	10	SAAD<20	SRRD>20
2	16	SAAD<20	SRRD<20
2	22	SAAD>20	SRWD>20
2	25	SAAD<20	SRWD 220
2	31	SAAD<20	SRWIK 20
2	37	SRWD>20	SRRD>20
2	54	SRWD>20	SRRD>2
2	60	SRWD≥2	SRRD≥20
2	66	SRWD≥20	SRRD<20
2	70	SRWD<2	SRRD>20
2	74	SRWD≥2	SRRD≥2
2	77	SRWD≥2	SRRD<2
2	81	SRWD<2	SRRD>2
2	85	SRWD<2	SRRD<2
3	2	EKAAD≥65	
3	3	EKAAD<65	
3	5	EKAAD≥65	
3	6	EKAAD<65	
3	7	EKAAD≥65	EKRRD≥65
3	8	EKAAD<65	EKRRD≥65
3	9	EKAAD<65	EKRRD<65
3	10	SAAD≥2	
3	12	SAAD>2	
3	16	SAAD 22	SRRD≥2
3	17	SAAD<2	SRRD≥2
3	19	SRRD<2	
3	22	EKAAD>65	EKRWD>65
3	23	EKAAD<65	EKRWD>65
3	24	EKAAD<65	EKRWD<65
3	25	SAAD>2	
3	27	SAAD<2	
3	31	SAAD≥2	SRWD>2
3	32	SAAD<2	SRWD>2

COORDINATES		IF CONDITION	
3	34	SRWD<2	
3	37	SAAD>20	
3	42	SAAD>2	
3	46	SAAD<2	
3	54	SAAD>2	
3	56	SAAD<2	
3	60	SAAD>2	
3	62	SAAD<2	
3	66	EKRRD>65	
3	68	EKRRD<65	
3	70	EKRWD>65	
3	72	EKRWD<65	
3	74	SAAD>2	
3	75	SAAD<2	
3	77	EKRRD>65	EKAAD>65
3	78	EKRRD>65	EKAAD<65
3	79	EKRRD<65	EKAAD>65
3	80	EKRRD<65	EKAAD<65
3	81	EKRWD>65	EKAAD>65
3	82	EKRWD>65	EKAAD<65
3	83	EKRWD<65	EKAAD>65
3	84	EKRWD<65	EKAAD<65
3	85	EKAAD<65	
3	86	EKRWD>65	EKRRD>65
3	87	EKRWD>65	EKRRD<65
3	88	EKRWD<65	EKRRD>65
3	89	EKRWD<65	EKRRD<65
4	10	EKRRD>65	
4	11	EKRRD<65	
4	12	EKRRD>65	EKAAD>65
4	13	EKRRD>65	EKAAD<65
4	14	EKRRD<65	EKAAD>65
4	15	EKRRD<65	EKAAD<65
4	17	EKAAD>65	
4	18	EKAAD<65	
4	19	EKRRD>65	EKAAD>65
4	20	EKRRD<65	EKAAD>65
4	21	EKRRD<65	EKAAD<65
4	25	EKRWD>65	
4	26	EKRWD<65	
4	27	EKAAD>65	EKRWD>65
4	28	EKAAD<65	EKRWD>65
4	29	EKAAD>65	EKRWD<65
4	30	EKAAD<65	EKRWD<65
4	32	EKAAD>65	
4	33	EKAAD<65	
4	34	EKAAD>65	EKRWD>65

COORDINATES		IF CONDITION	
4	35	EKAAD>65	EKRWD<65
4	36	EKAAD<65	EKRWD<65
4	37	EKAAD>65	
4	38	EKRWD>65	EKAAD>65
4	39	EKRWD>65	EKAAD<65
4	40	EKRWD<65	EKAAD>65
4	41	EKRWD<65	EKAAD<65
4	42	EKRWD>65	EKRRD>65
4	43	EKRWD>65	EKRRD<65
4	44	EKRWD<65	EKRRD>65
4	45	EKRWD<65	EKRRD<65
4	46	EKAAD<65	
4	50	EKAAD>65	
4	54	EKRWD>65	
4	55	EKRWD<65	
4	56	EKRWD>65	EKAAD>65
4	57	EKRWD>65	EKAAD<65
4	58	EKRWD<65	EKAAD>65
4	59	EKRWD<65	EKAAD<65
4	60	EKRRD>65	
4	61	EKRRD<65	
4	62	EKRRD>65	EKAAD>65
4	63	EKRRD>65	EKAAD<65
4	64	EKRRD<65	EKAAD>65
4	65	EKRRD<65	EKAAX 65
4	66	EKRWD>65	
4	67	EKRWD<65	
4	68	EKAAD>65	
4	69	EKAAD<65	
4	70	EKAAD>65	
4	71	EKAAD<65	
4	72	EKAAD>65	
4	73	EKAAD<65	
4	75	EKAAD>65	
4	76	EKAAD<65	
5	46	EKRWD>65	EKRRD>65
5	47	EKRWD>65	EKRRD<65
5	48	EKRWD<65	EKRRD>65
5	49	EKRWD<65	EKRRD<65
5	50	EKRWD>65	EKRWD>65
5	51	EKRWD>65	EKRRD<65
5	52	EKRWD<65	EKRRD>65
5	53	EKRWD<65	EKRRD<65

The next section presents the various methods used as perscribed by the navigation decision tree (Fig. 6.2) to evaluate the terms in the infinite series of $F(s)$. The asymptotic expansions are presented in appendix D. The ascending series for Modified Bessel Functions are :

$$I_n(z) = (z/2)^n \sum_{k=0}^{\infty} \frac{\left(\frac{z^2}{4}\right)^k}{k!\,(n+k)!} \tag{G.3}$$

$$K_n(z) = \frac{1}{2}(z/2)^{-n} \sum_{k=0}^{\infty} \frac{(n-k-1)!}{k!} \left(-\frac{z^2}{4}\right)^k$$

$$+ (-1)^{n+1} \ln(z/2)\, I_n(z) + (-1)\,\frac{1}{2}(z/2)^n$$

$$\cdot \sum_{k=0}^{\infty} \frac{\left(\frac{z^2}{4}\right)^k}{k!\,(n+k)!} \left[\, \psi(k+1) + \psi(n+k+1) \,\right] \tag{G.4}$$

where :

$$\psi(1) = -\gamma$$

$$\psi(n) = -\gamma + \sum_{k=1}^{n-1} k^{-1} \qquad (n > 2)$$

$$y = 0.5772156649 \qquad \text{(Euler constant)}$$

For the small argument approximation used in chapters 5 and 6, only the first term in the series is taken. However, for the approximations used in the numerical evaluation, the following is used :

For $I_n(z)$:

$$I_n(z) = \frac{(z/2)^n}{n!} \left[1 + \sum_{k=1}^{\infty} \frac{(z^2)^k}{k!\,(n+1)(n+2)\cdots(n+k)} \right] \tag{G.5}$$

For $K_n(z)$, only the first series is taken, assuming that $I_n(z)$ is negligible along with the third term which contains positive powers of the argument z, hence :

$$K_n(z) = 2^{n-1} z^{-n} (n-1)! \left[1 + \sum_{k=1}^{n-1} \frac{\left(\frac{z^2}{4}\right)^k}{k!\,(n-1)(n-2)\cdots(n-k)} \right] \tag{G.6}$$

For the ascending series we use the following notations :

$$I_n(z) \doteq \frac{(z/2)^n}{n!} \, FISMA_n(z) \tag{G.7}$$

$$K_n(z) = 2^{n-1} z^{-n} (n-1)! \, FKSMA_n(z) \tag{G.8}$$

while, for the asymptotic expansions, we use :

$$I_n(z) = \frac{1}{\sqrt{2\pi z}} e^{z} F_n(z) \tag{G.9}$$

$$K_n(z) = \sqrt{\pi/2z}\, e^{-z} G_n(z) \tag{G.10}$$

F and G are defined in appendix F.

EQUATIONS FOR THE CONSTANT PRESSURE CIRCULAR BOUNDARY

OPTION A : Complete asymptotic expansion

$$A_n = \frac{1}{2\sqrt{(SRRD)(SRWD)}}\, e^{2(SAAD) - SRRD - SRWD}$$

$$\cdot \frac{G_n(SRWD)F_n(SAAD)G_n(SRRD)}{G_n(SAAD)} \tag{G.11}$$

OPTION B : Partial asymptotic expansion (RWD,RRD)

$$\log A_n = \log I_n(SAAD) - (SRWD - SRRD)\log e - \log K_n(SAAD)$$

$$+ \log \left[\frac{\pi}{2\sqrt{(SRWD)(SRRD)}}\, G_n(SRRD)G_n(SRWD) \right] \tag{G.12}$$

OPTION C : Partial asymptotic expansion (RWD,RRD)

Small argument approximation (AAD)

$$\log A_n = \log \left[n\pi G_n(SRWD)G_n(SRRD) \frac{1}{\sqrt{(SRRD)(SRWD)}} \right] + 2n \log(SAAD)$$

$$- \left[(SRWD + SRRD) \right] \log e - 2n \log 2 - 2 \log(n!)$$

$$+ \log \left[\frac{FISMA_n(SAAD)}{FKSMA_n(SAAD)} \right] \tag{G.13}$$

OPTION D : Partial asymptotic expansion (RWD)

$$\log A_n = \log K_n(\mathrm{SRRD}) + \log I_n(\mathrm{SAAD}) - \log K_n(\mathrm{SAAD})$$

$$+ \log \left[\frac{\sqrt{\pi}}{\sqrt{2(\mathrm{SRWD})}} G_n(\mathrm{SRWD}) \right] - \mathrm{SRWD} \log e \qquad \text{(G.14)}$$

OPTION F : Partial asymptotic expansion (RWD)

Small argument approximation (AAD)

$$\log A_n = \log \left[\frac{\sqrt{\pi}}{\sqrt{2(\mathrm{SRWD})}} K_n(\mathrm{SRRD}) \right] + \log \left[2n\, G_n(\mathrm{SRWD}) \right] - \mathrm{SRWD} \log e$$

$$- 2 \log(n!) - 2n \log 2 + 2n \log(\mathrm{SAAD}) + \log \left[\frac{\mathrm{FISMA}_n(\mathrm{SAAD})}{\mathrm{FKSMA}_n(\mathrm{SAAD})} \right]$$

(G.15)

OPTION G : Partial asymptotic expansion (RWD)

Small argument approximation (RRD,AAD)

$$\log A_n = \log \left[\frac{\sqrt{\pi}}{\sqrt{2(\mathrm{SRWD})}} \right] + 2n \log(\mathrm{SAAD}) - n \log(\mathrm{SRRD}) - (\mathrm{SRWD}) \log e$$

$$- n \log 2 - \log(n!) + \log \left[\frac{\mathrm{FISMA}_n(\mathrm{SAAD})\,\mathrm{FKSMA}_n(\mathrm{SRRD})}{\mathrm{FKSMA}_n(\mathrm{SAAD})} \right] \qquad \text{(G.16)}$$

OPTION I : Partial asymptotic expansion (RRD)

$$\log A_n = \log K_n(\mathrm{SRWD}) + \log I_n(\mathrm{SAAD}) - \log K_n(\mathrm{SAAD}) - (\mathrm{SRRD}) \log e$$

$$+ \log \left[\frac{\sqrt{\pi}}{\sqrt{2(\mathrm{SRRD})}} \right] \qquad \text{(G.17)}$$

OPTION J : Partial asymptotic expansion (RRD)

Small argument approximation (AAD)

$$\log A_n = \log \left[\frac{\sqrt{\pi}}{\sqrt{2(\mathrm{SRRD})}} K_n(\mathrm{SRWD}) \right] + \log \left[2nG_n(\mathrm{SRRD}) \right] - (\mathrm{SRRD}) \log e$$

$$- 2\log(n!) - 2n\log 2 + 2n\log(\mathrm{SAAD}) + \log \left[\frac{\mathrm{FISMA}_n(\mathrm{SAAD})}{\mathrm{FKSMA}_n(\mathrm{SAAD})} \right]$$

$$\text{(G.18)}$$

OPTION K : Partial asymptotic expansion (RRD)

Small argument approximation (AAD)

$$\log A_n = \log \left[\frac{\sqrt{\pi}}{\sqrt{2(\mathrm{SRRD})}} G_n(\mathrm{SRRD}) \right] + 2n\log(\mathrm{SAAD}) - n\log(\mathrm{SRWD})$$

$$- (\mathrm{SRRD})\log e - n\log 2 - \log(n!) + \log \left[\frac{\mathrm{FISMA}_n(\mathrm{SAAD})\mathrm{FKSMA}_n(\mathrm{SRWD})}{\mathrm{FKSMA}_n(\mathrm{SAAD})} \right]$$

$$\text{(G.19)}$$

OPTION L : Small argument approximation (AAD)

$$\log A_n = \log K_n(SRWD) + \log K_n(SRRD) - 2n\log(SAAD) - \log 2n - 2n\log 2$$

$$- 2\log(n!) + \log \left[\frac{FISMA_n(SAAD)}{FKSMA_n(SAAD)} \right] \tag{G.20}$$

OPTION M : Small argument approximation (AAD.RRD)

$$\log A_n = \log K_n(SRWD) + 2n\log(SAAD) - n\log(SRRD) - n\log 2 - \log(n!)$$

$$+ \log \left[\frac{FISMA_n(SAAD)FKSMA_n(SRRD)}{FKSMA_n(SAAD)} \right] \tag{G.21}$$

OPTION N : Small argument approximation (RRD)

$$\log A_n = \log K_n(SRWD) + \log I_n(SAAD) - \log K_n(SAAD) + n\log 2 + \log(n!)$$

$$- n\log(SRRD) - \log 2n + \log \left[FKSMA_n(SRRD) \right] \tag{G.22}$$

OPTION O : Small argument approximation (AAD,RWD)

$$\log A_n = \log K_n(SRRD) + 2n\log(SAAD) - n\log(SRWD) - n\log 2 - \log(n!)$$

$$+ \log \left[\frac{FISMA_n(SAAD) FKSMA_n(SRWD)}{FKSMA_n(SAAD)} \right] \tag{G.23}$$

OPTION P : Small argument approximation (RWD)

$$\log A_n = \log K_n(SRRD) + \log I_n(SAAD) - \log K_n(SAAD) + n\log 2 + \log(n!)$$

$$- n\log(SRWD) - \log 2n + \log \left[FKSMA_n(SRWD) \right] \tag{G.24}$$

OPTION Q : Small argument approximation (AAD.RRD.RWD)

$$\log A_n = 2n\log(SAAD) - n\log \left[(SRWD)(SRRD) \right] - \log 2n$$

$$+ \log \left[\frac{FKSMA_n(SRRD) FISMA_n(SAAD) FKSMA_n(SRWD)}{FKSMA_n(SAAD)} \right] \tag{G.25}$$

OPTION Z : Simple program

$$A_n = \frac{K_n(SRWD) I_n(SAAD) K_n(SRRD)}{K_n(SAAD)} \tag{G.26}$$

$K_n(z)$ is evaluated using the "step up" method, where :

$$K_{n+1}(z) = K_{n-1}(z) + \frac{2n}{z} K_n(z) \tag{G.27}$$

For $I_n(z)$ the formula :

$$I_{n+1}(z) = I_{n-1}(z) - \frac{2n}{z} I_n(z) \qquad \text{(G.28)}$$

cannot be used due to the minus sign. For n > 10 the errors increase rapidly. $I_n(z)$ is evaluated using the ascending series.

EQUATIONS FOR THE NO-FLOW CIRCULAR BOUNDARY

OPTION A : Complete asymptotic expansion

$$A_n = \frac{1}{2\sqrt{(SRRD)(SRWD)}} \, e^{2(SAAD) - (SRRD) - (SRWD)}$$

$$\cdot \frac{G_n(SRWD)G_n(SRRD)\left[F_{n-1}(SAAD) + F_{n+1}(SAAD)\right]}{\left[G_{n-1}(SAAD) + G_{n+1}(SAAD)\right]} \qquad \text{(G.29)}$$

OPTION B : Partial asymptotic expansion (RWD,RRD)

$$\log A_n = \log \left[I_{n-1}(SAAD) + I_{n+1}(SAAD) \right] - \left[(SRRD) + SRWD) \right] \log e$$

$$- \log \left[K_{n-1}(SAAD) + K_{n+1}(SAAD) \right] + \log \left[\frac{\pi}{2\sqrt{(SRRD)(SRWD)}} \right]$$

$$+ \log \left[G_n(SRRD) G_n(SRWD) \right] \qquad (G.30)$$

OPTION C : Partial asymptotic expansion (RWD.RRD)

Small argument approximation (AAD)

$$\log A_n = \log \left[\frac{n\pi}{\sqrt{(SRRD)(SRWD)}} Gn(SRWD) G_n(SRRD) \right] + 2n\log(SAAD)$$

$$- \left[(SRWD) + (SRRD) \right] \log e - 2n\log 2 - 2\log(n!)$$

$$+ \log \left[\frac{2n}{(SAAD)} FISMA_{n-1}(SAAD) + \frac{(SAAD)}{2(n+1)} FISMA_{n+1}(SAAD) \right]$$

$$- \log \left[\frac{(SAAD)}{2(n-1)} FKSMA_{n-1}(SAAD) + \frac{2n}{(SAAD)} FKSMA_{n+1}(SAAD) \right] \qquad (G.31)$$

OPTION D : Partial asymptotic expansion (RWD)

$$\log A_n = \log K_n(\mathrm{SRRD}) + \log \left[I_{n-1}(\mathrm{SAAD}) + I_{n+1}(\mathrm{SAAD}) \right] - (\mathrm{SRWD})\log e$$

$$- \log \left[K_{n-1}(\mathrm{SAAD}) + K_{n+1}(\mathrm{SAAD}) \right] + \log \left[\frac{\sqrt{\pi}}{2\sqrt{(\mathrm{SRWD})}} G_n(\mathrm{SRWD}) \right]$$

(G.32)

OPTION F : Partial asymptotic expansion (RWD)

Small argument approximation (AAD)

$$\log A_n = \log \left[\frac{\sqrt{\pi}}{2\sqrt{(\mathrm{SRWD})}} K_n(\mathrm{SRRD}) \right] + \log \left[2nG_n(\mathrm{SRWD}) \right] - (\mathrm{SRWD})\log e$$

$$- 2\log(n!) - 2n\log 2 + 2n\log(\mathrm{SAAD})$$

$$+ \log \left[\frac{2n}{(\mathrm{SAAD})} \mathrm{FISMA}_{n-1}(\mathrm{SAAD}) + \frac{(\mathrm{SAAD})}{2(n+1)} \mathrm{FISMA}_{n+1}(\mathrm{SAAD}) \right]$$

$$- \log \left[\frac{(\mathrm{SAAD})}{2(n-1)} \mathrm{FKSMA}_{n-1}(\mathrm{SAAD}) + \frac{2n}{(\mathrm{SAAD})} \mathrm{FKSMA}_{n+1}(\mathrm{SAAD}) \right] \quad \text{(G.33)}$$

OPTION G : Partial asymptotic expansion (RWD)

Small argument approximation (AAD.RRD)

$$\log A_n = \log \left[\frac{\sqrt{\pi}}{2\sqrt{(SRWD)}} G_n(SRWD) \right] - 2n\log(SAAD) - (SRWD)\log e$$

$$- n\log(SRRD) - n\log 2 - \log(n!) + \log \left[FKSMA_n(SRRD) \right]$$

$$+ \log \left[\frac{2n}{(SADD)} FISMA_{n-1}(SAAD) + \frac{(SAAD)}{2(n+1)} FISMA_{n+1}(SAAD) \right]$$

$$- \log \left[\frac{(SAAD)}{2(n-1)} FKSMA_{n-1}(SAAD) + \frac{2n}{(SAAD)} FKSMA_{n+1}(SAAD) \right] \qquad (G.34)$$

OPTION I : Partial asymptotic expansion (RRD)

$$\log A_n = \log K_n(SRWD) + \log \left[I_{n-1}(SAAD) + I_{n+1}(SAAD) \right] - (SRRD)\log e$$

$$- \log \left[K_{n-1}(SAAD) + K_{n+1}(SAAD) \right] + \log \left[\frac{\sqrt{\pi}}{\sqrt{2(SRRD)}} G_n(SRRD) \right]$$

(G.35)

OPTION J : Partial asymptotic expansion (RRD)

Small argument approximation (AAD)

$$\log A_n = \log\left[\frac{\sqrt{p}}{\sqrt{-2(SRRD)}} K_n(SRWD)\right] + \log\left[2nG_n(SRRD)\right] - (SRRD)\log e$$

$$- \log(n!) - 2n\log 2 + 2n\log(SAAD)$$

$$+ \log\left[\frac{2n}{(SAAD)} FISMA_{n-1}(SAAD) + \frac{(SAAD)}{2(n+1)} FISMA_{n+1}(SAAD)\right]$$

$$- \log\left[\frac{(SAAD)}{2(n-1)} FKSMA_{n-1}(SAAD) + \frac{2n}{(SAAD)} FKSMA_{n+1}(SAAD)\right] \qquad (G.36)$$

OPTION K : Partial asymptotic expansion (RRD)

Small argument approximation (RWD.AAD)

$$\log A_n = \log\left[\frac{\sqrt{\pi}}{\sqrt{2(SRRD)}} G_n(SRRD)\right] + 2n\log(SAAD) - n\log(SRWD)$$

$$- (SRRD)\log e - n\log 2 - \log(n!) + \log\left[FKSMA_n(SRWD)\right]$$

$$+ \log\left[\frac{2n}{(SAAD)} FISMA_{n-1}(SAAD) + \frac{(SAAD)}{2(n+1)} FISMA_{n+1}(SAAD)\right]$$

$$- \log\left[\frac{(SAAD)}{2(n-1)} FKSMA_{n-1}(SAAD) + \frac{2n}{(SAAD)} FKSMA_{n+1}(SAAD)\right] \qquad (G.37)$$

OPTION L : <u>Small argument approximation (AAD)</u>

$$\log A_n = \log K_n(SRWD) + \log K_n(SRRD) + 2n\log(SAAD)$$

$$+ \log 2n - 2n\log 2 - 2\log(n!)$$

$$+ \log \left[\frac{2n}{(SAAD)} FISMA_{n-1}(SAAD) + \frac{(SAAD)}{2(n+1)} FISMA_{n+1}(SAAD) \right]$$

$$- \log \left[\frac{(SAAD)}{2(n-1)} FKSMA_{n-1}(SAAD) + \frac{2n}{(SAAD)} FKSMA_{n+1}(SAAD) \right] \qquad (G.38)$$

OPTION M : <u>Small argument approximation (AAD,RRD)</u>

$$\log A_n = \log K_n(SRWD) + 2n\log(SAAD) - n\log(SRRD) - n\log 2$$

$$- \log (n!) + \log \left[FKSMA_n(SRRD) \right]$$

$$+ \log \left[\frac{2n}{(SAAD)} FISMA_{n-1}(SAAD) + \frac{(SAAD)}{2(n+1)} FISMA_{n+1}(SAAD) \right]$$

$$- \log \left[\frac{(SAAD)}{2(n-1)} FKSMA_{n-1}(SAAD) + \frac{2n}{(SAAD)} FKSMA_{n+1}(SAAD) \right] \qquad (G.39)$$

OPTION N : <u>Small argument approximation (RRD)</u>

$$\log A_n = \log K_n(SRWD) + n\log 2 + \log(n!) - n\log(SRRD) - \log 2n$$

$$+ \log [FKSMA_n(SRRD) \} + \log [I_{n-1}(SAAD) + I_{n+1}(SAAD) \}$$

$$- \log [K_{n-1}(SAAD) + K_{n+1}(SAAD)] \qquad \text{(G.40)}$$

OPTION 0 : <u>Small argument approximation (AAD,RWD)</u>

$$\log A_n = \log K_n(SRRD) + 2n\log(SAAD) - n\log(SRWD) - n\log 2$$

$$- \log(n!) + \log [FKSMA_n(SRWD)]$$

$$+ \log [\frac{2n}{(SAAD)} FISMA_{n-1}(SAAD) + \frac{(SAAD)}{2(n+1)} FISMA_{n+1}(SAAD)$$

$$- \log [\frac{(SAAD)}{2(n-1)} FKSMA_{n-1}(SAAD) + \frac{2n}{(SAAD)} FKSMA_{n+1}(SAAD)] \qquad \text{(G.41)}$$

OPTION P : Small argument approximation (RWD)

$$\log A_n = \log K_n(SRRD) + \log\left[I_{n-1}(SAAD) + I_{n+1}(SAAD) \right] + n\log 2$$

$$- \log\left[K_{n-1}(SAAD) + K_{n+1}(SAAD) \right] + \log(n!) - n\log(SRWD)$$

$$- \log 2n + \log\left[FKSMA_n(SRWD) \right] \tag{G.42}$$

OPTION Q : Small argument approximation (AAD,RRD,RWD)

$$\log A_n = 2n\log(SAAD) - n\log\left[(SRRD)(SRWD) \right] - \log 2n$$

$$+ \log\left[FKSMA_n(SRRD)\ FKSMA_n(SRWD) \right]$$

$$+ \log\left[\frac{2n}{(SAAD)} FISMA_{n-1}(SAAD) + \frac{(SAAD)}{2(n+1)} FISMA_{n+1}(SAAD) \right]$$

$$- \log\left[\frac{(SAAD)}{2(n-1)} FKSMA_{n-1}(SAAD) + \frac{2n}{(SAAD)} FKSMA_{n+1}(SAAD) \right] \tag{G.43}$$

OPTION Z : Simple program

$$A_n = \frac{K_n(SRRD)\left[I_{n-1}(SAAD) + I_{n+1}(SAAD) \right] K_n(SRWD)}{\left[K_{n-1}(SAAD) + K_{n+1}(SAAD) \right]} \tag{6.44}$$

```
C*******************************************************************
C          THIS PROGRAM EVALUATES PD(TD) FOR A CONSTANT RATE
C          LINE SOURCE WELL EXTERIOR TO A CIRCULAR BOUNDARY
C          IN AN INFINITE SLAB SYSTEM.
C          TWO CASES ARE CONSIDERED:
C               ICASE=1   CONSTANT PRESSURE HOLE
C               ICASE=2   CLOSED BOUNDARY HOLE
C*******************************************************************
C
C
C                 VARIABLE DEFINITIONS
C              **************************
C
C          IOPT=OPTION FLAG FOR THE BESSEL FUNCTIONS ON IMSL
C          IER=ERROR FLAG FOR THE BESSEL FUNCTION ON IMSL
C          N=NUMBER OF TERMS IN THE STEHFEST ALGORITHM
C          M=V(I) CALCULATION FLAG
C          ICASE=TYPE OF HOLE FLAG
C          RRD=DIMENSIONLESS DISTANCE
C          RWD=DIMENSIONLESS DISTANCE TO THE HOLE
C          AAD=DIMENSIONLESS RADIUS OF THE HOLE
C          RRRD(I)=DISTANCE BETWEEN THE WELL AND THE PRESSURE POINT
C          SRRD=BESSEL FUNCTION ARGUMENT
C          SRWD=BESSEL FUNCTION ARGUMENT
C          SAAD=BESSEL FUNCTION ARGUMENT
C          SRRRD=BESSEL FUNCTION ARGUMENT
C          F=NORMALIZED RADIUS OF THE HOLE
C          E=NORMALIZED RADIUS TO THE PRESSURE POINT
C          EPSI=CONVERGENCE CRITERION FOR F(S)
C          EPSI1=CONVERGENCE CRITERION FOR THE BESSEL FUNCTIONS
C          DELTA=NTH TERM/SUMMATION TO N
C          DELTAA=N-1 TERN/SUMMATION TO N-1
C          DELT=CONVERGENCE RATIO
C          TTPI=THE CONSTANT PI
C          FACNU=FACTORIALS
C          PDSS(I)=STEADY STATE PD
C          PD=DIMENSIONLESS PRESSURE DROP
C          PDN=NORMALIZED PRESSURE DROP
C          PDLS=LINE SOURCE DIMENSIONLESS PRESSURE DROP
C          THETA(1)=0 DEG
C          THETA(2)=45 DEG
C          THETA(3)=90 DEG
C          THETA(4)=135 DEG
C          THETA(5)=180 DEG
C          ALFA=N*THETA IN F(S)
C          TD(II)=DIMENSIONLESS TIME
C          TD=DIMENSIONESS TIME
C          TDR=TD/RD**2, NORMALIZED DIMENSIONLESS TIME
C          SUM(NU,IJ)=TERMS IN THE INFINITE SUMMATION OF F(S)
C          NU=ORDER OF THE BESSEL FUNCTIONS
C          ICASE=BOUNDARY FLAG
C          IFLAG1=ANGLE FLAG FOR A GIVEN TD.
```

```
C          IFLAG2=FLAG FOR CALCULATING PD(TD/RD**2=0.1)
C          EEE=NATURAL CONSTANT
C          DEE=LOG BASE 10 OF EEE
C          BIAAD=I(N,Z), THE ARGUMENT OF AAD
C          BKAAD=K(N,Z), THE ARGUMENT OF AAD
C          BKRWD=K(N,Z), THE ARGUMENT OF RWD
C          BKRRD=K(N,Z), THE ARGUMENT OF RRD
C          EK---=LOG BASE 10 OF K(N,Z)
C
C
C
C                 LIST OF FUNCTIONS AND SUBROUTINES
C               ***************************************
C
C          FUNCTION PWD=THE STEHFEST ALGORITHM
C          FUNCTION PWDL=F(S)  FOR BOTH BOUNDARY CASES
C          FUNCTION SUMIN=GENERATES THE TERMS IN THE INFINITE SERIES
C          FUNCTION BESI=MODIFIED BESSEL FUNCTION I(NU,Z),ASC.SER.
C          FUNCTION BESIA=MODIFIED BESSEL FUNCTION I(NU,Z),ASY.EXP.
C          FUNCTION BESKA=MODIFIED BESSEL FUNCTION K(NU,Z),ASY.EXP.
C          FUNCTION BAAD=MODIFIED BESSEL FUNCTION K(N,Z),STEP
C          FUNCTION BRRD=MODIFIED BESSEL FUNCTION K(N,Z),STEP
C          FUNCTION BRWD=MODIFIED BESSEL FUNCTION K(N,Z),STEP
C          FUNCTION FKSMA=SMALL ARG. APPX. FOR K(N,Z),N DEPENDENT TERM
C          FUNCTION FISMA=SMALL ARG. APPX. FOR I(N,Z),N DEPENDENT TERM
C          SUBROUTINE FACT=GENERATES THE FACTORIALS TO 50
C
C
C
C                  MAIN PROGRAM
C                ******************
      IMPLICIT REAL*8 (A-H,O-Z)
      REAL*8 RRD,RWD,AAD,EPSI,TPI,TTPI
      REAL*8  EEE,DEE
      INTEGER IOPT,IER,N,M,ICASE
      DIMENSION PDSS(5),TD(100),PD(5,100)
      COMMON /FRAC3/FACNU(51)
      COMMON /FRAC1/THETA(5)
      COMMON /FRAC2/RRRD(5),RWD,RRD,AAD,EPSI,EPSI1,TTD,JJ
      COMMON /FRAC4/DEE,TTPI,ICASE
      COMMON /FRAC5/IOPT,IER
      COMMON /FRAC6/IFLAG1
      COMMON /FRAC99/IEND99
C
C
C          VARIABLE INPUT DATA
      ICASE=2
      N=8
      RRD=14.0D0
      RWD=20.0D0
      AAD=8.00D0
      EPSI=1.0D-13
```

```
      EPSI1=1.0D-15
C
C
C           CONSTANT DATA
      M=77777
      IOPT=1
      TTPI=3.141592654
      EEE=DEXP(1.0D0)
      DEE=DLOG10(EEE)
      IEND99=0
C           GENERATING THE FACTORIALS
      CALL FACT
C           GENERATING RRRD(I)
      DO 1 I=1,5
      TPI=TTPI/4.0
      THETA(I)=TPI*(I-1)
      RRRD(I)=(RRD**2+RWD**2-2*RRD*RWD*DCOS(THETA(I)))**0.5
1     CONTINUE
C
C
C           PRESETTING PD(JJ,II) TO ZERO
      DO 2 I=1,5
      DO 3 J=1,100
      PD(I,J)=0.0D0
3     CONTINUE
2     CONTINUE
C
C
C           DECIDING WHAT PROGRAM TO FOLLOW
      IF (ICASE.EQ.1) GO TO 1000
      IF (ICASE.EQ.2) GO TO 2000
      WRITE (6,3001)
3001  FORMAT (5X,'***ICASE WAS NOT SPECIFIED***')
      GO TO 1050
C
C
C
C              CONSTANT PRESSURE HOLE
C          ****************************
C
C
C           LONG TIME APPROXIMATON-DOUBLET MODEL
1000  W1=(AAD**2)/(RWD*RRD)
      W2=RRD/RWD
      DO 1001 I=1,5
      WCOS=DCOS(THETA(I))
      WW=1-2*W1*WCOS+(W1**2)
      WWW=1-2*W2*WCOS+(W2**2)
      WW=WW/WWW
      PDSS(I)=DLOG(RRD/AAD)+0.5*DLOG(WW)
1001  CONTINUE
C
```

```
C
      DO 1042 I=1,100
      TD(I)=1.0
1042  CONTINUE
C
C           THE TINE LOOP. WE CONSIDER SIX LOG CYCLES FOR
C           TD/RD**2 STARTING AT 0.1.
      II=0
      DO 1002 KKK=1,20
      DO 1003 KK=1,5
      IF (IEND99.EQ.1) GO TO 1041
      AB=KK
      ABB=KKK
      II=II+1
      TD(II)=AB*0.0002*(10.0**ABB)
C
C
C           NOW WE CONVERT TO TD/RD**2 FOR ANGLE=0
1020  TD(II)=TD(II)*(RRRD(1)**2)
      TTD=TD(II)
C     WRITE (6,1059) TTD
C1059  FORMAT (15X,D20.9)
C
C
      IFLAG1=0
C           THE ANGLE LOOP. THE ORDER OF CALCULATION IS
C           0,180,45,135,90 DEG. THE ANGLES ARE REARRANGED:
      DO 1021 JJJ=1,5
      IF (JJJ.EQ.1) JJ=1
      IF (JJJ.EQ.2) JJ=5
      IF (JJJ.EQ.3) JJ=4
      IF (JJJ.EQ.4) JJ=2
      IF (JJJ.EQ.5) JJ=3
      IF (IEND99.EQ.1) GO TO 1041
C      IF (JJ.GT.1) GO TO 1021
C
C           NOW THE ANGLES ARE THETA(JJ) AND THE RADII ARE
C           RRRD(JJ). WE NOW CHECK THE VALUE OF TD/RD**2:
      TDR=TD(II)/(RRRD(JJ)**2)
      IF (TDR.GE.0.0999.AND.TDR.LE.1.001D8) GO TO 1022
      PD(JJ,II)=0.0
      GO TO 1021
C
C
C           TD/RD**2 IS GREATER THAN 0.1 AND WE CONTINUE
C           WITH THE PD CALCULATION.
1022  PD(JJ,II)=PWD(TTD,N,M)
1021  CONTINUE
C      GO TO 1041
1003  CONTINUE
1002  CONTINUE
C
```

```
C
C           THE RESULTS
 1041  WRITE (6,1030)
 1030  FORMAT (///,20X,'THE RESULTS',/,20X,'***********',//)
       WRITE (6,1035) ICASE
 1035  FORMAT (10X,'ICASE=',I5,/)
       F=AAD/RWD
       E=RRD/RWD
       WRITE (6,1031) AAD,RWD,RRD
       WRITE (6,1032) F,E
 1031  FORMAT (10X,'AAD=',E12.5,/,10X,'RWD=',E12.5,/,10X,'RRD=',E12.5,/)
 1032  FORMAT (10X,'F=',E12.5,/,10X,'E=',El2.5,//)
       WRITE (6,1025)
 1025  FORMAT (10X,'THE STEADY STATE PRESSURES',/)
       DO 1026 I=1,5
       THET=THETA(I)*180.0/TTPI
       WRITE (6,1027) THET,PDSS(I)
 1027  FORMAT (10X,'THETA=',E12.5,10X,'PDSS=',D20.9)
 1026  CONTINUE
       WRITE (6,1028)
 1028  FORMAT (//)
C
C
       DO 1004 JJ=1,5
       THET=THETA(JJ)*180.0/TTPI
       WRITE (6,1033) THET
 1033  FORMAT (//,5X,'THETA=',E12.5,/)
       WRITE (6,1034)
 1034  FORMAT (14X,'TD',17X,'TD:RD**2',16X,'PD',19X,'PDN',/)
C
       DO 1005 II=1,100
       IF (PD(JJ,II).EQ.0.0) GO TO 1005
       PDN=PD(JJ,II)/PDSS(JJ)
       TTD=TD(II)
       TDR=TTD/(RRRD(JJ)**2)
       WRITE (6,1010) TTD,TDR,PD(JJ,II),PDN
 1010  FORMAT (5X,4(D20.9))
 1005  CONTINUE
 1004  CONTINUE
C
C
C
C           END OF THE CONST ANT PRESSURE CALCULATIONS
       GO TO 1050
C
C
C
C
C              CLOSED BOUNDARY HOLE
C            ************************
 2000  DO 2042 I=1,100
       TD(I)=1.0
```

```
2042  CONTINUE
C
C          THE TIME LOOP. WE CONSIDER SIX LOG CYCLES FOR
C          TD/RD**2 STARTING AT 0.1.
      II=0
      DO 2002 KKK=1,20
      DO 2003 KK=1,5
      IF (IEND99.EQ.1) GO TO 2041
      AB=KK
      ABB=KKK
      II=II+1
      TD(II)=AB*0.0002*(10.0**ABB)
C
C
C          NOW WE CONVERT TO TD/RD**2 FOR ANGLE=0
2020  TD(II)=TD(II)*(RRRD(1)**2)
      TTD=TD(II)
C     WRITE (6,2059) TTD
C2059  FORMAT (15X,D20.9)
C
C
      IFLAG1=0
C          THE ANGLE LOOP. THE ORDER OF CALCULATION IS
C          0,180,45,135,90 DEG. THE ANGLES ARE REARRANGED:
      DO 2021 JJJ=1,5
      IF (JJJ.EQ.1) JJ=1
      IF (JJJ.EQ.2)  JJ=5
      IF (JJJ.EQ.3) JJ=4
      IF (JJJ.EQ.4) JJ=2
      IF (JJJ.EQ.5) JJ=3
      IF (IEND99.EQ.1) GO TO 2041
C      IF (JJ.GT.1) GO TO 2021
C
C          NOW THE ANGLES ARE THETA(JJ) AND THE RADII ARE
C          RRRD(JJ). WE NOW CHECK THE VALUE OF TD/RD**2:
      TDR=TD(II)/(RRRD(JJ)**2)
      IF (TDR.GE.0.0999.AND.TDR.LE.1.001D8) GO TO 2022
      PD(JJ,II)=0.0
      GO TO 2021
C
C
C          TD/RD**2 IS GREATER THAN 0.1 AND WE CONTINUE
C          WITH THE PD CALCULATION.
2022  PD(JJ,II)=PWD(TTD,N,M)
2021  CONTINUE
C      GO TO 2041
2003  CONTINUE
2002  CONTINUE
C
C
C          THE RESULTS
2041  WRITE (6,2030)
```

```
2030  FORMAT (///,20X,'THE RESULTS',/,20X,'************',//)
      WRITE (6,2035) ICASE
2035  FORMAT (10X,'ICASE=',I5,/)
      F=AAD/RWD
      E=RRD/RWD
      WRITE (6 ,2031) AAD,RWD,RRD
      WRITE (6,2032) F,E
2031  FORMAT (10X,'AAD=',E12.5,/,10X,'RWD=',E12.5,/,10X,'RRD=',E12.5,/)
2032  FORMAT (10X,'F=',E12.5,/,10X,'E=',E12.5,//)
      DO 2004 JJ=1,5
      THET=THETA(JJ)*180.0/TTPI
      WRITE (6,2033) THET
2033  FORMAT (//,5X,'THETA=',E12.5,/)
      WRITE (6,2034)
2034  FORMAT (14X,'TD',17X,'TD:RD**2',16X,'PD',/)
      DO 2005 II=1,100
      IF (PD(JJ,II).EQ.0.0) GO TO 2005
      TTD=TD(II)
      TDR=TTD/(RRRD(JJ)**2)
      WRITE (6,2010) TTD,TDR,PD(JJ,II)
2010  FORMAT (5X,3(D20.9))
2005  CONTINUE
2004  CONTINUE
C
1050  STOP
      END
C
C
C                    THE STEHFEST ALGORITHM
C                 *****************************
C
      FUNCTION PWD(TD,N,M)
C          THIS FUNTION COMPUTES NUMERICALLY THE LAPLACE TRNSFORM
C          INVERSE OF F(S).
      IMPLICIT  REAL*8 (A-H,O-Z)
      DIMENSION G(50),V(50),H(25)
      COMMON /FRAC6/IFLAG1
      COMMON /FRAC99/IEND99
C
C          NOW IF THE ARRAY V(I) WAS COMPUTED BEFORE THE PROGRAM
C          GOES DIRECTLY TO THE END OF THE SUBROUTINE TO CALCULATE
C          F(S).
      IF (N.EQ.M) GO TO 17
      M=N
      DLOGTW=0.6931471805599
      NH=N/2
C
C          THE FACTORIALS OF 1 TO N ARE CALCULATED INTO ARRAY G.
      G(1)=1
      DO 1 I=2,N
      G(I)=G(I-1)*I
1     CONTINUE
```

```
C
C           TERMS WITH K ONLY ARE CALCULATED INTO ARRAY H.
      H(1)=2./G(NH-1)
      DO 6 I=2,NH
      FI=I
      IF(I-NH) 4,5,6
4     H(I)=FI**NH*G(2*I)/(G(NH-I)*G(I)*G(I-1))
      GO TO 6
5     H(I)=FI**NH*G(2*I)/(G(I)*G(I-1))
6     CONTINUE
C
C           THE TERMS (-1)**NH+1 ARE CALCULATED.
C           FIRST THE TERM FOR I=1
      SN=2*(NH-NH/2*2)-1
C
C           THE REST OF THE SN`S ARE CALCULATED IN THE MAIN ROUTINE.
C
C
C           THE ARRAY V(I) IS CALCULATED.
      DO 7 I=1,N
C
C           FIRST SET V(I)=0
      V(I)=0.
C
C           THE LIMITS FOR K ARE ESTABLISHED.
C           THE LOWER LIMIT IS K1=INTEG((I+1/2))
      K1=(I+1)/2
C
C           THE UPPER LIMIT IS K2=MIN(I,N/2)
      K2=I
      IF (K2-NH) 8,8,9
9     K2=NH
C
C           THE SUMMATION TERM IN V(I) IS CALCULATED.
8     DO 10 K=K1,K2
      IF (2*K-I) 12,13,12
12    IF (I-K) 11,14911
11    V(I)=V(I)+H(K)/(G(I-K)*G(2*K-I))
      GO TO 10
13    V(I)=V(I)+H(K)/G(I-K)
      GO TO 10
14    V(I)=V(I)+H(K)/G(2*K-I)
10    CONTINUE
C
C           THE V(I) ARRAY IS FINALLY CALCULATED BY WEIGHTING
C           ACCORDING TO SN.
      V(I)=SN*V(I)
C      WRITE (6,21) I,V(I)
C21    FORMAT (5X,'I=',I5,5X,'V(I)=',D20.9)
C
C           THE TERM SN CHANGES ITS SIGN EACH ITERATION.
      SN=-SN
```

```
7      CONTINUE
C
C          THE NUMERICAL APPROXIMATION IS CALCULATED.
17     PWD=0.
       A=DLOGTW/TD
       DO 15 I=1,N
       IF (IEND99.EQ.1) GO TO 18
C       WRITE (6,20) I
C20     FORMAT (5X,I5)
       ARG=A*I
       PWD=PWD+V(I)*PWDL(ARG,I)
15     CONTINUE
       PWD=PWD*A
       IFLAG1=1
18     RETURN
       END
C
C
C
C
C
C                 FUNCTION PWDL(ARG,IJ)
C              ****************************
C
C          THIS FUNCTION EVALUATES F(S) OF THE CONSTANT PRESSURE
C          BOUNDARY CASE FOR THE STEHFEST ALGORITHM. THE ARGUMENT
C          (S) IS FIXED BY THE ALGORITHM.
       FUNCTION PWDL(ARG,IJ)
       IMPLICIT REAL*8 (A-H,O-Z)
       REAL*8 SRRD,SRWD,SAAD,SRRRD,PWDL1,ALFA
       COMMON /FRAC12/SUM(50,16)
       COMMON /FRAC11/BIAAD(100),BKAAD(100),BKRWD(100),BKRRD(100)
       COMMON /FRAC1/THETA(5)
       COMMON /FRAC2/RRRD(5),RWD,RRD,AAD,EPSI,EPSI1,TTD,JJ
       COMMON /FRAC3/FACNU(51)
       COMMON /FRAC5/IOPT,IER
       COMMON /FRAC6/IFLAG1
       COMMON /FRAC99/IEND99
       DOUBLE PRECISION MM8SI0,MM8SI1,MM8SK0,MM8SK1
       DELTAA=1.0
C
C
C           FIRST WE CALCULATE THE LINE SOURCE TERM
       SRRRD=DSQRT(ARG)*RRRD(JJ)
       PWDL1=MMBSK0(IOPT,SRRRD,IER)
C
C
C          NOW WE CHECK IF THE MATRIX SUM(NU,IJ) IS COMPLETE
       IF (IFLAG1.EQ.1) GO TO 7
C
C          SETTING THE VECTOR SUM(KK,IJ) TO ZERO
       DO 1 KK=1,50
```

```
      SUM(KK,IJ)=0.0D0
1     CONTINUE
C
C
C          EVALUATING THE ARGUMENTS FOR THE BESSEL FUNCTIONS
      SRWD=DSQRT(ARG)*RWD
      SRRD=DSQRT(ARG)*RRD
      SAAD=DSQRT(ARG)*AAD
C
C
C          NOW WE START CONSIDRING THE TERMS IN THE SUMMATION.
C          NOTE THAT THE BESSEL FUNCTIONS ARE STORED IN AN ARRAY
C          OF WHICH THE INDEX IS SHIFTED UPWARDS BY 1  TO BE ABLE
C          TO HANDLE K(0,Z). K(0,SAAD) IS NOTED AS BKAAD(1).
      SUM(1,IJ)=SUMIN (SRRD,SRWD,SAAD,1,0)
      IF (IEND99.EQ.1) GO TO 6
7     PWDL=-SUM(1,IJ)+PWDL1
      DO 2 I=2,50
      NU=I
      NUU=NU-1
      IF (IFLAG1.EQ.1) GO TO 8
      SUM(NU,IJ)=SUMIN (SRRD,SRWD,SAAD,NU,NUU)
      IF (IEND99.EQ.1) GO TO 6
C     IF (SUM(NU,IJ).EQ.0.0) GO TO 3
8     ACE=SUM(NU,IJ)
      ACE=DABS(ACE)
      IF (ACE.LT.1.0D-45) GO TO 4
      ALFA=(I-1)*THETA(JJ)
      PWDL3=DCOS(ALFA)*SUM(NU,IJ)*2
      PWDL4=PWDL-PWDL3
C
C
C          NOW WE CHECK THE CONVERGENCE OF F(S)
      IF (PWDL3.EQ.0.0) GO TO 4
      DELTA=PWDL3/PWDL4
      DELTA=DABS(DELTA)
      DELT=DELTA/DELTAA
      DELTAA=DELTA
      IF (EPSI-DELTA) 3,4,4
3     PWDL=PWDL4
2     CONTINUE
C
C
C          THE SERIES CONVERGED.WE EVALUATE PWDL.
4     PWDL=PWDL/ARG
C      WRITE (6,5) NU,PWDL,DELTA,DELT,SRWD,SRRD,SAAD
c5     FORMAT (I5,1X,6(D20.9))
6     RETURN
      END
C
C
C
```

```
C
C                SUBROUTINE FACT
C              ******************
C
C           THIS SUBROUTINE EVALUATES FACTORIALS UP TO 50.
      SUBROUTINE FACT
      IMPLICIT REAL*8 (A-H,O-Z)
      COMMON /FRAC3/FACNU(51)
      FACNU(1)=1
      FACNU(2)=1.0D0
      DO 1 I=2,50
      FACNU(I+1)=FACNU(I)*I
1     CONTINUE
      RETURN
      END
C
C
C
C                FUNCTION BESKA (N,Z)
C             **************************
C           THIS FUNCTION EVALUATES THE N DEPENDENT SERIES FOR THE
C           ASYMPTOTIC EXPANSION OF K(N,Z)
C
      FUNCTION BESKA(N,Z)
      IMPLICIT REAL*8 (A-H,O-Z)
      REAL*8 AZ
      EPSI=1.0D-15
      FNU=(N**2)*4.0
      BESKA=1.0D0
      ZZ=Z*8.0
      AZ=1.0D0
      DO 1 I=1,100
      AZ=AZ*(FNU-((2*I-1)**2))/(ZZ*I)
      BESKA=BESKA+AZ
      DELTA=AZ/BESKA
      IF (DABS(DELTA).LT.EPSI) GO TO 2
1     CONTINUE
2     RETURN
      END
C
C
C                    FUNCTION BESIA (N,Z)
C                **************************
C
C            THIS FUNCTION EVALUATES THE N DEPENDENT SERIES FOR THE
C            ASYMPTOTIC EXPANSION OF I(N,Z)
      FUNCTION BESIA(N,Z)
      IMPLICIT REAL*8 (A-H,O-Z)
      REAL*8 AZ,FNU,ZZ,DELTA
      EPSI=1.0D-15
      FNU=(N**2)*4.0
      BESIA=1.0D0
```

```
      ZZ=Z*8.0
      AZ=1.0D0
      DO 1 I=1,100
      AZ=AZ*(-1)*(FNU-((2*I-1)**2))/(ZZ*I)
      BESIA=BESIA+AZ
      DELTA=AZ/BESIA
      IF (DABS(DELTA).LT.EPSI) GO TO 2
1     CONTINUE
2     RETURN
      END
C
C
C
C              FUNCTION SUMIN (SRRD,SRWD,SAAD,NU,NUU)
C           *****************************************
C
C          THIS FUNCTION EVALUATES THE TERMS IN THE INFINITE
C          SERIES IN F(S).
      FUNCTION SUMIN (SRRD,SRWD,SAAD,NU,NUU)
      IMPLICIT REAL*8 (A-H,O-Z)
      COMMON /FRAC12/SUM(50,16)
      COMMON /FRAC11/BIAAD(100),BKAAD(100),BKRWD(100),BKRRD(100)
      COMMON /FRAC4/DEE,TTPI,ICASE
      COMMON /FRAC3/FACNU(51)
      COMMON /FRAC99/IEND99
      DOUBLE PRECISION MMBSK0,MMBSK1,MMBSI0,MMBSI1
      IOPT=1
      NUU=NU-1
      NUUU=NUU
      IF (ICASE.EQ.2.AND.NU.EQ.1) NUUU=NUU+2
      NNU=NUUU+1
C
C          THIS PART IS THE SCREENING SECTION THAT PICKS THE
C          METHOD FOR EVALUATING THE F(S) TERNS.
C
      IF (SAAD.GE.100)  GO TO 251
      IF (SRWD.GE.100.AND.SRRD.GE.100) GO TO 252
      IF (SRWD.GE.100.AND.SRRD.LT.100) GO TO 253
      IF (SRWD.LT.100.AND.SRRD.GE.100) GO TO 254
      IF (SRWD.LT.100.AND.SRRD.LT.100) GO TO 255
C
252   IF (SAAD.GE.20) GO TO 256
      IF (SAAD.GE.2.0) GO TO 257
      IF (SAAD.LT.2.0)  GO TO 258
C
256   EKAAD=SAAD*DEE
      IF (EKAAD.GE.65)  GO TO 251
      GO TO 257
C
258   EKAAD=(-NU)*DLOG10(SAAD)+DLOG10(FACNU(NU))+(NU-1)*DLOG10(2.0D0)
      IF (EKAAD.GE.65) GO TO 259
      GO TO 257
```

```
C
253   IF (SAAD.GE.20.AND.SRRD.GE.20) GO TO 260
      IF (SAAD.LT.20.AND.SRRD.GE.20) GO TO 261
      IF (SAAD.LT.20.AND.SRRD.LT.20) GO TO 262
C
260   EKAAD=SAAD*DEE
      EKRRD=SRRD*DEE
      IF (EKAAD.GE.65.AND.EKRRD.GE.65) GO TO 251
      IF (EKAAD.LT.65.AND.EKRRD.GE.65) GO TO 257
      IF (EKAAD.LT.65.AND.EKRRD.LT.65) GO TO 263
C
261   IF (SAAD.GE.2.0) GO TO 264
      IF (SAAD.LT.2.0) GO TO 265
C
264   EKRRD=SRRD*DEE
      IF (EKRRD.GE.65) GO TO 257
      IF (EKRRD.LT.65) GO TO 263
C
265   EKRRD=SRRD*DEE
      EKAAD=(-NU)*DLOG10(SAAD)+DLOG10(FACNU(NU))+(NU-1)*DLOG10(2.0D0)
      IF (EKRRD.GE.65.AND.EKAAD.GE.65) GO TO 259
      IF (EKRRD.GE.65.AND.EKAAD.LT.65) GO TO 257
      IF (EKRRD.LT.65.AND.EKAAD.GE.65) GO TO 266
      IF (EKRRD.LT.65.AND.EKAAD.LT.65) GO TO 263
C
262   IF (SAAD.GE.2.0.AND.SRRD.GE.2.0) GO TO 263
      IF (SAAD.LT.2.0.AND.SRRD.GE.2.0) GO TO 267
      IF (SRRD.LT.2.0) GO TO 268
C
267   EKAAD=(-NU)*DLOG10(SAAD)+DLOG10(FACNU(NU))+(NU-1)*DLOG10(2.0D0)
      IF (EKAAD.GE.65) GO TO 266
      IF (EKAAD.LT.65) GO TO 263
C
268   EKRRD=(-NU)*DLOG10(SRRD)+DLOG10(FACNU(NU))+(NU-1)*DLOG10(2.0D0)
      EKAAD=(-NU)*DLOG10(SAAD)+DLOG10(FACNU(NU))+(NU-1)*DLOG10(2.0D0)
      IF (EKRRD.GE.65.AND.EKAAD.GE.65) GO TO 269
      IF (EKRRD.LT.65.AND.EKAAD.GE.65) GO TO 266
      IF (EKRRD.LT.65.AND.EKAAD.LT.65) GO TO 263
C
254   IF (SAAD.GE.20.AND.SRWD.GE.20) GO TO 270
      IF (SAAD.LT.20.AND.SRWD.GE.20) GO TO 271
      IF (SAAD.LT.20.AND.SRWD.LT.20) GO TO 272
C
270   EKAAD=SAAD*DEE
      EKRWD=SRWD*DEE
      IF (EKAAD.GE.65.AND.EKRWD.GE.65) GO TO 251
      IF (EKAAD.LT.65.AND.EKRWD.GE.65) GO TO 257
      IF (EKAAD.LT.65.AND.EKRWD.LT.65) GO TO 273
C
271   IF (SAAD.GE.2.0) GO TO 274
      IF (SAAD.LT.2.0) GO TO 275
C
```

```
274   EKRWD=SRWD*DEE
      IF (EKRWD.GE.65) GO TO 257
      IF (EKRWD.LT.65) GO TO 273
C
275   EKRWD=SRWD*DEE
      EKAAD=(-NU)*DLOG10(SAAD)+DLOG10(FACNU(NU))+(NU-1)*DLOG10(2.0D0)
      IF (EKRWD.GE.65.AND.EKAAD.GE.65) GO TO 259
      IF (EKRWD.GE.65.AND.EKAAD.LT.65) GO TO 257
      IF (EKRWD.LT.65.AND.EKAAD.GE.65) GO TO 276
      IF (EKRWD.LT.65.AND.EKAAD.LT.65) GO TO 273
C
272   IF (SAAD.GE.2.0.AND.SRWD.GE.2.0) GO TO 273
      IF (SAAD.LT.2.0.AND.SRWD.GE.2.0) GO TO 277
      IF (SAAD.LT.2.0.AND.SRWD.LT.2.0) GO TO 278
C
277   EKAAD=(-NU)*DLOG10(SAAD)+DLOG10(FACNU(NU))+(NU-1)*DLOG10(2.0D0)
      IF (EKAAD.GE.65) GO TO 276
      IF (EKAAD.LT.65) GO TO 273
C
278   EKAAD=(-NU)*DLOG10(SAAD)+DLOG10(FACNU(NU))+(NU-1)*DLOG10(2.0D0)
      EKRWD=(-NU)*DLOG10(SRWD)+DLOG10(FACNU(NU))+(NU-1)*DLOG10(2.0D0)
      IF (EKAAD.GE.65.AND.EKRWD.GE.65) GO TO 279
      IF (EKAAD.LT.65.AND.EKRWD.GE.65) GO TO 276
      IF (EKAAD.LT.65.AND.EKRWD.LT.65) GO TO 273
C
255   IF (SRWD.GE.20.AND.SRRD.GE.20) GO TO 280
      IF (SRWD.GE.20.AND.SRRD.GE.2.0) GO TO 281
      IF (SRWD.GE.2.0.AND.SRRD.GE.20) GO TO 282
      IF (SRWD.GE.20.AND.SRRD.LT.2.0) GO TO 304
      IF (SRWD.LT.2.0.AND.SRRD.GE.20) GO TO 305
      IF (SRWD.GE.2.0.AND.SRRD.GE.2.0) GO TO 283
      IF (SRWD.GE.2.0.AND.SRRD.LT.2.0) GO TO 284
      IF (SRWD.LT.2.0.AND.SRRD.GE.2.0) GO TO 285
      IF (SRWD.LT.2.0.AND.SRRD.LT.2.0) GO TO 286
C
280   IF (SAAD.GE.20) GO TO 287
      IF (SAAD.GE.2.0) GO TO 288
      IF (SAAD.LT.2.0) GO TO 289
C
287   EKAAD=SAAD*DEE
      EKRWD=SRWD*DEE
      EKRRD=SRRD*DEE
      IF (EKAAD.GE.65) GO TO 251
      IF (EKRWD.GE.65.AND.EKRRD.GE.65) GO TO 257
      IF (EKRWD.GE.65.AND.EKRRD.LT.65) GO TO 263
      IF (EKRWD.LT.65.AND.EKRRD.GE.65) GO TO 273
      IF (EKRWD.LT.65.AND.EKRRD.LT.65) GO TO 290
C
288   EKRWD=SRWD*DEE
      EKRRD=SRRD*DEE
      IF (EKRWD.GE.65.AND.EKRRD.GE.65) GO TO 257
      IF (EKRWD.GE.65.AND.EKRRD.LT.65) GO TO 263
```

```
      IF (EKRWD.LT.65.AND.EKRRD.GE.65) GO TO 273
      IF (EKRWD.LT.65.AND.EKRRD.LT.65) GO TO 290
C
289   EKAAD=(-NU)*DLOG10(SAAD)+DLOG10(FACNU(NU))+(NU-1)*DLOG10(2.0D0)
      IF (EKAAD.LT.65)  GO TO 291
      IF (EKAAD.GE.65)  GO TO 292
C
291   EKRWD=SRWD*DEE
      EKRRD=SRRD*DEE
      IF (EKRWD.GE.65.AND.EKRRD.GE.65) GO TO 257
      IF (EKRWD.GE.65.AND.EKRRD.LT.65) GO TO 263
      IF (EKRWD.LT.65.AND.EKRRD.GE.65) GO TO 273
      IF (EKRWD.LT.65.AND.EKRRD.LT.65) GO TO 290
C
292   EKRWD=SREID*DEE
      EKRRD=SRRD*DEE
      IF (EKRWD.GE.65.AND.EKRRD.GE.65) GO TO 259
      IF (EKRWD.GE.65.AND.EKRRD.LT.65) GO TO 266
      IF (EKRWD.LT.65.AND.EKRRD.GE.65) GO TO 276
      IF (EKRWD.LT.65.AND.EKRRD.LT.65) GO TO 293
C
281   IF (SAAD.GE.2.0) GO TO 294
      IF (SAAD.LT.2.0)  GO TO 295
C
294   EKRWD=SRWD*DEE
      IF (EKRWD.GE.65)  GO TO 263
      IF (EKRWD.LT.65)  GO TO 290
C
295   EKAAD=(-NU)*DLOG10(SAAD)+DLOG10(FACNU(NU))+(NU-1)*DLOG10(2.0D0)
      EKRWD=SRWD*DEE
      IF (EKRWD.GE.65.AND.EKAAD.GE.65) GO TO 266
      IF (EKRWD.GE.65.AND.EKAAD.LT.65) GO TO 263
      IF (EKRWD.LT.65.AND.EKAAD.GE.65) GO TO 293
      IF (EKRWD.LT.65.AND.EKAAD.LT.65) GO TO 290
C
282   IF (SAAD.GE.2.0)  GO TO 296
      IF (SAAD.LT.2.0)  GO TO 297
C
296   EKRRD=SRRD*DEE
      IF (EKRRD.GE.65)  GO TO 273
      IF (EKRRD.LT.65)  GO TO 290
C
297   EKRRD=SRRD*DEE
      EKAAD=(-NU)*DLOG10(SAAD)+DLOG10(FACNU(NU))+(NU-1)*DLOG10(2.0D0)
      IF (EKRRD.GE.65.AND.EKAAD.GE.65) GO TO 276
      IF (EKRRD.GE.65.AND.EKAAD.LT.65) GO TO 273
      IF (EKRRD.LT.65.AND.EKAAD.GE.65) GO TO 293
      IF (EKRRD.LT.65.AND.EKAAD.LT.65) GO TO 290
C
283   IF (SAAD.GE.2.0)  GO TO 290
      IF (SAAD.LT.2.0) GO TO 298
C
```

```
298   EKAAD=(-NU)*DLOG10(SAAD)+DLOG10(FACNU(NU))+(NU-1)*DLOG10(2.0D0)
      IF (EKAAD.GE.65)  GO TO 293
      IF (EKAAD.LT.65)  GO TO 290
C
284   EKAAD=(-NU)*DLOG10(SAAD)+DLOG10(FACNU(NU))+(NU-1)*DLOG10(2.0D0)
      EKRRD=(-NU)*DLOG10(SRRD)+DLOG10(FACNU(NU))+(NU-1)*DLOG10(2.0D0)
      IF (EKRRD.GE.65.AND.EKAAD.GE.65) GO TO 299
      IF (EKRRD.GE.65.AND.EKAAD.LT.65) GO TO 300
      IF (EKRRD.LT.65.AND.EKAAD.GE.65) GO TO 293
      IF (EKRRD.LT.65.AND.EKAAD.LT.65) GO TO 290
C
285   EKAAD=(-NU)*DLOG10(SAAD)+DLOG10(FACNU(NU))+(NU-1)*DLOG10(2.0D0)
      EKRWD=(-NU)*DLOG10(SRWD)+DLOG10(FACNU(NU))+(NU-1)*DLOG10(2.0D0)
      IF (EKRWD.GE.65.AND.EKAAD.GE.65) GO TO 301
      IF (EKRWD.GE.65.AND.EKAAD.LT.65) GO TO 302
      IF (EKRWD.LT.65.AND.EKAAD.GE.65) GO TO 293
      IF (EKRWD.LT.65.AND.EKAAD.LT.65) GO TO 290
C
286   EKAAD=(-NU)*DLOG10(SAAD)+DLOG10(FACNU(NU))+(NU-1)*DLOG10(2.0D0)
      IF (EKAAD.LT.65)  GO TO 290
      EKRRD=(-NU)*DLOG10(SRRD)+DLOG10(FACNU(NU))+(NU-1)*DLOG10(2.0D0)
      EKRWD=(-NU)*DLOG10(SRWD)+DLOG10(FACNU(NU))+(NU-1)*DLOG10(2.0D0)
      IF (EKRWD.GE.65.AND.EKRRD.GE.65) GO TO 303
      IF (EKRWD.GE.65.AND.EKRRD.LT.65) GO TO 301
      IF (EKRWD.LT.65.AND.EKRRD.GE.65) GO TO 299
      IF (EKRWD.LT.65.AND.EKRRD.LT.65) GO TO 293
C
304   EKRRD=(-NU)*DLOG10(SRRD)+DLOG10(FACNU(NU))+(NU-1)*DLOG10(2.0D0)
      IF (EKRRD.GE.65) GO TO 306
      IF (EKRRD.LT.65)  GO TO 307
C
306   EKRWD=SRWD*DEE
      IF (EKRWD.GE.65)  GO TO 269
      IF (EKRWD.LT.65)  GO TO 299
C
307   EKAAD=(-NU)*DLOG10(SAAD)+DLOG10(FACNU(NU))+(NU-1)*DLOG10(2.0D0)
      IF (EKAAD.GE.65)  GO TO 293
      IF (EKAAD.LT.65)  GO TO 290
C
305   EKRWD=(-NU)*DLOG10(SRWD)+DLOG10(FACNU(NU))+(NU-1)*DLOG10(2.0D0)
      IF (EKRWD.GE.65) GO TO 308
      IF (EKRWD.LT.65)  GO TO 309
C
308   EKRRD=SRRD*DEE
      IF (EKRRD.GE.65)  GO TO 279
      IF (EKRRD.LT.65)  GO TO 301
C
309   EKAAD=(-NU)*DLOG10(SAAD)+DLOG10(FACNU(NU))+(NU-1)*DLOG10(2.0D0)
      IF (EKAAD.GE.65)  GO TO 293
      IF (EKAAD.LT.65)  GO TO 290
C
C
```

```
C          THIS SECTION EVALUATES THE TERMS SUM(NU,IJ)
C
C
C          COMPLETE ASYMPTOTIC EXPANSION (AAD,RWD,RRD)  A
251    IF (ICASE.EQ.2) GO TO 351
       AR1=2*SAAD-SRRD-SRWD
       AR2=DSQRT(SRRD*SRWD)
       IF (DABS(AR1).GE.160) GO TO 499
       GNRWD=BESKA(NUU,SRWD)
       GNRRD=BESKA(NUU,SRRD)
       GNAAD=BESKA(NUU,SAAD)
       FNAAD=BESIA(NUU,SAAD)
       SUMIN=DEXP(AR1)*GNRWD*GNRRD*FNAAD/(2*AR2*GNAAD)
       GO TO 500
C
C          CLOSED BOUNDARY CASE
351    AR1=2*SAAD-SRWD-SRRD
       AR2=DSQRT(SRRD*SRWD)
       IF (DABS(AR1).GE.160) GO TO 499
       GNRWD=BESKA(NUU,SRWD)
       GNRRD=BESKA(NUU,SRRD)
       GNAAD1=BESKA(NUUU-1,SAAD)
       GNAAD2=BESKA(NUU+1,SAAD)
       FNAAD1=BESIA(NUUU-1,SAAD)
       FNAAD2=BESIA(NUU+1,SAAD)
       SUMIN=DEXP(AR1)*GNRWD*GNRRD*(FNAAD1+FNAAD2)/(2*AR2)
       SUMIN=-SUMIN/(GNAAD1+GNAAD2)
       GO TO 500
C
C
C
C          PARTIAL ASYMPTOTIC EXPANSION (RWD,RRD)  B
257    IF (ICASE.EQ.2) GO TO 352
       AR1=-SRWD-SRRD
       AR2=DSQRT(SRWD*SRRD)
       GNRWD=BESKA(NUU,SRWD)
       GNRRD=BESKA(NUU,SRRD)
       BIAAD(NU)=BESI(NUU,SAAD)
       BKAAD(NU)=BAAD(NUU,SAAD)
       DLAN=DLOG10(BIAAD(NU))+AR1*DEE+DLOG10(TTPI*GNRWD*GNRRD/(2*AR2))
       DLAN=DLAN-DLOG10(BKAAD(NU))
       IF (DLAN.LT.-60.0D0) GO TO 499
       SUMIN=10**DLAN
       GO TO 500
C
C          CLOSED BOUNDARY HOLE
352    AR1=-SRWD-SRRD
       AR2=DSQRT(SRWD*SRRD)
       GNRWD=BESKA(NUU,SRWD)
       GNRRD=BESKA(NUU,SRRD)
       BIAAD(NNU-1)=BESI(NUUU-1,SAAD)
       BIAAD(NU+1)=BESI(NUU+1,SAAD)
```

```
      BKAAD(NNU-1)=BAAD(NUUU-1,SAAD)
      BKAAD(NU+1)=BAAD(NUU+1,SAAD)
      DLAN=DLOG10(BIAAD(NNU-1)+BIAAD(NU+1))+AR1*DEE+DLOG10(TTPI*GNRWD)
      DLAN=DLAN+DLOG10(GNRRD/(2*AR2))
      DLAN=DLAN-DLOG10(BKAAD(NNU-1)+BKAAD(NU+1))
      IF (DLAN.LT.-60.0D0) GO TO 499
      SUMIN=-(10**DLAN)
      GO TO 500
C
C
C
C          PARTIAL ASYMPTOTIC EXPANSION (RWD,RRD)   C
C          SMALL ARGUMENT APPROXIMATION (AAD)
259   IF (ICASE.EQ.2)  GO TO 353
      GNRWD=BESKA(NUU,SRWD)
      FIAAD=FISMA(NUU,SAAD)
      FKAAD=FKSMA(NUU,SAAD)
      GNRRD=BESKA(NUU,SRRD)
      AR1=DSQRT(SRWD*SRRD)
      DLAN=DLOG10(TTPI*NUU*GNRWD*GNRRD/AR1)+2*NUU*DLOG10(SAAD)
      DLAN=DLAN-(SRWD+SRRD)*DEE-2*NUU*DLOG10(2.0D0)-2*DLOG10(FACNU(NU))
      DLAN=DLAN+DLOG10(FIAAD/FKAAD)
      IF (DLAN.LT.-60.0D0) GO TO 499
      SUMIN=10**DLAN
      GO TO 500
C
C          CLOSED BOUNDARY HOLE
353   GNRWD=BESKA(NUU,SRWD)
      FIAAD1=FISMA(NUUU-1,SAAD)
      FIAAD2=FISMA(NUU+1,SAAD)
      FKAAD1=FKSMA(NUUU-1,SAAD)
      FKAAD2=FKSMA(NUU+1,SAAD)
      GNRRD=BESKA(NUU,SRRD)
      AR1=DSQRT(SRWD*SRRD)
      DLAN=DLOG10(TTPI*NUU*GNRWD*GNRRD/AR1)+2*NUU*DLOG10(SAAD)
      DLAN=DLAN-(SRWD+SRRD)*DEE-2*NUU*DLOG10(2.0D0)-2*DLOG10(FACNU(NU))
      DLAN=DLAN+DLOG10((2*NUU*FIAAD1/SAAD)+SAAD*FIAAD2/(2*(NUU+1)))
      DLAN=DLAN-DLOG10((SAAD*FKAAD1/(2*(NUUU-1)))+2*NUU*FKAAD2/SAAD)
      IF (DLAN.LT.-60.0D0) GO TO 499
      SUMIN=-(10**DLAN)
      GO TO 500
C
C
C
C          PARTIAL ASYMPTOTIC EXPANSION (RWD)   D
263   IF (ICASE.EQ.2)  GO TO 354
      BIAAD(NU)=BESI(NUU,SAAD)
      BKRRD(NU)=BRRD(NUU,SRRD)
      BKAAD(NU)=BAAD(NUU,SAAD)
      BKRWD(NU)=BRWD(NUU,SRWD)
      GNRWD=BESKA(NUU,SRWD)
      DLAN=DLOG10(BIAAD(NU))+DLOG10(BKRRD(NU))-DLOG10(BKAAD(NU))
```

```
      DLAN=DLAN+DLOG10(DSQRT(TTPI/(2*SRWD))*GNRWD)-SRWD*DEE
      IF (DLAN.LT.-60.0D0) GO TO 499
      SUMIN=10**DLAN
      GO TO 500
C
C          CLOSED BOUNDARY HOLE
354   BIAAD(NNU-1)=BESI(NUUU-1,SAAD)
      BIAAD(NUU+1)=BESI(NUU+1,SAAD)
      BKRRD(NU)=BRRD(NUU,SRRD)
      BKAAD(NNU-1)=BAAD(NUUU-1,SAAD)
      BKAAD(NU+1)=BAAD(NUU+1,SAAD)
C      BKRWD(NU)=BRWD(NUU,SRWD)
      GNRWD=BESKA(NUU,SRWD)
      DLAN=DLOG10(BKRRD(NU))-DLOG10(BKAAD(NNU-1)+BKAAD(NU+1))
      DLAN=DLAN+DLOG10(BIAAD(NNU-1)+BIAAD(NU+1))
      DLAN=DLAN+DLOG10(DSQRT(TTPI/(2*SRWD))*GNRWD)-SRWD*DEE
      IF (DLAN.LT.-60.0D0) GO TO 499
      SUMIN=-(10**DLAN)
      GO TO 500
C
C
C
C          PARTIAL ASYMPTOTIC EXPANSION (RWD)    F
C          SMALL ARGUMENT APPROXIMATION (AAD)
266   IF (ICASE.EQ.2)  GO TO 356
      GNRWD=BESKA(NUU,SRWD)
      FIAAD=FISMA(NUU,SAAD)
      FKAAD=FKSMA(NUU,SAAD)
      BKRRD(NU)=BRRD(NUU,SRRD)
      AR1=DSQRT(TTPI/(2*SRWD))
      DLAN=DLOG10(BKRRD(NU)*AR1)+DLOG10(2*NUU*GNRWD)-SRWD*DEE
      DLAN=DLAN-2*DLOG10(FACNU(NU))-2*NUU*DLOG10(2.0D0)
      DLAN=DLAN+2*NUU*DLOG10(SAAD)
      DLAN=DLAN+DLOG10(FIAAD/FKAAD)
      IF (DLAN.LT.-60.0D0) GO TO 499
      SUMIN=10**DLAN
      GO TO 500
C
C         CLOSED BOUNDARY HOLE
356   GNRWD=BESKA(NUU,SRWD)
      FIAAD1=FISMA(NUUU-1,SAAD)
      FIAAD2=FISMA(NUU+1,SAAD)
      FKAAD1=FKSMA(NUUU-1,SAAD)
      FKAAD2=FKSMA(NUU+1,SAAD)
      BKRRD(NU)=BRRD(NUU,SRRD)
      AR1=DSQRT(TTPI/(2*SRWD))
      DLAN=DLOG10(BKRRD(NU)*AR1)+DLOG10(2*NUU*GNRWD)-SRWD*DEE
      DLAN=DLAN-2*DLOG10(FACNU(NU))-2*NUU*DLOG10(2.0D0)
      DLAN=DLAN+2*NUU*DLOG10(SAAD)
      DLAN=DLAN+DLOG10((2*NUU*FIAAD1/SAAD)+SAAD*FIAAD2/(2*(NUU+1)))
      DLAN=DLAN-DLOG10((SAAD*FKAAD1/(2*(NUUU-1)))+2*NUU*FKAAD2/SAAD)
      IF (DLAN.LT.-60.0D0) GO TO 499
```

```
      SUMIN=-(10**DLAN)
      GO TO 500
C
C
C
C           PARTIAL ASYMPTOTIC EXPANSION (RWD)   G
C           SMALL ARGUMENT APPROXIMATION (AAD,RRD)
269   IF (ICASE.EQ.2)  GO TO 357
      FKRRD=FKSMA(NUU,SRRD)
      FIAAD=FISMA(NUU,SAAD)
      FKAAD=FKSMA(NUU,SAAD)
      GNRWD=BESKA(NUU,SRWD)
      AR1=GNRWD*DSQRT(TTPI/(2*SRWD))
      DLAN=DLOG10(AR1)+2*NUU*DLOG10(SAAD)-NUU*DLOG10(SRRD)
      DLAN=DLAN-SRWD*DEE-NUU*DLOG10(2.0D0)-DLOG10(FACNU(NU))
      DLAN=DLAN+DLOG10(FKRRD*FIAAD/FKAAD)
      IF (DLAN.LT.-60.0D0) GO TO 499
      SUMIN=10**DLAN
      GO TO 500
C
C           CLOSED BOUNDARY HOLE
357   GNRWD=BESKA(NUU,SRWD)
      FKRRD=FKSMA(NUU,SRRD)
      FIAAD1=FISMA(NUUU-1,SAAD)
      FIAAD2=FISMA(NUU+1,SAAD)
      FKAAD1=FKSMA(NUUU-1,SAAD)
      FKAAD2=FKSMA(NUU+1,SAAD)
      AR1=GNRWD*DSQRT(TTPI/(2*SRWD))
      DLAN=DLOG10(AR1)+2*NUU*DLOG10(SAAD)-NUU*DLOG10(SRRD)
      DLAN=DLAN-SRWD*DEE-NUU*DLOG10(2.0D0)-DLOG10(FACNU(NU))
      DLAN=DLAN+DLOG10(FKRRD)
      DLAN=DLAN+DLOG10((2*NUU*FIAAD1/SAAD)+SAAD*FIAAD2/(2*(NUU+1)))
      DLAN=DLAN-DLOG10((SAAD*FKAAD1/(2*(NUUU-1)))+2*NUU*FKAAD2/SAAD)
      IF (DLAN.LT.-60.0D0) GO TO 499
      SUMIN=-(10**DLAN)
      GO TO 500
C
C
C
C           PARTIAL ASYMPTOTIC EXPANSION (RRD)   I
273   IF (ICASE.EQ.2)  GO TO 359
      BKRWD(NU)=BRWD(NUU,SRWD)
      GNRRD=BESKA(NUU,SRRD)
      BKAAD(NU)=BAAD(NUU,SAAD)
      BIAAD(NU)=BESI(NUU,SAAD)
      AR1=GNRRD*DSQRT(TTPI/(2*SRRD))
      DLAN=DLOG10(BKRWD(NU))+DLOG10(BIAAD(NU))-DLOG10(BKAAD(NU))
      DLAN=DLAN+DLOG10(AR1)-SRRD*DEE
      IF (DLAN.LT.-60.0D0) GO TO 499
      SUMIN=10**DLAN
      GO TO 500
C
```

```
C           CLOSED BOUNDARY HOLE
359    BKRWD(NU)=BRWD(NUU,SRWD)
       GNRRD=BESKA(NUU,SRRD)
       BKAAD(NNU-1)=BAAD(NUUU-1,SAAD)
       BKAAD(NU+1)=BAAD(NUU+1,SAAD)
       BIAAD(NNU-1)=BESI(NUUU-1,SAAD)
       BIAAD(NU+1)=BESI(NUU+1,SAAD)
       AR1=GNRRD*DSQRT(TTPI/(2*SRRD))
       DLAN=DLOG10(BKRWD(NU))+DLOG10(BIAAD(NNU-1)+BIAAD(NU+1))
       DLAN=DLAN-DLOG10(BKAAD(NNU-1)+BKAAD(NU+1))
       DLAN=DLAN+DLOG10(AR1)-SRRD*DEE
       IF (DLAN.LT.-60.0D0) GO TO 499
       SUMIN=-(10**DLAN)
       GO TO 500
C
C
C
C           PARTIAL ASYMPTOTIC EXPANSION (RRD)   J
C           SMALL ARGUMENT APPROXIMATION (AAD)
276    IF (ICASE.EQ.2) GO TO 360
       FIAAD=FISMA(NUU,SAAD)
       FKAAD=FKSMA(NUU,SAAD)
       BKRWD(NU)=BRWD(NUU,SRWD)
       GNRRD=BESKA(NUU,SRRD)
       AR1=BKRWD(NU)*DSQRT(TTPI/(2*SRRD))
       DLAN=DLOG10(AR1)+DLOG10(GNRRD*2*NUU)-SRRD*DEE
       DLAN=DLAN-2*DLOG10(FACNU(NU))-2*NUU*DLOG10(2.0D0)
       DLAN=DLAN+2*NUU*DLOG10(SAAD)
       DLAN=DLAN+DLOG10(FIAAD/FKAAD)
       IF (DLAN.LT.-60.0D0) GO TO 499
       SUMIN=10**DLAN
       GO TO 500
C
C           CLOSED BOUNDARY HOLE
360    BKRWD(NU)=BRWD(NUU,SRWD)
       FIAAD1=FISMA(NUUU-1,SAAD)
       FIAAD2=FISMA(NUU+1,SAAD)
       FKAAD1=FKSMA(NUUU-1,SAAD)
       FKAAD2=FKSMA(NUU+1,SAAD)
       GNRRD=BESKA(NUU,SRRD)
       AR1=BKRWD(NU)*DSQRT(TTPI/(2*SRRD))
       DLAN=DLOG10(AR1)+DLOG10(GNRRD*2*NUU)-SRRD*DEE
       DLAN=DLAN-2*DLOG10(FACNU(NU))-2*NUU*DLOG10(2.0D0)
       DLAN=DLAN+2*NUU*DLOG10(SAAD)
       DLAN=DLAN+DLOG10((2*NUU*FIAAD1/SAAD)+SAAD*FIAAD2/(2*(NUU+1)))
       DLAN=DLAN-DLOG10((SAAD*FKAAD1/(2*(NUUU-1)))+2*NUU*FKAAD2/SAAD)
       IF (DLAN.LT.-60.0D0) GO TO 499
       SUMIN=-(10**DLAN)
       GO TO 500
C
C
C
```

```
C          PARTIAL ASYMPTOTIC EXPANSION (RRD)   K
C          SMALL ARGUMENT APPROXIMATION (AAD,RWD)
279   IF (ICASE.EQ.2) GO TO 361
      FIAAD=FISMA(NUU,SAAD)
      FKAAD=FKSMA(NUU,SAAD)
      FKRWD=FKSMA(NUU,SRWD)
      GNRRD=BESKA(NUU,SRRD)
      AR1=GNRRD*DSQRT(TTPI/(2*SRRD))
      DLAN=DLOG10(AR1)+2*NUU*DLOG10(SAAD)-NUU*DLOG10(SRWD)
      DLAN=DLAN-SRRD*DEE-NUU*DLOG10(2.0D0)-DLOG10(FACNU(NU))
      DLAN=DLAN+DLOG10(FKRWD*FIAAD/FKAAD)
      SUMIN=10**DLAN
      GO TO 500
C
C          CLOED BOUNDARY HOLE
361   GNRRD=BESKA(NUU,SRRD)
      FIAAD1=FISMA(NUUU-1,SAAD)
      FIAAD2=FISMA(NUU+1,SAAD)
      FKAAD1=FKSMA(NUUU-1,SAAD)
      FKAAD2=FKSMA(NUU+1,SAAD)
      FKRWD=FKSMA(NUU,SRWD)
      AR1=GNRRD*DSQRT(TTPI/(2*SRRD))
      DLAN=DLOG10(AR1)+2*NUU*DLOG10(SAAD)-NUU*DLOG10(SRWD)
      DLAN=DLAN-SRWD*DEE-NUU*DLOG10(2.0D0)-DLOG10(FACNU(NU))
      DLAN=DLAN+DLOG10(FKRWD)
      DLAN=DLAN+DLOG10((2*NUU*FIAAD1/SAAD)+SAAD*FIAAD2/(2*(NUU+1)))
      DLAN=DLAN-DLOG10((SAAD*FKAAD1/(2*(NUUU-1)))+2*NUU*FKAAD2/SAAD)
      SUMIN=-(10**DLAN)
      GO TO 500
C
C
C
C
C          SMALL ARGUMENT APPROXIMATION (AAD)  L
293   IF (ICASE.EQ.2) GO TO 362
      FIAAD=FISMA(NUU,SAAD)
      FKAAD=FKSMA(NUU,SAAD)
      BKRWD(NU)=BRWD(NUU,SRWD)
      BKRRD(NU)=BRRD(NUU,SRRD)
      DLAN=DLOG10(BKRWD(NU))+DLOG10(BKRRD(NU))+2*NUU*DLOG10(SAAD)
      DLAN=DLAN+DLOG10(2.0D0*NUU)-2*NUU*DLOG10(2.0D0)
      DLAN=DLAN-2*DLOG10(FACNU(NU))
      DLAN=DLAN+DLOG10(FIAAD/FKAAD)
      SUMIN=10**DLAN
      GO TO 500
C
C          CLOSED BOUNDARY HOLE
362   BKRWD(NU)=BRWD(NUU,SRWD)
      FIAAD1=FISMA(NUUU-1,SAAD)
      FIAAD2=FISMA(NUU+1,SAAD)
      FKAAD1=FKSMA(NUUU-1,SAAD)
      FKAAD2=FKSMA(NUU+1,SAAD)
```

```
      BKRRD(NU)=BRRD(NUU,SRRD)
      DLAN=DLOG10(BKRWD(NU))+DLOG10(BKRRD(NU))+2*NUU*DLOG10(SAAD)
      DLAN=DLAN+DLOG10(2.0D0*NUU)-2*NUU*DLOG10(2.0D0)
      DLAN=DLAN-2*DLOG10(FACNU(NU))
      DLAN=DLAN+DLOG10((2*NUU*FIAAD1/SAAD)+SAAD*FIAAD2/(2*(NUU+1)))
      DLAN=DLAN-DLOG10((SAAD*FKAAD1/(2*(NUUU-1)))+2*NUU*FKAAD2/SAAD)
      SUMIN=-(10**DLAN)
      GO TO 500
C
C
C
C          SHALL ARGUMENT APPROXIMATION (AAD,RRD)    M
299   IF (ICASE.EQ.2) GO TO 363
      FIAAD=FISMA(NUU,SAAD)
      FKAAD=FKSMA(NUU,SAAD)
      FKRRD=FKSMA(NUU,SRRD)
      BKRWD(NU)=BRWD(NUU,SRWD)
      DLAN=DLOG10(BKRWD(NU))+2*NUU*DLOG10(SAAD)-NUU*DLOG10(SRRD)
      DLAN=DLAN-NUU*DLOG10(2.0D0)-DLOG10(FACNU(NU))
      DLAN=DLAN+DLOG10(FKRRD*FIAAD/FKAAD)
      SUMIN=10**DLAN
      GO TO 500
C
C          CLOSED BOUNDARY HOLE
363   BKRWD(NU)=BRWD(NUU,SRWD)
      FIAAD1=FISMA(NUUU-1,SAAD)
      FIAAD2=FISMA(NUU+1,SAAD)
      FKAAD1=FKSMA(NUUU-1,SAAD)
      FKAAD2=FKSMA(NUU+1,SAAD)
      FKRRD=FKSMA(NUU,SRRD)
      DLAN=DLOG10(BKRWD(NU))+2*NUU*DLOG10(SAAD)-NUU*DLOG10(SRRD)
      DLAN=DLAN-NUU*DLOG10(2.0D0)-DLOG10(FACNU(NU))
      DLAN=DLAN+DLOG10(FKRRD)
      DLAN=DLAN+DLOG10((2*NUU*FIAAD1/SAAD)+SAAD*FIAAD2/(2*(NUU+1)))
      DLAN=DLAN-DLOG10((SAAD*FKAAD1/(2*(NUUU-1)))+2*NUU*FKAAD2/SAAD)
      SUMIN=-(10**DLAN)
      GO TO 500
C
C
C
C          SMALL ARGUMENT APPROXIMATION (RRD)    N
300   IF (ICASE.EQ.2) GO TO 364
      FKRRD=FKSMA(NUU,SRRD)
      BKRWD(NU)=BRWD(NUU,SRWD)
      BKAAD(NU)=BAAD(NUU,SAAD)
      BIAAD(NU)=BESI(NUU,SAAD)
      DLAN=DLOG10(BKRWD(NU))+DLOG10(BIAAD(NU))-DLOG10(BKAAD(NU))
      DLAN=DLAN+NUU*DLOG10(2.0D0)+DLOG 0(FACNU(NU))-NUU*DLOG10(SRRD)
      DLAN=DLAN-DLOG10(2.0D0*NUU)+DLOG 0(FKRRD)
      SUMIN=10**DLAN
      GO TO 500
C
```

```
C          CLOSED BOUNDARY HOLE
364   BKRWD(NU)=BRWD(NUU,SRWD)
      FKRRD=FKSMA(NUU,SRRD)
      BKAAD(NNU-1)=BAAD(NUUU-1,SAAD)
      BKAAD(NU+1)=BAAD(NUU+1,SAAD)
      BIAAD(NNU-1)=BESI(NUUU-1,SAAD)
      BIAAD(NU+1)=BESI(NUU+1,SAAD)
      DLAN=DLOG10(BKRWD(NU))+DLOG10(BIAAD(NNU-1)+BIAAD(NU+1))
      DLAN=DLAN-DLOG10(BKAAD(NNU-1)+BKAAD(NU+1))
      DLAN=DLAN+NUU*DLOG10(2.0D0)+DLOG10(FACNU(NU))-NUU*DLOG10(SRRD)
      DLAN=DLAN-DLOG10(2.0D0*NUU)+DLOG10(FKRRD)
      SUMIN=-(10**DLAN)
      GO TO 500
C
C
C
C          SMALL ARGUMENT APPROXIMATION (RWD)   P
302   IF (ICASE.EQ.2)  GO TO 365
      FKRWD=FKSMA(NUU,SRWD)
      BKRRD(NU)=BRRD(NUU,SRRD)
      BKAAD(NU)=BAAD(NUU,SAAD)
      BIAAD(NU)=BESI(NUU,SAAD)
      DLAN=DLOG10(BKRRD(NU))+DLOG10(BIAAD(NU))-DLOG10(BKAAD(NU))
      DLAN=DLAN+NUU*DLOG10(2.0D0)+DLOG10(FACNU(NU))-NUU*DLOG10(SRWD)
      DLAN=DLAN-DLOG10(2.0D0*NUU)+DLOG10(FKRWD)
      SUMIN=10**DLAN
      GO TO 500
C
C          CLOSED BOUNDARY HOLE
365   BKRRD(NU)=BRRD(NUU,SRRD)
      FKRWD=FKSMA(NUU,SRWD)
      BKAAD(NNU-1)=BAAD(NUUU-1,SAAD)
      BKAAD(NU+1)=BAAD(NUU+1,SAAD)
      BIAAD(NNU-1)=BESI(NUUU-1,SAAD)
      BIAAD(NU+1)=BESI(NUU+1,SAAD)
      DLAN=DLOG10(BKRRD(NU))+DLOG10(BIAAD(NNU-1)+BIAAD(NU+1))
      DLAN=DLAN-DLOG10(BKAAD(NNU-1)+BKAAD(NU+1))
      DLAN=DLAN+NUU*DLOG10(2.0D0)+DLOG10(FACNU(NU))-NUU*DLOG10(SRWD)
      DLAN=DLAN-DLOG10(2.0D0*NUU)+DLOG10(FKRWD)
      SUMIN=-(10**DLAN)
      GO TO 500
C
C
C
C          SMALL ARGUMENT APPROXIMATION (AAD,RWD)   O
301   IF (ICASE.EQ.2)  GO TO 366
      FIAAD=FISMA(NUU,SAAD)
      FKAAD=FKSMA(NUU,SAAD)
      FKRWD=FKSMA(NUU,SRWD)
      BKRRD(NU)=BRRD(NUU,SRRD)
      DLAN=DLOG10(BKRRD(NU))+2*NUU*DLOG10(SAAD)-NUU*DLOG10(SRWD)
      DLAN=DLAN-NUU*DLOG10(2.0D0)-DLOG10(FACNU(NU))
```

```
      DLAN=DLAN+DLOG10(FKRWD*FIAAD/FKAAD)
      SUMIN=10**DLAN
      GO TO 500
C
C          CLOSED BOUNDARY HOLE
366   BKRRD(NU)=BRRD(NUU,SRRD)
      FIAAD1=FISMA(NUUU-1,SAAD)
      FIAAD2=FISMA(NUU+1,SAAD)
      FKAAD1=FKSMA(NUUU-1,SAAD)
      FKAAD2=FKSMA(NUU+1,SAAD)
      FKRWD=FKSMA(NUU,SRWD)
      DLAN=DLOG10(BKRRD(NU))+2*NUU*DLOG10(SAAD)-NUU*DLOG10(SRWD)
      DLAN=DLAN-NUU*DLOG10(2.0D0)-DLOG10(FACNU(NU))
      DLAN=DLAN+DLOG10(FKRWD)
      DLAN=DLAN+DLOG10((2*NUU*FIAAD1/SAAD)+SAAD*FIAAD2/(2*(NUU+1)))
      DLAN=DLAN-DLOG10((SAAD*FKAAD1/(2*(NUUU-1)))+2*NUU*FKAAD2/SAAD)
      SUMIN=-(10**DLAN)
      GO TO 500
C
C
C
C          SMALL ARGUMENT APPROXIMATION (AAD,RRD,RWD)   Q
303   IF(ICASE.EQ.2) GO TO 367
      FIAAD=FISMA(NUU,SAAD)
      FKAAD=FKSMA(NUU,SAAD)
      FKRWD=FKSMA(NUU,SRWD)
      FKRRD=FKSMA(NUU,SRRD)
      DLAN=2*NUU*DLOG10(SAAD)-NUU*DLOG10(SRWD*SRRD)-DLOG10(2.0D0*NUU)
      DLAN=DLAN+DLOG10(FKRWD*FKRRD*FIAAD/FKAAD)
      SUMIN=10**DLAN
      GO TO 500
C
C          CLOSED BOUNDARY HOLE
367   FIAAD1=FISMA(NUUU-1,SAAD)
      FIAAD2=FISMA(NUU+1,SAAD)
      FKAAD1=FKSMA(NUUU-1,SAAD)
      FKAAD2=FKSMA(NUU+1,SAAD)
      FKRWD=FKSMA(NUU,SRWD)
      FKRRD=FKSMA(NUU,SRRD)
      DLAN=2*NUU*DLOG10(SAAD)-NUU*DLOG10(SRWD*SRRD)-DLOG10(2.0D0*NUU)
      DLAN=DLAN+DLOG10(FKRWD*FKRRD)
      DLAN=DLAN+DLOG10((2*NUU*FIAAD1/SAAD)+SAAD*FIAAD2/(2*(NUU+1)))
      DLAN=DLAN-DLOG10((SAAD*FKAAD1/(2*(NUUU-1)))+2*NUU*FKAAD2/SAAD)
      SUMIN=-(10**DLAN)
      GO TO 500
C
C
C
C          SIMPLE PROGRAM    Z
290   IF (ICASE.EQ.2) GO TO 368
      BKRWD(NU)=BRWD(NUU,SRWD)
      BKRRD(NU)=BRRD(NUU,SRRD)
```

```
      BKAAD(NU)=BAAD(NUU,SAAD)
      BIAAD(NU)=BESI(NUU,SAAD)
      SUMIN=(BKRWD(NU)*BIAAD(NU)/BKAAD(NU))*BKRRD(NU)
      GO TO 500
C
C          CLOSED BOUNDARY HOLE
368   BKRWD(NU)=BRWD(NUU,SRWD)
      BKRRD(NU)=BRRD(NUU,SRRD)
      BKAAD(NNU-1)=BAAD(NUUU-1,SAAD)
      BKAAD(NU+1)=BAAD(NUU+1,SAAD)
      BIAAD(NNU-1)=BESI(NUUU-1,SAAD)
      BIAAD(NU+1)=BESI(NUU+1,SAAD)
      SUMIN=BKRWD(NU)*(BIAAD(NNU-1)+BIAAD(NU+1))
      SUMIN=-(SUMIN/(BKAAD(NNU-1)+BKAAD(NU+1)))*BKRRD(NU)
      GO TO 500
C
C
C
C
499   SUMIN=0.0D0
500   RETURN
      END
C
C
C
C
C
C
C                 FUNCTION BESI (NU,ARG)
C              *****************************
C          THIS FUNCTION EVALUATES THE MODIFIED BESSEL
C          FUNCTION I(NU,ARG).
C          THE ORDER IS LIMITED TO   NU<51
      FUNCTION BESI(NU,ARG)
      IMPLICIT REAL*8 (A-H,O-Z)
      REAL*8 A,AA,AAA,FNZ,B,BB,DELTA,EPSI,AEXP,C,CC
      COMMON /FRAC3/FACNU(51)
      COMMON /FRAC99/IEND99
C      WRITE (6,17) NU,ARG
C17    FORMAT (15X,I5,5X,E12.5)
C
C
C          CONVERGENCE CRITERION (FRACTION)


      EPSI=1.0D-15
C
C          THE ASYMPTOTIC EXPANSION OPTION IS BYPASSED
C          IN MOST CALCULATIONS.
      GO TO 5
C
```

```
C          NOW THE METHOD OF EVALUATING I IS CHOSEN
C          FOR ARG>=20    ASYMPTOTIC EXPANSION
C          FOR ARG<20     ASCENDING SERIES
C     IF (ARG.GE.20.0) GO TO 4
C     IF (ARG.LT.20.0) GO TO 5
C
C
C
C          ASYMPTOTIC EXPANSION
C          *********************
c4     A=(NU**2)*4
      AA=ARG*8
      AAA=2*ARG*3.141592654
      AAA=DSQRT(AAA)
      IFLAG3=0
      FNZ=1.0D0
      BB=1.0D0
      DDD=1.0D0
      DO 6 I=1,200
      D=(A-(2*I-1)**2)/(AA*I)
      DD=DABS(D)
      IF (IFLAG3.EQ.1) GO TO 14
      IF (DD.LT.DDD) IFLAG3=1
      GO TO 15
 14   II=I/2*2
      IF (DD.GT.DDD.AND.II.EQ.I) GO TO 7
 15   DDD=DD
      BB=BB*(-1)*D
      FNZ=FNZ+BB
C      WRITE (6,16) FNZ
C16    FORMAT (10X,E12.5)
      DELTA=BB/FNZ
      DELTA=DABS(DELTA)
      IF (EPSI-DELTA) 6,7,7
6     CONTINUE
C
C
C           CHECK FOR EXPONENT MAG
7     E=DEXP(1.0D0)
      AEXP=ARG*DLOG10(E)-DLOG10(AAA)+DLOG10(FNZ)
      IF (DABS(AEXP).GT.70.0) GO TO 8
      BESI=DEXP(ARG)*FNZ/AAA
      GO TO 9
C
C
C          EXPONENT MAG OVERFLOW


8     WRITE (6,101) AEXP
101   FORMAT (5X,'EXPONENT OF I',D20.9,I5,D20.9)
      BESI=10**AEXP
      GO TO 9
```

```
C
            ASCENDING SERIES
            ****************
            FIRST CHECK FOR EXPONENT MAG
      C=NU*DLOG10(ARG/2)-DLOG10(FACNU(NU+1))
      CC=DABS(C)
      IF (CC.GT.70.0) GO TO 10
      B=1.0D0
      BB=B
      AA=(ARG/2)**2
      AAA=1/FACNU(NU+1)
      DO 11 I=1,200
      BB=BB*AA/(I*(I+NU))
      B=B+BB
      DELTA=BB/B
      IF (EPSI-DELTA) 11,12,12
11    CONTINUE
C
C
C             SECOND CHECK FOR EXPONENT HAG
12    B=B*AAA
      CCC=NU*(DLOG10(ARG/2.))
      IF (CCC.GT.69.) GO TO 27
      C=DLOG10(B)+CCC
      CC=DABS (C)
      IF (CC.GT.69.) GO TO 10
      BESI=B*((ARG/2.)**NU)
      GO TO 9
27    C=DLOG10(B)+CCC
      CC=DABS(C)
      IF (CC.GT.69.) GO TO 10
      BESI=10.**C
      GO TO 9
C
C
C             EXPONENT HAG OVERFLOW
10    WRITE (6,101) CC,NU,ARG
      IEND99=1
      BESI=1.0D-70
C
C
9     RETURN
      END
C
C
C
C                FUNCTION BAAD (N,Z)
```

```
C           *************************
C          THIS FUNCTION EVALUATES K(N,Z) USING THE "STEP-UP
C          METHOD". WE USE K(0,Z) AND K(1,Z) TO EVALUATE THE
C          HIGHER ORDERS.
      FUNCTION BAAD(N,Z)
      IMPLICIT REAL*8 (A-H,O-Z)
      COMMON /FRAC11/BIAAD(100),BKAAD(100),BKRWD(100),BKRRD(100)
      COMMON /FRAC12/SUM(50,16)
      COMMON /FRAC5/IOPT,IER
      DOUBLE PRECISION MMBSK0,MMBSK1
      IF (N.EQ.0) GO TO 1
      IF (N.EQ.1) GO TO 2
      EKAAD=DLOG10(BKAAD(N))
      EKAAD=DABS(EKAAD)
      IF (EKAAD.GE.70) IEND99=1
      BAAD=BKAAD(N-1)+(BKAAD(N)/Z)*2*(N-1)
      GO TO 3
1     BAAD=MMBSK0(IOPT,Z,IER)
      GO TO 3
2     BAAD=MMBSK1(IOPT,Z,IER)
3     RETURN
      END
C
C
C
C              FUNCTION BRWD (N,Z)
C           *************************
C          THIS FUNCTION EVALUATES K(N,Z) USING THE "STEP-UP
C          METHOD". WE USE K(0,Z) AND K(1,Z) TO EVALUATE THE
C          HIGHER ORDERS.
      FUNCTION BRWD(N,Z)
      IMPLICIT REAL*8 (A-H,O-Z)
      COMMON /FRAC11/BIAAD(100),BKAAD(100),BKRWD(100),BKRRD(100)
      COMMON /FRAC12/SUM(50,16)
      COMMON /FRAC5/IOPT,IER
      COMMON /FRAC99/IEND99
      DOUBLE PRECISION MMBSK0,MMBSK1
      IF (N.EQ.0) GO TO 1
      IF (N.EQ.1) GO TO 2
      EKRWD=DLOG10(BKRWD(N))
      EKRWD=DABS(EKRWD)
      IF (EKRWD.GE.70) IEND99=1
      BRWD=BKRWD(N-1)+(BKRWD(N)/Z)*2*(N-1)
      GO TO 3
1     BRWD=MMBSK0(IOPT,Z,IER)
      GO TO 3
2     BRWD=MMBSK1(IOPT,Z,IER)
3     RETURN
      END
C
C
C
```

```
C              FUNCTION BRRD (N,Z)
C           *************************
C           THIS FUNCTION EVALUATES K(N,Z) USING THE "STEP-UP
C           METHOD". WE USE K(0,Z) AND K(1,Z) TO EVALUATE THE
C           HIGHER ORDERS.
      FUNCTION BRRD(N,Z)
      IMPLICIT REAL*8 (A-H,O-Z)
      COMMON /FRAC11/BIAAD(100),BKAAD(100),BKRWD(100),BKRRD(100)
      COMMON /FRAC12/SUM(50,16)
      COMMON /FRAC5/IOPT,IER
      COMMON /FRAC99/IEND99
      DOUBLE PRECISION MMBSK0,MMBSK1
      IF (N.EQ.0) GO TO 1
      IF (N.EQ.1) GO TO 2
      EKRRD=DLOG10(BKRRD(N))
      EKRRD=DABS(EKRRD)
      IF (EKRRD.EQ.70)  IEND99=1
      BRRD=BKRRD(N-1)+(BKRRD(N)/Z)*2*(N-1)
      GO TO 3
1     BRRD=MMBSK0(IOPT,Z,IER)
      GO TO 3
2     BRRD=MMBSK1(IOPT,Z,IER)
3     RETURN
      END
C
C
C
C
      FUNCTION FISMA(NU,ARG)
C           THIS FUNCTION EVALUATES THE NON-EXPONENTIAL
C           TERMS IN THE ASCENDING SERIES FOR I(NU,ARG).
C           NU FACTORIAL IS FACTORED OUT WITH THE EXPONENTIAL
      IMPLICIT REAL*8 (A-H,O-Z)
      EPSI1=1.0D-15
      A=(ARG**2)/4.0
      B=1.0D0
      BB=1.0D0
      DO 1 I=1,200
      BB=BB*A/(I*(NU+I))
      B=B+BB
      DELTA=BB/B
      IF (DELTA.LT.EPSI1) GO TO 2
1     CONTINUE
2     FISMA=B
      RETURN
      END
C
C
C
      FUNCTION FKSMA(NU,ARG)
C           THIS FUNCTION EVALUATES THE NON-EXPONENTIAL
C           TERMS IN THE ASCENDING SERIES FOR K(NU,ARG).
```

```
C           NU FACTORIAL IS FACTORED OUT WITH THE EXPONENTIAL
      IMPLICIT REAL*8 (A-H,O-Z)
      EPSI1=1.0D-15
      B=1.0D0
      BB=1.0DD
      A=(ARG**2)/4.0
      KK=NU-1
      DO 1 I=1,KK
      BB=BB*A/(I*(NU-I))
      B=B+BB
      DELTA=BB/B
      IF (DELTA.LT.EPSI1) GO TO 2
1     CONTINUE
2     FKSMA=B
      RETURN
      END
```

APPENDIX H : TABLES FOR PRESSURE TIME TYPE CURVES

In this appendix, we use the following notations :

a_D = AAD

r'_D = RWD

r_D = RRD

θ = THETA

p_{Dss} = PDSS

t_D = TD

t_D / r_D^2 = TD:RD**2

p_D = PD

p_{DN} = PDN = normalized pressure drop

r_1 = R1

r_2 = R2

TABLE H1 :

CONSTANT PRESSURE INTERNAL BOUNDARY

AAD= 0.20000D+01
RWD= 0.20000D+02
RRD= 0.19640D+02

F= 0.10000D+00
E= 0.98200D+00

THE STEADY STATE PRESSURES

THETA= 0.0	PDSS= 0.629156914D+01
THETA= 0.45000D+02	PDSS= 0.255342104D+01
THETA= 0.90000D+02	PDSS= 0.194689881D+01
THETA= 0.13500D+03	PDSS= 0.168668159D+01
THETA= 0.18000D+03	PDSS= 0.161044649D+01

THETA= 0.0

TD	TD:RD**2	PD	PDN
0.129599997D-01	0.999999975D-01	0.124198 D-01	0.197405 D-02
0.259199993D-01	0.199999995D+00	0.736016 D-01	0.116984 D-01
0.518399987D-01	0.399999990D+00	0.216265 D+00	0.343738 D-01
0.777599980D-01	0.599999985D+00	0.337574 D+00	0.536551 D-01
0.103679997D+00	0.799999980D+00	0.437690 D+00	0.695677 D-01
0.129599997D+00	0.999999975D+00	0.521993 D+00	0.829670 D-01
0.259199993D+00	0.199999995D+01	0.811571 D+00	0.128993 D+00
0.518399987D+00	0.399999990D+01	0.112834 D+01	0.179342 D+00
0.777599980D+00	0.599999985D+01	0.132093 D+01	0.209953 D+00
0.103679997D+01	0.799999980D+01	0.145966 D+01	0.232004 D+00
0.129599997D+01	0.999999975D+01	0.156816 D+01	0.249248 D+00
0.259199993D+01	0.199999995D+02	0.190854 D+01	0.303349 D+00
0.518399987D+01	0.399999990D+02	0.225200 D+01	0.357940 D+00
0.777599980D+01	0.599999985D+02	0.245370 D+01	0.389998 D+00
0.103679997D+02	0.799999980D+02	0.259702 D+01	0.412778 D+00
0.129599997D+02	0.999999975D+02	0.270828 D+01	0.430462 D+00
0.259199993D+02	0.199999995D+03	0.305420 D+01	0.485444 D+00
0.518399987D+02	0.399999990D+03	0.340045 D+01	0.540478 D+00
0.777599980D+02	0.599999985D+03	0.360254 D+01	0.572598 D+00
0.103679997D+03	0.799999980D+03	0.374447 D+01	0.595157 D+00
0.129599997D+03	0.999999975D+03	0.385271 D+01	0.612360 D+00
0.259199993D+03	0.199999995D+04	0.416866 D+01	0.662578 D+00
0.518399987D+03	0.399999990D+04	0.443765 D+01	0.705333 D+00
0.777599980D+03	0.599999985D+04	0.457000 D+01	0.726370 D+00
0.103679997D+04	0.799999980D+04	0.465336 D+01	0.739619 D+00
0.129599997D+04	0.999999975D+04	0.471252 D+01	0.749022 D+00
0.259199993D+04	0.199999995D+05	0.487015 D+01	0.774077 D+00
0.518399987D+04	0.399999990D+05	0.499660 D+01	0.794174 D+00
0.777599980D+04	0.599999985D+05	0.505966 D+01	0.804198 D+00
0.103679997D+05	0.799999980D+05	0.510047 D+01	0.810683 D+00
0.129599997D+05	0.999999975D+05	0.513014 D+01	0.815400 D+00
0.259199993D+05	0.199999995D+06	0.521300 D+01	0.828569 D+00
0.518399987D+05	0.399999990D+06	0.528430 D+01	0.839902 D+00
0.777599980D+05	0.599999985D+06	0.532167 D+01	0.845842 D+00
0.103679997D+06	0.799999980D+06	0.534651 D+01	0.849790 D+00
0.129599997D+06	0.999999975D+06	0.536491 D+01	0.852714 D+00

AAD= 0.40000D+01
RWD= 0.20000D+02
RRD= 0.19680D+02

F= 0.20000D+00
E= 0.98400D+00

THE STEADY STATE PRESSURES

THETA=	0.0	PDSS=	0.568697536D+01
THETA=	0.45000D+02	PDSS=	0.183982346D+01
THETA=	0.90000D+02	PDSS=	0.125556007D+01
THETA=	0.13500D+03	PDSS=	0.101609050D+01
THETA=	0.18000D+03	PDSS=	0.948039430D+00

THETA= 0.0

TD	TD:RD**2	PD	PDN
0.102399997D-01	0.999999975D-01	0.124198 D-01	0.218391 D-02
0.204799995D-01	0.199999995D+00	0.736016 D-01	0.129421 D-01
0.4095999900-01	0.399999990D+00	0.216265 D+00	0.380282 D-01
0.614399984D-01	0.599999985D+00	0.337574 D+00	0.593593 D-01
0.819199979D-01	0.799999980D+00	0.037690 D+00	0.769636 D-01
0.102399997D+00	0.999999975D+00	0.521993 D+00	0.917874 D-01
0.204799995D+00	0.199999995D+01	0.811571 D+00	0.142707 D+00
0.409599990D+00	0.399999990D+01	0.112834 D+01	0.198408 D+00
0.614399984D+00	0.599999985D+01	0.132093 D+01	0.232274 D+00
0.819199979D+00	0.799999980D+01	0.145966 D+01	0.256668 D+00
0.102399997D+01	0.999999975D+01	0.156816 D+01	0.275746 D+00
0.204799995D+01	0.199999995D+02	0.190854 D+01	0.335599 D+00
0.409599990D+01	0.399999990D+02	0.225200 D+01	0.395994 D+00
0.614399984D+01	0.599999985D+02	0.245370 D+01	0.431460 D+00
0.819199979D+01	0.799999980D+02	0.259702 D+01	0.456661 D+00
0.102399997D+02	0.999999975D+02	0.270828 D+01	0.476225 D+00
0.204799995D+02	0.199999995D+03	0.305420 D+01	0.537051 D+00
0.409599990D+02	0.399999990D+03	0.340045 D+01	0.597937 D+00
0.614399984D+02	0.599999985D+03	0.360238 D+01	0.633444 D+00
0.819199979D+02	0.799999980D+03	0.374385 D+01	0.658321 D+00
0.102399997D+03	0.999999975D+03	0.385134 D+01	0.677222 D+00
0.204799995D+03	0.199999995D+04	0.416126 D+01	0.731719 D+00
0.409599990D+03	0.399999990D+04	0.441705 D+01	0.776697 D+00
0.614399984D+03	0.599999985D+04	0.453852 D+01	0.798056 D+00
0.819199979D+03	0.799999980D+04	0.461304 D+01	0.811159 D+00
0.102399997D+04	0.999999975D+04	0.466484 D+01	0.820268 D+00
0.204799995D+04	0.199999995D+05	0.479781 D+01	0.843649 D+00
0.409599990D+04	0.399999990D+05	0.489851 D+01	0.861356 D+00
0.614399984D+04	0.599999985D+05	0.494663 D+01	0.869818 D+00
0.819199979D+04	0.799999980D+05	0.497703 D+01	0.875163 D+00
0.102399997D+05	0.999999975D+05	0.499878 D+01	0.878988 D+00
0.204799995D+05	0.199999995D+06	0.505798 D+01	0.889398 D+00
0.409599990D+05	0.399999990D+06	0.510724 D+01	0.898060 D+00
0.614399984D+05	0.599999985D+06	0.513249 D+01	0.902500 D+00
0.819199979D+05	0.799999980D+06	0.514907 D+01	0.905415 D+00
0.102399997D+06	0.999999975D+06	0.516124 D+01	0.907556 D+00

AAD= 0.60000D+01
RWD= 0.20000D+02
RRD= 0.19720D+02

F= 0.30000D+00
E= 0.98600D+00

THE STEADY STATE PRESSURES

THETA=	0.0	PDSS=	0.536285589D+01
THETA=	0.45000D+02	PDSS=	0.139980788D+01
THETA=	0.90000D+02	PDSS=	0.854448560D+00
THETA=	0.13500D+03	PDSS=	0.647301034D+00
THETA=	0.18000D+03	PDSS=	0.591100700D+00

THETA= 0.0

TD	TD:RD**2	PD	PDN
0.783999980D-02	0.999999975D-01	0.124198 D-01	0.231590 D-02
0.156799996D-01	0.199999995D+00	0.736016 D-01	0.137243 D-01
0.313599992D-01	0.399999990D+00	0.216265 D+00	0.403265 D-01
0.470399988D-01	0.599999985D+00	0.337574 D+00	0.629468 D-01
0.627199984D-01	0.799999980D+00	0.437690 D+00	0.816151 D-01
0.783999980D-01	0.999999975D+00	0.521993 D+00	0.973349 D-01
0.156799996D+00	0.199999995D+01	0.811571 D+00	0.151331 D+00
0.313599992D+00	0.399999990D+01	0.112834 D+01	0.210400 D+00
0.470399988D+00	0.599999985D+01	0.132093 D+01	0.246312 D+00
0.627199984D+00	0.799999980D+01	0.145966 D+01	0.272181 D+00
0.783999980D+00	0.999999975D+01	0.156816 D+01	0.292411 D+00
0.156799996D+01	0.199999995D+02	0.190854 D+01	0.355882 D+00
0.313599992D+01	0.399999990D+02	0.225200 D+01	0.419927 D+00
0.470399988D+01	0.599999985D+02	0.245370 D+01	0.457536 D+00
0.627199984D+01	0.799999980D+02	0.259702 D+01	0.484261 D+00
0.783999980D+01	0.999999975D+02	0.270828 D+01	0.505007 D+00
0.156799996D+02	0.199999995D+03	0.305419 D+01	0.569509 D+00
0.313599992D+02	0.399999990D+03	0.340044 D+01	0.634074 D+00
0.470399988D+02	0.599999985D+03	0.360226 D+01	0.671705 D+00
0.627199984D+02	0.799999980D+03	0.374337 D+01	0.698018 D+00
0.783999980D+02	0.999999975D+03	0.385026 D+01	0.717951 D+00
0.156799996D+03	0.199999995D+04	0.415556 D+01	0.774879 D+00
0.313599992D+03	0.399999990D+04	0.440177 D+01	0.820789 D+00
0.470399988D+03	0.599999985D+04	0.451575 D+01	0.842043 D+00
0.627199984D+03	0.799999980D+04	0.456438 D+01	0.854839 D+00
0.783999980D+03	0.999999975D+04	0.463137 D+01	0.863602 D+00
0.156799996D+04	0.199999995D+05	0.474865 D+01	0.885470 D+00
0.313599992D+04	0.399999990D+05	0.483338 D+01	0.901270 D+00
0.470399988D+04	0.599999985D+05	0.487236 D+01	0.908540 D+00
0.627199984D+04	0.799999980D+05	0.489644 D+01	0.913029 D+00
0.783999980D+04	0.999999975D+05	0.491341 D+01	0.916193 D+00
0.156799996D+05	0.199999995D+06	0.495846 D+01	0.924593 D+00
0.313599992D+05	0.399999990D+06	0.499473 D+01	0.931357 D+00
0.470399988D+05	0.599999985D+06	0.501292 D+01	0.934749 D+00
0.627199984D+05	0.799999980D+06	0.502473 D+01	0.936950 D+00
0.783999980D+05	0.999999975D+06	0.503333 D+01	0.938554 D+00

AAD= 0.80000D+01
RWD= 0.20000D+02
RRD= 0.19760D+02

F= 0.40000D+00
E= 0.98800D+00

THE STEADY STATE PRESSURES

THETA=	0.0	PDSS=	0.515039724D+01
THETA=	0.45000D+02	PDSS=	0.106420713D+01
THETA=	0.90000D+02	PDSS=	0.576588181D+00
THETA=	0.13500D+03	PDSS=	0.409926093D+00
THETA=	0.18000D+03	PDSS=	0.367182922D+00

THETA= 0.0

TD	TD:RD**2	PD	PDN
0.575999985D-02	0.999999975D-01	0.124198 D-01	0.241143 D-02
0.115199997D-01	0.199999995D+00	0.736016 D-01	0.142904 D-01
0.230399994D-01	0.399999990D+00	0.216265 D+00	0.419900 D-01
0.345599991D-01	0.599999985D+00	0.337574 D+00	0.655434 D-01
0.460799988D-01	0.799999980D+00	0.437690 D+00	0.849818 D-01
0.575999985D-01	0.999999975D+00	0.521993 D+00	0.101350 D+00
0.115199997D+00	0.199999995D+01	0.811571 D+00	0.157574 D+00
0.230399994D+00	0.399999990D+01	0.112834 D+01	0.219079 D+00
0.345599991D+00	0.599999985D+01	0.132093 D+01	0.256473 D+00
0.460799988D+00	0.799999980D+01	0.145966 D+01	0.283409 D+00
0.575999985D+00	0.999999975D+01	0.156816 D+01	0.304473 D+00
0.115199997D+01	0.199999995D+02	0.190854 D+01	0.370562 D+00
0.230399994D+01	0.399999990D+02	0.225200 D+01	0.437249 D+00
0.345599991D+01	0.599999985D+02	0.245370 D+01	0.476410 D+00
0.460799988D+01	0.799999980D+02	0.259702 D+01	0.504237 D+00
0.575999985D+01	0.999999975D+02	0.270828 D+01	0.525839 D+00
0.115199997D+02	0.199999995D+03	0.305419 D+01	0.593001 D+00
0.230399994D+02	0.399999990D+03	0.340044 D+01	0.660229 D+00
0.345599991D+02	0.599999985D+03	0.360215 D+01	0.699393 D+00
0.460799988D+02	0.799999980D+03	0.374295 D+01	0.726731 D+00
0.575999985D+02	0.999999975D+03	0.384934 D+01	0.747387 D+00
0.115199997D+03	0.199999995D+04	0.415067 D+01	0.805893 D+00
0.230399994D+03	0.399999990D+04	0.438878 D+01	0.852126 D+00
0.345599991D+03	0.599999985D+04	0.449660 D+01	0.873059 D+00
0.460799988D+03	0.799999980D+04	0.456049 D+01	0.885464 D+00
0.575999985D+03	0.999999975D+04	0.460370 D+01	0.893854 D+00
0.115199997D+04	0.199999995D+05	0.470906 D+01	0.914311 D+00
0.230399994D+04	0.399999990D+05	0.478218 D+01	0.928507 D+00
0.345599991D+04	0.599999985D+05	0.481465 D+01	0.934812 D+00
0.460799988D+04	0.799999980D+05	0.483427 D+01	0.938622 D+00
0.575999985D+04	0.999999975D+05	0.484788 D+01	0.941264 D+00
0.115199997D+05	0.199999995D+06	0.488310 D+01	0.948101 D+00
0.230399994D+05	0.399999990D+06	0.491045 D+01	0.953412 D+00
0.345599991D+05	0.599999985D+06	0.492383 D+01	0.95601'1 D+00
0.460799988D+05	0.799999980D+06	0.493240 D+01	0.957675 D+00
0.575999985D+05	0.999999975D+06	0.493860 D+01	0.958877 D+00

AAD= 0.10000D+02
RWD= 0.20000D+02
RRD= 0.19800D+02

F= 0.50000D+00
E= 0.99000D+00

THE STEADY STATE PRESSURES

THETA= 0.0	PDSS= 0.499721227D+01
THETA= 0.45000D+02	PDSS= 0.781821844D+00
THETA= 0.90000D+02	PDSS= 0.372432260D+00
THETA= 0.13500D+03	PDSS= 0.249776611D+00
THETA= 0.18000D+03	PDSS= 0.220 123921D+00

THETA= 0.0

TD	TD:RD**2	PD	PDN
0.399999990D-02	0.999999975D-01	0.124198 D-01	0.248536 D-02
0.799999980D-02	0.199999995D+00	0.736016 D-01	0.147285 D-01
0.159999996D-01	0.399999990D+00	0.216265 D+00	0.432772 D-01
0.239999994D-01	0.599999985D+00	0.337574 D+00	0.675526 D-01
0.319999992D-01	0.799999980D+00	0.437690 D+00	0.875868 D-01
0.399999990D-01	0.999999975D+00	0.521993 D+00	0.104456 D+00
0.799999980D-01	0.199999995D+01	0.811571 D+00	0.162404 D+00
0.159999996D+00	0.399999990D+01	0.112834 D+01	0.225795 D+00
0.239999994D+00	0.599999985D+01	0.132093 D+01	0.264335 D+00
0.319999992D+00	0.799999980D+01	0.145966 D+01	0.292096 D+00
0.399999990D+00	0.999999975D+01	0.156816 D+01	0.313807 D+00
0.799999980D+00	0.199999995D+02	0. 190854 D+0 1	0.381922 D+00
0.159999996D+01	0.399999990D+02	0.225200 D+01	0.450653 D+00
0.239999994D+01	0.599999985D+02	0.245370 D+01	0.491014 D+00
0.319999992D+01	0.799999980D+02	0.259702 D+01	0.519694 D+00
0.399999990D+01	0.999999975D+02	0.270828 D+01	0.541959 D+00
0.799999980D+01	0.199999995D+03	0.305418 D+01	0.611178 D+00
0.159999996D+02	0.399999990D+03	0.340044 D+01	0.680468 D+00
0.239999994D+02	0.599999985D+03	0.360206 D+01	0.720813 D+00
0.319999992D+02	0.799999980D+03	0.374258 D+O1	0.748934 D+00
0.399999990D+02	0.999999975D+03	0.384851 D+01	0.770132 D+00
0.799999980D+02	0.199999995D+04	0.414629 D+01	0.829721 D+00
0.159999996D+03	0.399999990D+04	0.437719 D+01	0.875926 D+00
0.239999994D+03	0.599999985D+04	0.447955 D+01	0.896410 D+00
0.319999992D+03	0.799999980D+04	0.453930 D+01	0.908367 D+00
0.399999990D+03	0.999999975D+04	0.457924 D+01	0.916359 D+00
0.799999980D+03	0.199999995D+05	0.467457 D+O1	0.935436 D+00
0.159999996D+04	0.399999990D+05	0.473836 D+01	0.348201 D+00
0.239999994D+04	0.599999985D+05	0.476579 D+01	0.953690 D+00
0.319999992D+04	0.799999980D+05	0.47820 1 D+O1	0.956936 D+00
0.399999990D+04	0.999999975D+05	0.479308 D+01	0.959152 D+00
0.799999980D+04	0.199999995D+06	0.482095 D+01	0.964729 D+00
0.159999996D+05	0.399999990D+06	0.484174 D+O1	0.968889 D+00
0.239999994D+05	0.599999985D+06	0.485162 D+01	0.970867 D+00
0.319999992D+05	0.799999980D+06	0.485786 D+0 1	0.972114 D+00
0.399999990D+05	0.999999975D+06	0.486231 D+01	0.973005 D+00

AAD= 0.12000D+02
RWD= 0.20000D+02
RRD= 0.19840D+02

F= 0.60000D+00
E= 0.99200D+00

THE STEADY STATE PRESSURES

THETA=	0.0	PDSS=	0.488027348D+01
THETA=	0.45000D+02	PDSS=	0.533906032D+00
THETA=	0.90000D+02	PDSS=	0.222079701D+00
THETA=	0.13500D+03	PDSS=	0.141672794D+00
THETA=	0.18000D+03	PDSS=	0.123271442D+00

THETA= 0.0

TD	TD:RD**2	PD	PDN
0.255999994D-02	0.999999975D-01	0.124198 D-01	0.254491 D-02
0.511999987D-02	0.199999995D+00	0.736016 D-01	0.150814 D-01
0.102399997D-01	0.399999990D+00	0.216265 D+00	0.443142 D-01
0.153599996D-01	0.599999985D+00	0.337574 D+00	0.691713 D-01
0.204799995D-01	0.799999980D+00	0.437690 D+00	0.896855 D-01
0.255999994D-01	0.999999975D+00	0.521993 D+00	0.106959 D+00
0.511999987D-01	0.199999995D+01	0.811571 D+00	0.166296 D+00
0.102399997D+00	0.399999990D+01	0.112834 D+01	0.231205 D+00
0.153599996D+00	0.599999985D+01	0.132093 D+01	0.270669 D+00
0.204799995D+00	0.799999980D+01	0.145966 D+01	0.299095 D+00
0.255999994D+00	0.999999975D+01	0.156816 D+01	0.321326 D+00
0.511999987D+00	0.199999995D+02	0.190854 D+01	0.391073 D+00
0.102399997D+01	0.399999990D+02	0.225200 D+01	0.461451 D+00
0.153599996D+01	0.599999985D+02	0.245370 D+01	0.502779 D+00
0.204799995D+01	0.799999980D+02	0.259702 D+01	0.532147 D+00
0.255999994D+01	0.999999975D+02	0.270828 D+01	0.554945 D+00
0.511999987D+01	0.199999995D+03	0.305418 D+01	0.625822 D+00
0.102399997D+02	0.399999990D+03	0.340044 D+01	0.696772 D+00
0.153599996D+02	0.599999985D+03	0.360197 D+01	0.738068 D+00
0.204799995D+02	0.799999980D+03	0.374224 D+01	0.766809 D+00
0.255999994D+02	0.999999975D+03	0.384775 D+01	0.788431 D+00
0.511999987D+02	0.199999995D+04	0.414227 D+01	0.848779 D+00
0.102399997D+03	0.399999990D+04	0.436656 D+01	0.894737 D+00
0.153599996D+03	0.599999985D+04	0.446394 D+01	0,914692 D+00
0.204799995D+03	0.799999980D+04	0.451993 D+01	0.926163 D+00
0.255999994D+03	0.999999975D+04	0.455690 D+01	0.933739 D+00
0.511999987D+03	0.199999995D+05	0.464328 D+01	0.951439 D+00
0.102399997D+04	0.399999990D+05	0.469903 D+01	0.962862 D+00
0.153599996D+04	0.599999985D+05	0.472226 D+01	0.967623 D+00
0.204799995D+04	0.799999980D+05	0.473572 D+01	0.970380 D+00
0.255999994D+04	0.999999975D+05	0.474476 D+01	0.972232 D+00
0.511999987D+04	0.199999995D+06	0.476687 D+01	0.976764 D+00
0.102399997D+05	0.399999990D+06	0.478264 D+01	0.979995 D+00
0.153599996D+05	0.599999985D+06	0.478988 D+01	0.981478 D+00
0.204799995D+05	0.799999980D+06	0.479435 D+01	0.982395 D+00
0.255999994D+05	0.999999975D+06	0.479750 D+01	0.983041 D+00

AAD= 0.14000D+02
RWD= 0.20000D+02
RRD= 0.19880D+02

F= 0.70000D+00
E= 0.99400D+00

THE STEADY STATE PRESSURES

THETA=	0.0	PDSS=	0.478749174D+01
THETA=	0.45000D+02	PDSS=	0.318338399D+00
THETA=	0.90000D+02	PDSS=	0.115850105D+00
THETA=	0.13500D+03	PDSS=	0.710709086D-01
THETA=	0.18000D+03	PDSS=	0.612734171D-01

THETA= 0.0

TD	TD:RD**2	PD	PDN
0.143999996D-02	0.999999975D-01	0.124198 D-01	0.259423 D-02
0.287999993D-02	0.199999995D+00	0.736016 D-01	0.153737 D-01
0.575999985D-02	0.399999990D+00	0.216265 D+00	0.451730 D-01
0.863999978D-02	0.599999985D+00	0.337574 D+00	0.705118 D-01
0.115199997D-01	0.799999980D+00	0.437690 D+00	0.914236 D-01
0.143999996D-01	0.999999975D+00	0.521993 D+00	0.109032 D+00
0.287999993D-01	0.199999995D+01	0.811571 D+00	0.169519 D+00
0.575999985D-01	0.399999990D+01	0.112834 D+01	0.235686 D+00
0.863999978D-01	0.599999985D+01	0.132093 D+01	0.275914 D+00
0.115199997D+00	0.799999980D+01	0.145966 D+01	0.304892 D+00
0.143999996D+00	0.999999975D+01	0.156816 D+01	0.327553 D+00
0.287999993D+00	0.199999995D+02	0.190854 D+01	0.398652 D+00
0.575999985D+00	0.399999990D+02	0.225200 D+01	0.470394 D+00
0.863999978D+00	0.599999985D+02	0.245370 D+01	0.512523 D+00
0.115199997D+01	0.799999980D+02	0.259702 D+01	0.542460 D+00
0.143999996D+01	0.999999975D+02	0.270828 D+01	0.565700 D+00
0.287999993D+01	0.199999995D+03	0.305418 D+01	0.637950 D+00
0.575999985D+01	0.399999990D+03	0.340043 D+01	0.710275 D+00
0.863999978D+01	0.599999985D+03	0.360189 D+01	0.752355 D+00
0.115199997D+02	0.799999980D+03	0.374192 D+01	0.781604 D+00
0.143999996D+02	0.999999975D+03	0.384705 D+01	0.803563 D+00
0.287999993D+02	0.199999995D+04	0.413853 D+01	0.864447 D+00
0.575999985D+02	0.399999990D+04	0.435665 D+01	0.910007 D+00
0.863999978D+02	0.599999985D+04	0.444940 D+01	0.929381 D+00
0.115199997D+03	0.799999980D+04	0.450189 D+01	0.940344 D+00
0.143999996D+03	0.999999975D+04	0.453612 D+01	0.947494 D+00
0.287999993D+03	0.199999995D+05	0.461425 D+01	0.963814 D+00
0.575999985D+03	0.399999990D+05	0.466273 D+01	0.973940 D+00
0.863999978D+03	0.599999985D+05	0.468226 D+01	0.978020 D+00
0.115199997D+04	0.799999980D+05	0.469333 D+01	0.980332 D+00
0.143999996D+04	0.999999975D+05	0.470065 D+01	0.981860 D+00
0.287999993D+04	0.199999995D+06	0.471803 D+01	0.985492 D+00
0.575999985D+04	0.399999990D+06	0.472983 D+01	0.987956 D+00
0.863999978D+04	0.599999985D+06	0.473502 D+01	0.989041 D+00
0.115199997D+05	0.799999980D+06	0.473815 D+01	0.989694 D+00
0.143999996D+05	0.999999975D+06	0.474032 D+01	0.990147 D+00

AAD= 0.16000D+02
RWD= 0.20000D+02
RRD= 0.19920D+02

F= 0.80000D+00
E= 0.99600D+00

THE STEADY STATE PRESSURES

THETA=	0.0	PDSS=	0.471177992D+01
THETA=	0.45000D+02	PDSS=	0.146099921D+00
THETA=	0.90000D+02	PDSS=	0.473828766D-01
THETA=	0.13500D+03	PDSS=	0.282979656D-01
THETA=	0.18000D+03	PDSS=	0.242526116D-01

THETA= 0.0

TD	TD:RD**2	PD	PDN
0.639999984D-03	0.999999975D-01	0.124198 D-01	0.263591 D-02
0.127999997D-02	0.199999995D+00	0.736016 D-01	0.156207 D-01
0.255999994D-02	0.399999990D+00	0.216265 D+00	0.458989 D-01
0.383999990D-02	0.599999985D+00	0.337574 D+00	0.716448 D-01
0.511999987D-02	0.799999980D+00	0.437690 D+00	0.928927 D-01
0.639999984D-02	0.999999975D+00	0.521993 D+00	0.110784 D+00
0.127999997D-01	0.199999995D+01	0.811571 D+00	0.172243 D+00
0.255999994D-01	0.399999990D+01	0.112834 D+01	0.239473 D+00
0.383999990D-01	0.599999985D+01	0.132093 D+01	0.280348 D+00
0.511999987D-01	0.799999980D+01	0.145966 D+01	0.309791 D+00
0.639999984D-01	0.999999975D+01	0.156816 D+01	0.332817 D+00
0.127999997D+00	0.199999995D+02	0.190854 D+01	0.405058 D+00
0.255999994D+00	0.399999990D+02	0.225200 D+01	0.477952 D+00
0.383999990D+00	0.599999985D+02	0.245370 D+01	0.520759 D+00
0.511999987D+00	0.799999980D+02	0.259702 D+01	0.551177 D+00
0.639999984D+00	0.999999975D+02	0.270828 D+01	0.574790 D+00
0.127999997D+01	0.199999995D+03	0.305417 D+01	0.648200 D+00
0.255999994D+01	0.399999990D+03	0.340043 D+01	0.721688 D+00
0.383999990D+01	0.599999985D+03	0.360181 D+01	0.764428 D+00
0.511999987D+01	0.799999980D+03	0.374162 D+01	0.794100 D+00
0.639999984D+01	0.999999975D+03	0.384639 D+01	0.816335 D+00
0.127999997D+02	0.199999995D+04	0.413500 D+01	0.877589 D+00
0.255999994D+02	0.399999990D+04	0.434730 D+01	0.922645 D+00
0.383999990D+02	0.599999985D+04	0.443567 D+01	0.941402 D+00
0.511999987D+02	0.799999980D+04	0.448486 D+01	0.951840 D+00
0.639999984D+02	0.999999975D+04	0.451650 D+01	0.958556 D+00
0.127999997D+03	0.199999995D+05	0.458691 D+01	0.973499 D+00
0.255999994D+03	0.399999990D+05	0.462864 D+01	0.982356 D+00
0.383999990D+03	0.599999985D+05	0.464478 D+01	0.985782 D+00
0.511999987D+03	0.799999980D+05	0.465370 D+01	0.987674 D+00
0.639999984D+03	0.999999975D+05	0.465948 D+01	0.988900 D+00
0.127999997D+04	0.199999995D+06	0.467275 D+01	0.991718 D+00
0.255999994D+04	0.399999990D+06	0.468127 D+01	0.993526 D+00
0.383999990D+04	0.599999985D+06	0.468484 D+01	0.994284 D+00
0.511999987D+04	0.799999980D+06	0.468693 D+01	0.994727 D+00
0.639999984D+04	0.999999975D+06	0.468834 D+01	0.995026 D+00

AAD= 0.18000D 02
RWD= 0.20000D 02
RRD= 0.19960D 02

F= 0.90000D 00
E= 0.99800D 00

THE STEADY STATE PRESSURES

THETA=	0.00000D 00	PDSS=	0.4648655300 01
THETA=	0.45000D 02	PDSS=	0.359885758D-01
THETA=	0.90000D 02	PDSS=	0.108117383D-01
THETA=	0.13500D 03	PDSS=	0.636170248D-02
THETA=	0.18000D 03	PDSS=	0.543509740D-02

THETA= 0.00000D OD

TD	TD:RD**2	PD	PDN
0.159999996D-03	0.999999975D-01	0.120198 D-01	0.267 171 D-02
0.319999992D-03	0.199999995D 00	0.736016 D-01	0. 158328 D-01
0.639999984D-03	0.399999990D 00	0.216265 D 00	0.465221 D-01
0.959999976D-03	0.599999985D 00	0.337574 D 00	0.726177 D-01
0.127999997D-02	0.799999980D 00	0.437690 D 00	0.941541 D-01
0.159999996D-02	0.999999975D 00	0.521993 D 00	0.112289 D 00
0.319999992D-02	0.199999995D 01	0.811571 D 00	0.174582 D 00
0.639999984D-02	0.399999990D 01	0.112834 D 01	0.242725 D 00
0.959999976D-02	0.599999985D 01	0.132093 D 01	0.284155 D 00
0.127999997D-01	0.799999980D 01	0.145966 D 01	0.313998 D 00
0.159999996D-01	0.999999975D 01	0.156816 D 01	0.337336 D 00
0.319999992D-01	0.199999995D 02	0.190854 D 01	0.410558 D 00
0.639999984D-01	0.399999990D 02	0.225200 D 01	0.484443 D 00
0.959999976D-01	0.599999985D 02	0.245370 D 01	0.527830 D 00
0.127999997D 00	0.799999980D 02	0.259702 D 01	0.558661 D 00
0.159999996D 00	0.999999975D 02	0.270828 D 01	0.582595 D 00
0.319999992D 00	0.199999995D 03	0.305417 D 01	0.657001 D 00
0.639999984D 00	0.399999990D 03	0.340043 D 01	0.731487 D 00
0.959999976D 00	0.599999985D 03	0.360174 D 01	0.774793 D 00
0.127999997D 01	0.799999980D 03	0.374134 D 01	0.804823 D 00
0.159999996D 01	0.999999975D 03	0.384576 D 01	0.827286 D 00
0.319999992D 01	0.199999995D 04	0.413165 D 01	0.888785 D 00
0.639999984D 01	0.399999990D 04	0.433839 D 01	0.933257 D 00
0.9599999763) 01	0.599999985D 04	0.442259 D 01	0.951370 D 00
0.127999997D 02	0.799999980D 04	0.446862 D 01	0.961273 D 00
0.159999996D 02	0.999999975D 04	0.449780 D 01	0.967549 D 00
0.319999992D 02	0.199999995D 05	0.456085 D 01	0.981112 D 00
0.639999984D 02	0.399999990D 05	0.459621 D 01	0.988719 D 00
0.959999976D 02	0.599999985D 05	0.460918 D 01	0.991509 D 00
0.127999997D 03	0.799999980D 05	0.461609 D 01	0.992996 D 00
0.159999996D 03	0.999999975D 05	0.462046 D 01	0.993934 D 00
0.319999992D 03	0.199999995D 06	0.463004 D 01	0.995996 D 00
0.639999984D 03	0.399999990D 06	0.463567 D 01	0.997208 D 00
0.959999976D 03	0.599999985D 06	0.463790 D 01	0.997688 D 00
0.1279999971) 04	0.799999980D 06	0.063901 D 01	0.997926 D 00
0.159999996D 04	0.999999975D 06	0.463993 D 01	0.998125 D 00

TABLE **H.2** :

NO–FLOW INTERNAL **BOUNDARY**

AAD= 0.60000D+01
RWD= 0.20000D+02
RRD= 0.19720D+02

F= 0.30000D+00
E= 0.98600D+00

THETA= 0.0

TD	TD:RD**2	PD
0.783999980D-02	0.999999975D-01	0.124198 D-01
0.156799996D-01	0.199999995D+00	0.736016 D-01
0.313599992D-01	0.399999990D+00	0.216265 D+00
0.470399988D-01	0.599999985D+00	0.337574 D+00
0.627199984D-01	0.799999980D+00	0.437690 D+00
0.783999980D-01	0.999999975D+00	0.521993 D+00
0.156799996D+00	0.199999995D+01	0.811571 D+00
0.313599992D+00	0.399999990D+01	0.112834 D+01
0.470399988D+00	0.599999985D+01	0.132093 D+01
0.627199984D+00	0.799999980D+01	0.145966 D+01
0.783999980D+00	0.999999975D+01	0.156816 D+01
0.156799996D+01	0.199999995D+02	0.190854 D+01
0.313599992D+01	0.399999990D+02	0.225200 D+01
0.470399988D+01	0.599999985D+02	0.245370 D+01
0.627199984D+01	0.799999980D+02	0.259702 D+01
0.783999980D+01	0.999999975D+02	0.270828 D+01
0.156799996D+02	0.199999995D+03	0.305925 D+01
0.313599992D+02	0.399999990D+03	0.340050 D+01
0.470399988D+02	0.599999985D+03	0.360374 D+01
0.627199984D+02	0.799999980D+03	0.374930 D+01
0.783999980D+02	0.999999975D+03	0.386359 D+01
0.156799996D+03	0.199999995D+04	0.422890 D+01
0.313599992D+03	0.399999990D+04	0.460452 D+01
0.470399988D+03	0.599999985D+04	0.482299 D+01
0.627199984D+03	0.799999980D+04	0.497583 D+01
0.783999980D+03	0.999999975D+04	0.509296 D+01
0.156799996D+04	0.199999995D+05	0.544978 D+01
0.313599992D+04	0.399999990D+05	0.579974 D+01
0.470399988D+04	0.599999985D+05	0.600296 D+01
0.627199984D+04	0.799999980D+05	0.614684 D+01
0.783999980D+04	0.999999975D+05	0.625835 D+01
0.156799996D+05	0.199999995D+06	0.660450 D+01
0.313599992D+05	0.399999990D+06	0.695063 D+01
0.470399988D+05	0.599999985D+06	0.715316 D+01
0.627199984D+05	0.799999980D+06	0.729688 D+01
0.783999980D+05	0.999999975D+06	0.740837 D+01
0.156799996D+06	0.199999995D+07	0.775476 D+01
0.313599992D+06	0.399999990D+07	0.810122 D+01
0.470399988D+06	0.599999985D+07	0.830391 D+01
0.627199984D+06	0.799999980D+07	0.844772 D+01
0.783999980D+06	0.999999975D+07	0.855928 D+01
0.156799996D+07	0.199999995D+08	0.890582 D+01
0.313599992D+07	0.399999990D+08	0.925238 D+01
0.470399988D+07	0.599999985D+08	0.945510 D+01
0.627199984D+07	0.799999980D+08	0.959894 D+01
0.783999980D+07	0.999999975D+08	0.971051 D+01

AAD= 0.10000D+02
RWD= 0.20000D+02
RRD= 0.19800D+02

F= 0.50000D+00
E= 0.99000D+00

THETA= 0.0

TD	TD:RD**2	PD
0.399999990D-02	0.999999975D-01	0.124198 D-01
0.799999980D-02	0.199999995D+00	0.736016 D-01
0.159999996D-01	0.399999990D+00	0.216265 D+00
0.239999994D-01	0.599999985D+00	0.337574 D+00
0.319999992D-01	0.799999980D+00	0.437690 D+00
0.399999990D-01	0.999999975D+00	0.521993 D+00
0.799999980D-01	0.199999995D+01	0.811571 D+00
0.159999996D+00	0.399999990D+01	0.112834 D+01
0.239999994D+00	0.599999985D+01	0.132093 D+01
0.319999992D+00	0.799999980D+01	0.145966 D+01
0.399999990D+00	0.999999975D+01	0.156816 D+01
0.799999980D+00	0.199999995D+02	0.190854 D+01
0.159999996D+01	0.399999990D+02	0.225200 D+01
0.239999994D+01	0.599999985D+02	0.245370 D+01
0.319999992D+01	0.799999980D+02	0.259702 D+01
0.399999990D+01	0.999999975D+02	0.270828 D+01
0.799999980D+01	0.199999995D+03	0.305426 D+01
0.159999996D+02	0.399999990D+03	0.340051 D+01
0.239999994D+02	0.599999985D+03	0.360403 D+01
0.319999992D+02	0.799999980D+03	0.375051 D+01
0.399999990D+02	0.999999975D+03	0.386643 D+01
0.799999980D+02	0.199999995D+04	0.424645 D+01
0.159999996D+03	0.399999990D+04	0.465715 D+01
0.239999994D+03	0.599999985D+04	0.490410 D+01
0.319999992D+03	0.799999980D+04	0.507848 D+01
0.399999990D+03	0.999999975D+04	0.521197 D+01
0.799999980D+03	0.199999995D+05	0.561113 D+01
0.159999996D+04	0.399999990D+05	0.598534 D+01
0.239999994D+04	0.599999985D+05	0.619556 D+01
0.319999992D+04	0.799999980D+05	0.634226 D+01
0.399999990D+04	0.999999975D+05	0.645510 D+01
0.799999980D+04	0.199999995D+06	0.680263 D+01
0.159999996D+05	0.399999990D+06	0.714837 D+01
0.239999994D+05	0.599999985D+06	0.735048 D+01
0.319999992D+05	0.799999980D+06	0.749390 D+01
0.399999990D+05	0.999999975D+06	0.760518 D+01
0.799999980D+05	0.199999995D+07	0.795102 D+01
0.159999996D+06	0.399999990D+07	0.829711 D+01
0.239999994D+06	0.599999985D+07	0.849965 D+01
0.319999992D+06	0.799999980D+07	0.864338 D+01
0.399999990D+06	0.999999975D+07	0.875489 D+01
0.799999980D+06	0.199999995D+08	0.910131 D+01
0.159999996D+07	0.399999990D+08	0.944780 D+01
0.239999994D+07	0.599999985D+08	0.965050 D+01
0.319999992D+07	0.799999980D+08	0.979433 D+01
0.399999990D+07	0.999999975D+08	0.990589 D+01

AAD= 0.12000D+02
RWD= 0.20000D+02
RRD= 0.19840D+02

F= 0.60000D+00
E= 0.99200D+00

THETA= 0.0

TD	TD:RD**2	PD
0.255999994D-02	0.999999975D-01	0.124198 D-01
0.511999987D-02	0.199999995D+00	0.736016 D-01
0.102399997D-01	0.399999990D+00	0.216265 D+00
0.153599996D-01	0.599999985D+00	0.337574 D+00
0.204799995D-01	0.799999980D+00	0.437690 D+00
0.255999994D-01	0.999999975D+00	0.521993 D+00
0.511999987D-01	0.199999995D+01	0.811571 D+00
0.102399997D+00	0.399999990D+01	0.112834 D+01
0.153599996D+00	0.599999985D+01	0.132093 D+01
0.204799995D+00	0.799999980D+01	0.145966 D+01
0.255999994D+00	0.999999975D+01	0.156816 D+01
0.511999987D+00	0.199999995D+02	0.190854 D+01
0.102399997D+01	0.399999990D+02	0.225200 D+01
0.153599996D+01	0.599999985D+02	0.245370 D+01
0.204799995D+01	0.799999980D+02	0.259702 D+01
0.255999994D+01	0.999999975D+02	0.270828 D+01
0.511999987D+01	0.199999995D+03	0.305427 D+01
0.102399997D+02	0.399999990D+03	0.340052 D+01
0.153599996D+02	0.599999985D+03	0.360415 D+01
0.204799995D+02	0.799999980D+03	0.375102 D+01
0.255999994D+02	0.999999975D+03	0.386764 D+01
0.511999987D+02	0.199999995D+04	0.425426 D+01
0.102399997D+03	0.399999990D+04	0.468186 D+01
0.153599996D+03	0.599999985D+04	0.494412 D+01
0.204799995D+03	0.799999980D+04	0.513151 D+01
0.255999994D+03	0.999999975D+04	0.527607 D+01
0.511999987D+03	0.199999995D+05	0.571175 D+01
0.102399997D+04	0.399999990D+05	0.611723 D+01
0.153599996D+04	0.599999985D+05	0.634013 D+01
0.204799995D+04	0.799999980D+05	0.649314 D+01
0.255999994D+04	0.999999975D+05	0.660955 D+01
0.511999987D+04	0.199999995D+06	0.696286 D+01
0.102399997D+05	0.399999990D+06	0.730999 D+01
0.153599996D+05	0.599999985D+06	0.751210 D+01
0.204799995D+05	0.799999980D+06	0.765538 D+01
0.255999994D+05	0.999999975D+06	0.776651 D+01
0.511999987D+05	0.199999995D+07	0.811187 D+01
0.102399997D+06	0.399999990D+07	0.845757 D+01
0.153599996D+06	0.599999985D+07	0.865999 D+01
0.204799995D+06	0.799999980D+07	0.880357 D+01
0.255999994D+06	0.999999975D+07	0.891501 D+01
0.511999987D+06	0.199999995D+08	0.926129 D+01
0.102399997D+07	0.399999990D+08	0.960769 D+01
0.153599996D+07	0.599999985D+08	0.981036 D+01
0.204799995D+07	0.799999980D+08	0.995417 D+01
0.255999994D+07	0.999999975D+08	0.100657 D+02

AAD= 0.14000D+02
RWD= 0.20000D+02
RRD= 0.19880D+02

F= 0.70000D+00
E= 0.99400D+00

THETA= 0.0

TD	TD:RD**2	PD
0.143999996D-02	0.999999975D-01	0.124198 D-01
0.287999993D-02	0.199999995D+00	0.736016 D-01
0.575999985D-02	0.399999990D+00	0.216265 D+00
0.863999978D-02	0.599999985D+00	0.337574 D+00
0.115199997D-01	0.799999980D+00	0.437690 D+00
0.143999996D-01	0.999999975D+00	0.521993 D+00
0.287999993D-01	0.199999995D+01	0.811571 D+00
0.575999985D-01	0.399999990D+01	0.112834 D+01
0.863999978D-01	0.599999985D+01	0.132093 D+01
0.115199997D+00	0.799999980D+01	0.195966 D+01
0.143999996D+00	0.999999975D+01	0.156816 D+01
0.287999993D+00	0.199999995D+02	0.190854 D+01
0.575999985D+00	0.399999990D+02	0.225200 D+01
0.863999978D+00	0.599999985D+02	0.245370 D+01
0.115199997D+01	0.799999980D+02	0.259702 D+01
0.143999996D+01	0.999999975D+02	0.270828 D+01
0.287999993D+01	0.199999995D+03	0.305427 D+01
0.575999985D+01	0.399999990D+03	0.340053 D+01
0.863999978D+01	0.599999985D+03	0.360426 D+01
0.115199997D+02	0.799999980D+03	0.375149 D+01
0.143999996D+02	0.999999975D+03	0.386877 D+01
0.287999993D+02	0.199999995D+04	0.426159 D+01
0.575999985D+02	0.399999990D+04	0.470568 D+01
0.863999978D+02	0.599999985D+04	0.498340 D+01
0.115199997D+03	0.799999980D+04	0.518429 D+01
0.143999996D+03	0.999999975D+04	0.534064 D+01
0.287999993D+03	0.199999995D+05	0.581879 D+01
0.575999985D+03	0.399999990D+05	0.627029 D+01
0.863999978D+03	0.599999985D+05	0.651754 D+01
0.115199997D+04	0.799999980D+05	0.668518 D+01
0.143999996D+04	0.999999975D+05	0.681109 D+01
0.287999993D+04	0.199999995D+06	0.718368 D+01
0.575999985D+04	0.399999990D+06	0.753849 D+01
0.863999978D+04	0.599999985D+06	0.774215 D+01
0.115199997D+05	0.799999980D+06	0.788585 D+01
0.143999996D+05	0.999999975D+06	0.799708 D+01
0.287999993D+05	0.199999995D+07	0.834211 D+01
0.575999985D+05	0.399999990D+07	0.868723 D+01
0.863999978D+05	0.599999985D+07	0.888930 D+01
0.115199997D+06	0.799999980D+07	0.903275 D+01
0.143999996D+06	0.999999975D+07	0.914407 D+01
0.287999993D+06	0.199999995D+08	0.949006 D+01
0.575999985D+06	0.399999990D+08	0.983627 D+01
0.863999978D+06	0.599999985D+08	0.100388 D+02
0.115199997D+07	0.799999980D+08	0.101826 D+02
0.143999996D+07	0.999999975D+08	0.102941 D+02

AAD= 0.16000D+02
RWD= 0.20000D+02
RRD= 0.19920D+02

F= 0.80000D+00
E= 0.99600D+00

THETA= 0.0

TD	TD:RD**2	PD
0.639999984D-03	0.999999975D-01	0.124198 D-01
0.127999997D-02	0.199999995D+00	0.736016 D-01
0.255999994D-02	0.399999990D+00	0.216265 D+00
0.383999990D-02	0.599999985D+00	0.337574 D+00
0.511999987D-02	0.799999980D+00	0.437690 D+00
0.639999984D-02	0.999999975D+00	0.521993 D+00
0.127999997D-01	0.199999995D+01	0.811571 D+00
0.255999994D-01	0.399999990D+01	0.112834 D+01
0.383999990D-01	0.599999985D+01	0.132093 D+01
0.511999987D-01	0.799999980D+01	0.145966 D+01
0.639999984D-01	0.999999975D+01	0.156816 D+01
0.127999997D+00	0.199999995D+02	0,190854 D+01
0.255999994D+00	0.399999990D+02	0.225200 D+01
0.383999990D+00	0.599999985D+02	0.245370 D+01
0.511999987D+00	0.799999980D+02	0.259702 D+01
0.639999984D+00	0.999999975D+02	0.270828 D+01
0.127999997D+01	0.199999995D+03	0.305428 D+01
0.255999994D+01	0.399999990D+03	0.340053 D+01
0.383999990D+01	0.599999985D+03	0.360437 D+01
0.511999987D+01	0.799999980D+03	0.375193 D+01
0.639999984D+01	0.999999975D+03	0.386981 D+01
0.127999997D+02	0.199999995D+04	0.426853 D+01
0.255999994D+02	0.399999990D+04	0.472877 D+01
0.383999990D+02	0.599999985D+04	0.502212 D+01
0.511999987D+02	0.799999980D+04	0.523704 D+01
0.639999984D+02	0.999999975D+04	0.540590 D+01
0.127999997D+03	0.199999995D+05	0.593126 D+01
0.255999994D+03	0.399999990D+05	0.644002 D+01
0.383999990D+03	0.599999985D+05	0.672340 D+01
0.511999987D+03	0.799999980D+05	0.691664 D+01
0.639999984D+03	0.999999975D+05	0.706172 D+01
0.127999997D+04	0.199999995D+06	0.748507 D+01
0.255999994D+04	0.399999990D+06	0.787149 D+01
0.383999990D+04	0.599999985D+06	0.808517 D+01
0.511999987D+04	0.799999980D+06	0.823320 D+01
0.639999984D+04	0.999999975D+06	0.834661 D+01
0.127999997D+05	0.199999995D+07	0.669441 D+01
0.255999994D+05	0.399999990D+07	0.903954 D+01
0.383999990D+05	0.599999985D+07	0.924122 D+01
0.511999987D+05	0.799999980D+07	0.938437 D+01
0.639999984D+05	0.999999975D+07	0.949545 D+01
0.127999997D+06	0.199999995D+08	0.984082 D+01
0.255999994D+06	0.399999990D+08	0.101866 D+02
0.383999990D+06	0.599999985D+08	0.103890 D+02
0.511999987D+06	0.799999980D+08	0.105326 D+02
0.639999984D+06	0.999999975D+08	0.106441 D+02

AAD= 0.18000D+02
RWD= 0.20000D+02
RRD= 0.19960D+02

F= 0.90000D+00
E= 0.99800D+00

THETA= 0.0

TD	TD:RD**2	PD
0.159999996D-03	0.999999975D-01	0.124198 D-01
0.319999992D-03	0.199999995D+00	0.736016 D-01
0.639999984D-03	0.399999990D+00	0.216265 D+00
0.959999976D-03	0.599999985D+00	0.337574 D+00
0.127999997D-02	0.799999980D+00	0.437690 D+00
0.159999996D-02	0.999999975D+00	0.521993 D+00
0.319999992D-02	0.199999995D+01	0.811571 D+00
0.639999984D-02	0.399999990D+01	0.112834 D+01
0.959999976D-02	0.599999985D+01	0.132093 D+01
0.127999997D-01	0.799999980D+01	0.145966 D+01
0.159999996D-01	0.999999975D+01	0.156816 D+01
0.319999992D-01	0.199999995D+02	0.190854 D+01
0.639999984D-01	0.399999990D+02	0.225200 D+01
0.959999976D-01	0.599999985D+02	0.245370 D+01
0.127999997D+00	0.799999980D+02	0.259702 D+01
0.159999996D+00	0.999999975D+02	0.270828 D+01
0.319999992D+00	0.199999995D+03	0.305428 D+01
0.639999984D+00	0.399999990D+03	0.340054 D+01
0.959999976D+00	0.599999985D+03	0.360446 D+01
0.127999997D+01	0.799999980D+03	0.375234 D+01
0.159999996D+01	0.999999975D+03	0.387079 D+01
0.319999992D+01	0.199999995D+04	0.427514 D+01
0.639999984D+01	0.399999990D+04	0.475123 D+01
0.959999976D+01	0.599999985D+04	0.506043 D+01
0.127999997D+02	0.799999980D+04	0.528992 D+01
0.159999996D+02	0.999999975D+04	0.547209 D+01
0.319999992D+02	0.199999995D+05	0.605013 D+01
0.639999984D+02	0.399999990D+05	0.662829 D+01
0.959999976D+02	0.599999985D+05	0.695926 D+01
0.127999997D+03	0.799999980D+05	0.718896 D+01
0.159999996D+03	0.999999975D+05	0.736362 D+01
0.319999992D+03	0.199999995D+06	0.788325 D+01
0.639999984D+03	0.399999990D+06	0.836334 D+01
0.959999976D+03	0.599999985D+06	0.862420 D+01
0.127999997D+04	0.799999980D+06	0.880046 D+01
0.159999996D+04	0.999999975D+06	0.893209 D+01
0.319999992D+04	0.199999995D+07	0.931802 D+01
0.639999984D+04	0.399999990D+07	0.967942 D+01
0.959999976D+04	0.599999985D+07	0.988431 D+01
0.127999997D+05	0.799999980D+07	0.100282 D+02
0.159999996D+05	0.999999975D+07	0.101400 D+02
0.319999992D+05	0.199999995D+08	0.104846 D+02
0.639999984D+05	0.399999990D+08	0.108298 D+02
0.959999976D+05	0.599999985D+08	0.110316 D+02
0.127999997D+06	0.799999980D+08	0.111749 D+02
0.159999996D+06	0.999999975D+08	0.112859 D+02

AAD= 0.19000D+02
RWD= 0.20000D+02
RRD= 0.19980D+02

F= 0.95000D+00
E= 0.99900D+00

THETA= 0.0

TD	TD:RD**2	PD
0.399999990D-04	0.999999975D-01	0.124198 D-01
0.799999980D-04	0.199999995D+00	0.736016 D-01
0.159999996D-03	0.399999990D+00	0.216265 D+00
0.239999994D-03	0.599999985D+00	0.337574 D+00
0.319999992D-03	0.799999980D+00	0.437690 D+00
0.399999990D-03	0.999999975D+00	0.521993 D+00
0.799999980D-03	0.199999995D+01	0.811571 D+00
0.159999996D-02	0.399999990D+01	0.112834 D+01
0.239999994D-02	0.599999985D+01	0.132093 D+01
0.319999992D-02	0.799999980D+01	0.145966 D+01
0.399999990D-02	0.999999975D+01	0.156816 D+01
0.799999980D-02	0.199999995D+02	0.190854 D+01
0.159999996D-01	0.399999990D+02	0.225200 D+01
0.239999994D-01	0.599999985D+02	0.245370 D+01
0.319999992D-01	0.799999980D+02	0.259702 D+01
0.399999990D-01	0.999999975D+02	0.270828 D+01
0.799999980D-01	0.199999995D+03	0.305429 D+01
0.159999996D+00	0.399999990D+03	0.340053 D+01
0.239999994D+00	0.599999985D+03	0.360431 D+01
0.319999992D+00	0.799999980D+03	0.375211 D+01
0.399999990D+00	0.999999975D+03	0.387063 D+01
0.799999980D+00	0.199999995D+04	0.427728 D+01
0.159999996D+01	0.399999990D+04	0.476114 D+01
0.239999994D+01	0.599999985D+04	0.507835 D+01
0.319999992D+01	0.799999980D+04	0.531536 D+01
0.399999990D+01	0.999999975D+04	0.550450 D+01
0.799999980D+01	0.199999995D+05	0.611123 D+01
0.159999996D+02	0.399999990D+05	0.672989 D+01
0.239999994D+02	0.599999985D+05	0.709050 D+01
0.319999992D+02	0.799999980D+05	0.734399 D+01
0.399999990D+02	0.999999975D+05	0.753870 D+01
0.799999980D+02	0.199999995D+06	0.812921 D+01
0.159999996D+03	0.399999990D+06	0.869161 D+01
0.239999994D+03	0.599999985D+06	0.900634 D+01
0.319999992D+03	0.799999980D+06	0.921063 D+01
0.399999990D+03	0.999999975D+06	0.939185 D+01
0.799999980D+03	0.199999995D+07	0.985187 D+01
0.159999996D+04	0.399999990D+07	0.102822 D+02
0.239999994D+04	0.599999985D+07	0.105250 D+02
0.319999992D+04	0.799999980D+07	0.106805 D+02
0.399999990D+04	0.999999975D+07	0.107928 D+02
0.799999980D+04	0.199999995D+08	0.111605 D+02
0.159999996D+05	0.399999990D+08	0.115099 D+02
0.239999994D+05	0.599999985D+08	0.116970 D+02
0.319999992D+05	0.799999980D+08	0.118422 D+02
0.399999990D+05	0.999999975D+08	0.119569 D+02

TABLE **H.3** :

CONSTANT PRESSURE **LINEAR** BOUNDARY

2C'=100
R1= 1.0
R2= 99.0

TD	PD	TD	PD
0.100000016D 00	0.124574657D-01	0.100000016D 05	0.447973396D 01
0.200000033D 00	0.732067097D-01	0.200000033D 05	0.453569610D 01
0.300000049D 00	0.146277220D D0	0.300000049D 05	0.455510547D 01
0.400000066D 00	0.216125925D 00	0.400000066D 05	0.456495758D 01
0.500000082D 00	0.279886847D 00	0.500000082D 05	0.457091680D 01
0.600000098D 00	0.337620829D 00	0.600000098D 05	0.457490977D 01
0.700000115D 00	0.390014748D 00	0.700000115D 05	0.457777183D 01
0.800000131D 00	0.437811021D 00	0.800000131D 05	0.457992382D 01
0.900000148D 00	0.481668671D 00	0.900000148D 05	0.4551600533 01
0.100000016D 01	0.522141381D 00	0.100000016D 06	0.458294449; 01
0.2000000333 01	0.811712893D 00	0.200000033D 06	0.458901356D 01
0.300000049D 01	0.994660006D 00	0.300000049D 06	0.459104484D 01
0.400000066D 01	0.112845503D 01	0.400000066D 06	0.459206203D 01
0.500000082D 01	0.123394932D 01	0.500000082D 06	0.4592672853 01
0.600000098D 01	0.13210374713 01	0.600000098D 06	0.459308027D 01
0.700000115D 01	0.139519346D 01	0.700000115D 06	0.459337138D 01
0.800000131D 01	0.145976397D 01	0.800000131D 06	0.459358977D 01
0.900000148D 01	0.151694475D 01	0.900000148D 06	0.459375967D 01
0.100000016D 02	0.156825428D 01	0.100000016D 07	0.459389560D 01
0.200000033D 02	0.190863609D 01	0.200000033D 07	0.4594507542 01
0.300000049D 02	0.210929612D 01	0.300000049D 07	0.459471160D 01
0.400000066D 02	0.225209928D 01	0.400000066D 07	0.459481365D 01
0.500000082D 02	0.236304781D 01	0.500000082D 07	0.459487485D 01
0.600000098D 02	0.245379288D 01	0.600000098D 07	0.459491570D 01
0.700000115D 02	0.253057117D 01	0.700000115D 07	0.459494487D 01
0.800000131D 02	0.259711403D 01	0.800000131D 07	0.4594966743 01
0.900000148D 02	0.265583219D 01	0.900000148D 07	0.459498375D 01
0.100000016D 03	0.270837374D 01	0.100000016D 08	0.459499736D D1
0.200000033D 03	0.305432274D 01	0.2050000333 08	0.459505860D 01
0.300000049D 03	0.325683162D 01	0.300000049D 08	0.4595079029 01
0.400000066D 03	0.340042825D 01	0.400000066D 08	0.459508923D 01
0.500000082D 03	0.351144809D 01	0.500000082D 08	0.459509535D 01
0.600000098D 03	0.360150495D 01	0.600000098D 08	0.459509943D 01
0.700000115D 03	0.367677462D 01	0.700000115D 08	0.4595102350 01
0.800000131D 03	0.374097735D 01	0.800000131D 08	0.459510454D 01
0.900000148D 03	0.379656050D 01	0.900000148D 08	0.459510624D 01
0.100000016D 04	0.384523868D 01	0.100000016D 09	0.459510760D 01
0.200000033D 04	0.412893074D 01	0.200000033D 09	0.459511373D 01
0.300000049D 04	0.425708326D 01	0.300000049D 09	0.459511577D 01
0.400000066D 04	0.4330056310 01	0.400000066D 09	0.459511679D 01
0.500000082D 04	0.437714781D 01	0.500000082D 09	0.459511740D 01
0.600000098D 04	0.441004358D 01	0.600000098D 09	0.459511781D 01
0.700000115D 04	0.443431818D 01	0.700000115D 09	0.459511810D 01
0.800000131D 04	0.445296647D 01	0.800000131D 09	0.459511832D 01
0.900000148D 04	0.446774065D 01	0.900000148D 09	0.459511849D 01

TABLE *H.4* :

NO-FLOW LINEAR **BOUNDARY**

2C'=100
R1= 1.0
R2= 99.0

TD	PD	TD	PD
0.100000016D 0D	0.124574657D-01	0.100000016D 05	0.553971027D 01
0.200000033D 00	0.732067097D-01	0.200000033D 05	0.617688282D 01
0.300000049D 00	0.146277220D 00	0.300000049D 05	0.656293439D 01
0.400000066D 00	0.216125925D 00	0.400000066D 05	0.684076226D 01
0.500000082D 00	0.279886847D 00	0.500000082D 05	0.705794534D 01
0.6090300985 00	0.337620829D 00	0.6000000965 05	0.723627310D 01
0.700000115D 00	0.390014748D 00	0.700000115D 05	0.738756113D 01
0.800000131D 00	0.437811021D 00	0.8000001310 05	0.751894008D 01
0.900000148D 00	0.481668671D 00	0.900000148D 05	0.763504575D 01
0.100000016D 01	0.522141381D 00	0.100000016D 06	0.7739062333 01
0.200000033D 01	0.811712893D 00	0.2000000335 06	0.8426139195 01
0.300000049D 01	0.994660006D 00	0.300000049D 06	0.882957261D 01
0.400000066D 01	0.112845503D 01	0.400000066D 06	0.9116237262 01
0.500000082D 01	0.123394932D 01	0.500000082D 06	0.933876989D 01
0.600000098D 01	0.132103747D 01	0.600000098D 06	0.952068394D 01
0.700000115D 01	0.139519346D 01	0.700000115D 06	0.9674543453 01
0.800000131D 01	0.145976397D 01	0.800000131D 06	0.0807856415 01
0.900000148D 01	0.151694475D 01	0.900000148D 06	0.9925469523 01
0.100000016D 02	0.156825428D 01	0.100000016D 07	0.100306941D Q
0.200000033D 02	0.190863609D 01	0.200000033D 07	0.107232292D 02
0.300000049D 02	0.210929612D 01	0.300000049D 07	0.111284902D 02
0.400000066D 02	0.225209928D 01	0.400000066D 07	0.114160702D 02
0.500000082D 02	0.236304781D 01	0 500000082D 07	0.116391525D 02
0.600000098D 02	0.245379288D 01	0.600000098D 07	0.118214332D 02
0.700000115D 02	0.253057117D 01	0.700000115D 07	0.119755547D 02
0.800000131D 02	0.259711403D 01	0.800000131D 07	0.1210506433 C2
0.900000148D 02	0.265583219D 01	0.900000148D 07	0.122268303D 02
0.100000016D 03	0.270837374D 01	0.100000016D 08	0.123321772D 02
0.200000033D 03	0.305432310D 01	0.200000033D 08	0.130252631D 02
0.300000049D 03	0.325686288D 01	0.300000049D 08	0.134307078D 02
0.400000066D 03	0.340074006D 01	0.400000066D OS	0.137183797D 02
0.500000082D 03	0.351273881D 01	0.500000082D 08	0.139415171D 02
0.600000098D 03	0.360492019D 01	0.6000000985 08	0.141238346D 02
0.700000115D 03	0.368374169D 01	0.700000115D 08	0.142779823D 02
0.800000131D 03	0.375302571D 01	0.800000131D 08	0.144115115D 02
0.900000148D 03	0.381519088D 01	0.900000148D 08	0.145292929D 02
0.100000016D 04	0.387184545D 01	0.100000016D 09	0.146346520D 02
0.200000033D 04	0.428117557D 01	0.200000033D 09	0.153277931D 02
0.300000049D 04	0.455844650D 01	0.300000049D 09	0.157332561D 02
0.400000066D 04	0.477313469D 01	0.400000066D 09	0.160209372D 02
0.500000082D 04	0.494917424D 01	0.500000082D 09	0.162440801D 02
0.600000098D 04	0.509859169D 01	0.600000098D 09	0.1642640133 02
0.700000115D 04	0.522846183D 01	0.700000115D 09	0.1658055170 02
0.800000131D 04	0.534334046D 01	0.800000131D 09	0.167140828D 02
0.900000148D 04	0.544634585D 01	0.900000148D 09	0.168318657D 02

TABLE **H.5** :

THE LINE SOURCE

LINE SOURCE

TD	PD	TD	PD
0.100000016D 00	0.124574657D-01	0.100000016D 05	0.500972212D 01
0.200000033D 00	0.732067097D-01	0.200000033D 05	0.535628946D 01
0.300000049D 00	0.146277220D 00	0.300000049D 05	0.555901993D 01
0.400000066D 00	0.216125925D 00	0.400000066D 05	0.570285992D 01
0.500000082D 00	0.279886847D 00	0.500000082D 05	0.5914431073 01
0.600000098D 00	0.337620829D 00	0.600000098D 05	0.590559143D 01
0.700000115D 00	0.390014748D 00	0.700000115D 05	0.598266648D 01
0.800000131D 00	0.437611021D 00	0.800000131D 05	0.6049431953 01
0.900000148D 00	0.481668671D 00	0.900000148D 05	0.610832329D 01
0.100000016D 01	0.522141381D 00	0.100000016D 06	0.616100341D 01
0.200000033D 01	0.811712893D 00	0.200000033D 06	0.6507576383 01
0.300000049D 01	0.994660006D 00	0.300000049D 06	0.6710306123 01
0.400000066D 01	0.1158455030 01	0.400000066D 06	0.6854149663 01
0.500000082D 01	0.123394932D 01	0.500000082D 06	0.696572137D 01
0.600000098D 01	0.132103747D 01	0.600000098D 06	0.705688211D 01
0.700000115D 01	0.1395193460 01	0.700000115D 06	0.713395742D 01
0.800000131D 01	0.145976397D 01	0.800000131D 06	0.720072309D 01
0.900000148D 01	0.151694475D 01	0.900000148D 06	0.725961459D 01
0.1000000163 02	0.156825428D 01	0.100000016D 07	0.7312294833 01
0.200000033D 02	0.190863609D 01	0.200000033D 07	0.765886836D 01
0.300000049D 02	0.210929612D 01	0.300000049D 07	0.786160090D 01
0.400000066D 02	0.225209928D 01	0.400000066D 07	0.800544192D 01
0.500000082D 02	0.236304781D 01	0.500000082D 07	0.811701369D 01
0.600000098D 02	0.245379288D 01	0.600000098D 07	0.820817446D 01
0.700000115D 02	0.253057117D 01	0.700000115D 07	0.828524980D 01
0.800000131D 02	0.259711403D 01	0.800000131D 07	0.835201550D 01
0.900000148D 02	0.265583219D 01	0.900000148D 07	0.841090701D 01
0.100000016D 03	0.270837374D 01	0.100000016D 08	0.846358727D 01
0.200000033D 03	0.305432292D 01	0.200000033D 08	0.881016085D 01
0.300000049D 03	0.325684725D 01	0.300000049D 08	0.9012893405 01
0.400000066D 03	0.340058415D 01	0.400000066D 08	0.9156734443 01
0.500000082D 03	0.351209345D 01	0.500000082D 08	0.926830621D 01
0.600000098D 03	0.360321257D 01	0.600000098D 08	0.935946699D 01
0.700000115D 03	0.368025815D 01	0.700000115D 08	0.943654233D 01
0.800000131D 03	0.374700153D 01	0.800000131D 08	0.950330803D 01
0.900000148D 03	0.380587569D 01	0.900000148D 08	0.9562199553 01
0.100000016D 04	0.385854206D 01	0.100000016D 09	0.961487980D 01
0.200000033D 04	0.420505316D 01	0.200000033D 09	0.996145339D 01
0.300000049D 04	0.440776488D 01	0.300000049D 09	0.101641859D 02
0.400000066D 04	0.455159550D 01	0.400000066D 09	0.103080270D 02
0.500000082D 04	0.466316103D 01	0.500000082D 09	0.104195988D 02
0.600000098D 04	0.475431764D 01	0.600000098D 09	0.105107595D 02
0.700000115D 04	0.483139000D 01	0.700000115D 09	0.105878349D 02
0.800000131D 04	0.489815347D 01	0.800000131D 09	0.106546006D 02
0.900000148D 04	0.495704325D 01	0.900000148D 09	0.107134921D 02